

***COMPARISON OF DIFFERENT TYPES OF
ZEOLITES USED AS SOLID ACID CATALYSTS IN
THE TRANSESTERIFICATION REACTION OF
JATROPHA-TYPE OIL FOR BIODIESEL
PRODUCTION***

By

Gaétan LEMOINE

A thesis submitted to the Faculty of the

WORCESTER POLYTECHNIC INSTITUTE

In partial fulfillment of the requirements for the Degree of

Master of Science

In

Chemical Engineering

by

May 2013

APPROVED

Dr. Robert W. Thompson, Advisor

Dr. David DiBiasio, Head of Department

Acknowledgements

First and foremost, I would like to thank the École Nationale Supérieure des Industries Chimiques (ENSIC, Nancy, France) to have allowed me to take advantage of their partnership with the Worcester Polytechnic Institute for two years.

I would like to thank my advisor Professor Thompson for his time and help throughout my master program and also Professor Clark for his great help and very relevant advice for all the experimental part of my project. I would like to thank Ying Yang as well as Susan Yen for their priceless help for the Gas Chromatography and EDX analysis. I would also like to thank the faculty, staff and students of the Chemical Engineering department and more particularly Felicia Vidito, Tiffany Royal and Paula Moravek.

I would like to thank my friends and coworkers at WPI Thomas Gabry, Julien Courtois, Liang-Chih “Stanley” Ma, Tatiana Popova, Anuj Singh, Jeffrey Swanna, Kathleen Wang, Adrian Boteanu, Yuwei Zhai and all those I forgot here... I would like to say a special thank you to Federico Guazzone not only for his great support and insight on the direction that this thesis should take but also for all the experiences, ideas and values he shared with me over this past two years. Also a great thank you to Alessandro Mora and Jun “Ivan” Ma (the Italian-Chinese-French team) for their awesomeness which made my experience in Worcester incredibly rich. And obviously, an infinite thank you to Kelsey for all the love and happiness we have been sharing together.

Last but not least, I would like to thank my family and friends overseas for their support and trust during the past two years.

Abstract

Sustainable energy management has become a high priority for many countries. A great majority of our energy stocks comes from non-renewable fossil fuels, which are currently dwindling. Biofuels are one of the most promising solutions being researched to address this urgent problem. In particular, using transesterified *Jatropha curcas* L. oil appears to be a promising method of producing biofuels due to several properties of the plant, such as the high oil yield of its seeds and the fact that it does not compete with food crops.

The literature mentions many attempts of using zeolites as solid acid catalysts in transesterification reactions of vegetable oils with high free fatty acid (FFA) content. The acid catalysis prevents soap formation and emulsification, which can be observed in the basic process. The use of a solid catalyst makes the separation and purification of the final products steps easier to implement in comparison to catalysis in homogeneous conditions. However, the efficiency of the zeolite in the heterogeneous transesterification reaction of vegetable oil is not well-known yet and varies on the structure of the catalyst used.

This project aims at better understanding the relationship between the type of zeolite used and the yield of this particular reaction using reconstituted *Jatropha* oil from Sesame seed oil, which has a similar composition. Five different types of zeolites were compared: Y, X, Beta, Mordenite & ZSM-5. Non-catalyzed reactions as well as homogeneously catalyzed – with H_2SO_4 – reactions were also implemented. Since we take advantage of the catalytic properties of different zeolites, the one that were not already in

hydrogen form were ion-exchanged and the ion-exchanged species were then analyzed by Energy-Dispersive X-Ray spectroscopy (EDX).

Three alcohol-to-oil ratios were tested at atmospheric pressure and at $T=115^{\circ}\text{C}$ for each catalyst in order to determine the influence of this ratio. All experiments were conducted in an airtight autoclave with butan-1-ol in order to obtain a biofuel whose cetane index is higher than regular petroleum-based diesels.

Table of contents

| | | |
|------|---|----|
| I. | Introduction..... | 11 |
| II. | Background..... | 15 |
| | II.1 – Economic and Environmental aspects..... | 15 |
| | II.2 – General aspects of biofuels | 18 |
| | II.3 – Jatropha Curcas | 20 |
| | II.3.1 –The plant..... | 20 |
| | II.3.2 – The great potential of the plant | 21 |
| | II.4 – Transesterification of Jatropha oil..... | 31 |
| | II.4.1 – Overhaul presentation of the reaction..... | 31 |
| | II.4.2 – Parameters of the reaction | 33 |
| | II.5 – General presentation of the Zeolites | 44 |
| | II.5.1 – Zeolites’ structures | 44 |
| | II.5.2 – Applications | 47 |
| | II.5.3 – Properties and structures | 49 |
| III. | Determination of the Acid Value of the Sesame oil | 53 |
| | III.1- Introduction | 53 |
| | III.2- Experimental | 54 |
| | III.2.1 - Experimental device..... | 54 |
| | III.2.2 - Chemical reaction and location of the equivalence..... | 55 |
| | III.3 - Results | 57 |
| | III.4 – Conclusions..... | 58 |
| IV. | Determination of the Fatty Acid Composition of the Sesame oil – Recreation of artificial Jatropha oil..... | 59 |
| | IV.1 – Introduction – Necessity of the FA analysis | 59 |
| | IV.2 – Theory – Methods of analysis of the FA composition of vegetable oils | 61 |
| | IV.2.1 – The Transesterification step..... | 61 |
| | IV.2.2 – The separation of the compounds | 62 |
| | IV.2.3 – The analysis of the compounds..... | 63 |
| | IV.3 – Experimental | 63 |
| | IV.3.1 – Transesterification in alkaline medium..... | 64 |
| | IV.3.2 – Post-treatment of the transesterified oil | 66 |
| | IV.3.3 – Gas Chromatography and Mass Spectroscopy analysis (GC-MS)..... | 67 |

| | |
|--|-----|
| IV.3.4 – Recreation of the artificial Jatropha oil | 68 |
| IV.4 – Results | 69 |
| IV.4.1 – GC-MS Analysis..... | 69 |
| IV.4.2 – Amounts of FAs added to the Sesame oil | 72 |
| IV.5 – Conclusions..... | 73 |
| V. Ion-exchange process on the 13-X zeolite | 75 |
| V.1 – Introduction..... | 75 |
| V.1.1 – necessity of the ion-exchange step | 75 |
| V.1.2 – ion exchange processes..... | 76 |
| V.1.3 – Post treatment of the ion-exchanged zeolite | 78 |
| V.2 – Experimental | 79 |
| V.2.1 – Pretreatment..... | 79 |
| V.2.2 – Ion-exchange step | 79 |
| V.2.3 – Conductimetric analysis | 81 |
| V.2.4 – EDX spectroscopy analysis | 85 |
| V.3 – Results | 86 |
| V.3.1 – Conductimetric analysis | 86 |
| V.3.2 – Basicity of the untreated zeolite 13-X - Washing step and pH variations..... | 90 |
| V.3.3 – EDX spectroscopy analysis | 92 |
| V.4 – Conclusions..... | 95 |
| VI. Transesterification of recreated Jatropha oil with zeolites as catalysts | 96 |
| VI.1 – Introduction..... | 96 |
| VI.1.1 – Composition of Jatropha oil | 96 |
| VI.1.2 –The reaction | 99 |
| VI.2 – Experimental | 102 |
| VI.2.1 – Reactants and Parameters of reaction..... | 102 |
| VI.2.2 – Experimental device | 106 |
| VI.2.3 – Analysis of the samples | 108 |
| VI.3 – Results and discussion..... | 109 |
| VI.3.1 – Homogeneous and heterogeneous catalysis | 109 |
| VI.3.2 – Influence of the molar butanol-to-oil ratio | 111 |
| VI.3.3 – Compared efficiencies of the zeolites | 112 |
| VI.3.4 – Global results of the transesterification reactions..... | 120 |
| VI.4 – Conclusions..... | 121 |

| | | |
|-------|--|-----|
| VII. | Conclusions..... | 122 |
| VIII. | Recommendations | 124 |
| IX. | Appendices | 132 |
| | Appendix A: Standard curves obtained for the calibration of the gas chromatograph | 132 |
| | Appendix B: Determination by calculation of the quantity of FA needed to recreate Jatropha oil from Sesame oil..... | 134 |
| | Appendix C: Determination of the butanol-to-oil weight ratios corresponding to the three molar ratios..... | 138 |
| | Appendix D: EDX Analysis reports | 141 |
| | Appendix E: EnzyChrom Assay Kit's manual..... | 154 |
| | Appendix F: Determination of the glycerol concentration of a sample..... | 155 |
| | Appendix G: Results of the transesterification reactions with the different catalysts. 5 zeolites (13-X-type, Y-type, ZSM-5, Mordenite & Beta), H ₂ SO ₄ and non-catalyzed reaction. Butanol-to-oil ratios tested: 3:1, 6:1 and 15:1. | 158 |
| | Appendix H: Specifications and characteristics of the Parr reactor..... | 179 |

List of figures

| | |
|---|-----|
| Figure 1 - The annual range in mass of total FFCO ₂ emissions. The range was calculated from the maximum and minimum monthly values of total FFCO ₂ emissions for the calendar year. The dashed line is a linear regression through the annual values | 16 |
| Figure 2 - Per-capita energy consumption by sectoral end use in (A) the developing world and (B) the developed world (in gigajoules) in 2000[4] | 17 |
| Figure 3 - <i>Jatropha</i> field in Chiapas, Mexico (3a); <i>Jatropha</i> plant and whole seeds in Guanacaste, Costa Rica (3b) | 21 |
| Figure 4 - Compositions of <i>Jatropha</i> fruits[8]..... | 22 |
| Figure 5 - Balances of the three steps of the transesterification reaction | 33 |
| Figure 6 - Tetrahedra of oxygen coordinated with silicon (left) and aluminum (right)..... | 45 |
| Figure 7 - Examples of a truncated octahedron (left), the β-framework building unit and a truncated cuboctahedron (right), the α-framework building unit[83]..... | 46 |
| Figure 8 - The structure of the A-type zeolite, assembly of truncated octahedron and double four-member rings (D4R) | 47 |
| Figure 9 - The three channel system. The 1-D channel system of the L-type zeolite (a). The 2-D channel system of Mordenite (b). The 3-D channel system of Faujasite (c).[90] | 52 |
| Figure 10 – Experimental set up for the determination of the AV of the sesame oil by titration with KOH in ethanol | 55 |
| Figure 11 - Different forms of phenolphthalein depending on the value of pH..... | 55 |
| Figure 12 - Evolution of the coloration of the solution around the equivalence (Left: before the equivalence; middle: equivalence; right: after the equivalence)..... | 57 |
| Figure 13 - Skeletal formula of the four main FA found in Sesame oil | 59 |
| Figure 14 - Overall FAME production reaction from triglycerides | 64 |
| Figure 15 - Non-diluted sample (chromatogram) | 70 |
| Figure 16 - 100-time diluted sample (chromatogram)..... | 70 |
| Figure 17 - Flow diagram for countercurrent operation | 77 |
| Figure 18 - Flow diagram for crossflow operation [111]..... | 77 |
| Figure 19 - Balances of the three ion-exchange processes on zeolite 13X | 78 |
| Figure 20 – Ion-Exchange set up using a solution of Ammonium Chloride (NH ₄ Cl) at 1mol.L ⁻¹ at a constant temperature of 65°C for 40 minutes | 80 |
| Figure 21 – Experimental set up for the titration of the ion-exchange solutions (containing NH ₄ ⁺) by an aqueous solution of Potassium Hydroxide (KOH) at 4.10 ⁻³ mol.L ⁻¹ | 83 |
| Figure 22 - Dosages of NH ₄ ⁺ by OH ⁻ followed by conductimetry | 87 |
| Figure 23 – Number of moles of NH ₄ ⁺ exchanged vs. experiment n° | 88 |
| Figure 24 - Langmuir and Freundlich adsorption models applied to our ion-exchange process | 89 |
| Figure 25 - EDX Analysis of the 13-X zeolite Before calcination and the four ion-exchange steps..... | 92 |
| Figure 26 - EDX Analysis of the 13-X zeolite After the four ion-exchange steps and calcination | 92 |
| Figure 27 - EDX Analysis of the ZSM-5 zeolite before calcination | 94 |
| Figure 28 – General structure of a triglyceride with R ₁ , R ₂ and R ₃ saturated or unsaturated alkyl groups..... | 96 |
| Figure 29 - Acid-catalyzed mechanism of the transesterification reaction | 100 |
| Figure 30 - Overhaul balance of the saponification reaction | 101 |
| Figure 31 -The transesterification device: Stirring controller, autoclave, heating mantle (a); open reactor (b); reactor's head (c); temperature controller and thermocouple (d) | 108 |
| Figure 32 - Transesterification of recreated <i>Jatropha</i> oil with butanol at 115°C using H ₂ SO ₄ (1%wt.) as liquid acid catalyst for three butanol-to-oil molar ratios (3:1, 6:1 & 15:1) | 110 |

| | |
|--|------------|
| <i>Figure 33 - Transesterification of recreated Jatropha oil with butanol at 115°C using Y-type zeolite (1%wt.) as solid acid catalyst for three butanol-to-oil molar ratios (3:1, 6:1 & 15:1).....</i> | <i>113</i> |
| <i>Figure 34 - Transesterification of recreated Jatropha oil with butanol at 115°C using 13-X-type zeolite (1%wt.) as solid acid catalyst for three butanol-to-oil molar ratios (3:1, 6:1 & 15:1).....</i> | <i>113</i> |
| <i>Figure 35 - Transesterification of recreated Jatropha oil with butanol at 115°C using Beta zeolite (1%wt.) as solid acid catalyst for three butanol-to-oil molar ratios (3:1, 6:1 & 15:1).....</i> | <i>115</i> |
| <i>Figure 36 - Non-catalyzed transesterification of recreated Jatropha oil with butanol at 115°C for three butanol-to-oil molar ratios (3:1, 6:1 & 15:1).....</i> | <i>116</i> |
| <i>Figure 37 - Transesterification of recreated Jatropha oil with butanol at 115°C using Mordenite (1%wt.) as solid acid catalyst for three butanol-to-oil molar ratios (3:1, 6:1 & 15:1).....</i> | <i>117</i> |
| <i>Figure 38 - Models of the four main Fatty Acids and determination of the chain length taking into account the spatial set up of the molecules ($d_{\text{Palmitic acid}} = 1.387 \text{ nm}$, $d_{\text{Stearic acid}} = 0.802 \text{ nm}$, $d_{\text{Oleic acid}} = 1.368 \text{ nm}$, $d_{\text{Linoleic acid}} = 1.249 \text{ nm}$).....</i> | <i>118</i> |
| <i>Figure 39 - Transesterification of recreated Jatropha oil with butanol at 115°C using ZSM-5 (1%wt.) as solid acid catalyst for three butanol-to-oil molar ratios (3:1, 6:1 & 15:1).....</i> | <i>119</i> |
| <i>Figure 40 - Maximum conversions reached for each catalyst and each of the three butanol-to-oil molar ratio (3:1, 6:1 & 15:1) in the transesterification reaction of recreated Jatropha oil with butanol at 115°C.....</i> | <i>120</i> |
| <i>Figure 41 – The OD depends on the glycerol concentration in each well.....</i> | <i>155</i> |

List of tables

| | |
|--|-----|
| Table 1 - Examples of production of biogas by digestion of the seedcake in anaerobic reactors | 23 |
| Table 2 - Some physicochemical properties of <i>Jatropha curcas</i> oil and Diesel fuel [5]..... | 27 |
| Table 3 - Compared standards (ASTM) for petroleum-based diesel and biodiesel[23]..... | 29 |
| Table 4 - Uses of the different part of <i>Jatropha</i> plants in direct energy or energy carriers | 30 |
| Table 5 - Specific gravity of the alcohols and organic co-solvent (Note: most vegetable oils have a specific gravity within the 0.80-0.95 range) | 37 |
| Table 6 - Classification and performances of different catalysts used in transesterification of several vegetable oils | 44 |
| Table 7 - pKa of the Fatty Acids found in sesame oil [95]..... | 56 |
| Table 8 - Sesame oil composition (in % FA)[96, 97]..... | 60 |
| Table 9 - FA profile of the triglycerides in <i>Jatropha</i> oil..... | 68 |
| Table 10 - Results of the GC-MS on the diluted sample of sesame oil - Quantity of matter [mol] of each FAME in 1 gram of oil..... | 71 |
| Table 11 - Amount of each FA in the FFA fraction of the <i>Jatropha</i> oil..... | 72 |
| Table 12 - Quantity of matter and weight of each FA added per gram of sesame oil | 73 |
| Table 13 - Molar ionic conductivity of some useful ions | 84 |
| Table 14 - Results of the dosages of the NH_4^+ ions with OH^- | 88 |
| Table 15 - pH of the washing solutions | 91 |
| Table 16 - Weight and Atomic composition of both samples..... | 93 |
| Table 17 - Weight and Atomic composition for the three analyses | 94 |
| Table 18 - FA composition[118] and FFA content[108] of common plants oils..... | 97 |
| Table 19 - FA profile of the triglycerides in <i>Jatropha</i> oil..... | 97 |
| Table 20 - Structural characteristics of the zeolites used (* ZSM-5 structure obtained thanks to the idealized unit cell composition[121] and the outcome of the EDX Analysis) | 104 |
| Table 21 - Peaks' areas for the calibration sample, the studied sample and Relative peak area (Arbitrary unit) ND ¹ : Non Detected | 134 |
| Table 22 - Amount of each FA in the FFA fraction of both oils | 135 |
| Table 23 - Amount of FAs added per gram of sesame oil..... | 137 |
| Table 24 – Amounts of each liquid according to the butanol-to-oil molar ratio | 139 |
| Table 25 – Weight of each zeolite with respect to the molar ratio in each batch..... | 140 |
| Table 26– theoretical value of the maximum glycerol concentration reached with respect to the butanol-to-oil ratio..... | 157 |

I. *Introduction*

From the industrial revolution in the 18th and 19th centuries until now, mankind's needs in energy have been growing faster and faster to enable the development of the industries producing the world's goods and fuels necessary to meet transportation and residential needs. Nonetheless, the natural resources on which the economy and growth are based have been dwindling and finding new sources of renewable energies, more than a mere option, has become a necessity nowadays.

On top of the urge to address the concern of a fossil fuel shortage, it is also crucial to find a new source of energy that is going to be sustainable and which will meet environmental requirements. Many attempts have been developed and one of them particularly attracted scientists' and industrialists' attentions: biofuels.

Biofuels aims at making fuels from biomass. All parts of organic waste from plants and animals can be used in order to produce several kinds of biofuels mainly liquid and gaseous according to different processes. This study focused on the asset that is represented by the vegetable oil and more particularly the great potential that lies in Jatropha oil. This oil comes from a plant whose characteristics make it a strong candidate to the production of biodiesel on a large scale. On top of avoiding the unfavorable competition with the food crops, the plant has been proven to have high oil content and to be able to grow under harsh climatic conditions. The other parts of the plants (mainly the fibrous material from the wood-type by-products) can also be taken advantage of in the production of other types of fuels and extra-energy. And last but not least, the biodiesel produced from raw Jatropha oil does not require any modification of the engines and can be used exactly in the same way as petroleum-based diesel.

It was important to understand how to make the most of all the assets of the plant and how to produce biodiesel efficiently from Jatropha oil. The physical and chemical characteristics of the raw oil added constraints to the reaction transforming it into biofuel. Indeed, the major concern came from the high Free Fatty Acid (FFA) content of Jatropha oil in comparison to other vegetable oils whose use in biodiesel production has already been studied in depth. This forced us to adapt the type of catalysis and to choose a catalyst able to both esterify the FFA and transesterify the triglycerides of the oil and at the same time, avoid the formation of unwanted species by saponification (which renders the separations steps very time and energy consuming). Taking into consideration this particular aspect led us to choose acidic species as catalysts. Amongst dozens of types of acid catalyst, the choice of a heterogeneous species was done regarding separation and corrosion aspects.

The transesterification and esterification reactions can be implemented in thousands of different ways acting on all the reaction parameters such as the type or reactor, the temperature, the pressure, the nature of the transesterifying alcohol the amount of each reactant, the quantity of catalyst... In all the experiments implemented, all the parameters were kept identical from one experiment to another except the alcohol-to-oil molar ratio. Three different molar alcohol-to-oil ratios were tested (3:1, 6:1 and 15:1) in order to determine if a general trend can be observed when the amount of alcohol increased with respect to the number of moles of triglycerides.

The nature of the alcohol is also a parameter of paramount importance in that reaction. The chain length as well as the structure of the alcohol chain (linear versus branched) not only play on the kinetics (reaction rate) and thermodynamics (feasibility and yield) of the reaction but also dramatically influences the properties and efficiency of the final biodiesel. The only alcohol tested in all the batches was butan-1-ol.

Besides the production of biodiesel from Jatropha oil, one of the goals of the project was first and foremost to compare the efficiency of different varieties of zeolites as solid acid catalysts of the transesterification reaction. The particular structures of the zeolites combined with their acidic properties make them potentially efficient catalysts of the reactions between the alcohol and the FFA on the one hand, and between the butanol and the triglycerides of the oil on the other hand. Each zeolite has a particular framework characterized, amongst others, by the dimension of the channels, the pore size and the Silicon-to-Aluminum ratio. The nature of the positive counter-ion also has a strong influence on the properties of the zeolites. Frameworks containing hydrogen ions H^+ as positive counter-ions exhibit Brønsted acidic properties. The influence of the nature of this cation was not studied since all the zeolites used were either already in their H-form or went through a four-step ion-exchange process in order to be in the desired form. Five different types of zeolites were tested (ZSM-5, X-type, Y-type, Mordenite and Beta zeolites) and compared to a non-catalyzed reaction and to a homogeneously catalyzed reaction with H_2SO_4 .

It is important to note that due to the difficulties to obtain real raw Jatropha oil from suppliers, the oil used was Jatropha-type oil carefully reconstituted from unrefined Sesame oil. The whole interest of choosing Sesame oil as a starting point was to begin with oil which nature and proportion of each Fatty Acid (FA) were similar to the ones of Jatropha oil. This reconstitution first of all implied an accurate analysis of the Sesame oil's composition by Gas Chromatography-Mass Spectroscopy (GC-MS) analysis, measurement of the Acid Value (AV) of the oil and eventually, addition of the missing FFAs in the right proportions to the initial Sesame oil in order to have reconstituted Jatropha oil with the exact same composition and properties as raw Jatropha oil.

In summary, the specific objectives of the project were to:

- Recreate Jatropha oil from unrefined Sesame oil by measuring the AV of the latter as well as determining accurately the composition of its FA. The goal of those two primary steps was to add the right amount of each FFA to the oil;
- Obtain each zeolite in its H-form. The natures of the counter-ions of the zeolites whose counter-ion was unknown, was determined by Energy-Dispersive X-ray spectroscopy (EDX) analysis. Ion-exchange steps were implemented for the one which was not in its H-form. All zeolites were calcined before being used as catalyst;
- Implement the transesterification (and esterification) reaction of the Jatropha-type oil using the different zeolites and, in each case, for the three butanol-to-oil ratios;
- Follow the conversion of the reaction by measuring its yield throughout the reaction time thanks to a colorimetric method;
- Understand the influence of the alcohol-to-oil ratio in the reaction;
- Compare the efficiencies of the zeolites and understand their differences with respect to their properties.

II. *Background*

II.1 – Economic and Environmental aspects

In the past few decades, dozens of studies have been done in order to find alternatives to the petrol-based fuels on which our entire economy has been based for more than 60 years. By definition, fossil fuels are non-renewable and the reserves of oil, coal and natural gas are depleting dramatically. It is very hard to predict with accuracy when the fossil fuels supplies are going to be exhausted but even if scientists do not agree on the amount of time remaining before the shortage of fossil fuels, the great majority of them is aware that it is just a matter of time before the reserves are totally diminished. Shafiee and Topal [1] recently developed a new formula to compute the depletion of the three main non-renewable fuels: oil, coal and gas. The results of the calculations exhibited alarming acknowledgement: the approximate depletion times would be 35, 107 and 37 years respectively.

On the other side, the environmental and climatic impacts of the petroleum-based fuels have been concerning scientists and government all over the world for years. Among all the drawbacks of the use of traditional fossil fuels, the one which attracts more attention is the gigantic amount of carbon dioxide (CO₂) that their combustion implies. The total mass of CO₂ emissions due to fossil fuel over the 1950 to 2006 period of time was calculated by Andres et al. [2]. The plot on **Figure 1** shows the growth in the amplitude of the annual cycle over 56 years. From the data, the average Fossil Fuel CO₂ (FFCO₂) emission was multiplied by more than 4.5 in less than 60 years.

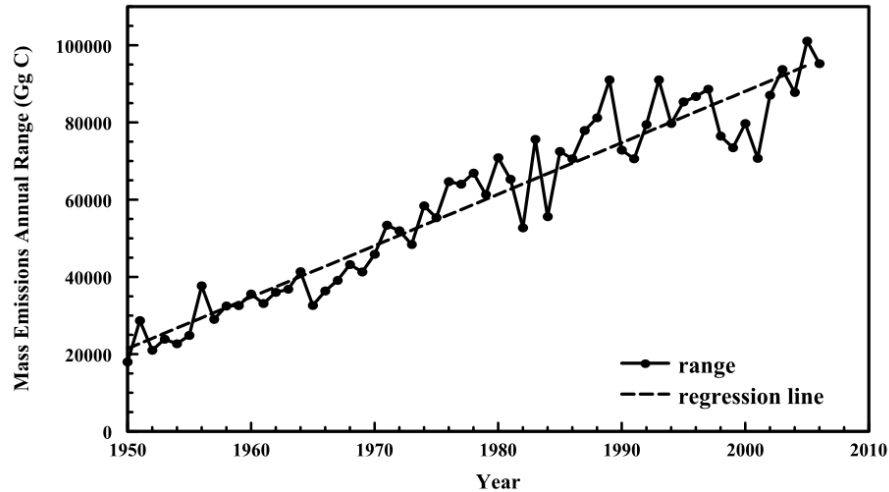


Figure 1 - The annual range in mass of total FFCO₂ emissions. The range was calculated from the maximum and minimum monthly values of total FFCO₂ emissions for the calendar year. The dashed line is a linear regression through the annual values

Two approaches to unravel the FFCO₂ emissions problem are commonly used. The first one tackles the consequence of the fossil fuels consumption and tries to find solutions to limit the environmental impact of the emissions without necessarily acting on the emissions themselves. Solutions such as capture of the CO₂ followed by ocean storage, geological storage or mineral carbonation were studied and proposed[3]. Unlike the first approach, the second one focuses on the source of the problem: the FFCO₂ emissions. This second approach aims at developing innovative processes and new types of fuel which could be used to substitute the current processes and fuels in order to cut the CO₂ emissions.

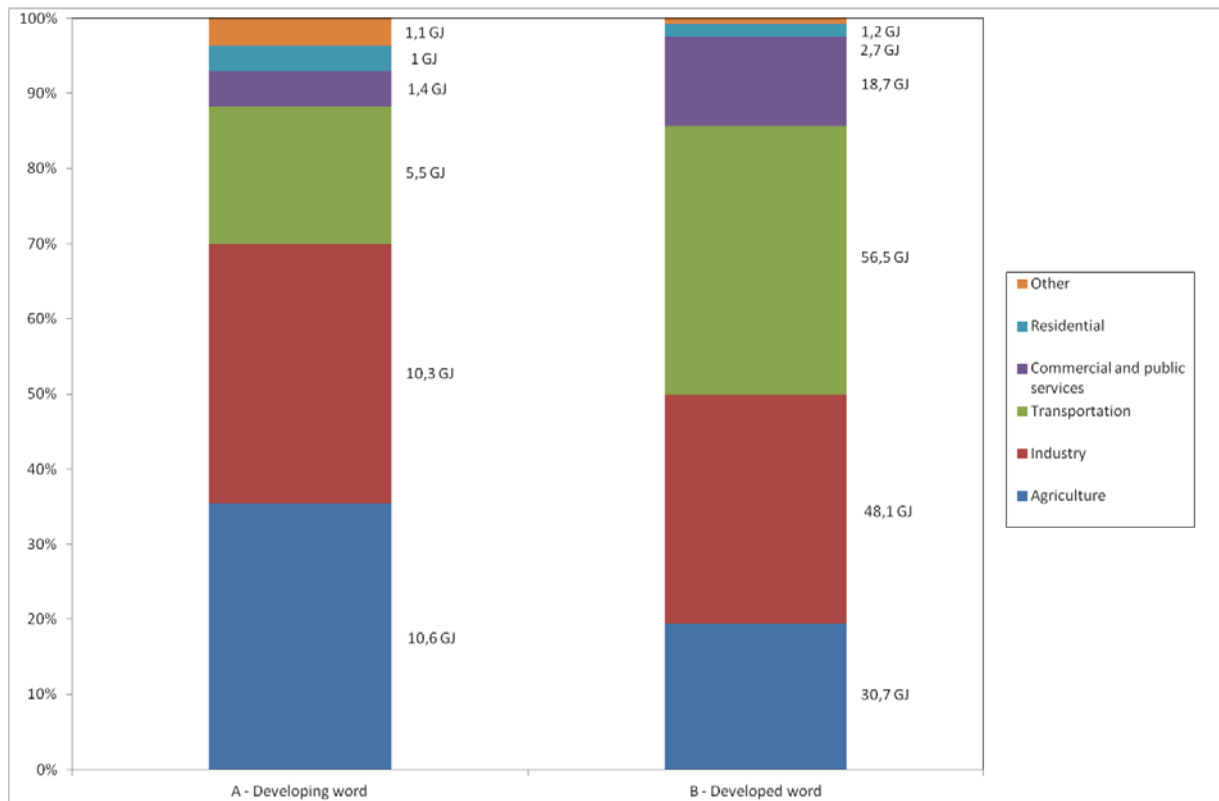


Figure 2 - Per-capita energy consumption by sectoral end use in (A) the developing world and (B) the developed world (in gigajoules) in 2000[4]

Figure 2 (A & B) show the distribution (in both the developing and in the developed world) of the consumption of energy from the primary sources (of which fossil fuels represent 95% of the total consumption with petroleum - 44%, natural gas - 26% and coal - 25%).[4] All the human activities in both developing and developed worlds are closely related to the abundance of fossil fuels and particularly the proficiency of petroleum. Solutions to reduce the weight of the petroleum-based fuels in human activities are being developed. However, many of those new options are efficient and economically acceptable but require dramatic changes in order to adapt technologies to those new sources of energy, more particularly in the transportation area.

Biofuels seem to be a viable solution to overcome this problem. Indeed, producing biofuels aims at using biomass to produce a fuel (liquid fuels, biogases) which could be either

mixed with regular fuels or even used as a total replacement of the common types of fuels. Scientists and industrialists start to understand the full potential of biomass and natural materials that were considered so far as organic wastes. On top of the thousands of compounds that can be produced from biomass, its energetic potential is considered by many as a promising way to face the pending energetic crisis.

II.2 – General aspects of biofuels

Unlike petroleum-based fuels, biofuels are renewable and non-fossil and they can be found in many different forms. They can be produced from oil, alcohol obtained by fermentation processes, wood coal or gaseous fuels derived from plants and animal biomass. Since the start of their use as energy sources, biofuels haven't stopped evolving in order to match more and more the objectives of the sustainable development. This rapid evolution allowed us to classify them into three groups: the first, the second and the third generation.

First-generation biofuels gather solid biofuels, bioalcohols, biodiesels processed from vegetable oils (in some cases the vegetable oil can be used as a fuel without any chemical modification), biogas and syngas, all produced from vegetable oil, starch and sugars.

The first generation of biofuels has the huge advantage that the production methods of the crops are very well understood and controlled. Also, the liquid fuels (biodiesels and bioalcohols) can be used in regular engines initially designed to be run with petroleum-derived fuels without any modification of their technologies.

However, the first generation of biofuels presents drawbacks which question their sustainability. Growing the crops dedicated to biofuel production takes over arable land that could be used for food production. This is highly questionable knowing that in the meantime 925 millions of people starved in 2010. (Source: Food and Agriculture Organization (FAO) of the United Nations) Also, when the cost of transportation is taken into account, the energetic and CO₂ emissions balances are mediocre. Finally, the development at a large scale of the cultivation of crops dedicated to biodiesel production would interfere with ecosystems.

In front of all those disadvantages, the urge to develop a second generation of biofuels was a priority.

Second-generation biofuels are produced from more sustainable biomass. Indeed, the main criterion in the development of that second generation of biofuels was to eliminate the dependence towards feedstock.

Biofuels belonging to the second generation are mostly bioalcohols issued from the fermentation of organic wastes (cellulosic material) or synthetic diesel obtained by pyrolysis, gasification and Fischer-Tropsch process. (See section I.3.2.1).

The advantages of the second generation of biofuels make them good candidates to progressively replace traditional fuels.

Third-generation biofuels based on algae and microalgae have been arising in the past few years. In terms of oil, theoretical yields of microalgae are tremendous in comparison to terrestrial plants. Due to the lack of studies, many questions have to be addressed (regarding the economic and technical feasibility of the cultures and their impact

on the environment) in order to know the long-term potential of this new generation of biofuels. According to a report of GreenTech Market research (GMT, 2010), a **fourth generation** of biofuels using petroleum-like hydroprocessing or advanced biochemistry starts appearing. Solar-to-fuel method based on the Joule-biotechnology is an example of the implementation of those emerging technologies.

Among those different options, scientists and industrialists have focused their attention on the most promising candidates. One of them, *Jatropha Curcas*, particularly retained their attention due to its high energetic potential combined with properties of the plant that allow it to grow on lands unsuitable for food crops.

II.3 – *Jatropha Curcas*

II.3.1 – The plant

Jatropha curcas is originally from the Mexican/Central American region but was introduced in other tropical and subtropical regions of the world where its acclimation made its cultivation possible.

This perennial species is a seed-bearing shrub or small tree (biggest specimens can reach 6 m) that has the quality to adapt and grow under numerous climatic conditions from dry tropical to moist subtropical or wet tropical forest. It can support rainfalls from 200mm/year to 2380mm/year, 200mm/year being sufficient for seed production. It does best in drier tropical area and is undemanding on soil, being well adapted to poorer soils.[5]

Jatropha curcas fruits are 2.5cm long, ovoid, black and have 2 or 3 halves. Seed production goes from 0.4 to over 12t/ha/year. Kernels and seeds have a high oil content. On average, 100 kg of whole seeds (hulls/husks + kernels) lead to 28-30 kg of oil.[6]

Except for a very few species, the great majority of Jatropha curcas fruits contains toxins that makes them non-edible. The main toxins are phorbol esters (biodegradable biotoxin), hydrogen cyanide, toxalbumin curcin (phytotoxin) and tetramethylpyrazine (TMPZ)[7].



Figure 3 - Jatropha field in Chiapas, Mexico (3a); Jatropha plant and whole seeds in Guanacaste, Costa Rica (3b)

II.3.2 – The great potential of the plant

Several projects have been running worldwide (India, Zimbabwe, Mexico...) to implement the culture of Jatropha with a view to producing energy from the plant. Indeed, most parts of the plant can be used in energy production. [8] The potential of the plant mainly comes from four parts: The wood-products, the shells hulls and husks, the seed oil and eventually the press-cake obtained after press of the whole seeds.



Figure 4 - Compositions of Jatropha fruits[8]

11.3.2.1 – The press-cake

The press-cake is the compact fibrous material obtained after press of the whole seeds. It can be used for several different purposes.

Fertilizer

The presence of toxins inside the plant is a drawback in the way it prevents the plant from being used as fodder and cattle food. But those toxic compounds also confer natural pesticide and bioinsecticide when the seedcake is used as a fertilizer. The fact that the toxins are biodegradable over a short period of time makes it a good fertilizer for crops[9].

Bioogas production

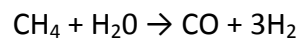
Biogas (mainly methane CH_4) can be produced in anaerobic reactors by digestion while the press-cake is used as a feed for the bacteria. **Table 1** gathers the gas production

yields obtained by Staubman et al.[10] and Radhakrishna[11] when cake was used as a feed for bacteria in anaerobic reactors. Several studies showed co-digestion using two or more substrates was an even more efficient way to obtain high yields for the biogas production.

| | Nature of the feed | Volume of biogas [m ³ per kg of feed] |
|---------------------|--|--|
| Staubman et al.[10] | dry seed press cake | 0,446 (70% CH ₄) |
| Radhakrishna[11] | solvent extracted kernel cake (de-oiled) | 0,5 |

Table 1 - Examples of production of biogas by digestion of the seedcake in anaerobic reactors

The traditional fermentation process can be followed by a steam reforming step in order to produce hydrogen H₂ from methane CH₄ following the equilibrium:



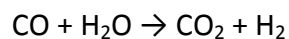
Bio-alcohol (and other chemicals) production

One of the most widespread anaerobic digestion processes is the Acetone-Butanol-Ethanol (ABE) process that allows the lignocellulosic material to be digested by bacteria in anaerobic conditions. The most common bacteria used for that matter are *Saccharomyces cerevisiae* and *Clostridium acetobutylicum*[12] but current researches try to find other more efficient bacteria species to reach higher yields[13]. Other studies focused on a modification of the reactor itself to a Fibrous-Bed reactor[14] or a two-step process where butyric acid would be produced first to be finally turned into bio-butanol in a second step[15]. Mixing 90% of regular gasoline with 10% of this bio-alcohol would allow to use this bio-alcohol in regular engines without needing any modification. The main drawback of those bioprocesses is the fact that they often need (costly) pretreatments with enzymes and/or acid hydrolysis[16]. Nonetheless, in spite of those pretreatment steps, the process uses only a

fraction of the lignocellulose (cellulose and hemicelluloses) and does not take advantage of the lignin.

Pyrolysis

Another efficient process to make energy from lignocellulosic product is pyrolysis. This process is an incomplete thermal degradation of the combustible in absence of air and it leads to ashes, tars, gaseous products and other condensable liquids. The main products of the reaction are the gases compounds: hydrogen H₂, carbon monoxide CO, carbon dioxide CO₂ and hydrocarbon gases. The hydrogen yield can be increased by a gas-shift reaction between the carbon monoxide and the water vapor[17] following the equilibrium:



II.3.2.2 – Shells, Husks & Hulls

Amongst all those by-products of the cultivation of Jatropha, shells, husks and hulls are also lignocellulosic materials whose energetic potential has to be taken into account. They can either be used just as they are but after grinding them, briquettes can also be formed and used as sources of energy. Once more, several processes can be implemented to produce direct energy or products that are important energy carriers.

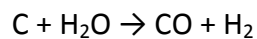
In the manner of the press-cake, those parts of the plant can be used as feed for **pyrolysis** in order to produce H₂, CO₂, CO and other volatile hydrocarbons. Anaerobic digestions can also be implemented from them to produce biogas or bio-alcohols.

Combustion

Direct combustion is an easy way to produce direct energy. However, more mature processes allow to treat those by-products more efficiently in terms of energy.

Gasification

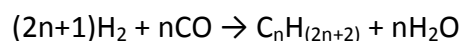
The gasification step gathers several processes. It not only includes a pyrolysis step but also allows the char produced during this previous step to react with steam in order to produce more hydrogen and carbon monoxide following the reaction



Gasification can also be followed by a water-gas shift reaction to produce more H₂. Vyas and Singh concluded that a gasification process implemented in an open core gasifier was very effective when Jatropha husks were used as feedstock [6].

The Fischer-Tropsch process

Synthetic hydrocarbons can be produced from hydrogen and carbon monoxide thanks to the Fischer-Tropsch process following the equilibrium:



Gasification processes combined with the Fischer-Tropsch reaction are being studied to produce sustainable transportation fuels at a large scale.

II.3.2.3 – Wood products

Sotolongo et al. showed that on average, a hectare of Jatropha plantation produces more than 20 tons of woody biomass only due to pruning over a period of six years.[18] It

goes without saying that this represents a direct source of energy by combustion or pyrolysis.

Bio-oil production

If the woody by-products undergo a fast pyrolysis followed by a rapid quench, Bio-oil can be produced. Bio-oil is a dark brown mixture of several hundreds of liquid organic compounds. It is obtained when the products of the fast pyrolysis of cellulose, hemicelluloses and lignin are “frozen” by quench. All the potential of bio-oil has not been deeply understood yet but the literature already shows applications of this oil from heat and electricity production to syn-gas and specialty chemicals productions.[19]

II.3.2.4 – Jatropha oil

The fact that most parts of the Jatropha plant can be used makes it very interesting in a Life-Cycle Approach (LCA) since the energy balance would be negative (Energy spent – Energy produced <0). But among all those by-products and the multiple ways they can be treated to produce energy or efficient energy carriers, it is important to keep in mind that the main purpose of Jatropha plantations is the production of Jatropha oil. This oil, obtained after press of the whole seeds is the reason of industrialists’ and scientists’ enthusiasm. Indeed, the high oil content of the Jatropha seeds combined with the properties of the plant makes Jatropha oil an easily available and promising resource with an astonishing energetic potential.

The oil can be extracted from the seeds in two main ways. On the one hand, it can be extracted by mechanical expellers. In that case, engine driven screw presses are more efficient than manual ram press. Increasing the yield can be done by increasing the number of passes[9] On the other hand, chemical extraction processes of the kernel’s oil have been

developed and exhibited good yields. Among the extractions methods, the best-known are the extraction using n-hexane, water (after ultrasolnic pretreatment), supercritical CO₂ or bio-renewable solvents such as bio-ethanol, isopropyl alcohol...

Raw Jatropha oil found several applications unrelated to energy production: it is the case for soap or biocides productions. However, it can be directly used after or before chemical treatment as a fuel.

Some of the physicochemical characteristics of Jatropha oil and regular diesel fuel are compared in **Table 2**[5].

| Property | Jatropha curcas oil | Diesel fuel |
|--------------------------------------|---------------------|-----------------|
| Viscosity (cP or mPa.s) | 75,7 at 20°C | 2-4,3 at 37,8°C |
| Ignition temperature (°C) | 340 | 51,7 |
| Conradson Carbon Residue Index (wt%) | 0,46 | 0,35 |
| Caloric power (MJ/kg) | 38,781 | 42,951 |
| Freezing point (°C) | 5 | ND |

Table 2 - Some physicochemical properties of Jatropha curcas oil and Dielsel fuel [5]

Jatropha curcas oil and Diesel fuel have comparable caloric powers. However, viscosity and ignition point of both liquids are very different. This is due to the structure of the oil itself which is mostly composed of high molecular weight molecules: the triglycerides.

Due to these differences, Jatropha oil can be used as a fuel in two ways: Direct use without chemical treatment; or after chemical modification.

Use of the Crude oil as a fuel

In the past, several studies have proved the use of pure Jatropha oil was doable in motor running at constant speed and low heat rejection diesel engines but was generally less efficient in terms of energy and smoke emission than the use of regular diesel.[20] Moreover, the high viscosity of crude Jatropha oil makes the injection and ignition steps improper and less efficient than in a regular diesel engine. Also, using high-viscosity crude Jatropha oil increases the risk of fouling, gum formation, coking in the engine and thickening of lubricating oil inside the motor. It is easy to understand that all those drawbacks make the crude Jatropha oil impossible to be used in regular diesel engines and thus, economically not viable.[21]

More promising results were obtained when blends of crude Jatropha oil and regular Diesel were tested. For instance Pramanik[22] showed up to 40-50%vol. in vegetable oils allowed to reach good efficiencies without any modification of the engine and any preheating of the blend.

Despite those results, the long-term impacts of the use of blends of diesel and vegetable oil remain unknown and best efficiencies are only reachable for relatively low Jatropha oil fractions and are very sensitive to the quality of the oil.

The best way to make the most of the capacities of the oil is to modify its chemical structure by transesterifying it. Transesterified Jatropha achieves better results in unadjusted diesel engines than the pure Jatropha oil used straight or in blends.[9]

Use of the transesterified oil as a fuel

Behind the idea of modifying the chemical structure of the components of the oil, there was a strong will to keep using Jatropha oil as an energy source but without modifying the engines. Indeed, the transesterification reaction of the triglycerides of the oil in presence

of a short-chain alcohol leads to Fatty Acid Alkyl Esters (The alkyl group depending on the nature of the alcohol used); this decreases dramatically the viscosity of the oil which enables to reach viscosities comparable to the one of regular diesel fuels.

Kywe and Oo[21] compared the viscosities of the crude Jatropha oil to the one of the biodiesel derived from the same oil. The kinematic viscosity decreased from $41.51\text{mm}^2\cdot\text{s}^{-1}$ in the crude oil to $5.384\text{mm}^2\cdot\text{s}^{-1}$ when the transesterification was run with methanol and $4.009\text{mm}^2\cdot\text{s}^{-1}$ with ethanol was the alcohol used during the transesterification step. Those numbers were within the limit of the American Society for Testing Materials (ASTM) for biodiesels and regular petro-diesel. Helwani et al. [23] compared the standards for diesel and biodiesel based on the ASTM (**Table 3**). Properties of both fuels are very similar and in some cases, properties of the biodiesel surpass the petroleum-based diesel such as higher flash point and cetane number, better lubricating power and low sulfur concentration.

| Property | Petroleum-based Diesel | Biodiesel |
|--------------------------------|---|--|
| Composition | Hydrocarbon (C ₁₀ -C ₂₁) | FAAE (C ₁₂ -C ₂₂) |
| Specific gravity (g/mL) | 0,85 | 0,88 |
| Flash point (K) | 333-353 | 373-443 |
| Water (wt%) | 0,05 | 0,05 |
| Oxygen (wt%) | 0 | 11 |
| Sulfur (wt%) | 0,05 | 0,05 |
| Cetane number | 40-55 | 48-60 |

Table 3 - Compared standards (ASTM) for petroleum-based diesel and biodiesel[23]

Scientists have now understood that using the altered (transesterified) Jatropha oil was the best way to make the most of the energetic power of the plant without any modification of the engines that have been running on regular petro-diesel so far.

This work being based on the transesterification reaction of this particular oil, a deeper description of Jatropha oil and its use reported by the literature is done in the next section (See Section 1.4).

Table 4 gathers all the uses presented above of the different part of the plant.

| | Press-cake | Shells, Hulls & Husks | Wood Products | Jatropha oil |
|------------------------|-------------------------------------|---|--------------------|--|
| Direct use | Fertilizer | Combustion | Combustion | Fuel (using the crude oil) |
| After treatment | Pyrolysis | | Pyrolysis | |
| | CH ₄ production (Biogas) | H ₂ production (Gasification, water-gas shift) | | BioDiesel production (transesterification) |
| | Bioalcohols production | Synthetic hydrocarbons (Fischer-Tropsch process) | Bio-oil production | Soaps production |
| | Other Chemicals | | | Biocides production |

Table 4 - Uses of the different part of Jatropha plants in direct energy or energy carriers

11.3.2.5 – Criticism about the use of Jatropha oil

In spite of all the bright aspects of the potential of Jatropha, more and more studies, article and official reports question the actual sustainability of Jatropha cultivation. In 2010, the NL Agency published a report [24] in the frame work of the Netherlands Programmes Sustainable Biomass in which the major drawbacks are stated. The international network “*friends of the earth*” published a report supported by the Dutch government as well as the European commission that showed the evidence of the unsustainability of the Jatropha farming.[25] The legitimacy of the interest in Jatropha cultivation has also been exposed to the general public by the news agency Reuters in the article “*Biofuel jatropha falls from wonder-crop pedestal*”[26]. One of the main interests of Jatropha is the ability of the plant to grow on wastelands which would enable to make the most of lands that cannot be used for

food crops. However, the reality was proved to be slightly different from the bright expectations since cultures of Jatropha on true wastelands exhibited yields that were far too low to be of economic interest. In order to be viable, Jatropha plants would have to be grown on fertile lands with additional use of fertilizers and irrigation. On the one hand, this would have an impact on food security increasing the competition with food crops and increasing land pressure; on the other hand, it has been proved that under the same conditions and using the same resources, production of crops for food purposes would be much more profitable than farming Jatropha.

Other aspects of the cultivation of Jatropha have been misestimated. It is the case of the seed yields which had been unrealistically overestimated. On the contrary, costs of land and labor have often been underestimated.

If good progresses have been done regarding the oil processing efficiency, value-creation from the by-products (from both farming and oil process) is not efficient enough.

All those drawbacks were analyzed by Kumar et al.[27] and held responsible of the failure of the National Biodiesel Mission Phase-I. However, if the numerous technological, environmental, economic and social issues are addressed, the possibility of local production and use of Jatropha oil and products were not ruled out.

II.4 – Transesterification of Jatropha oil

II.4.1 – Overhaul presentation of the reaction

The transesterification reaction takes place between the ester group of a molecule and the alcohol function of another one – in the case of an intermolecular reaction – or the same one – if the reaction is intramolecular reaction. The presence of a catalyst is essential

for the reaction to occur. In our case, it is an intermolecular reaction (two different molecules involved) where a triglyceride (TG) reacts with three molecules of alcohol to lead to a molecule of glycerol and three molecules of Fatty Acid Alkyl Esters (FAAE). Those FAAE are the objective of the whole process in our case: the Biodiesel.

In fact, obtaining those final products from the initial reagents is a combination of three successive independent reactions:

- A first molecule of alcohol (R-OH) reacts with the triglyceride to lead to a single molecule of FAAE and an intermediate: a di-glyceride;
- Then, the di-glyceride reacts with another molecule of alcohol to lead to a second molecule of FAAE and the second intermediate: a mono-glyceride;
- Eventually, the mono-glyceride reacts with the last molecule of alcohol to lead to the glycerol and a third molecule of FAAE.

Figure 5 shows the balance of those three steps.

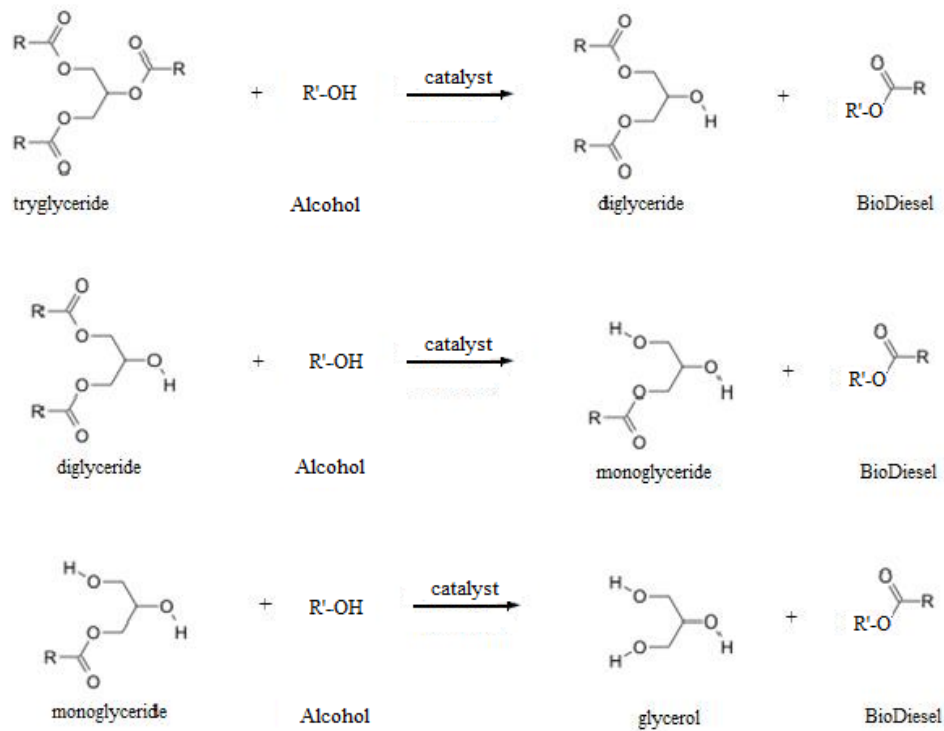


Figure 5 - Balances of the three steps of the transesterification reaction

The transesterification of triglycerides of vegetable oils is a well-known and well-controlled process that has been deeply studied in the literature. That is the reason why many parameters can be modified offering an almost infinite amount of possibilities to realize that reaction.

II.4.2 – Parameters of the reaction

II.4.2.1 – Types of reactors

If the transesterification reactions are done most of the time following batch processes, several other type of reactors can reach better conversion in a few particular cases (usually determined by a singular catalyst).

The batch process

The batch processes have been widely studied in the past thanks to its facility of implementation.[28] In some cases, several batch unit are put in series in order to reach higher conversions.[29]

The main limitation of the process is its scale: for large-size production, continuous processes are often preferred.

The plug-flow reactors

The use of the plug flow reactor is less widespread than the use of batch processes but in some cases, in spite of the material constraints it implies, it exhibits obvious assets. It is the case when an oil has to be pretreated in acidic media and then transesterified in basic media. Putting two plug-flow reactors in series for each treatment allow a better yield and in less time than with a batch process.

Due to the high viscosity of the reactants, the main issue of the plug-flow reactors is the mass transfer. This problem can be unraveled using the following and very particular type of reactor.

The oscillatory-flow reactors

Due to the singular geometry of the oscillatory-flow reactors, the literature exhibits only a few studies about them. However, they seem to be a promising way to overcome the

main concerns raised by the plug-flow reactors. The amplitude and frequency of the flow inside the reactor can be set in order to decrease the mass transfer limitation.[30]

II.4.2.2 – Influence of the temperature

The influence of the temperature is of paramount importance. If high temperatures are required to allow the reaction to occur, it jeopardizes the sustainability of the process. The literature reports low activation energies for the transesterification reaction. Depending on the type of alcohol used and the quality and nature of the oil, the activation energy varies. Kinetics of transesterification of Soybean oil was studied by Nouredini and Zhu and compared to other literature results. They reported an activation energy (E_a) within the 8 Kcal/mol to 18.5Kcal/mol range.[31] These relatively small values of E_a enable the reaction to occur in mild temperature conditions.

However, depending on the quality of the oil and the type of catalysis used, the temperature conditions might be adapted to the particular reaction.

II.4.2.3 – Nature of the alcohol

The nature of the triglyceride is closely related to the nature of the oil and it is hard to have an influence on it. Nevertheless, the nature of the second reagent is easily manipulable. Among the alcohol family, only a few of them were commonly used in transesterification reactions. Short chain alcohols from methanol to pentanol have been widely used. Nonetheless, several factors had to be taken into account for the choice of the alcohol.

Cost and availability

Cost of raw materials is one of the primary concerns for the implementation of a process. That is why methanol was the most common alcohol used for transesterification of vegetable oils purposes. However, the increasing production of bio-ethanol and bio-butanol from biomass makes the use of these two alcohols more and more common. On top of that, including bio-alcohols into the transesterification process makes it 100% environment-friendly by the production of a sustainable fuel from a renewable resource. Also, the ethanol produced by fermentation of sugars is much less toxic than non-renewable methanol.

Reaction aspects

The type of alcohol used also has a direct influence on the rates of reaction and conversions reached. Usually, the smaller the carbonated chain of the alcohol, the higher reactivity thanks to greater polarity of the species.

However, in the case of a transesterification with a short chain alcohol, the reaction takes place between two phases: the heavy lower phase containing the oil and a lighter alcoholic phase. As a consequence, in addition to the kinetics, mass transfer limitation becomes a limiting process. The mass transfer influence can be reduced by the choice of an alcohol with a longer chain. Kildiran et al. [32] shown that better yields are reached using ethanol, propanol and butanol than using methanol. The formation of emulsions between the alcohol, the oil and the reaction intermediates (mono- and di-glycerides) favors the reaction. The emulsion is all the more stable that the alcohol's chain is long. With longer

chain alcohols and with a large alcohol-to-oil ratio, the diffusion limiting issue is avoided by the formation of a single-phased system.

In order to avoid those mass transfer limitation issues, another technique was established using a co-solvent. For that matter, organic solvents such as TetraHydroFuran (THF), ethoxyethane and (1,4)-dioxane are the most common co-solvent. Their specific gravities shown in **Table 5** enables them to gather both phases (the oil and the alcohol phase) and consequently to avoid any mass transfer issue.

| Alcohol | Specific gravity |
|--------------|------------------|
| Methanol | 0,7918 |
| Ethanol | 0,789 |
| Propanol | 0,8034 |
| Butanol | 0,81 |
| THF | 0,8892 |
| 1,4 dioxane | 1,033 |
| Ethoxyethane | 0,7134 |

Table 5 - Specific gravity of the alcohols and organic co-colvent (Note: most vegetable oils have a specific gravity within the 0.80-0.95 range)

The nature of the carbonated chain also has a strong influence. If linear chains gave good results, the presence of ramifications or a position of the alcohol group in the middle of the chain increase the steric bulk and makes the reaction hard to occur.[33] Isopropanol which does not carry its alcohol group at the end of its carbonated chain, did not allow to reach high conversions due to the repulsion caused by the additional methyl group compared to ethanol.

II.4.2.4 – The alcohol-to-oil molar ratio

The mechanism of a transesterification reaction between a triglyceride and a mono-alcohol involves one mole of triglyceride for three moles of alcohol. Yet, in practice, the

stoichiometric ratio is not used and an excess of alcohol is mandatory to reach good conversions. Usually the smaller ratio studied in the literature is 6:1; this allowed to shift the equilibrium towards the formation of the products and enabled to reach better conversions.[34, 35]

Literature exhibits a wide range of alcohol-to-oil ratios going from 6:1 up to 30:1.[36, 37] In some publications, the molar ratio can reach 245:1.[38] This value contradicted other studies' results in which high ratios were avoided in order to prevent from increasing the glycerol solubility in the ester phase which causes the indirect reaction to take place and consequently reduces the yield of the direct reaction.[39]

II.4.2.5 – The nature of the catalyst

The literature exhibits dozens of different catalysts for the particular transesterification of vegetable oils. Depending on the nature and quality of the oil, some catalysts fit better than others and the difference of conversion between two different types of catalysts can be dramatic.

II.4.2.5.a –Homogeneous catalyses

Both acidic and basic species can be used as catalysts. Most studies focused on the use and comparison of basic catalysts due to the fast kinetics they involve.

Their great availability and very low cost make potassium hydroxide (KOH) and sodium **hydroxide** (NaOH) the two most common bases used for that purpose.[21, 40] **Alkoxydes** such as Sodium methoxide (CH_3ONa) are less common but allow to reach higher conversions and already include the transesterifying alcohol in their structure.[35]

Eventually, **Carbonates** can also be used as catalytic species in alkaline homogeneous processes.[23]

Nonetheless, even if the reaction kinetics can be up to 4000 times faster using a basic catalyst than an acid catalyst[36, 41], the quality of the oil is the main parameter to take into account while choosing the type of catalyst. Indeed, oils with high Free Fatty Acid (FFA) and/or water contents must not be transesterified in alkaline medium due to the unwanted formation of large amounts of soaps. (See Section V.1.2.1). **Inorganic acids** are the most common homogeneous acid catalysts used in transesterification of vegetable oils. Among them, Sulfuric Acid and hydrochloric acid gave high conversion in transesterification of several vegetable oils with methanol [40, 42]. **Organic acids** such as p-Toluenesulfonic acid or supported organic acids also exhibited good yields[42, 43].

The main interests of using homogeneous catalyses are the availability of the catalysts combined with a very good knowledge of the processes involving them due to dozens of studies. Nonetheless, with the view to making chemical processes as efficient and as respectful of the environment as possible, the trend is now to use heterogeneous catalyses.

II.4.2.5.b –Heterogeneous catalyses

Thanks to the easy way to separate them from the main liquid phase(s) at the end of the reaction, the heterogeneous catalysts have the advantage to considerably simplify the final separation units (which are then reduced to simple decantation/filtration units) and

most of them can be regenerated and reused later whether continuous or batch process are dealt with. These properties also have an impact on the sustainability of the process since less energy is spent on separation processes (distillation, extraction), less catalyst is needed due to its reuse and risks of release of toxic liquid catalytic waste downstream are avoided.

Such as homogeneous catalysts, heterogeneous catalysts can be divided into two main families: the basic heterogeneous catalysts and the basic homogeneous catalysts.

Among the basic heterogeneous catalysts, the **Alkali earth metal oxides** (MgO, CaO, SrO) and the **transition and mixed metal oxides** (Li/CaO, ZnO/Ba...) showed almost total conversions when used in the transesterification of several different vegetable oils. [44-46] Other studies have shown **Hydrotalcites**, **Alkali metal oxides** and **basic zeolites** were also usable for that purpose. [33, 47, 48]

Once again, basic heterogeneous catalyst usually exhibit a good yield when they are used for the transesterification reaction of oils with low FFA content but are not well adapted when the FFA content reaches only 1 or 2%wt. The acid solid catalysts are well adapted for that matter. **Solid HeteropolyAcids** and **mixed metal oxides** are the most efficient catalysts in terms of conversion. [42, 49, 50]

In the past few years, **zeolites** have been attracting scientists' attention. Their particular structures can be tailored in dozens of different ways and their catalytic properties adjusted to reach particular goals. Usually used in detergents or in catalytic processes in the petroleum industry, their uses have been widened to a very large panel of chemical reactions and particularly transesterification of oils for the production of Biodiesel. On the one hand, the particular structures exhibited by the zeolites are often an advantage in a way that they enable the catalysis of certain reactions, preventing others to occur at the same time which makes the process very specific. On the other hand, this great specificity can be a drawback

if the zeolite is not perfectly adapted to the type of reaction it is supposed to catalyze. As a consequence, yields of transesterification reactions of vegetable oils were not found as satisfying as with other types of catalysts. Sasidharan et al. observed less than 30% of conversion for conversions of beta-keto ester with **H-ZSM-5** [51] and Brito et al. only 26% of conversion of waste cooking oil using **H-Mordenite**. [52] Nonetheless, the type of zeolite and its properties make an important difference in the conversion. The same reaction implemented by Sasidharan et al. with **H-Y** zeolite exhibited a yield over 85%. [51]

Thus, it seems that zeolites can be adapted in order to reach industrialists' expectations regarding the yields of reaction as well as a great availability combined with very low costs.

This project aims at studying the efficiency of different types of zeolites used as heterogeneous acid catalysts in transesterification reactions. Section 1.5 details the structures and properties of the zeolites.

II.4.2.5.c – Other types of catalyses

Other types of catalyses have been marginally studied mostly due to their cost.

Enzymatic processes involving lipases were studied by Shah and Gupta [53]. Although the yields obtained were comparable to the one obtained using other types of catalysts, implementing those reactions require highly controlled conditions and are usually much more expensive than the other methods. These drawbacks make enzymatic processes impossible to implement at large industrial scales.

The use of Lewis Acids (AlCl_3 , ZnCl_2) was studied by Soriano et al. [54] and enabled them to reach conversions higher than 80% (with AlCl_3).

Methods without catalysts were also studied [55] but they required a supercritical methanol treatment of the oil which is not as energy efficient as processes using other types of catalysts.

Table 6 gathers and classifies the different catalysts used by previous works on transesterification of several vegetable oils. **Table 6** also provides the conversion reached for each catalyst.

| Phase | Property | Catalyst | Structure | Feedstock | Conversion | Reference | |
|---------------|---------------------------------|---------------------------|-------------------------------------|--|---------------|-----------|------|
| Homogeneous | Basic | Hydroxydes | KOH | Rapeseed oil | 98,50% | [40] | |
| | | | NaOH | - | - | | |
| | | Alkoxides | CH ₃ ONa | Vegetable oils | >98% | [35, 37] | |
| | | Carbonates | K ₂ CO ₃ | - | - | [56] | |
| | Na ₂ CO ₃ | | - | - | | | |
| | Acid | Inorganic Acids | H ₂ SO ₄ | Rapeseed oil | 97,50% | [40] | |
| | | | H ₃ PO ₄ | Vegetable oil | - | [42] | |
| | | | HCl | Vegetable oil | - | [42] | |
| | | | BuSn(OH) ₃ | Vegetable oil | - | [42] | |
| | | | Al(OR) ₃ | Vegetable oil | - | [42] | |
| | | Organic Acids | p-Toluenesulfonic acid | Vegetable oil | - | [42] | |
| | | | Sulfonated biochar activated carbon | Esterification of FA | 90-100% | [43] | |
| | | | wood based activated carbon | Esterification of FA | 97% | [43] | |
| heterogeneous | Basic | Alkali earth metal oxides | MgO | Soybean oil | 99% | [44] | |
| | | | | Soybean oil | 98% | [57] | |
| | | | | Sunflower oil | 94% | [58] | |
| | | | CaO | Soybean oil | 95% | [59] | |
| | | | | Jatropha oil | 93% | [37] | |
| | | | | CaO supported on silicate | Sunflower oil | 95% | [60] |
| | | | | Ca(OCH ₃) ₂ (calcium methoxide) | Soybean oil | 98% | [48] |

| | | | | | | | | |
|------|-----------------------------------|-----------------------|---|---|---|--------------|----------|--|
| | | | SrO | Soybean oil | 95% | [45] | | |
| | Alkali metal oxides | | Al ₂ O ₃ /KNO ₃ | Soybean oil | 87% | [61] | | |
| | | | Al ₂ O ₃ /Na/NaOH | Soybean oil | 83% | [62] | | |
| | Transition and mixed metal oxides | | ZnO/Sr(NO ₃) ₂ | Soybean oil | 93% | [63] | | |
| | | | ZnO/Ba | Soybean oil | 95% | [46] | | |
| | | | ZnO/KF | Soybean oil | 87% | [64] | | |
| | | | Li/CaO | Karanja oil | 95% | [65] | | |
| | | | KF/Al ₂ O ₃ | Soybean oil | 99% | [66] | | |
| | Hydrotalcites | | Mg-Al HT | Soybean oil | 80% | [47] | | |
| | | | | Rapeseed oil | 91% | [67] | | |
| | Zeolites | | ETS-10 | Soybean oil | 95% | [33] | | |
| Acid | Mixed metal oxides | | ZnO | Palm oil | 86% | [49] | | |
| | | | | Coconut oil | 78% | | | |
| | | | VOPO ₄ ·2H ₂ O | Soybean oil | 80% | [68] | | |
| | | | ZrO ₂ /WO ₃ ²⁻ | Sunflower oil | 97% | [69] | | |
| | | | ZrO ₂ /SO ₄ ²⁻ | Palm oil | 90% | [49] | | |
| | | | ZrO ₂ /SO ₄ ²⁻ | Coconut oil | 86% | | | |
| | | | Al ₂ O ₃ /PO ₄ ³⁻ | Palm oil | 69% | [70] | | |
| | | | Al ₂ O ₃ /TiO ₂ /ZnO | Rapeseed oil | 94% | [71] | | |
| | | | Al ₂ O ₃ /ZrO ₂ /WO ₃ | Soybean oil | 90% | [50] | | |
| | | | TiO ₂ /SO ₄ ²⁻ | Cottonseed oil | 90% | [72] | | |
| | | Solid HeteropolyAcids | | Cs _x H _{x-3} PW ₁₂ O ₄₀ | Eruca Sativa | 99% | [42] | |
| | | | | H ₃ PW ₁₂ O ₄₀ ·6H ₂ O | Waste cooking oil | 87% | [73] | |
| | | | | H ₃ PW ₁₂ O ₄₀ /K-10 clay | Sunflower oil | 92% | [50] | |
| | | | | | Soybean oil | 95% | | |
| | | | | | Palm oil | 94% | | |
| | | | | | Karanja oil | 93% | | |
| | | | | | Ag _{0.5} H _{2.5} PW ₁₂ O ₄₀ | Jatropha oil | 93% | |
| | | | | | Ag _{0.5} H _{2.5} PW ₁₂ O ₄₀ | Castor oil | 80% | |
| | | | | Zr _{0.7} H _{0.2} PW ₁₂ O ₄₀ /nanotube | Waste cooking oil | 97% | [74] | |
| | | | | H ₃ PW ₁₂ O ₄₀ /ZrO ₂ | Canola oil | 90% | [75] | |
| | | Zeolites | | H-ZSM-5 | beta-keto ester | <30% | [51] | |
| | | | | H-Beta | Soybean oil | 36% | [76] | |
| | | | | La-Beta | beta-keto ester | 80% | [51] | |
| | | | | | Soybean oil | 50% | [76] | |
| | | | | H-Y | beta-keto ester | 85% | [51] | |
| | | | | H-Mordenite | Waste cooking oil | 26% | [52, 77] | |

| | | | | | | |
|-------|---|-------------------------|---------------|-----------------|----------|------|
| | | | | beta-keto ester | 65% | [51] |
| | Metallic complexes | Zn/I ₂ | Soybean oil | 96% | [78] | |
| | | Cyanide-Fe/Zn complexes | Sunflower oil | 97% | [79] | |
| | | | Vegetable oil | 60% | [80] | |
| Other | Enzymatic | immobilized lipase | Vegetable oil | 98% | [53] | |
| | | P. cepacia lipase | Vegetable oil | - | [54] | |
| | Lewis species | ZnCl ₂ | Vegetable oil | - | [55, 81] | |
| | | AlCl ₃ | Vegetable oil | - | | |
| | Non-catalytic supercritical transesterification | None | Vegetable oil | - | [23] | |

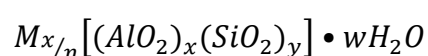
Table 6 - Classification and performances of different catalysts used in transesterification of several vegetable oils

II.5 – General presentation of the Zeolites

The interest in zeolites and their application has not stopped increasing for decades. This can be explained by the exceptional versatility of those particular structures and the almost infinite variety of use they allow. On top of the 34 different species of zeolite minerals (natural), hundreds of structures can be artificially tailor made; this widens the scope of use of those materials.

II.5.1 – Zeolites' structures

Zeolites are crystalline, hydrated aluminosilicates. The general formula representing their structure could be written as follows:



In this general formula we can note that M is the positive counter ion of valence $+n$ which balances the positive charge due to the $x (AlO_2^-)$ groups. The ratio y/x represents the

Silicon-to-Aluminium ratio and is a parameter of paramount importance to describe the zeolite's properties (See Section 1.5.3.1). Eventually, the sum $(x + y)$ represents the total number of tetrahedral in a unit cell of the particular zeolite.

What the general formula does not tell us about is the spatial arrangement of the atoms in the material which confers them very particular properties. The microscopic structure of each zeolite is based on the tetrahedral formed between a small silicon (Si^{4+}) or Aluminum (Al^{3+}) cation and four oxygen atoms. **Figure 6** shows the tetrahedral of oxygen coordinated with silicon and aluminum.

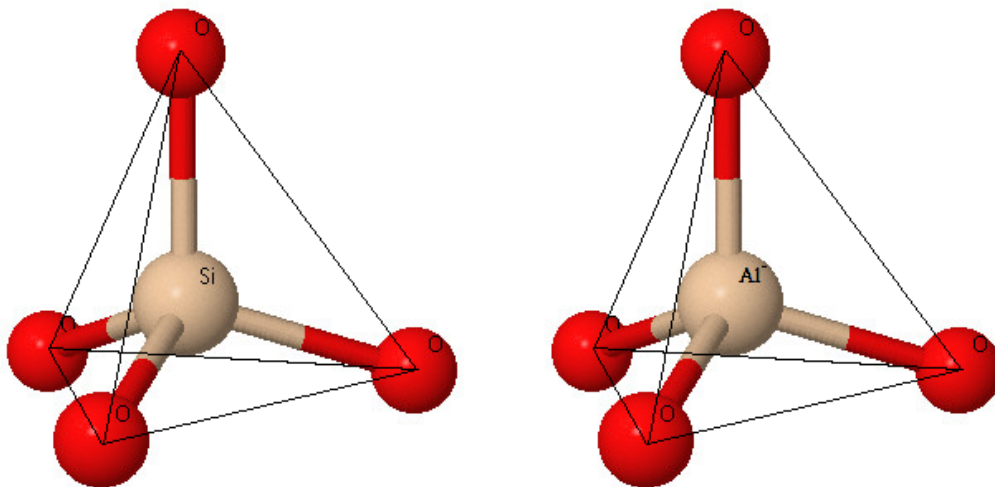


Figure 6 - Tetrahedra of oxygen coordinated with silicon (left) and aluminum (right)

Those tetrahedra are the primary units from which the whole structure is built. They are then gathered in particular structures named Secondary Building Units (SBU) by Meier[82]. Often, those layouts can be described as polyhedral units. For instance, if we consider the example of the α -framework[83], the aluminum and silicon atoms are located

at the vertexes of a truncated cuboctahedron. **Figure 7** shows the truncated octahedron and the truncated cuboctahedron structures in which the vertexes of the polyhedral unit are occupied by the aluminum and silicon atoms; the oxygen atoms are not shown but they are located around the mid-points of the lines joining two tetrahedral sites (Al or Si).

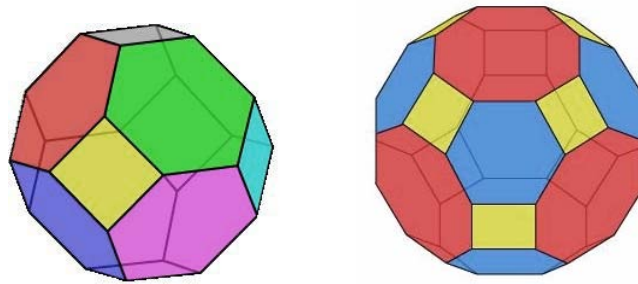


Figure 7 - Examples of a truncated octahedron (left), the β -framework building unit and a truncated cuboctahedron (right), the α -framework building unit[83]

The SBUs are usually used in order to classify the zeolites in groups and are the elementary units from which the topology can be described. It is important to note that in many cases, several SBUs are necessary to describe a particular topology. Thanks to the example of the structure of the A-type zeolite, **Figure 8** illustrates how the assembly of several SBUs can lead to the description the actual spatial structure of the zeolite. The assembly of 8 truncated octahedron units with 8 double four-member rings (D4R) creates a supercage on the middle of the structure of the A-type zeolite.

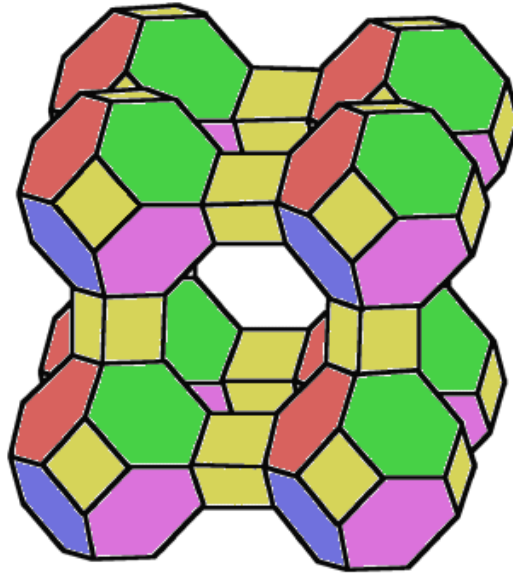


Figure 8 - The structure of the A-type zeolite, assembly of truncated octahedron and double four-member rings (D4R)

Eventually, the zeolite material is the inorganic polymer for which the elementary building blocks are those particular assemblies of SBUs. The great number of SBUs as well as the variety of combinations that can be done from them enable to build an almost infinite number of zeolite structures.

II.5.2 – Applications

The microporous structure (ultraporosity) they exhibit makes them very good adsorbents. **Separation processes** make the most of that property and more particularly gas-gas and gas-vapor separation processes. Kusakabe et al. [84] studied the permeances of several gases through a Y-type zeolite membrane. The great selective adsorption of CO₂ makes this particular use of zeolite an excellent gas-gas separation process spread in the natural gas industry. Modifying the hydration degree of the zeolite was shown to have a strong influence on the permeability to water vapor and every type of gas.[85]

Zeolites can also be used as **molecular sieves** allowing only the molecules that fit in the pores of the zeolite to go through it. An application of this property was implemented by Van Hoof et al. [86] in which organic solvents were dehydrated using NaA-type zeolite.

Molecular confinement is also enabled thanks to the particular structures of the zeolites. The most striking examples are the attempts in the nineties on the site of the Tchernobyl catastrophe [87] and later in 2011 off the coast of Fukushima, Japan, scientists have used quantities of zeolites in order to absorb as much as possible the radioactive pollution by cesium 137.

Another application of the zeolites uses the affinity of the structure towards different cations. It is possible to use zeolites as **ion-exchange** materials in order to remove cations from a solution. The ion exchange takes place between the zeolite and a solution containing cations exhibiting a higher affinity towards the zeolite than the positive counter-ion already in the structure. This property has been used in Part IV for the ion-exchange of the 13-X-type zeolite.

Eventually, zeolites are also used as **catalysts** for a variety of reactions thanks to the high concentration of active acid (Lewis and Brønsted) sites they exhibit. Above all, the interest in using zeolites as catalyst also comes from their specificity towards certain molecules. Indeed, the catalytic activity combined with the restriction in the limit size of the reactants – penetration of the species depending on their size in comparison to the pores' sizes – fosters only certain chemical reactions and thus makes zeolites specific catalysts.

II.5.3 – Properties and structures

The great variety of uses of zeolites is mainly due to particular characteristics of their structures. The activity of a particular zeolite depends on how its properties are tuned.

II.5.3.1 – The Silicon-to-Aluminum (Si/Al) Ratio

The Silicon-to-Aluminum ratio is one of the parameters which govern the zeolite's reactivity.

First, based on the general formula of the zeolite the number of charged entities within the structure is closely related to the amount of aluminum atoms. The more AlO_4^- groups in the zeolite, the more negative charge that needs to be balanced and consequently, the more positive counter-ions. On top of assuring the electro-neutrality of the structure, those positive ions play an important role in the reactivity of the zeolite due to their location outside of the Al-O-Si framework. As explained above, their number is closely related to the number of AlO_4^- units and consequently to the Si/Al ratio. The nature of the counter-ions is also decisive for the reactivity of the zeolite and is tackled in Section I.5.3.2.

Second, if the Silicon-to-Aluminum ratio has a strong influence on the reactivity (and catalytic power) of the zeolite, it also has a huge impact of its affinity towards water. Indeed, the higher Si/Al ratio, the more hydrophobic the zeolite and vice-versa. [88] Decreasing the Si/Al ratio increases the affinity of the zeolite towards water and in the case of a reaction between organic species catalyzed by the acid properties of the zeolite, water molecules are more likely to adsorb on the surface of the zeolite causing a deactivation of the catalyst and thus a drop in conversion. On the other side increasing the Si/Al ratio decreases the affinity

of water towards the catalyst which is more available to interact with organic species and efficiently play the role of acid catalyst for the organic reaction.

II.5.3.2 – The nature of the counter-ion

The more common positive simple counter-ions found in the zeolites are alkali such as Li^+ , Na^+ or K^+ , alkali earth like Mg^{2+} , Ca^{2+} or Ba^{2+} and more rarely elements belonging to other columns of the periodic classification such as La^{3+} . Groups of atoms such as ammonium cation NH_4^+ are also common structures which balance the negative charge of the zeolite framework. However, the nature of the cation determines the acidic catalytic power of the zeolite. The higher Brønsted acidity of a zeolite is obtained when the extraframework cation is hydrogen H^+ .

The determination of the acidity of zeolites has been widely studied and it is now well known that zeolites exhibit both types of acid sites: the proton-donating groups (Brønsted sites) and the electron-accepting functionalities (Lewis sites).[89] If both of them play a role in the reactivity of the zeolite, the Brønsted properties of the catalyst seemed to predominate.

II.5.3.3 – The channel system and the pore size

On the one hand, the empirical chemical formula of the zeolite (Silicon-to-Aluminum ratio and nature of the positive counter-ion) is a decisive parameter influencing the properties of the zeolite. On the other hand, the special layout of the atoms in space is of paramount importance and also governs the reactivity of the zeolite and its catalytic power.

The spatial disposition of the atoms and tetrahedra in the zeolites can be characterized by the dimension D and the pore size of the microporous structure of the zeolite.

The dimension D of the channel system of a zeolite is the number which characterizes if the void channels are intersecting each other or not. This number can go from one to three depending on the type of zeolite. The channels allow molecular diffusion of reactants within the zeolite.

In the one-dimensional (1-D) channel system, the channels do not intersect each other. It is the case of zeolites such as Mordenite or the L-type zeolite (LTL) shown in **Figure 9.a**. The channels are parallel and consequently do not intersect. Molecular diffusion is limited to a single direction in that case. This structure can be pictured by a system of parallel tubes.

The two-dimensional (2-D) channel system exhibits two different channel systems that are linked. In this particular set up, we can either see a main channel system in which channels are parallel and linked thanks to a smaller channel system or two channel systems that cross each other. **Figure 9.b** exhibits the 2-D Mordenite (MOR) framework.

The three-dimensional (3-D) channel system exhibits three intersecting channel systems. Those three channels can either be equivalent in diameter or the diameter can also depend on the direction in the Cartesian coordinates (X, Y, Z). The Faujasite (FAU) structure displayed in **Figure 9.c** is an example of 3-D channel system. In the Faujasite system, the channels in the three directions are equidimensional.

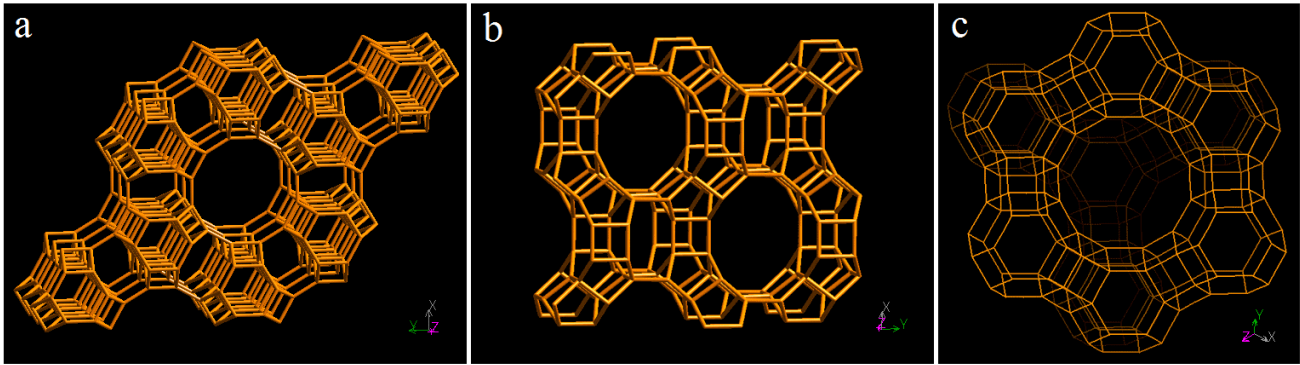


Figure 9 - The three channel system. The 1-D channel system of the L-type zeolite (a). The 2-D channel system of Mordenite (b). The 3-D channel system of Faujasite (c).[90]

Whatever dimension of the channel system, the size of those channels is the parameter that will determine if a particular molecule (reactant or not) can enter in the lattice of the zeolite or will only be able to stay outside of the framework and react on the external surface of the zeolite. The diameter of a channel is determined by the type of structure and the number of oxygen atoms that are on the edge of the aperture ring. Basing the determination on the number of oxygen atoms is an approximation since the temperature and kinetic energies of a diffusive molecule can affect whether or not a molecule will be able to enter the structure or not. However, this assumption is valid in general.

III. *Determination of the Acid Value of the Sesame oil*

III.1- Introduction

Due to major differences in their compositions, all the vegetable oils do not have the same efficiency regarding the production of biofuels. As Ramos & al. showed[91], the fatty acid composition of the crude oil has a huge impact on the physical properties of the derived biofuel which has to meet governmental requirements.

The nature of the fatty acids contained in the crude oil is one of the most important parameter but the amount of Free Fatty Acids (FFA) in the crude oil is also a parameter of paramount importance. Indeed, if the FFA contents of two crude oils are very different, the chemical processes that will produce biodiesel from them will be radically different. As detailed in Section V.2.1.1, it is much more profitable to implement the transesterification step of a vegetable oil with a low FFA content in basic catalysis whereas the same step will be done with an acidic catalyst for an oil with a high FFA content.

Thus, determining the amount of FFA helped us justifying the use of an acidic catalyst. In order to do so, it is possible to measure the Acidic Value (AV) also called Acidic Number (N) of the oil. The AV corresponds to the weight of potassium hydroxide (KOH) needed to neutralize the FFA present in 1 gram of oil. Thanks to this value and knowing the nature and quantity of the fatty acids in the oil, we can obtain an accurate value of the FFA content in wt%.

III.2- Experimental

III.2.1 - Experimental device

In order to determine the Acid Value of the sesame oil, we followed the colorimetric titration of the Free Fatty Acids (FFA) contained in the oil by a solution of KOH in the presence of phenolphthalein as an indicator[92, 93].

The reactions could not take place in aqueous solution due to the immiscibility of water and oil. Consequently, all the solutions prepared were 95% vol. ethanol-based solutions.

The titration solution was a potassium hydroxide (KOH) solution at 10^{-1} mol.L⁻¹ in ethanol (95% vol.). An ethanolic solution of phenolphthalein at 10 g.L⁻¹ was also prepared.

Common values of Acid values of crude sesame oil were reported to be between 1 and 4 mg. Knowing that, 10 g of sesame oil were dosed[93]. To ensure a good miscibility between the different reactants, 100mL of a solvent mixture 1/1 vol. of 95% vol. ethanol and diethyl ether were added to the sesame oil sample. Due to the particular hazardous properties and volatilities of the compound used, both preparation of the solution and titration were carried out under the hood and with containers sealed as much as possible.

Figure 10 describes the experimental devices used.

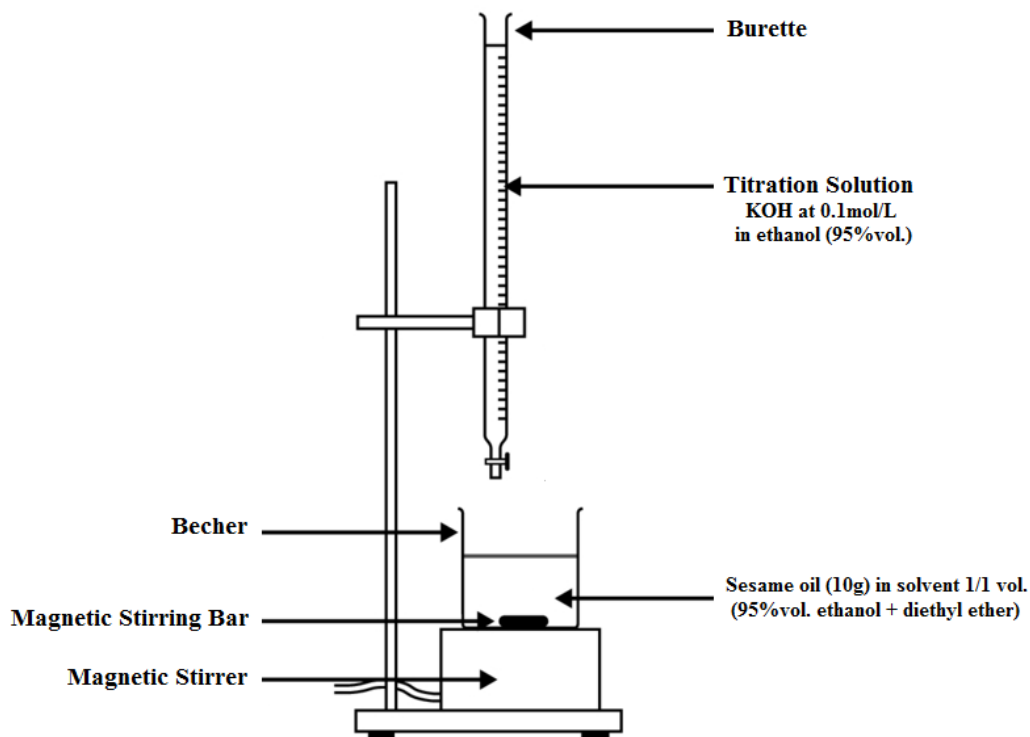


Figure 10 – Experimental set up for the determination of the AV of the sesame oil by titration with KOH in ethanol

III.2.2 - Chemical reaction and location of the equivalence

The dosage is carried out in the presence of phenolphthalein. This colored indicator is colorless when $0 < \text{pH} < 8.2$ and turns pink when $8.2 < \text{pH} < 12$ [94](**Figure 11**).

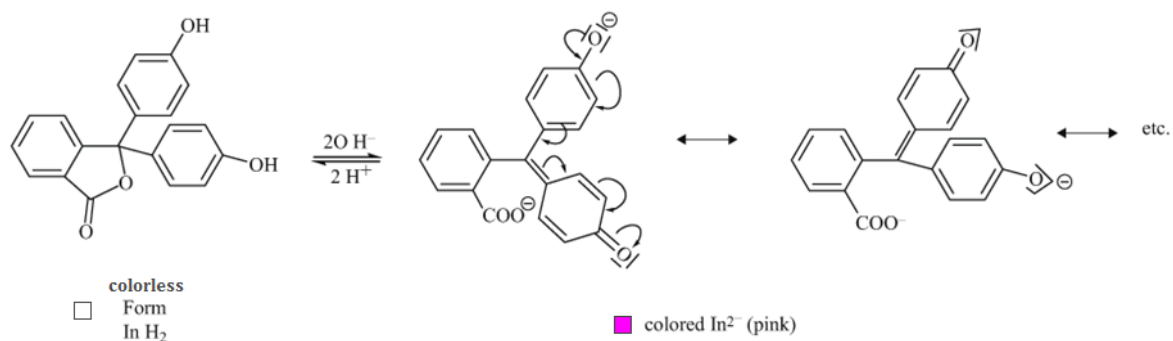


Figure 11 - Different forms of phenolphthalein depending on the value of pH

The free fatty acids are derived from the triglycerides present in the oil (See Part III). Thus, the main Fatty Acids dosed in this experiment are of the same nature as the FA present in the triglycerides and analyzed by GC-MS. **Table 7** summarizes the main FA found in the triglycerides structure after analyzing the oil and gives the pKa for each of them[95].

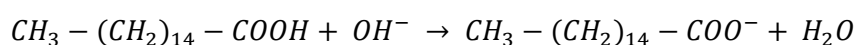
| Acid | Notation | pKa |
|----------|----------|-------|
| Palmitic | C 16:0 | 4,78 |
| Stearic | C 18:0 | 10,15 |
| Oleic | C 18:1 | 9,85 |
| Linoleic | C 18:2 | 9,24 |

Table 7 - pKa of the Fatty Acids found in sesame oil [95]

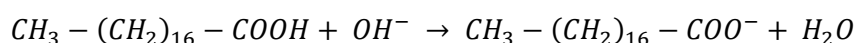
The values of the pKa of the four main FA found in the oil allowed us to classify those acids among the weak acids. Since the titration was done with a strong base, the equivalence should be expected for basic values of pH. The color change zone for phenolphthalein is located at pH = 8.2 which enabled us to do the dosage using phenolphthalein as an indicator.

The four chemical reactions taking place during the titration were:

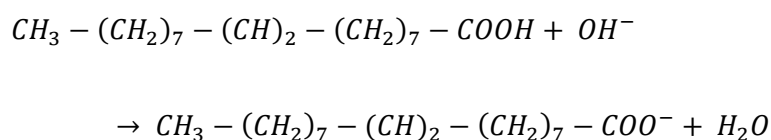
Palmitic acid:



Stearic acid:



Oleic acid:



Linoleic acid:

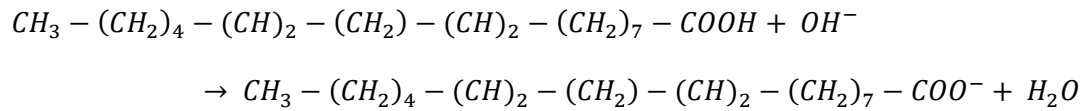


Figure 12 shows the color evolution of the titration medium around the equivalence.

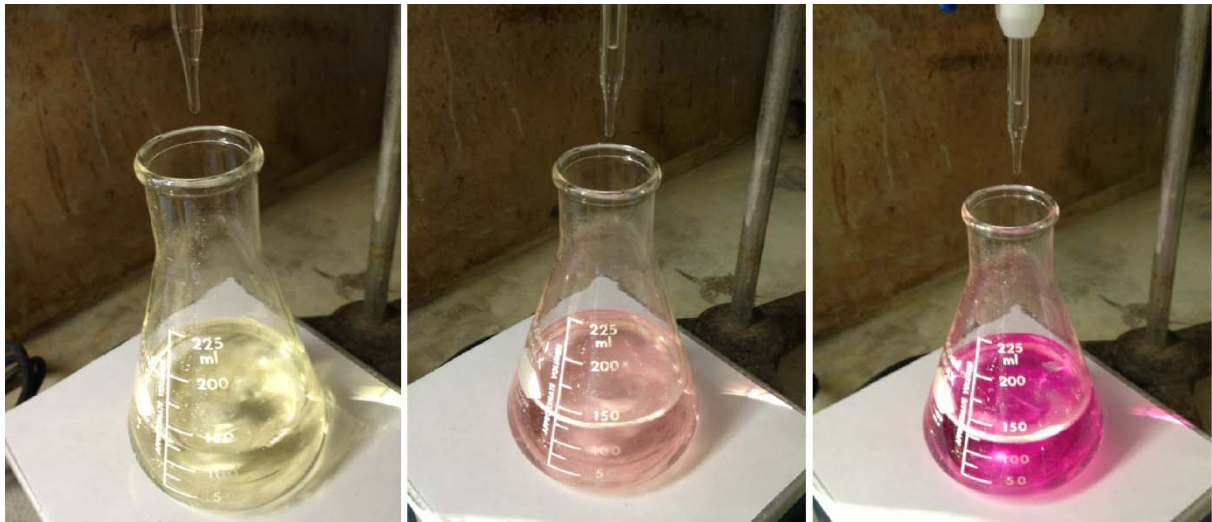


Figure 12 - Evolution of the coloration of the solution around the equivalence (Left: before the equivalence; middle: equivalence; right: after the equivalence)

III.3 - Results

The equivalent volume of the solution of KOH at at $10^{-1} \text{ mol.L}^{-1}$ poured was $V_{eq} = 2.45$ mL. The weight of KOH necessary to neutralize 1g of oil is then given by:

$$AV[mg] = \frac{M[mg.mol^{-1}].C[mol.L^{-1}].V_{eq}[L]}{m_{oil}[g]} = \frac{56100 . 10^{-1} . 2.45 . 10^{-3}}{10} = 1.374 \frac{mg}{g}$$

The acid value found seemed in good agreement with the values found for sesame oil in the literature.

III.4 – Conclusions

This analysis allowed us to know how much FFA the initial sesame oil contained. The result found was in good agreement with the common AV for sesame oil found in the literature. From the number found, it was possible to determine how much of each of the four main FA we needed to add to the sesame oil in order to recreate the high FFA content Jatropha oil. The method of calculation of the quantity of each FFA can be found in Appendix B.

IV. *Determination of the Fatty Acid Composition of the Sesame oil – Recreation of artificial Jatropha oil*

IV.1 – Introduction – Necessity of the FA analysis

The nature of the Fatty Acids (FA) of Sesame oil can be easily found in the literature.[96, 97] The main fatty acids present in the oil (as Free Fatty Acids and as part of the structure of the triglycerides) are Palmitic Acid (C 16:0), Stearic Acid (C 18:0), Oleic Acid (C 18:1 cis 9) and Linoleic Acid (C 18:2 cis 9, cis 12). Their skeletal formulas can be found on

Figure 13.

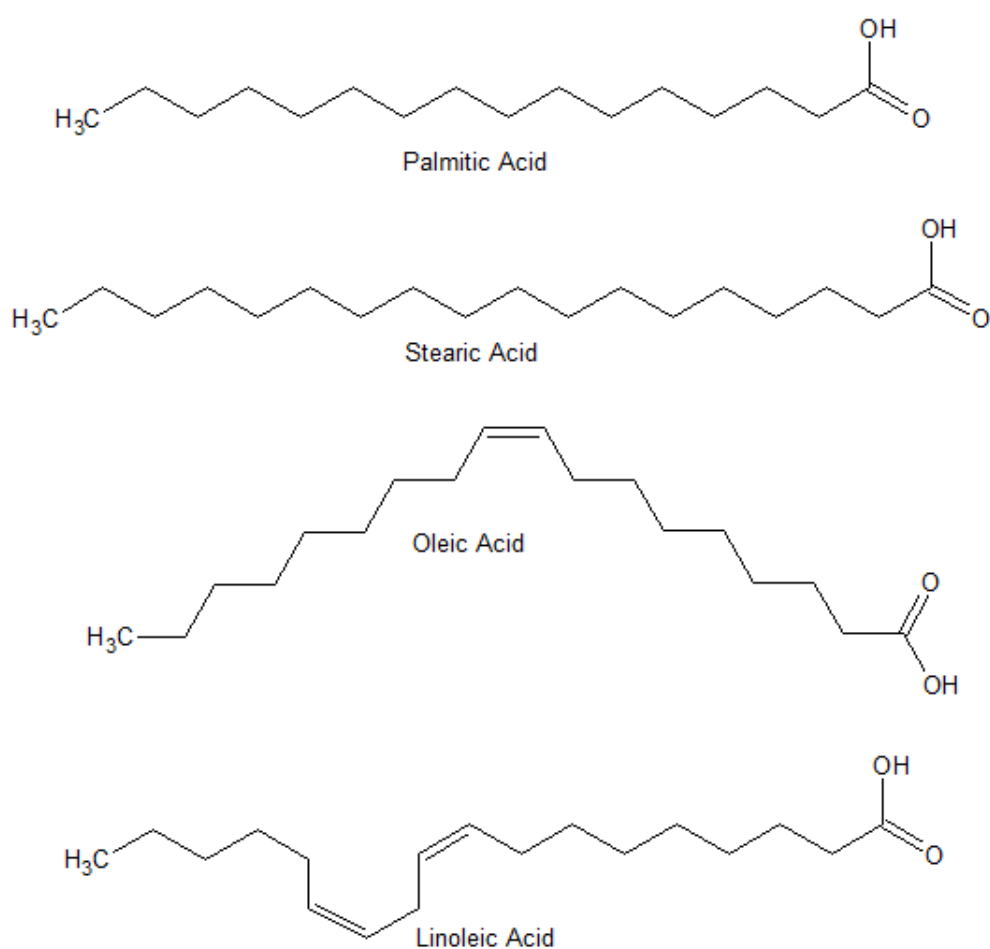


Figure 13 - Skeletal formula of the four main FA found in Sesame oil

Hwang [96] gathers the results on several studies [98-100] about different sesame oils' compositions. **Table 8** presents the FA composition of sesame oil. All together, those four FA represent more than 98% of the FA contained in the oil. Thus, we can reasonably neglect the other FA in the oil and only consider those four FA.

| | O'Connor & Herb [98] | Codex Alimentarius [99] | Cultivated [100] | Wild [100] | Crocker [97] |
|----------------------------------|-------------------------|----------------------------|---------------------|----------------|-----------------|
| Myristic (C14:0) | ND-0,1 | < 0,5 | | | |
| Palmitic (C16 :0) | 7,9 - 12 | 7,0 - 12 | 9,0 - 9,6 | 8,2 - 12,7 | 8 - 12 |
| Palmitoleic (C16:1) | 0,1 - 0,2 | < 0,5 | 0,1 - 0,2 | 0,2 - 0,3 | |
| Heptadecanoic (C17:0) | ND - 0,2 | | | | |
| Heptadecenoic (C17:1) | ND - 0,2 | | | | |
| Stearic (C18:0) | 4,8 - 6,1 | 3,5 - 6,0 | 5,6 - 6,4 | 5,6 - 9,1 | 4 - 7 |
| Oleic (C18:1) | 35,9 - 42,3 | 35 - 50 | 41,9 - 45,2 | 34,3 - 48,1 | 35 - 45 |
| Linoleic (C18:2) | 41,5 - 47,9 | 35 - 50 | 38,0 - 41,6 | 33,2 - 48,4 | 37 - 48 |
| Linolenic (C18:3) | 0,3 - 0,4 | < 1,0 | 0,5 - 0,6 | 0,6 - 0,9 | |
| Arachidic (C20:0) | 0,3 - 0,6 | < 1,0 | 0,3 | 0,2 - 0,8 | |
| Eicosenoic (C20:1) | ND - 0,3 | < 0,5 | 0,1 | 0,1 | |
| Behenic (C22:0) | ND - 0,3 | < 1,0 | 0,1 | 0,1 | |
| Lignoceric (C24:0) | ND - 0,3 | | trace | trace | |

Table 8 - Sesame oil composition (in % FA)[96, 97]

Although their nature is well known, the percentage of each of those four main FA can vary dramatically from a sample to another. [96, 98-100] Moreover, the Sesame oil (obtained from Kevala international LLC) used as a starting point for our experiments did not have a perfectly well-known Fatty Acid (FA) composition. As a consequence, an analysis of the nature and the amount of each FA present in the oil was necessary before going any further in its use.

IV.2 – Theory – Methods of analysis of the FA composition of vegetable oils

Several methods exist to determine the FA composition of an oil. The most common methods are based on separation followed by analysis of the chemical compounds. The separation step is usually a chromatographic step. At the end of this step, the different components have been separated depending on their molecular weight, their affinity with the stationary phase, their volatility... The analysis of the components of the original mixture can be done thanks to different kind of devices.

IV.2.1 – The Transesterification step

Prior to the separation/analysis steps, all the most common methods require a transesterification step. This first mandatory step aims at chemically transforming the triglycerides (TG) of the oil thanks to the transesterification reaction. This enables to decrease the viscosity and increase the volatility of the mixture.

Indeed, the Fatty Acid Methyl Esters (FAME) formed by the reaction have much shorter molecular weights than the initial oil mostly composed of triglycerides. The breakage of the triglycerides into small-chained molecules allows the use of chromatographic devices to separate the different compounds at relatively low temperatures. Using directly the triglycerides in the columns would have three main drawbacks:

- Damage of the column due to the high temperature necessary to evaporate the triglycerides;
- Fouling - and eventually clogging - of the device because of the residues of TG along the column;

- Damage of the structure of the TG due to the high temperatures. Loss of accuracy of the final result of the chromatography (detection of other chemicals formed during the thermolysis of the initial compounds).

IV.2.2 – The separation of the compounds

Once the mixture of FAME obtained, compounds have to be separated from one another for further analysis. The main method used for that matter is the Gas Chromatography (GC).

The literature[101] shows another efficient method to directly analyze a mixture of TG without any pretreatment (transesterification) step: the Reverse-Phase High-Performance Liquid Chromatography (RP-HPLC) followed by a Refractive Index (RI) detector. This method gives accurate results but its implementation becomes very delicate for complex mixtures of TG.

The method chosen here was a good compromise between accuracy and relatively easy implementation. After the required transesterification step with methanol, the mixture of FAMEs in hexane underwent a GC. The main parameters to take into account to choose the characteristics of the column are the physical interactions between the three phases of the column.

Indeed, the individual partition (or adsorption equilibrium properties) determines the rate at which each component will move through the system[102]. It also determines the degree of separation of the different compounds in the sample. It is also required to make sure no

chemical interaction or transformation take place between the different phases inside the device.

The main criterion for the choice of the carrier gas (mobile phase) is the non-interaction with the components and column material (stationary phase). Hydrogen H₂ is a common choice due to its low viscosity and high diffusion coefficient.

IV.2.3 – The analysis of the compounds

Each component of the initial FAME mixture has been separated. The goal of the following and last step is to analyze the nature and the amount of each component. Two main technologies are commonly used for that purpose:

- The Flame Ionization detector (FID)[103];
- The Mass spectroscopy analysis (MS)[104].

Both methods are equivalent in terms of accuracy. However, the FID is not as inconvenient for an online analysis directly in a production chain whereas MS detectors are ideal candidates for continuous analysis. Moreover, MS offers a higher sensibility than FID which allows to analyze much diluted samples.

IV.3 – Experimental

The method chosen for the FA analysis of the oil was a Gas Chromatography followed by a Mass Spectroscopy (GC-MS).

In a first step, the triglycerides of the crude Sesame oil were transesterified in alkaline medium using methanol. At the end of this first step Fatty Acids Methyl Esters (FAME) were obtained and ready to be analyzed in a second step by GC-MS.

IV.3.1 – Transesterification in alkaline medium

The triglycerides are the main components of the Sesame oil we are using. Each triglyceride is composed by a back-bone of glycerol to which are attached three FA. The transesterification step with methanol (MeOH) aims at breaking apart each triglyceride into three FAMEs and a glycerol molecule. A balance of the reaction is given on **Figure 14**.

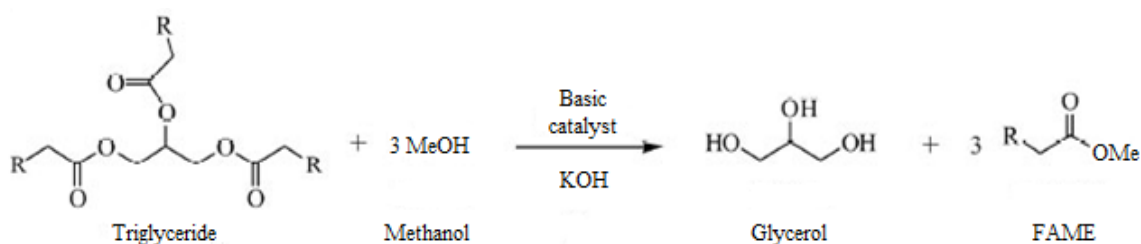
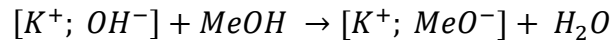


Figure 14 - Overall FAME production reaction from triglycerides

Prior to the any reaction, both the oil and the methanol were dried using Sodium Sulfate (Na₂SO₄). This white solid is a powerful desiccant when used at moderate temperatures. It forms with the moisture contained in solutions an hydrate Na₂SO₄·10H₂O by capturing ten water molecules. This compound does not interact with the other components of the oil under those conditions.

Then, an alkaline catalytic solution was prepared by dissolution of 5.6 g of potassium hydroxide (KOH) in 100 ml of dry methanol. The concentration of the methanolic solution

obtained was 1 mol.L⁻¹ of KOH. This allowed the formation of potassium methoxide [K⁺; MeO⁻] given by the following equilibrium:



All the reactants were separately brought to a temperature of 60°C before being put together in the preheated reactor. This temperature avoids the vaporization of the methanol ($T_{\text{methanol}}^{\text{eb}} = 64.7^\circ\text{C}$) and enables a good reaction yield [105].

The transesterification reaction was carried out with an oil to methanol weight ratio of 1:10 (12 g of dry oil, 120 ml of dry methanol) and catalyzed by adding 1.5 ml of the methanolic potassium hydroxide solution to the medium. The transesterification reaction was implemented in the Parr reactor for 30 minutes with an overhead stirrer running at 1000 rpms.

Once the reaction done, the media was rapidly cooled down to room temperature thanks to a bath of cold water.

Contrary to the expected observation, a single-phased system was observed. Indeed, instead of observing a bottom phase mainly composed of glycerol and most of the unreacted methanol separated from an upper layer containing the FAME and a small amount of alcohol, we observed only one phase containing all the unreacted chemicals and the products. This is due to the very high alcohol to oil ratio used for the experiment. The huge excess of methanol increases the solubility of the glycerol. This could be an issue at a large scale since it makes the separation steps more delicate and it can favor the reverse reaction between glycerol and FAME which would lead to the formation of mono-, di- and triglycerides. [39, 106] However for our analytic purposes in that section we needed to focus

our attention on the esterification reaction itself and not specially its yield. The conversion was not determined but the expected values in those conditions are roughly 97%[105].

IV.3.2 – Post-treatment of the transesterified oil

The post-treatment steps were described in details by Braithwaite and Stock [102] and by the Health Services of the Indian Ministry of Health[92] .

The FAMEs were extracted by a mixture of hexane isomers due to their non-polarity and thus, their affinity with non-polar solvents. The high alcohol to oil ratio allows the reaction to be almost complete so the amount of mono-, di- and triglycerides extracted by the hexane phase was neglected. The mixture of hexane isomers was obtained from Pharmco-Aaper (Brookfield, CT).

The washing step with water aimed at removing the unreacted methanol and the glycerol formed during the transesterification. The content of the reactor was poured in a separating funnel. The reactor was rinsed with 40mL of hexane which was introduced in the separating funnel. Due to long carbonated chains, the FAME and remaining triglycerides are non-polar. Thus they pass into the upper hexane layer. The bottom layer contains the polar compounds such as the glycerol, the methanol, the potassium methoxide and the potential soaps formed by saponification of the Free Fatty Acids (FFA) initially present in the oil.

The upper layer was sucked off the funnel and washed with 100 ml of deionized water to remove the traces of polar compounds. The non-polar phase underwent this process two more times with 40mL of water and the polar phase was washed again with 60mL of hexane.

In the end, the solution of FAME in hexane is dried with sodium sulfate and a part of the solvent is evaporated on a water bath at 68°C. It is important not to raise the temperature too high in order not to damage the FAME. A temperature of 68°C enabled to evaporate part of the hexane without impacting on the structure of the FAME.

A 50mL of solution of FAME (Approximately 5% to 10%wt.[92]) in hexane are kept for the GC-MS chromatography.

IV.3.3 – Gas Chromatography and Mass Spectroscopy analysis (GC-MS)

The sample was analyzed twice with different degrees of dilution. The first run was done with the sample right after the extraction steps with hexane. The first chromatogram showed FAMEs concentration that were too high to be determined accurately and needed to be decreased. Thus, the sample underwent a dilution by 100.

The percentage of each FA found with that method was the actual percentage of this particular FA both as a Free Fatty Acid (FFA) and within the triglyceride structures. It is important to state that we made the assumption that the molar fraction of each FA in the FFA part of the oil was the same as the molar fraction of the same FA within the triglyceride structures.

This assumption can be justified by the mechanism of formation of the FFA within the oil by chemical decomposition of the triglycerides[107]. Over time, the FFA content of the oil increases due to the hydrolysis, photolysis and thermolysis of the triglycerides. Indeed, even if the kinetics of those reactions is slow (characteristic time in months), it does affect the composition of the oil. (See Section V.2.1.6).

Considering the FA composition of the FFA and the FA composition of the triglycerides as equivalent was a justified assumption.

IV.3.4 – Recreation of the artificial Jatropha oil

The literature [37, 97, 103] reports the nature and the FA profile of the triglycerides contained in Jatropha oil. The results are gathered in **Table 9**. Jatropha oil contains in great majority the same four as the ones found in Sesame oil and we can observe the results presented by the different sources are consistent with each other. We based our reflection on the FA profile described by Akbar et al.[103].

| | Crocker[97] | Akbar et al.[103] | Endalew[37] |
|-------------------------|--------------------|--------------------------|--------------------|
| Palmitic (C16:0) | 11 to 16 | 14,2 | 14,1 - 15,3 |
| Stearic (C18:0) | 6 to 15 | 7 | 3,7 - 9,8 |
| Oleic (C18:1) | 34 to 45 | 44,7 | 34,3 - 45,8 |
| Linoleic (C18:2) | 30 to 50 | 32,8 | 29,0 - 44,2 |

Table 9 - FA profile of the triglycerides in Jatropha oil

The purpose was to recreate artificial Jatropha oil that would have the same acid value as the one reported in the literature (See Part II) and which would also have a composition of FFA qualitatively and quantitatively similar to the one observed in natural Jatropha oil.

Once the molar percentage of each FA in the sesame oil known thanks to the GC-MC analysis, it was possible to recreate artificial Jatropha oil by adding the right amount of each FA to the original sesame oil to finally end up with an oil whose AV and FFA profile were exactly equal to the ones of natural Jatropha oil.

Technical grade Palmitic, Stearic and Linoleic acids were bought from Sigma Aldrich. Technical grade Oleic acid was bought from Consolidated Chemical.

IV.4 – Results

IV.4.1 – GC-MS Analysis

The Gas Chromatograph used for the separation of the different compounds of our samples was the 7890A GC using automated splitless injection (Agilent G4513A, 7693A auto-sampler injector) from Agilent Technologies. The Mass Spectrometer for the detection of the compounds was the 5975C MS equipped with a triple-axis detector from Agilent Technologies as well. The software interface and databank were also provided by the same company.

Helium was the carrier gas maintained at a flow rate of $1 \text{ mL}\cdot\text{min}^{-1}$. The column used was Stabilwax[®] Cat#10623 (30 m x 0.25 mm x 0.25 μm) with polyethylene glycol as the stationary phase. Column temperature was held at 125°C for 1 min, elevated first at $10^\circ\text{C}\cdot\text{min}^{-1}$ for 5 min to 175°C and then at $6^\circ\text{C}\cdot\text{min}^{-1}$ to reach 250°C when all FAMES of interest had been eluted.

As it can be seen on **Figure 15**, the chromatogram obtained while analyzing the non-diluted sample does not allow any relevant conclusion regarding its FAME composition. After a dilution by 100, the sample underwent a new GC-MS analysis in the exact same conditions. The chromatogram obtained for the diluted sample (presented on **Figure 16**) exhibits clear peaks which match the theoretical composition of the oil.

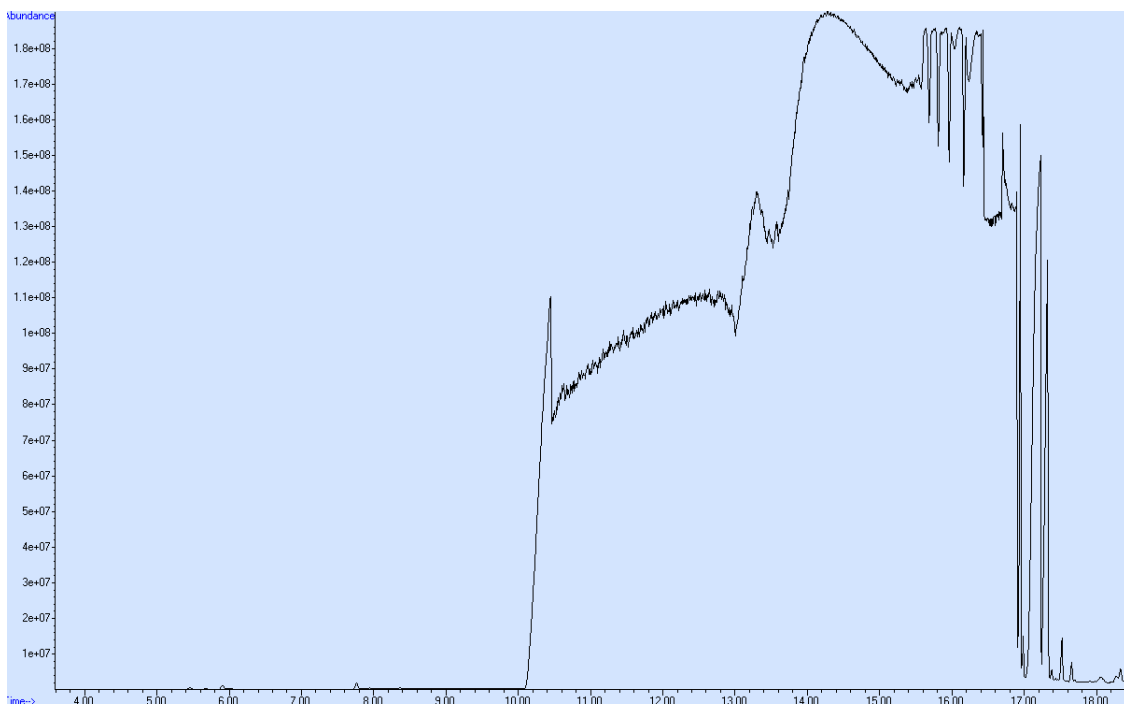


Figure 15 - Non-diluted sample (chromatogram)

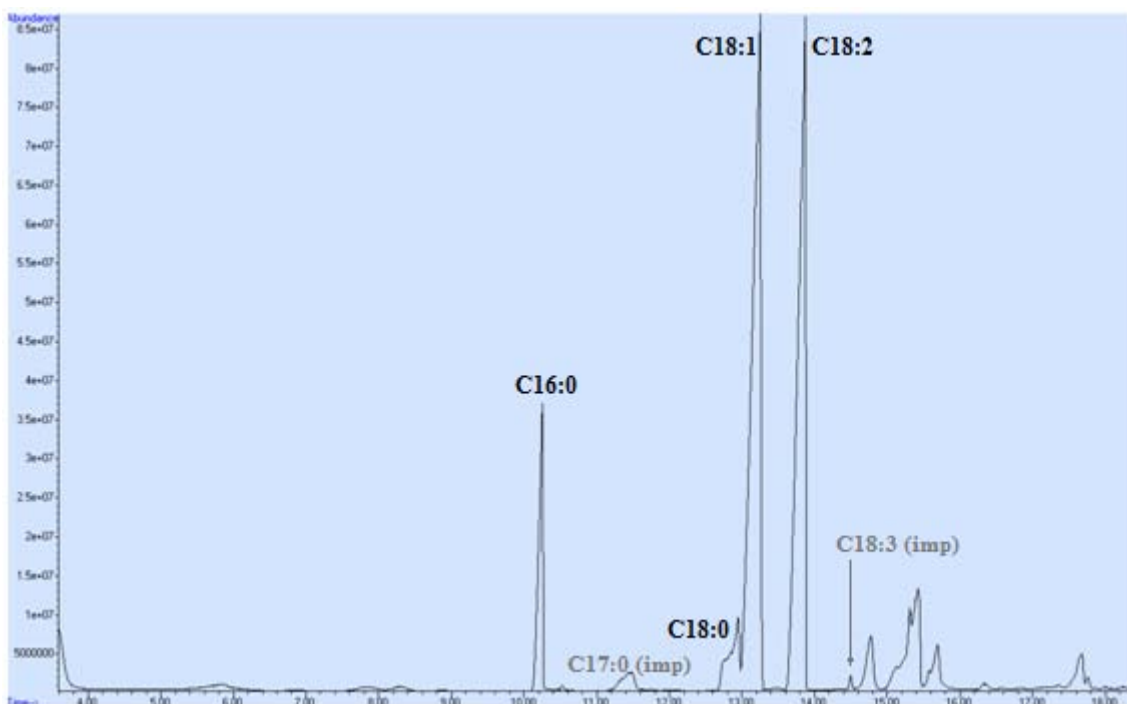


Figure 16 - 100-time diluted sample (chromatogram)

The retention times of the separated compounds contained in the sample match the retention times of the four FAMES found in the databank of the CG-MS software (OpenLAB CDS ChemStation Edition, Agilent Technologies). The area under each peak was proportional

to the amount of each compound present in the sample. Thanks to the calibration curve and the area of each peak, we were able to obtain the percentage of each FAME considering that the Palmitic, Stearic, Oleic and Linoleic FAMES were the only FAMES present in the oil. The results are gathered in **Table 10**. The details of the determination of the data presented in **Table 10** thanks to the calibration values of the column and the chromatogram (**Figure 16**) can be found in Appendix A.

| | Molar Fraction | Quantity of matter ($\times 10^{-5}$) [mol] |
|------------------|----------------|---|
| Palmitic (C16:0) | 0.0721 | 0.1802 |
| Stearic (C18:0) | 0.1021 | 0.2553 |
| Oleic (C18:1) | 0.3446 | 0.8616 |
| Linoleic (C18:2) | 0.4812 | 1.2029 |
| Total | 1 | 2.5 |

Table 10 - Results of the GC-MS on the diluted sample of sesame oil - Quantity of matter [mol] of each FAME in 1 gram of oil

This analysis permitted us to check that the percentage of each FAME was within the ranges of values found in the literature for sesame oils [97-100].

On the chromatogram shown in **Figure 16**, other smaller peaks were visible. Comparing the retention times of those peaks with the databank of the software allowed us to determine the possible nature of the minor compounds detected. Those compounds are indicated as impurities (imp) on **Figure 16**. At $t \approx 11.2$ minutes, 14-methyl Palmitic acid (C17:0) was detected. Also, around $t \approx 14.45$ minutes, traces of Linolenic acid (C18:3) were detected.

IV.4.2 – Amounts of FAs added to the Sesame oil

Thanks to the AV of the sesame oil that we determined in Part II ($AV_{\text{sesame}} = 1.374 \text{ mg}_{\text{KOH}}/\text{g}_{\text{oil}}$ i.e. $2.5 \times 10^{-5} \text{ mole}_{\text{FFA}}/\text{g}_{\text{oil}}$) and with the results of the GC-MS analysis, the quantity of matter of each of the four main FA was computed.

The AV found in the literature for the Jatropha oil was $28 \text{ mg}_{\text{KOH}}/\text{g}_{\text{oil}}$ [37] which corresponds to 5×10^{-4} mole of KOH at the equivalence. Thus, it was deduced that 1g of Jatropha oil contained 5×10^{-4} mole of FFA. We assumed that only the four main FA were present in the oil (i.e. the sum of their four molar fractions was equal to 1). Using the FA profile described by Akbar et al.[103], the molar fraction of each FA in the Jatropha oil was computed.

Molar fraction in the FFA fraction and quantity of matter [mol] of each FA are gathered in **Table 11** for both Sesame and Jatropha oil.

| | Sesame oil | | Jatropha oil [103] | |
|-------------------------|----------------|---|--------------------|---|
| | Molar Fraction | Quantity of matter ($\times 10^{-5}$) [mol] | Molar fraction | Quantity of matter ($\times 10^{-4}$) [mol] |
| Palmitic (C16:0) | 0.0721 | 0.1802 | 0.143 | 0.715 |
| Stearic (C18:0) | 0.1021 | 0.2553 | 0.071 | 0.355 |
| Oleic (C18:1) | 0.3446 | 0.8616 | 0.453 | 2.265 |
| Linoleic (C18:2) | 0.4812 | 1.2029 | 0.333 | 1.665 |
| Total | 1 | 2.5 | 1 | 5 |

Table 11 - Amount of each FA in the FFA fraction of the Jatropha oil

Using Sesame oil as a starting point, the amounts of each FA which needed to be added to the oil were computed to reach a composition close to the Jatropha oil composition.

For each Fatty Acid FA_i, the amount N_{FA_i} of FA_i that needed to be added to the sesame oil was computed according to the relation below:

$$x_{FA_i,J} = \frac{N_{FA_i} + N_{FA_i,S}}{\sum_i N_{FA_i,S} + \sum_i N_{FA_i}}$$

With $x_{FA_i,J}$ the molar fraction of the particular FA_i in the Jatropha oil, Note that $\sum_i x_{FA_i,J} = 1$

N_{FA_i} the quantity of matter [mol] of the particular FA_i that has to be added to 1g of oil,

$N_{FA_i,S}$ the quantity of matter [mol] of the particular FA_i in 1g of the Sesame oil.

The amounts N_{FA} of each of the four FA that were added per gram of sesame oil are presented in **Table 12**. The detail of the calculations can be found in Appendix B. We can easily verify that the total amount of FFA in the recreated oil (FA added to the oil on the one hand, and FA already present in the sesame oil on the other hand) equals the total amount of FFA in the Jatropha oil taken as a reference[103].

| | Quantity of matter (x10 ⁻⁵) [mol] | Weight added [mg] |
|-------------------------|---|-------------------|
| Palmitic (C16:0) | 6.97 | 17.87 |
| Stearic (C18:0) | 3.29 | 9.36 |
| Oleic (C18:1) | 21.79 | 61.54 |
| Linoleic (C18:2) | 15.45 | 43.33 |
| Total | 47.5 | 132.1 |

Table 12 - Quantity of matter and weight of each FA added per gram of sesame oil

IV.5 – Conclusions

The important amounts of Fatty Acids added to the initial sesame oil justify this process. Indeed, those quantities allow us to better visualize the important impact of the high Free Fatty Acid content than the only knowledge of the Acid Value of Jatropha oil. It

was also important to measure with accuracy the natures and exact amounts of the Fatty Acids contained in the oil since, on top of having an influence on the kinetics of reaction of transesterification, the nature and quantity of the different Fatty Acid Esters were reported to have a direct impact on the quality of the fuel itself[108, 109].

The oil obtained at the end of that step had a FFA content almost identical to the one of the genuine Jatropha oil. This sought characteristic enabled us to carry on our work and to tackle the transesterification reactions.

V. *Ion-exchange process on the 13-X zeolite*

V.1 – Introduction

In the past three decades, the industry has widened the field of application of the zeolites. Their catalytic properties are now combined with their high ion-exchange power. This property can not only be used to remove particular ions from waste water (such as metal ions) but also enables to modify the structure of the zeolite itself in order to impart a particular chemical or physical property to it.

In this project, the Brønsted acidity of the zeolites was used for catalytic purposes and consequently, it was mandatory to obtain the hydrogen-form of each zeolite. That is why ion-exchange processes were implemented.

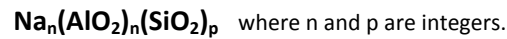
V.1.1 – necessity of the ion-exchange step

Every zeolite structure is composed of two different elements which determine its physical and chemical properties:

- A fixed basis made of the aluminum, silica and oxygen atoms linked with covalent bonds. In a way, this fixed structure can be considered as the “skeleton” of the zeolite. It is important to notice that this microporous molecular structure of the zeolites is made of aluminum oxide groups and silicon dioxide groups commonly known as silica SiO_2 . Since the valence structure of aluminum is $3s^2 3p^1$, the aluminum oxide group is negatively charged which makes the entire structure negatively charged. To counterbalance those charges, positive species have to be present in the structure.

- The counter-cation, often a sodium, potassium, calcium or hydrogen atom which role is to compensate the negative charge of the structure.

For instance, the general structure of a dry zeolite in a sodium form can be written as:



The Brønsted acidity of the zeolite comes mostly from the presence of hydrogen atoms in its structure. Among the five different zeolites used, only three (Y-type, Mordenite and Beta) were known to be in hydrogen form. The positive counter-ion in the 13-X-typezeolite was Na^+ . In order to enhance the Brønsted acidity of those three solids, an ion-exchange step was necessary.

V.1.2 – ion exchange processes

The ion exchange process can be done following several different paths. It can either be a countercurrent operation in which the zeolite and the solution move countercurrent to each other in a stagewise manner. It can also be a crossflow process where the zeolite powder goes through several fresh batches of the solution which contains the cation to exchange in the zeolite structure.

Both processes are illustrated in **Figure 17** and **Figure 18**[110]. It can clearly be seen on **figure 18** that the zeolite encounters several batches of fresh exchange solution whose concentration $N_{T_0 v_0}$ is constant. The nomenclature presented below **Figure 17** and **Figure 18** was also developed by Howard S. Sherry[110].

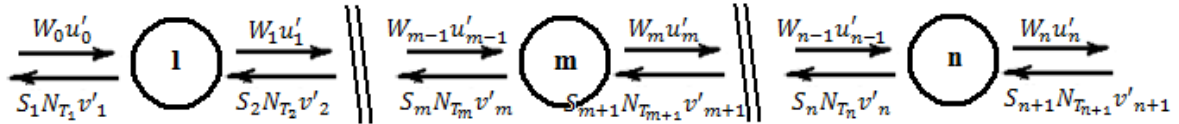


Figure 17 - Flow diagram for countercurrent operation

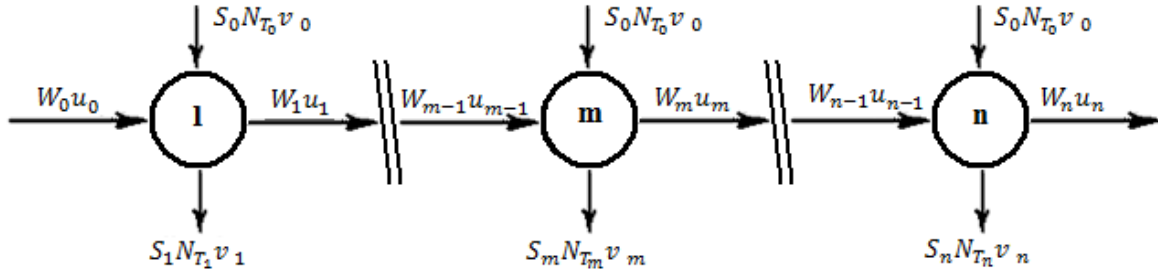


Figure 18 - Flow diagram for crossflow operation [111]

With

- $C = N_T v$ = In batch process, number of equivalent of salt in solution fed into a stage
- $C' = N_T v'$ = In continuous process, number of equivalent of salt in solution flowing per time unit
- m = index of the stage in a multistage process
- n = index of the last stage in a multistage process
- N_T = total normality
- $Q = Wu$ = in batch process, number of equivalent of zeolite fed into a stage
- $Q' = Wu'$ = in continuous process, equivalent of zeolite flowing per time unit
- S = fraction of the interesting ion in solution
- u = in batch process, weight (in g) of dry zeolite entering a stage
- u' = in continuous process, weight (in g) of dry zeolite flowing per time unit
- v = in batch process, volume (in L) of solution entering a stage
- v' = in continuous process, volume (in L) of solution flowing per time unit

Here and in most laboratory operations, we operated following the crossflow operation[111].

Depending on the later use of the zeolite, different counter-cation can be inserted in the structure of the zeolite by ion-exchange processes.

Uni-univalent exchanges can be made by replacing a cation by another cation. For instance, it is the case when the initial sodium, potassium or any other single-charge cation

is replaced by another single-charge cation such as lithium, silver, etc in a one-for-one process.

Di-univalent exchanges can also be implemented. It occurs for example when a single charge sodium cation Na^+ is replaced by a double charge calcium cation Ca^{2+} in a two-for-one process. Eventually, rare earth ion-exchange processes can be done on certain types of zeolites like X and Y-type zeolites. They involve multiple charged ions such as lanthanum cations La^{3+} [111]. **Figure 19** illustrates the three examples of ion-exchange processes on zeolites.

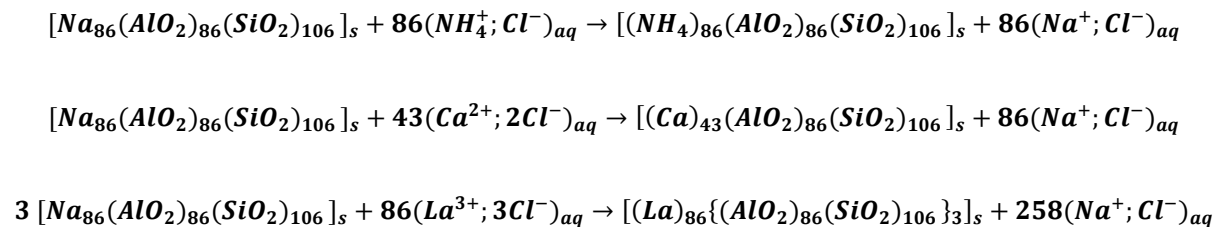
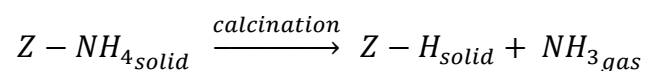


Figure 19 - Balances of the three ion-exchange processes on zeolite 13X

V.1.3 – Post treatment of the ion-exchanged zeolite

In some cases the fresh ion-exchanged solid cannot be used right away and need a last step to be catalytically efficient. Indeed, it is the case when a hydrogen form of the zeolite is needed. The main process to obtain the H-form of the zeolite is to pass by an intermediate form where the counter-cation is an ammonium anion NH_4^+ . Eventually, a calcination step allow the ammonia removal, the counter-cation becomes H^+ and an gaseous ammonia NH_3 comes out of the solid zeolite. The reaction path can be written as follows:

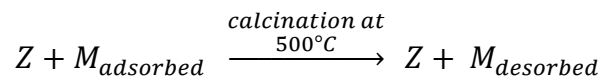


Where Z stands for the zeolite structure

V.2 – Experimental

V.2.1 – Pretreatment

First and foremost, species such as water, oxygen, nitrogen or other molecules can be adsorbed at the surface and inside the pores of the zeolites. To avoid any perturbation during the ion exchange process, the zeolites were pretreated by calcinations in an oven at 500°C for 3 hours. We have:



Where Z stands for the zeolite structure and M, any species initially adsorbed in the zeolite.

The zeolite was not preconditioned in its sodium form by making the zeolite go through several batches of Sodium Chloride (NaCl) since we assumed that 100% of the counter-cations present in the structure were sodium ions. This hypothesis was confirmed later on thanks to the EDX-Analysis [112] (See Section IV.3.3).

V.2.2 – Ion-exchange step

A solution of ammonium chloride (NH₄Cl) at $C_{NH_4Cl} = 1 \text{ mol} \cdot L^{-1}$ was obtained by dissolving 53.45g of anhydrous NH₄Cl in 1000mL of deionized water. This solution was used as the exchanged solution.

Working with zeolites in solution requires mild conditions since zeolites' structures are quite sensitive to extreme pH values[113]. When a pH of 4 or lower is reached, the crystalline lattice can be partially or even totally perturbed due to the fact that aluminum atoms are solubilized as aluminum hydrates[114]. It is also important to mention that each

solution was brought to 60°C and maintained at that temperature during the entire time of the ion-exchange process. Those constant mild conditions were kept up not only to ensure an isothermal process but also to avoid damaging the zeolite structure by reaching high temperatures.

Then, 10g of the freshly calcined zeolite were introduced in a 2000mL 3-neck flask and fitted with a reflux condenser. 1000mL of the NH_4Cl solution were introduced in the flask. This first batch was heated at 65°C with continuous mechanic agitation during 40 minutes. A diagram of the experimental device is provided in **Figure 20**.

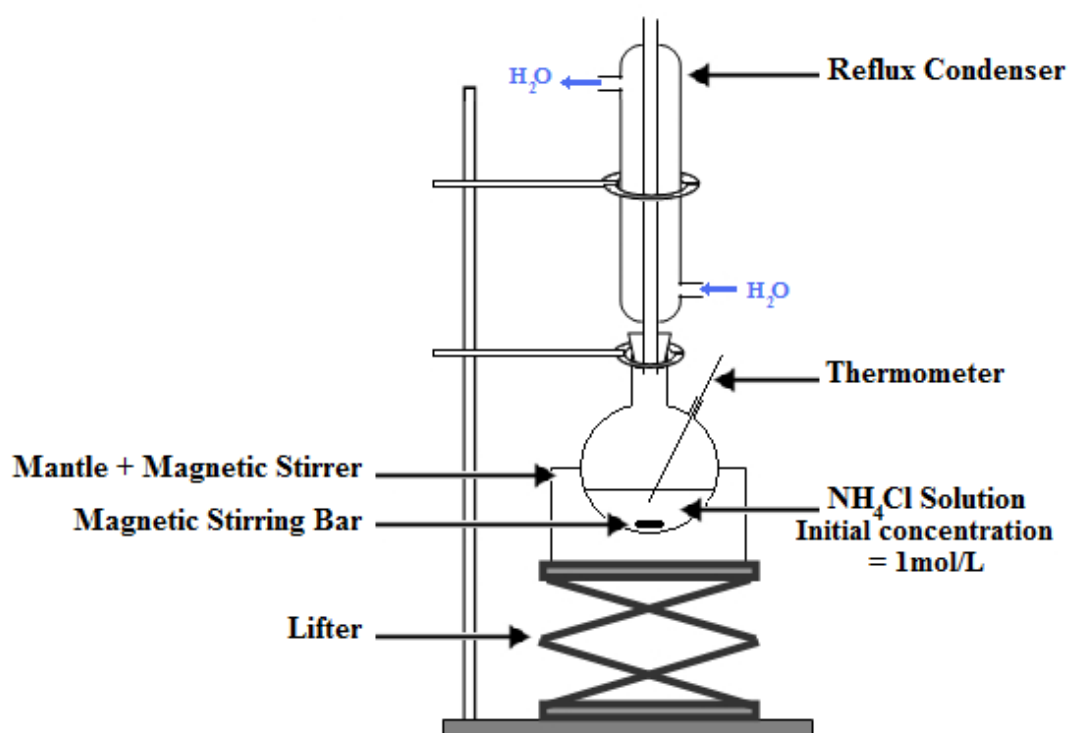
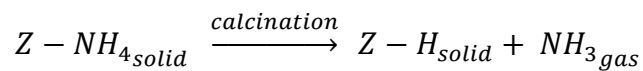


Figure 20 – Ion-Exchange set up using a solution of Ammonium Chloride (NH_4Cl) at $1\text{mol}\cdot\text{L}^{-1}$ at a constant temperature of 65°C for 40 minutes

After 40 minutes of reaction, the solution was filtered with a sintered glass funnel. The filtrate was kept for further analysis and the powder was used one more time in another ion-exchange step. The zeolite powder underwent four identical ion-exchange steps, every

time with a freshly made solution of (NH₄Cl) at $C_{NH_4Cl} = 1 \text{ mol. L}^{-1}$. The filtrate of each step was kept for further analysis (See Section IV.3.1).

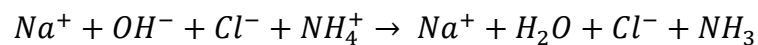
After the four batches, half of the powder obtained by the final filtration is calcined at 500°C for 3 hours and kept in a close dry hermetic container to be used as the acidic catalyst in the esterification/transesterification step (See Part V). This calcination step leads to the H-form of the zeolite according to the following balance:



V.2.3 – Conductimetric analysis

V.2.3.a – Theory

The concentration in ammonium cations (NH₄⁺) can be determined by several methods including conductimetric dosage by a sodium hydroxide solution whose concentration is perfectly known. The reaction which takes place in the medium is:



The conductivity of a solution containing p ions is related to the molar ionic conductivity of each ion with the formula:

$$\sigma = \sum_{i=1}^p \lambda_i \cdot [X_i]$$

Where σ is the conductivity of the solution [S.m⁻¹];

λ_i is the molar ionic conductivity of the ion i [S.m²/mol]

$[X_i]$ is the molar concentration of the ion i [mol.m⁻³]

In conductimetry, it is essential that the concentration of the analyzed solution does not exceed $10^{-2} \text{ mol.L}^{-1}$.

V.2.3.b – Analysis

In order to make sure the ion-exchange took place, the ammonium cations remaining in solution were dosed by a solution of sodium hydroxide (NaOH) at $4 \cdot 10^{-3} \text{ mol.L}^{-1}$. The dosage is followed with a conductivity meter (WTW Portable pH/Conductivity Tester, Model DUO-60. Model 16467-116).

As explained in the previous section, the concentration of the different species in solution should not exceed $10^{-2} \text{ mol.L}^{-1}$. Consequently, before being dosed, the exchanged solution of ammonium chloride was diluted by 100.

The experimental device used for the dosage is presented in **Figure 21**.

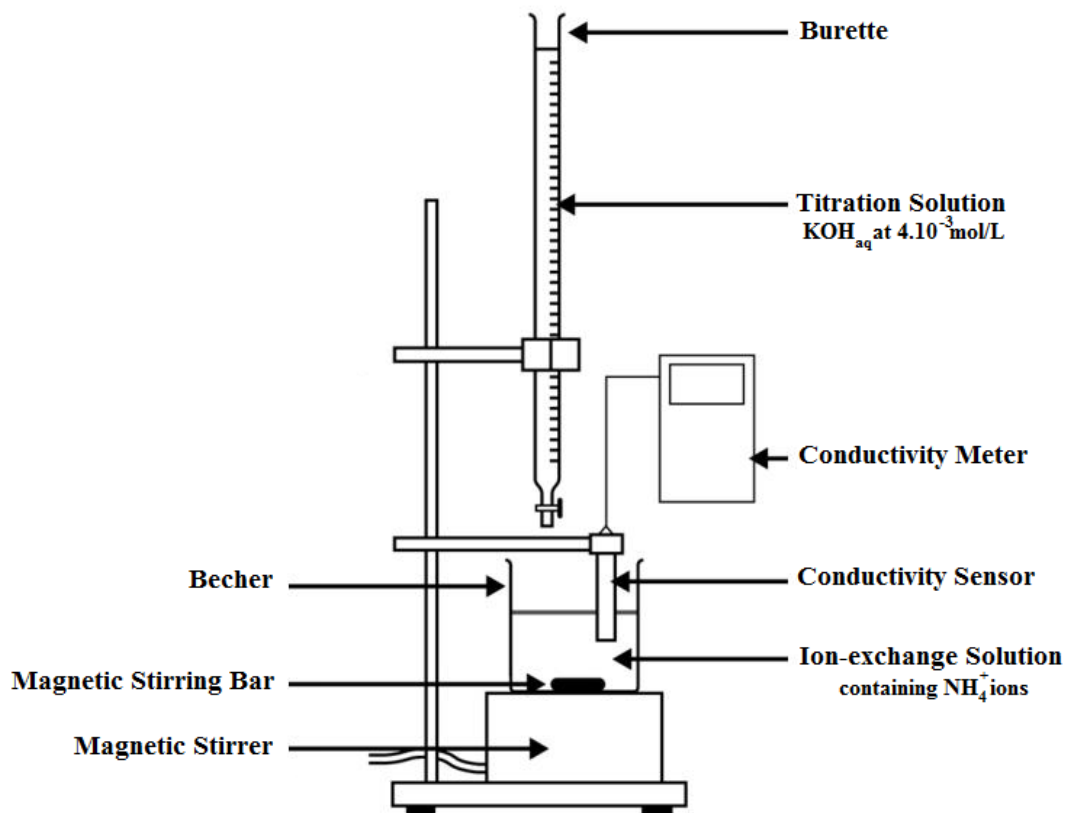
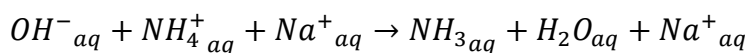


Figure 21 – Experimental set up for the titration of the ion-exchange solutions (containing NH_4^+) by an aqueous solution of Potassium Hydroxide (KOH) at $4.10^{-3} \text{ mol.L}^{-1}$

At the beginning of the addition of the NaOH solution, the conductivity of the solution is supposed to slightly decrease from its initial value since the hydroxide and ammonium ions react together to form water and ammonia, two uncharged species following the balance:



Charged species → *Uncharged species*

Table 13 gives the molar ionic conductivity of the different ions present in the solution. Since $\lambda_{\text{OH}^-} > \lambda_{\text{NH}_4^+} > \lambda_{\text{Na}^+}$, the disappearance of the hydroxide and ammonium

ions surpasses the addition of sodium ions to the medium which confirm the decrease in conductivity at the beginning.

| Ion | OH ⁻ | NH ₄ ⁺ | Na ⁺ | Cl ⁻ | H ₃ O ⁺ |
|--|-----------------|------------------------------|-----------------|-----------------|-------------------------------|
| Molar ionic conductivity λ in S.m ² /mol (x10 ⁻⁴) | 198,6 | 73,5 | 50,1 | 76,3 | 349,8 |

Table 13 - Molar ionic conductivity of some useful ions

After the equivalence, all the ammonium cations have disappeared to form ammonia. The conductivity of the solution starts increasing since the addition of ions is not anymore compensated by the reaction.

Plotting the conductivity with respect to the volume of NaOH solution poured will lead to a V-shaped curve whose slope-break point gives us the equivalent volume V_{eq} .

$$\text{Then, we have } C_{OH^-} \cdot V_{eq} = C_{NH_4^+} \cdot V_{NH_4^+}$$

$$\rightarrow C_{NH_4^+} = \frac{C_{OH^-} \cdot V_{eq}}{V_{NH_4^+}} \quad \text{with } C_{OH^-} = 4 \cdot 10^{-3} \text{ mol} \cdot L^{-1}$$

$$V_{NH_4^+} = 50 \text{ mL}$$

Eventually, the concentration $C_{exchanged}$ of the initial exchange solution is obtained multiplying the concentration $C_{NH_4^+}$ by 100 since the exchanged solution was diluted by 100 prior to the dosage.

For each zeolite used, the plots of the conductivity with respect to the volume of the sodium hydroxide (NaOH) at $4 \cdot 10^{-3} \text{ mol} \cdot L^{-1}$ are presented below.

V.2.4 – EDX spectroscopy analysis

V.2.4.a – Theory

The conductimetric analysis of the batches of exchange solution provided good qualitative results and the trend of the decrease in exchange with respect to the number of the batch was relevant. However, the results obtained thanks to that method were not quantitatively accurate (See Section IV.3). A second set of analysis was done in order to conclude about the efficiency of the ion-exchange process. This second batch of analysis aimed at focusing on the product of the ion-exchange process itself – the zeolite – rather than on the exchange solution.

The elemental analysis of each sample was made using an Energy-Dispersive X-ray (EDX) spectrometer (AMRAY Scanning electron microscope model 1610 Turbo). This technique enables to determine the raw chemical composition of a powder based on the response of the sample to X-ray excitation. This powerful analysis method is not efficient for elements whose atomic number is lower than 12 (Carbon) which did not affect our measurements.

V.2.4.b – Analysis

The EDX analysis was initially done in order to overcome the lack of accuracy of the conductimetric analysis on the 13-X zeolite (See Section IV.3). Then, the EDX analysis was used as a tool to know the elemental composition of the ZSM-5 zeolite and thus to conclude about the kind of treatment was necessary to obtain its hydrogen form. In other words, for the ZSM-5 zeolite, the interest of using that method was double:

- Know the exact composition of the zeolite to know (or check) the Si/Al ratio and the nature of the positive counter-ion;
- Apply to appropriate kind of treatment in order to obtain the H-form of the zeolite;
- In the case of an ion-exchange process, check if the composition after treatment was in agreement with the expected product.

For the sake of accuracy, several measurements were done on each sample. The different analyses done on each sample were consistent. Complete reports can be found in Appendix C.

V.3 – Results

V.3.1 – Conductimetric analysis

Since the ion-exchange process was done 4 times, the dosage of the exchange solution was done 4 times too. **Figure 22.a** to **Figure 22.d** shows the four different plots of σ (μS) = f [V(mL)] for each waste solution. It is important to note that only for the two first titrations, the concentration of the solution of sodium hydroxide was $1 \cdot 10^{-3} \text{mol} \cdot \text{L}^{-1}$ and not $4 \cdot 10^{-3} \text{mol} \cdot \text{L}^{-1}$ as it is for all the following experiments. That can explain the very slow increase of conductivity after the equivalence for dosage 1 and 2 in comparison to the followings.

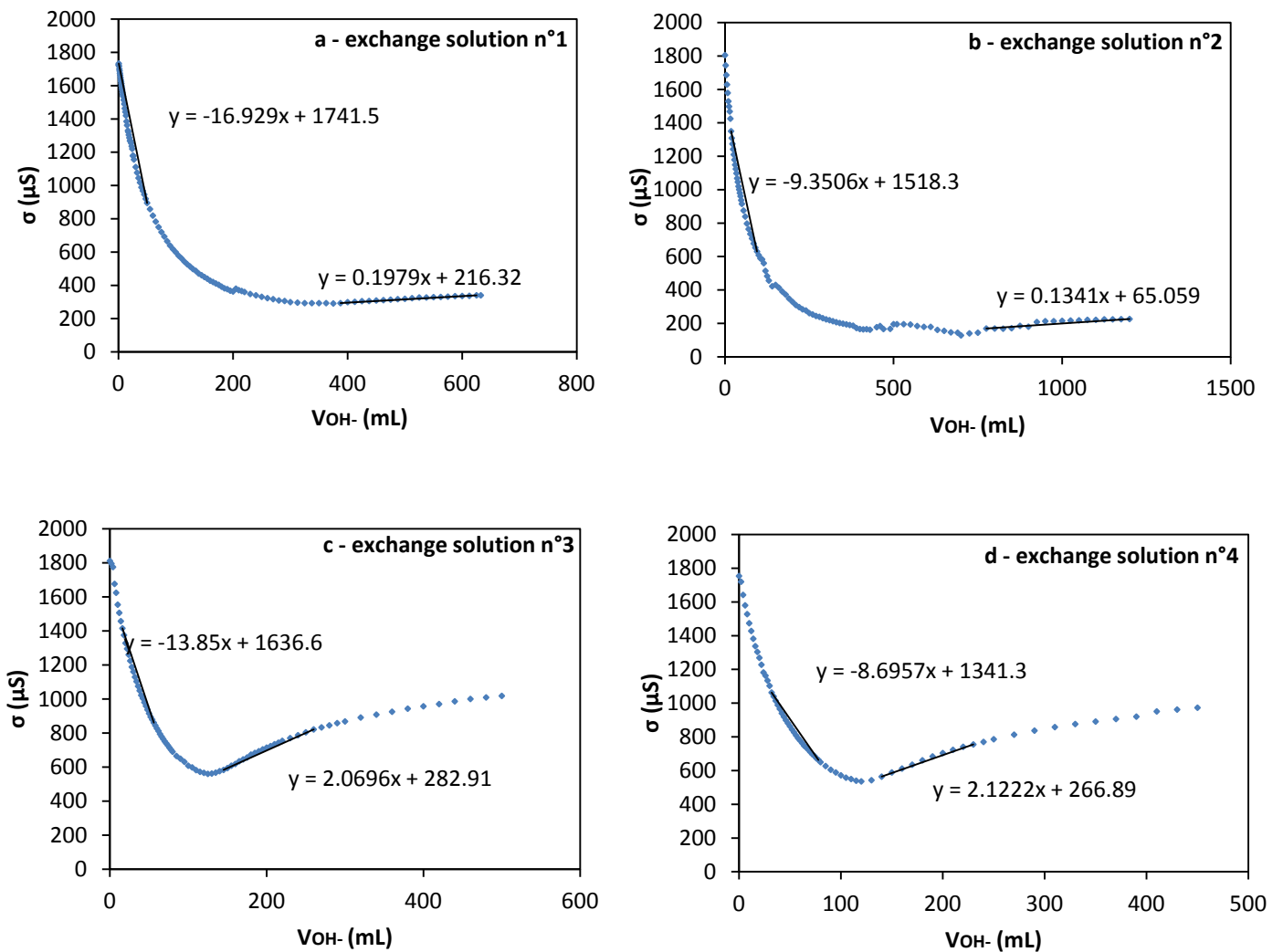


Figure 22 - Dosages of NH_4^+ by OH^- followed by conductimetry

For each dosage linear regressions were done on both parts of the V-shaped curve. The abscissa of the intersection point of the two linear regression lines give us the equivalent volume of sodium hydroxide poured. **Table 14** gathers the results of the four dosages for the ion-exchange process made on 13-X zeolite. **Figure 23** shows the amount of ammonium ion exchanged during the four experiments. We verified that the quantity of matter exchanged decreased gradually with the number of the experiment.

| Experiment n° | C _{OH-} [mol/L] | V _{eq} [mL] | mol of NH ₄ ⁺ in solution before ion-exchange | mol of NH ₄ ⁺ in solution after ion-exchange | mol of NH ₄ ⁺ exchanged [mol] |
|-----------------------|--------------------------|----------------------|---|--|---|
| 1 | 10 ⁻³ | 89,052 | 1 | 0,1781 | 0,8219 |
| 2 | 10 ⁻³ | 153,22 | 1 | 0,3064 | 0,693561 |
| 3 | 4. 10 ⁻³ | 85,033 | 1 | 0,6807 | 0,31973677 |
| 4 | 4. 10 ⁻³ | 99,32 | 1 | 0,7945 | 0,205 |
| Total exchanged [mol] | | | | | 2,04019777 |

Table 14 - Results of the dosages of the NH₄⁺ ions with OH⁻

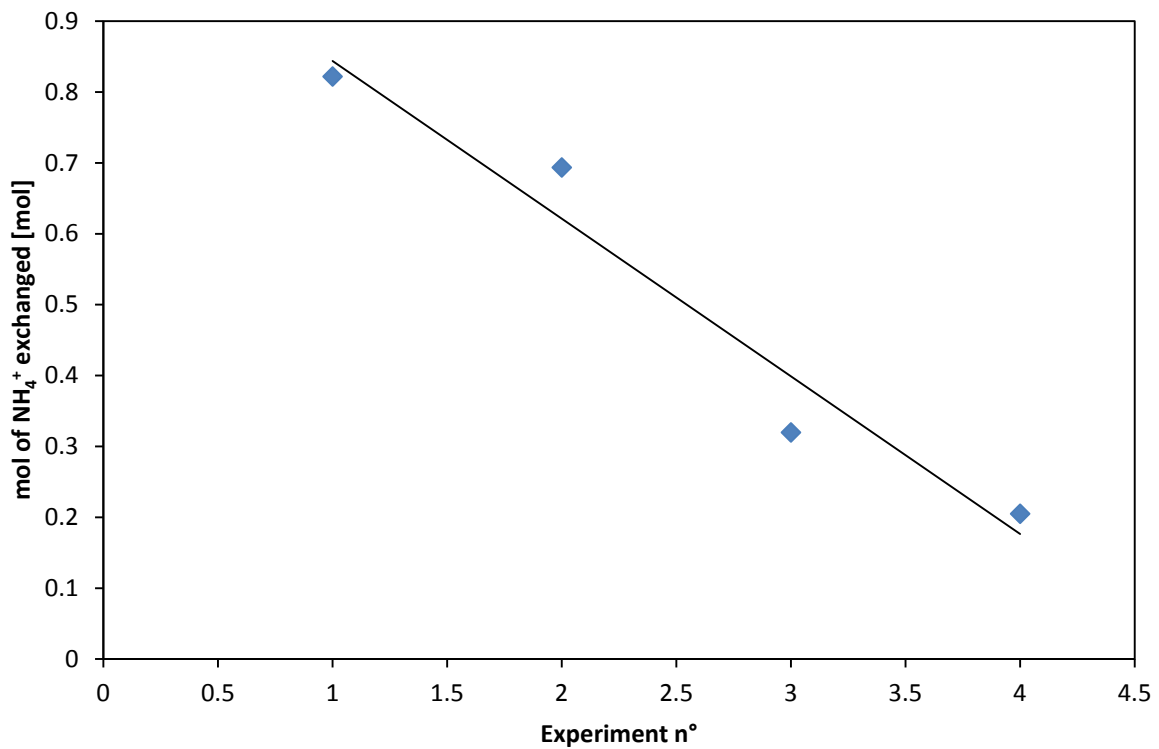


Figure 23 – Number of moles of NH₄⁺ exchanged vs. experiment n°

The literature shows several examples of ion-exchange processes involving zeolites [112], [115], [116]. The main purpose of those processes is to remove ammonium cations from waste water. Models of adsorption of ammonium cations can be developed introducing the Langmuir and Freundlich adsorption models. The isotherms of Langmuir and Freundlich are respectively given by the following expressions:

- Isotherm of Langmuir:

$$q_e = \frac{q_0 \cdot C_e \cdot b}{(1 + b \cdot C_e)}$$

- Isotherm of Freundlich:

$$q_e = K \cdot C_e^{1/n}$$

Where - C_e is the equilibrium concentration of NH_4^+ in the solution in mol.L^{-1} ;

- C_0 is the initial concentration of NH_4^+ in the solution in mol.L^{-1} ;

- q_e is the equilibrium adsorption capacity in mol.L^{-1} (assumed to be $C_0 - C_e$);

- q_0 is the maximal (monolayer) adsorption capacity in mol.L^{-1} ;

- b is the coefficient of Langmuir isotherm in L.mol^{-1} ;

- K and n are the coefficients of Freundlich isotherm.

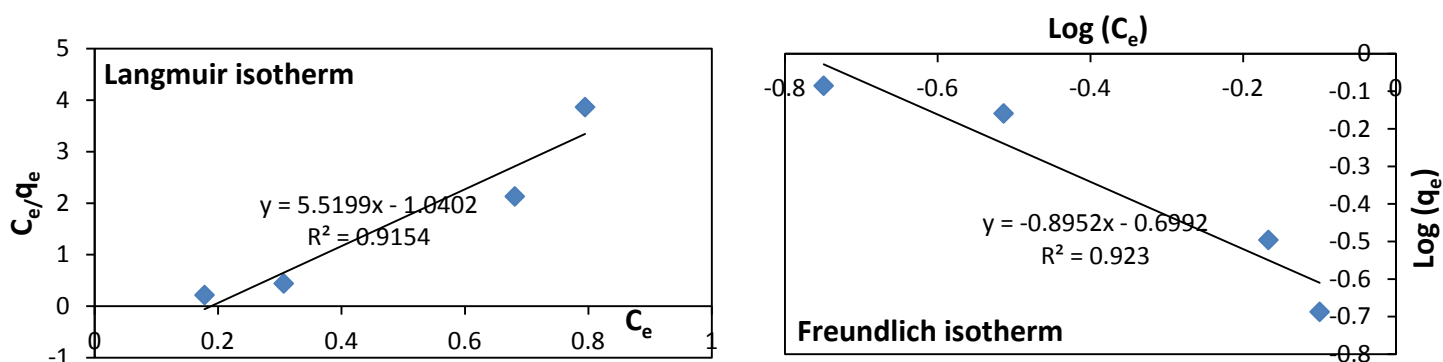


Figure 24 - Langmuir and Freundlich adsorption models applied to our ion-exchange process

Both models were applied to our case (with $C_0 = 1 \text{ mol.L}^{-1}$) and the plots can be found on **Figure 24**. It can be easily seen that neither of the two models fits to our case. This can be explained by two factors. First, the zeolite was reused for each experiment and consequently, its exchange capacity was decreasing as we saw on **Figure 23**. Langmuir and Freundlich models work in the case of the study of a fresh zeolite contacting solutions of various known concentration[112], [115].

The second argument that can be brought up here is the quality of the zeolite initially used. Poor washing steps during the manufacturing steps might have left traces of unknown products. Those traces will be studied later on (IV.3.2).

As **Table 14** shows, 2.04 moles of ions NH_4^+ were exchanged according to the titrations. Thanks to the chemical formula $\text{Na}_{86}(\text{AlO}_2)_{86}(\text{SiO}_2)_{106}$ of the compound provided by Sigma-Aldrich, it is possible to determine the maximum number of moles of sodium exchangeable in 10 grams of the dry zeolite.

$$n_{\text{exchangeable}} = 86 \cdot \frac{m_{\text{Na}_{86}(\text{AlO}_2)_{86}(\text{SiO}_2)_{106}}}{M_{\text{Na}_{86}(\text{AlO}_2)_{86}(\text{SiO}_2)_{106}}} = 86 \cdot \frac{10 \text{ [g]}}{13412 \text{ [g} \cdot \text{mol}^{-1}]} = 0.064 \text{ moles of Na}$$

This result is contradictory with the total amount of NH_4^+ which reacted during the ion-exchange process. Indeed, the titrations lead to a quantity of ion exchanged 31 times higher than the actual exchangeable amount of ions. This can be explained by the fact that another reaction involving ammonium ions could have taken place in the solution and disturb the measurement. Another set of analysis was done to explain the apparent irrelevance of the previous result.

V.3.2 – Basicity of the untreated zeolite 13-X - Washing step and pH variations

After the inconsistency of the previous analysis, analyses were done on the untreated zeolite in order to understand which other reaction could have taken place between the ammonium cation and a compound present in the zeolite powder perturbing the titration results.

1 g of untreated 13-X zeolite was thoroughly washed several times using 100mL of distilled water at 65°C for each wash. The pH of each filtered solution was measured. The washing steps were stopped once the pH of the washing solution reached a neutral value. Results of those wash are given below (**Table 15**).

| Washing batch n° | 1 | 2 | 3 | 4 | 5 | 6 | 7 | 8 | 9 |
|------------------|-----|-----|-----|---|-----|-----|-----|---|-----|
| pH | 9,8 | 9,5 | 9,1 | 9 | 8,7 | 8,6 | 8,2 | 8 | 7,8 |

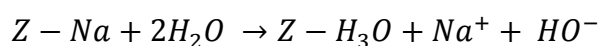
Table 15 - pH of the washing solutions

Note: The pH of the pure water used at that temperature was 6.1 (measured).

The high values of pH for the first washing batches prove that basic species are present in the structure of the untreated zeolites. Those species solubilize during the washing steps. This pH change can have two main causes:

- Basic compounds remaining from the production process of the zeolite (zeolite not thoroughly washed at the end of the fabrication process)
- A reaction between the zeolite powder and the solution.

The second option corresponds to an ion-exchange reaction between water molecules and the cations of the zeolites following the balance below:



The previous washing step of the zeolite cannot indicate us if the pH change is due to one cause or another. Further analyses were done using Energy-Dispersive X-Ray Spectroscopy (EDX).

V.3.3 – EDX spectroscopy analysis

V.3.3.a – the 13-X Zeolite

For the 13-X zeolite, the structure before and after the four ion exchange steps and calcination were analyzed.

Figure 25, **Figure 26** and **Table 16** present the output of the EDX analysis on both samples of zeolite 13-X.

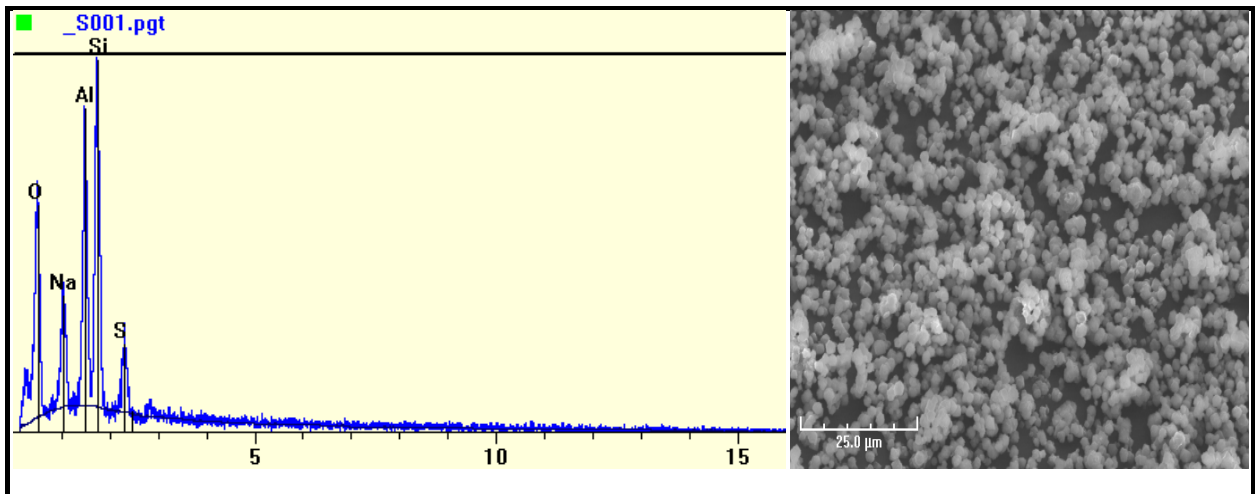


Figure 25 - EDX Analysis of the 13-X zeolite Before calcination and the four ion-exchange steps

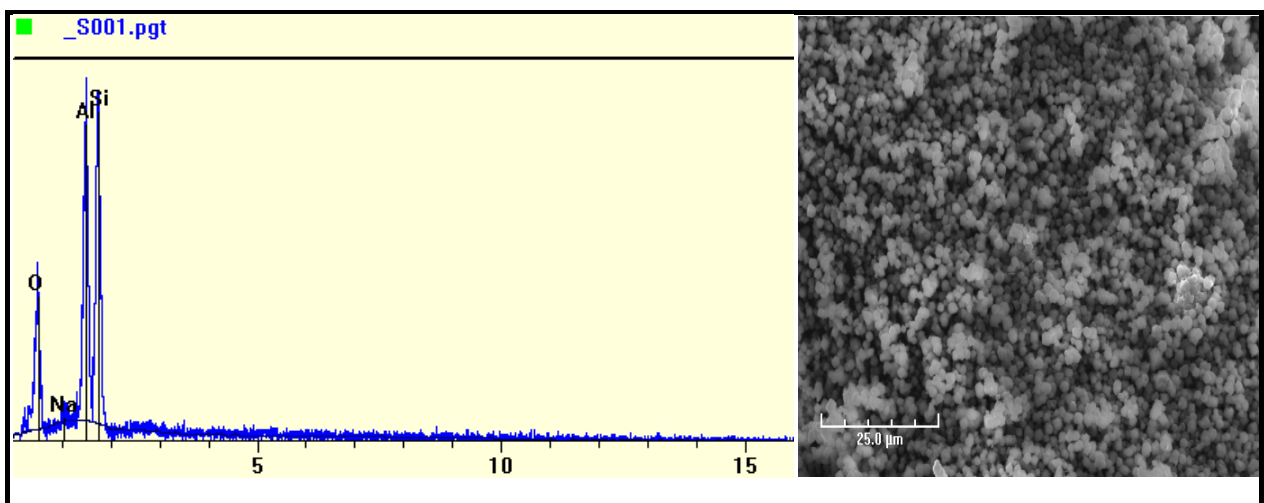


Figure 26 - EDX Analysis of the 13-X zeolite After the four ion-exchange steps and calcination

| | |
|---------------------|--------------------|
| Before ion-exchange | After ion-exchange |
|---------------------|--------------------|

| Element | Wt% | At% | Wt% | At% |
|---------|---------------|---------------|---------------|---------------|
| Na | 10.48 | 9.90 | 0.87 | 0.85 |
| Al | 20.12 | 16.21 | 29.40 | 24.35 |
| Si | 27.18 | 21.03 | 37.54 | 29.86 |
| O | 35.65 | 48.41 | 32.19 | 44.94 |
| S | 6.56 | 4.45 | 0 | 0 |
| Total | 100.00 | 100.00 | 100.00 | 100.00 |

Table 16 - Weight and Atomic composition of both samples

The comparison between the EDX Analysis of both samples is an evidence of the efficiency of the ion-exchange and calcination steps. Indeed, the elemental analysis of the raw sample which did not undergo the steps contains shows 9.9 at% of Sodium in the structure. Whereas the sodium content of the sample after exchange was only 0.85 at%. As expected the sample lost more than 91.1% of its sodium content thanks to the ion-exchange process. The calcination step implemented after the exchange allows the freshly-exchanged ammonium cations to vanish at the expense of lonely protons. That is why the ammonium content cannot be observed in the second sample.

In the first EDX analysis appears a significant atomic quantity of Sulfur. This amount of sulfur was without a doubt a remaining quantity of a compound containing sulfur used in the zeolite production process. The literature shows several examples where compounds of that nature are used in neutralizing steps during the process. [111, 117] This observation can also be related to the unexpectedly high values of pH of the water solutions used to wash the zeolite in Section IV.3.2.

Comparing both data sets collected from the analyses also show that the ion-exchange and calcination steps did not affect the fixed structure of the zeolite since the values of the Si/Al ratio before and after the exchange steps remain equals.

V.3.3.b – the ZSM-5 zeolite

For the ZSM-5 zeolite, the structure before calcinations was analyzed. **Figure 27** and **Table 17** present the output of the EDX analysis on the ZSM-5 zeolite.

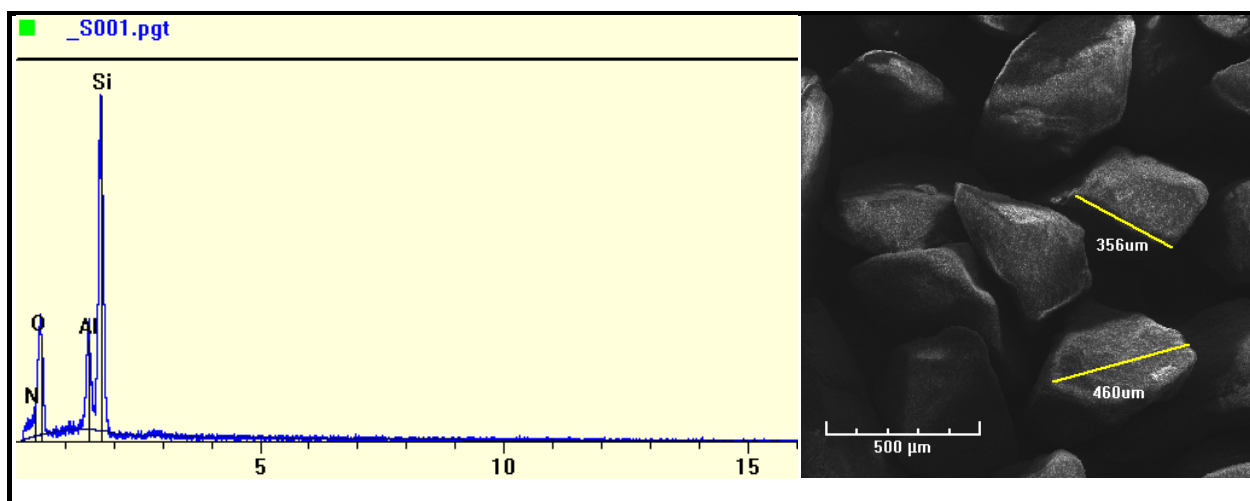


Figure 27 - EDX Analysis of the ZSM-5 zeolite before calcination

| Element | First analysis | | Second analysis | | Second analysis | |
|-------------|----------------|--------|-----------------|--------|-----------------|--------|
| | Wt% | At% | Wt% | At% | Wt% | At% |
| Al | 7.82 | 5.08 | 11.18 | 7.55 | 7.89 | 5.10 |
| Si | 25.22 | 15.75 | 28.92 | 18.75 | 24.17 | 15.02 |
| O | 30.13 | 33.04 | 25.82 | 29.38 | 30.56 | 33.32 |
| N | 36.83 | 46.13 | 34.09 | 44.32 | 37.38 | 46.56 |
| Total | 100.00 | 100.00 | 100.00 | 100.00 | 100.00 | 100.00 |
| Si/Al Ratio | 3.10 | | 2.48 | | 2.94 | |

Table 17 - Weight and Atomic composition for the three analyses

The analysis on the sample shows here that the Si/Al ratio was 2.84 for the ZSM-5 zeolite. It also told us that the counter-ion was ammonium NH_4^+ . The unexpected result is in the amount of Nitrogen present in the sample. Since NH_4^+ is part of the structure in order to compensate the negative charge due to the aluminum atoms (one negative charge per aluminum atom), the atomic percentage of Al and N should be equal. We observed a much higher percentage of nitrogen than aluminum. This observation can be explained by the fact

that the sample did not undergo the calcinations step before being analyzed. Thus, the nitrogen (N₂) adsorbed from the air was remaining at the surface of the zeolite.

A calcination step at 450°C for 3 hours unraveled the problem and allowed us to obtain the ZSM-5 zeolite in its right H-form.

The three zeolites (Y-type, Mordenite and Beta) already were in their Hydrogen form. Beta and Mordenite were ordered from Zeolyst and the Y-type zeolite from Sigma-Aldrich. Both suppliers provided the MSDS and the technical specification data sheets of the products. Thus, they only underwent a calcinations step at 450°C for 3 hours and were not analyzed by EDX spectroscopy.

V.4 – Conclusions

The catalytic power of a zeolite is closely related to the nature of the positive counter-ion balancing the negative charge of the silicon/aluminum/oxygen framework. Consequently, it was essential to know the nature of this cation prior to the implementation of any transesterification reaction of vegetable oil using the different type of zeolites as solid acid catalysts for the main reaction. In the case of the 13-X-type zeolite, the lack of accuracy of the conductimetric analysis was overcome by a second set of analyses done by Energy-Dispersive X-Ray spectroscopy. This EDX analyses aimed at knowing if the ion-exchange process worked efficiently in the case of the 13-X-type zeolite. They also enabled us to know which treatment was appropriate for the ZSM-5 zeolite prior to use it as catalyst in the main transesterification reaction of the recreated Jatropha oil.

VI. *Transesterification of recreated Jatropha oil with zeolites as catalysts*

VI.1 – Introduction

VI.1.1 – Composition of Jatropha oil

VI.1.1.1 – Triglycerides and Fatty Acids

Jatropha oil, like every vegetable oil is mainly composed of triglycerides. Triglycerides are Fatty Acids Triesters formed with the combination of a glycerol molecule – the backbone of the triglyceride – and three molecules of Fatty Acids link to the glycerol thanks to an ester group. **Figure 28** shows the general structure of a triglyceride.

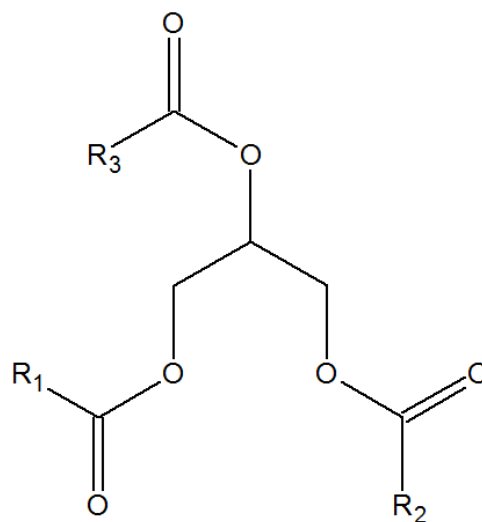


Figure 28 – General structure of a triglyceride with R₁, R₂ and R₃ saturated or unsaturated alkyl groups

Fatty Acids (FAs) encountered in the triglycerides' structures are long carbonated chains ended by a carboxylic acid group. They can either be saturated, monounsaturated or polyunsaturated. In plants and vegetable oils the chain lengths of the FAs typically vary from 14 to 18 carbon atoms. The international normalized nomenclature the fatty acid is written C

n:m, n corresponding to the number of carbons (including the carbon of the carboxylic acid group) and m standing for the number of double bonds C=C in the chain. Sometimes, the notation includes the location of the double bonds and the conformation *cis* or *trans* that it exhibits (i.e. for Linoleic Acid: C 18:2 *cis* 9, *cis* 12). **Table 18** presents the FAs encountered in the triglycerides' structures found in common types of plants and vegetables oils[118].

| Type of oil | Rapeseed | Corn | Cotton | Linseed | Palm | Peanut | Sesame | Soybean | Sunflower | Coconut | Olive |
|-----------------------|-------------------------|------|--------|---------|------|--------|--------|---------|-----------|-------------|-------------|
| FFA content (%) [108] | | 0.15 | | 0.23 | 0.85 | | | | 0.2 | 1.2 | 0.4 |
| Name of the FA | Normalized nomenclature | | | | | | | | | | |
| Butyric | C4:0 | | | | | | | | | | |
| Caproic | C6:0 | | | | | | | | | | |
| Caprylic | C8:0 | | | | | | | | | | |
| Capric | C10:0 | | | | | | | | | | |
| Lauric | C12:0 | | | | | | | | | | |
| Myristic | - | 0.0 | 0.8 | - | 1.0 | 0.1 | - | 0.1 | - | 13.0 - 19.0 | 0.1-1.2 |
| Palmitic | 4.8 | 10.9 | 22.7 | 5.3 | 43.5 | 9.5 | 8.9 | 10.3 | 5.4 | 8.0 - 11.0 | 7.0 - 16.0 |
| Palmitoleic | 0.5 | - | 0.8 | - | 0.3 | 0.1 | 0.2 | 0.2 | 0.2 | 0 - 1 | 1.6 |
| Stearic | 1.6 | 1.8 | 2.3 | 4.1 | 4.3 | 2.2 | 4.8 | 3.8 | 3.5 | 1.0 - 3.0 | 1.0 - 3.0 |
| Oleic | 53.8 | 24.2 | 17.0 | 20.2 | 36.6 | 44.8 | 39.3 | 22.8 | 45.3 | 5.0 - 8.0 | 65.0 - 85.0 |
| Linoleic | 22.1 | 58.0 | 51.5 | 12.7 | 9.1 | 32.0 | 41.3 | 51.0 | 39.8 | Traces-2.5 | 4.0-15.0 |
| Linolenic | 11.1 | 0.7 | 0.2 | 53.3 | 0.2 | - | 0.3 | 6.8 | 0.2 | | |
| Arachidic | C20:0 | | | | | | | | | | |
| Others | 6.1 | 4.4 | 4.7 | 4.4 | 5.0 | 11.3 | 5.2 | 5.0 | 5.6 | 0 - 0.04 | 0.1 - 0.3 |

Table 18 - FA composition[118] and FFA content[108] of common plants oils

Table 19 shows the nature and amount of the different FA found in Jatropha oil. Alike most types of plants (See **Table 18**), Jatropha oil exhibits high Oleic and Linoleic contents (more than 79% of the total FA content). Significant amounts of two other FA – Palmitic and Stearic Acid – are found and only traces of other FA (Non-reported here) are measured.

| | Crocker[96] | Akbar et al.[102] | Endalew[36] |
|------------------|-------------|-------------------|-------------|
| Palmitic (C16:0) | 11 to 16 | 14,2 | 14,1 - 15,3 |
| Stearic (C18:0) | 6 to 15 | 7 | 3,7 - 9,8 |
| Oleic (C18:1) | 34 to 45 | 44,7 | 34,3 - 45,8 |
| Linoleic (C18:2) | 30 to 50 | 32,8 | 29,0 - 44,2 |

Table 19 - FA profile of the triglycerides in Jatropha oil

VI.1.1.2 –Free Fatty Acid content

Free Fatty Acids (FFA) are species naturally present in the every type of vegetable/plant oil. They come from the decomposition of a triglyceride into a glycerol molecule and three Free Fatty Acids molecules. Due to their carboxylic acid structure described above, their amount affects the chemical properties and reactivity of the oil towards other Brønsted species.

In acid oils, the FFA content can vary from 0.5% up to 40%. However, most vegetable/plant oils have low FFA content. One of the typical characteristics of Jatropha oil is that the Free Fatty Acid (FFA) content is naturally much higher than in other vegetable/plant oils. Freshly pressed Jatropha oil can have more than 22% of FFA in its raw composition [21] whereas the FFA content of the plants presented in **Table 18** ranges from 0.15% et 1.2%[108].

Initially, every type of oil has a different amount of FFA in its composition but with time, the FFA content increases. Khan, Bhatti and Sardar[107] quantified this increase on several batches of Soybean oil, Cotton seed oil and sunflower oil after a ten-month period of storage. The sealed groups underwent increases of 99.4%, 104% and 119.25% respectively whereas the unsealed groups experienced a much more important increase of 1066.4%, 1085.4% and 1241% respectively.

The dramatic rancidity of the oil after unsealed storage is due to the chemical decomposition of the triglycerides into FFA, monoglycerides, diglycerides and glycerol. Factors such as light rise in temperature, presence of moisture in the medium or even lipolytic enzyme lipase can accelerate significantly the amount of FFA in the oil which directly

affects the reactivity, chemical and physical properties of the oil and consequently its use in the industry.

The Free Fatty Acid content, characterized by the Acid Value of the oil (See Part II) has an enormous impact on the type of catalysis used in the transesterification reaction. The influence in the choice of the catalyst of the high AV ($28 \text{ mg}_{\text{KOH}}/\text{g}_{\text{oil}}$ [37]) in the case of Jatropha oil was studied in depth in Section V.2.1.1.

VI.1.2 - The reaction

VI.1.2.1 - Presentation of the transesterification reaction

The transesterification reaction takes place between an ester group and an alcohol group and can be either intra- or extra-molecular. In our case, it is an extra-molecular reaction between the three ester groups of a triglyceride molecule and three molecules of alcohol in presence of a catalyst. However, the mechanism of the reaction was shown to be closely related to the type of catalyst used[40]. **Figure 29** shows the mechanism of the reaction catalyzed by an acidic species (See Section V.1.2.1).

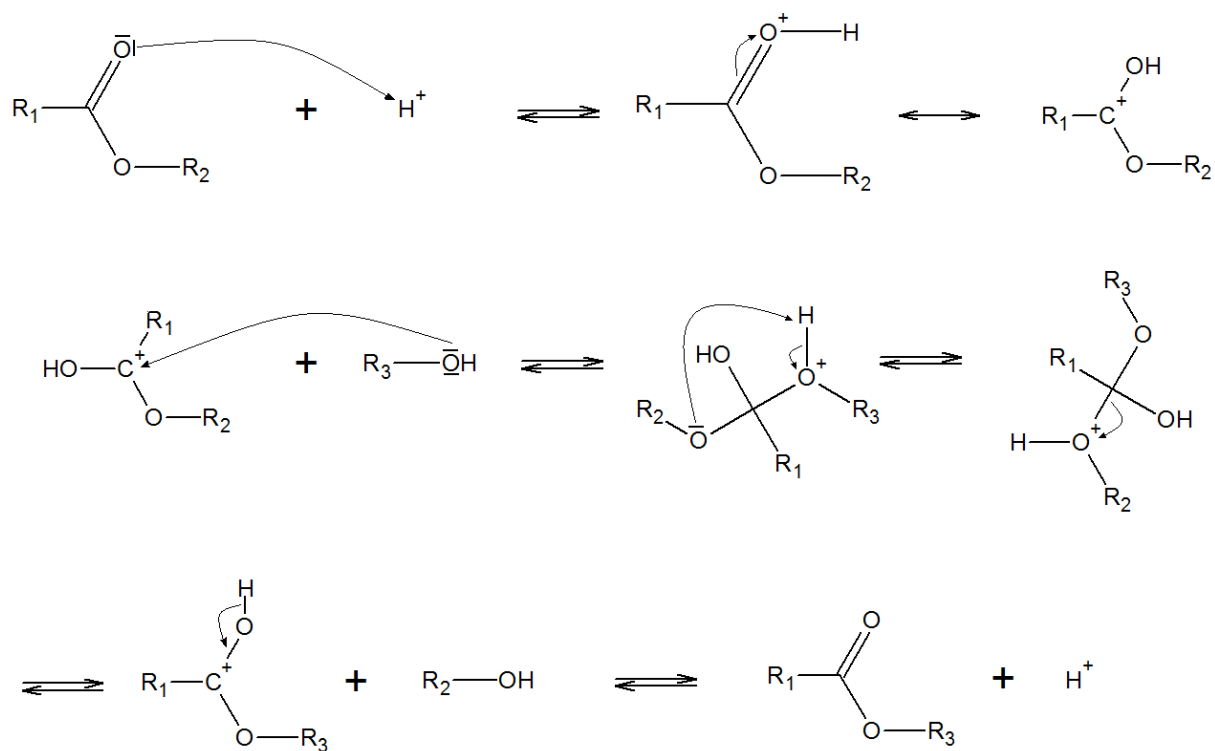


Figure 29 - Acid-catalyzed mechanism of the transesterification reaction

The mechanism presented in **Figure 29** only shows one transesterification step. However, it is important to notice that in the acid-catalyzed reaction between a triglyceride and butanol, three transesterification steps occur to finally lead to three molecules of Fatty Acid Butyl Esters (FABEs) and a molecule of glycerol. The entire mechanism being very similar to the one presented in **Figure 29** is not presented here.

The acid-catalyzed transesterification reactions are characterized by two consecutive and reversible substitutions preceded by a step of protonation of the carbonyl group (forming an unstable tetrahedral intermediate) whereas the alkali-catalyzed reactions are based on a reversible addition–elimination mechanism. In the reaction catalyzed with an acid species, the carbon atom of the carbonyl group of the triglyceride becomes more electrophilic by the catalyst and more susceptible to be attacked by alcohol.

The main differences between the acidic and the alkali-catalyzed mechanism come from the degree of polarization of the carbonyl group of the triglyceride, the nucleophile strength of the alcohol and also from the ability of the substituted group to leave the tetrahedral intermediate. Those differences between both mechanisms have a strong influence on the kinetics of the reaction. They are able to explain why the alkali-catalyzed reaction was shown to have a much greater reaction rate than the same reaction catalyzed in acidic medium.

VI.1.2.1 – Unwanted parasitic reaction

In general, the conditions used for the transesterification reaction are also ideal for another unwanted side reaction involving the triglycerides of the oil. This particular reaction called Saponification involves the formation of soaps (i.e. ionic species composed of a carboxylic ion and a positive counter-ion such as Na^+) would particularly occur when a nucleophilic (basic) species is present in the medium. It can also marginally happen when the water content of the oil is high.

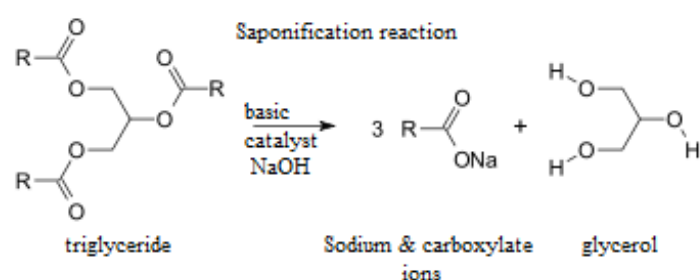


Figure 30 - Overhaul balance of the saponification reaction

The effects of this reaction have to be minimized or even avoided since it creates emulsions and renders the separation steps of the diesel phase particularly energy and time consuming.

However, in our experiments, the use of an acid catalyst prevents the formation of soaps and only the acid-catalyzed transesterification reaction of the triglycerides as well as the acid-catalyzed esterification reaction of the FFA occur in the media.

VI.2 – Experimental

VI.2.1 – Reactants and Parameters of reaction

VI.2.1.1 – Choice of the alcohol

Many parameters were taken into account while choosing the type of alcohol used in the transesterification reaction. First of all regarding the feasibility of the reaction, long chain linear alcohols (With more than 6 carbon atoms in their chain) as well as non-linear species such as isopropanol and tertiobutanol were not considered due to the slow (or even null) kinetics they involve.

Among the small chain linear alcohols, butanol was chosen for quality purposes. Indeed, working with a longer chain imparts a higher energy density to the final fuel thanks to a higher Cetane Number (C#). C# of linear chain alcohols were proven to increase linearly with the number of carbon atom in their chain[119].

Whithin the scope of sustainable development, we kept in mind that the two alcohols mainly produced from biomass are ethanol and butanol (ABE process). The choice between them was made considering the fact butanol has a greater Lower Heating Value (LHV) and its combustion releases less Volatile Organic Compounds (VOC) than ethanol[12].

The main drawback regarding the choice of butanol is its good miscibility with glycerol as well as oil. Butanol played the role of a co-solvent during the reaction and did not

allow different phases to separate. On the one hand, the single-phased liquid system did not present any matter diffusion as a two-phase system would. But on the other hand, it rendered the separation of the products and the reactants hard.

Working with longer chain alcohols had an influence on the reaction conditions and more particularly on the temperature conditions.

VI.2.1.2 – Butanol-to-oil ratios

Even if the stoichiometric ratio is 3:1, higher ratios are usually chosen in order to increase the solubility of the mono-, di- and triglycerides in the alcohol phase[120].

Three molar Butanol-to-oil ratios were tested: 3:1 (stoichiometric ratio), 6:1 and 15:1. The choice of those different ratios was made regarding previous studies and in order to determine its influence on both the progression of the reaction overtime and the final yield reached.

VI.2.1.1 – Choice of the catalyst

Choosing an acid catalysis was justifiable by the fact that the high FFA content of the oil did not permit us to use a basic catalysis. On top of that, the choice of an heterogeneous catalysis is more interesting in our case than an homogeneous acid catalyst which would highly foster corrosion of the reactor and its components in those harsh conditions.

The primary goal of our study is to compare the activity of different zeolites as solid acid catalysts in the transesterification reaction between butanol and high FFA Jatropha oil. Thus, five different types of zeolites were tested: X-type (13-X) zeolite, Y-type zeolite, Mordenite, Beta and ZSM-5. Their properties are gathered in **Table 20**.

| Nature of the zeolite | Chemical formula (before treatments) | Dimension | Pore size (Å) | Si/Al ratio | Cation | Treatment | Shape |
|-----------------------|---|-----------|---------------|-------------|--------------|-------------------------|----------------|
| X-type (13-X) | $\text{Na}_{86}[(\text{AlO}_2)_{86}(\text{SiO}_2)_{106}] \cdot 264\text{H}_2\text{O}$ | 3-D | 7,4 | 1,23 | H^+ | Ion-exchanged, calcined | Powder (2µm) |
| Y-type | $\text{H}_{56}[(\text{AlO}_2)_{56}(\text{SiO}_2)_{136}] \cdot 250\text{H}_2\text{O}$ | 3-D | 7,4 | 2,43 | H^+ | Calcined | Powder (2µm) |
| Mordenite | $\text{H}_8[(\text{AlO}_2)_8(\text{SiO}_2)_{40}] \cdot 24\text{H}_2\text{O}$ | 2-D | 6,7 - 7,0 | 5 | H^+ | Calcined | Powder (2µm) |
| Beta | $\text{H}_2[(\text{AlO}_2)_2(\text{SiO}_2)_{150}] \cdot 4\text{H}_2\text{O}$ | 3-D | 6,68 | 75 | H^+ | Calcined | Powder (2µm) |
| ZSM-5 | $(\text{NH}_4)_{52}[(\text{AlO}_2)_{52}(\text{SiO}_2)_{44}] \cdot 16\text{H}_2\text{O}$ | 2-D | 5,5 | 2,84 | H^+ | Calcined | Grains (0,4mm) |

Table 20 - Structural characteristics of the zeolites used (* ZSM-5 structure obtained thanks to the idealized unit cell composition[121] and the outcome of the EDX Analysis)

Since it is hard to quantify accurately the molar amount of active catalytic sites within a zeolite, all the experiments were run with a fixed weight of zeolite corresponding to 1%wt. of the total weight of reactants in the batch.

In order to have landmarks as references, three batches were also ran without catalyst (one for each Butanol-to-oil ratio) and three other with sulfuric acid at 98.5%mol as a catalyst. For the latter, the quantity of catalyst was also chosen as 1%wt. of the total weight of the reactants.

VI.2.1.4 – Choice of the temperature

For all the batches, the reaction temperature was maintained constant at 115°C. This particular temperature was chosen taking into account several factors and physical properties.

First of all 117°C is the vaporization temperature of the butanol under atmospheric pressure. In order to avoid a raise in pressure due to the appearance of a significant amount of vapor phase, the temperature was kept below the vaporization temperature of the

alcohol. A two-degree Celsius margin of precaution was kept in order to avoid any unexpected pressure increase in case of an overshoot in temperature control.

Working with harsh temperature conditions also exhibits several other mechanistic advantages. Indeed, the kinetics and thermodynamics of the transesterification reaction are governed by the energy gradient between the reactants and the products of the reaction as well as the steric mobility of the reactants towards each other. Thus, applying intense reaction conditions to the batch allowed to reach higher conversions with the relatively long chained butan-1-ol.

Finally, working at higher temperatures decreased the viscosity of the mixture and limited the effect of diffusion of the reactants toward each other and toward the catalyst. Increasing the temperature for that reason is even more justified because of the high content of long-chained and unsaturated Fatty Acids such as Oleic and Linoleic acids [122].

VI.2.1.5 – Stirring conditions

One of the concerns regarding the medium in which the reaction took place was the homogeneity of the solution. The transesterification required two reactants whose specific gravities were different from each other leading to the formation of a biphasic liquid mixture. On top of that, the choice of a heterogeneous catalyst added one more phase to the system. Moreover, the expected products of the reaction (the Biodiesel made of the Fatty Acid Butyl Esters (FABE) and the alcohol phase containing the glycerol as well as the unreacted butanol) were not miscible either. It is then easy to understand that mass transfer limitation had an important influence on the feasibility of the reaction from its beginning until its end.

A high mixing rate was chosen to overcome the mass transfer limitation. With a stirring-speed of 1000 rpm, we assumed the medium was well-stirred and the contact between phases (i.e. reactants) was ideal.

V.2.1.6 – Moisture content of the oil and storage conditions

Either the transesterification reaction itself (with the unwanted side reaction of saponification) or the natures of the catalysts (zeolites) are sensitive to the presence of water in the medium. Wright et al. observed that a rise of water content of 0.11% to 0.57%mol caused the yield of the transesterification reaction of cottonseed oil with ethanol to drop from 89.4% to 61.8%[123]. Thus, the alcohol used was dry butanol (with less than 0.01%wt. of water), traces of water were removed from the oil using a powerful desiccant (Calcium Chloride CaCl_2) and the material was carefully dried before each experiment.

To avoid penetration of moisture inside the bottles of reactants, all containers were carefully sealed using parafilm. Moreover, the reactants were kept away from the light (thanks to smoked glass bottles) in order to avoid the increase of the FFA content.

VI.2.2 – Experimental device

Among all the different types of reactors commonly used and presented in the background section (Batch reactors, plug-flow reactors, oscillatory flow reactors – See section I.4.2.1), the reactor used for our purpose was a well-stirred batch reactor. The reactor was a donation from the company Sepracor given to the Chemical Engineering department of the Worcester Polytechnic Institute by Robert Pritko. The device include à 450mL stainless steel vessel, sealed to an airtight head. A mechanical stirring agitator, a sampling line as well as a

pressure relief valve, a vent and an emergency rupture disk (2000psig) were part of the reactor's head. The head of the reactor also exhibited a gas inlet which was not used for our purposes and was plugged carefully by a safety rupture disk of the same nature as the first one.

Figure 31.a to **Figure 31.c** show pictures of the device. Specifications of the reactor and its components can be found in Appendix H.

In order to control the stirring speed, the stirring propeller was activated by a Parr motor whose speed was controlled by a Parr 4842 controller.

The temperature control was guaranteed by a Eurotherm 2116 temperature controller and the temperature was measured with a K-type thermocouple (Chromel [Ni:90%, Cr:10%]-Alumel[Ni:95%, Mn:2%, Al:2%,Si:1%]) . The temperature controller can be seen on **Figure**

31.d.



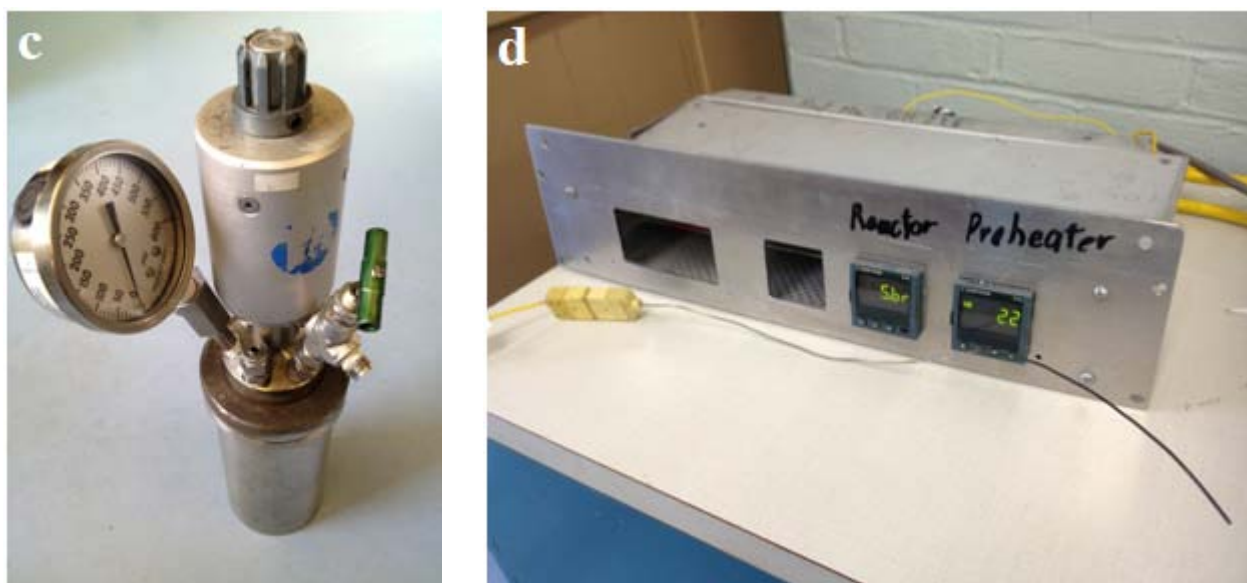


Figure 31 -The transesterification device: Stirring controller, autoclave, heating mantle (a); open reactor (b); reactor's head (c); temperature controller and thermocouple (d)

VI.2.3 – Analysis of the samples

In order to follow the conversion of the reaction overtime, we chose to follow the concentration of glycerol in the media overtime. Indeed according to the balance of the reaction, the formation of glycerol was a good indicator of the yield of the transesterification reaction since it is the compound formed at the end of the three transesterification steps of the tri-, di- and mono- glycerides. The concentration of glycerol in the medium showed the global conversion of the triglycerides into biodiesel. However, it is important to notice that this method enabled to measure the conversion of the transesterification reaction only and did not take into account the formation of FABEs from FFA thanks to the esterification reaction. Consequently, the actual production of biodiesel (as FABEs) was slightly higher than the conversion measured.

The detailed procedure of determination of the glycerol concentration in the reactor overtime is detailed in Appendices E & F.

VI.3 – Results and discussion

In this section, the following graphs show the conversions (in %) that were observed with each catalyst for the three butanol-to-oil ratio tested (3:1, 6:1 and 15:1). The method of determination of those numerical values of conversions is reported in Appendix F. Also, the calibration curves and raw data for each experiment are provided in Appendix G.

VI.3.1 – Homogeneous and heterogeneous catalysis

A reference reaction using a liquid acid catalyst (H_2SO_4 at 98%wt.) was implemented in the same conditions as the reactions with zeolites. This reaction enabled to reach high values of conversion between 17% – for a butanol-to-oil ratio of 3:1 – and up to 74.4% for a 15:1 ratio. **Figure 32** show the evolution of the conversion with respect to time for the three different butanol-to-oil ratios.

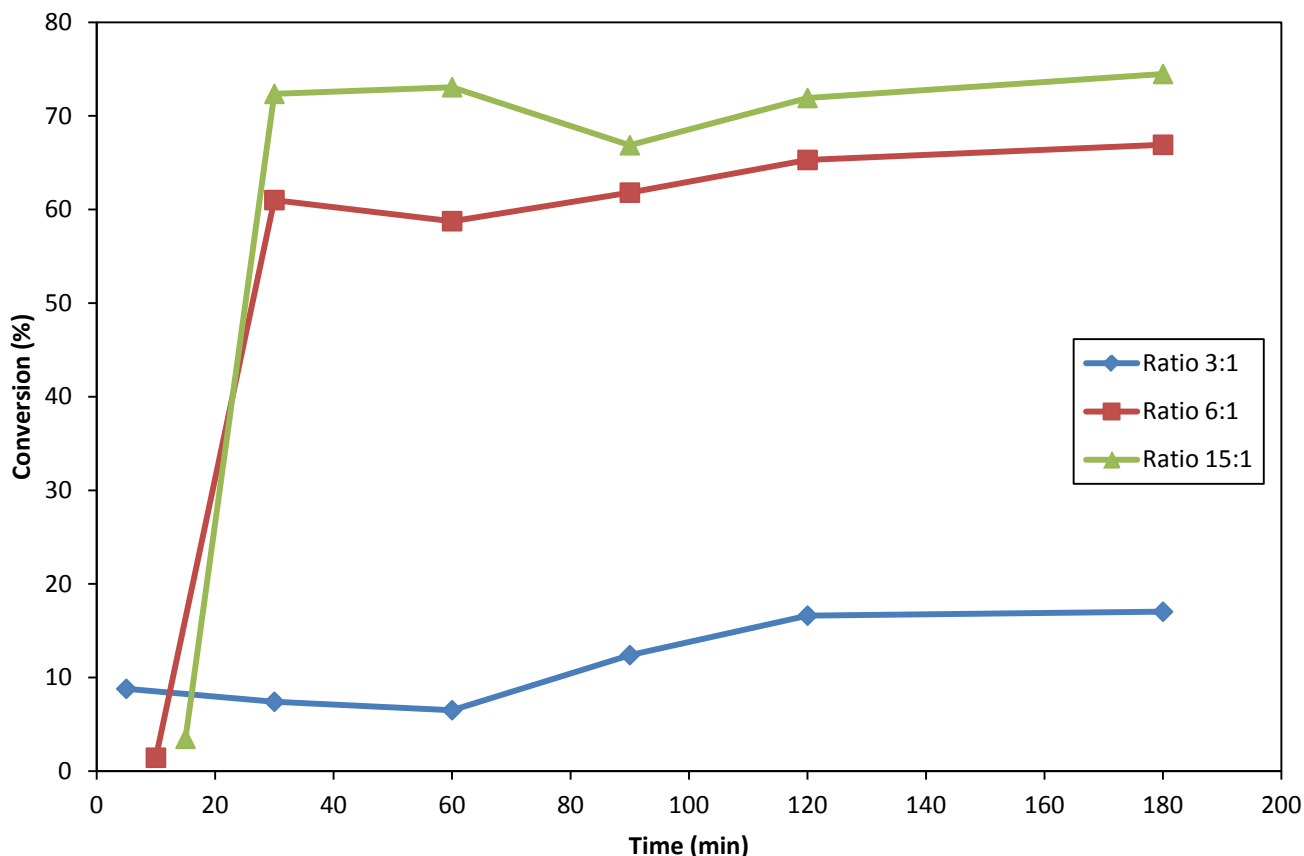


Figure 32 - Transesterification of recreated Jatropha oil with butanol at 115°C using H₂SO₄ (1%wt.) as liquid acid catalyst for three butanol-to-oil molar ratios (3:1, 6:1 & 15:1)

The yields reached using H₂SO₄ as catalyst for the transesterification reactions are lower than those reported in the literature. Nimcevic et al. [40] implemented transesterification of rapeseed oil in the exact same conditions and observed final conversions of 96.4% and 96% for 6:1 and 15:1 butanol-to-oil molar ratios respectively after 4 hours of conversion. This major difference can be explained by the nature of the oil. Indeed, the oil used in our case was recreated Jatropha oil with a much higher FFA content than the rapeseed oil used by Nimcevic et al. The parallel esterification reaction of the FFA observed in our experiments did not occur in the rapeseed oil batch and consequently did not affect the yield of the transesterification reaction.

VI.3.2 – Influence of the molar butanol-to-oil ratio

Many studies concluded that in homogeneous catalysis, the best alcohol-to-oil ratio was around 6:1.[34, 120] However, in all the experiments implemented by us with any type of zeolite used as acid catalyst, the conversions reached increased with the butanol-to-oil ratio.

This can be explained by the fact that higher butanol-to-oil molar ratios increase the **solubility** of the triglycerides in butanol and consequently allow a better contact between the reactants. Thus, the greater butanol-to-oil ratio, the higher probability of reaction between the species.

Another explanation from this acknowledgement is the evolution of the **viscosity** of the reactive medium. Indeed, the viscosity of a butanol/oil mixture decreases when the butanol-to-oil ratio increases. This is due to the lower viscosity of butanol in comparison to the oil. Consequently, in the batches with a low butanol-to-oil ratio (i.e. high viscosity) a diffusion limiting process towards the solid zeolites particles in suspension in the mixture was observed. On the contrary, increasing the butanol-to-oil ratio decreased the viscosity and decreased the impact of the diffusion of the reactants towards the catalyst particles.

The acknowledgement that a high butanol-to-oil molar ratio is necessary for acid-catalyzed transesterification is relevant to the observation made by Freedman et al. [34] during the transesterification of various vegetable oils with sulfuric acid as a catalyst. High conversions were reached for a alcohol-to-oil molar ratio of 30:1. Zheng et al. [38] noticed that an alcohol-to-oil molar ratio of 245 :1 was necessary in order to reach good conversions of waste oil with methanol in acidic catalysis.

Also, the nature of the alcohol involved in the transesterification step had an important influence on the reaction medium. Indeed, the main difference with the use of

small-chained alcohols – such as methanol or ethanol – and butanol is that the latter is less reactive than the two others due to its bigger size. The steric bulk implied by its size also decreases its activity that has to be compensated by a higher butanol-to-oil ratio.

VI.3.3 – Compared efficiencies of the zeolites

For a fixed butanol-to-oil ratio, the compared efficiencies of the different catalysts (zeolites & H₂SO₄) bring to the light several properties of the zeolites and their influence on their ability to catalyze the transesterification reaction.

The four main criteria that come out in order to explain the outcomes of the different reactions are:

- The hydrophobicity of the zeolite increasing with the silicon-to-aluminum ratio;
- The acidity decreasing when the silicon-to-aluminum ratio increases;
- The pore size of the zeolite which limits the diffusion within their structures;
- The zeolite particles size.

VI.3.3.a – Hydrophobicity of the catalyst

As explained in Section I.5.3.1, zeolites with low silicon-to-aluminum ratios are less hydrophobic than zeolites with high Si/Al ratios. This result was observed comparing the efficiencies of Y-type zeolite and 13-X-type zeolite. **Figure 33** and **Figure 34** exhibit the results obtained using Y-type and 13-X-type zeolites.

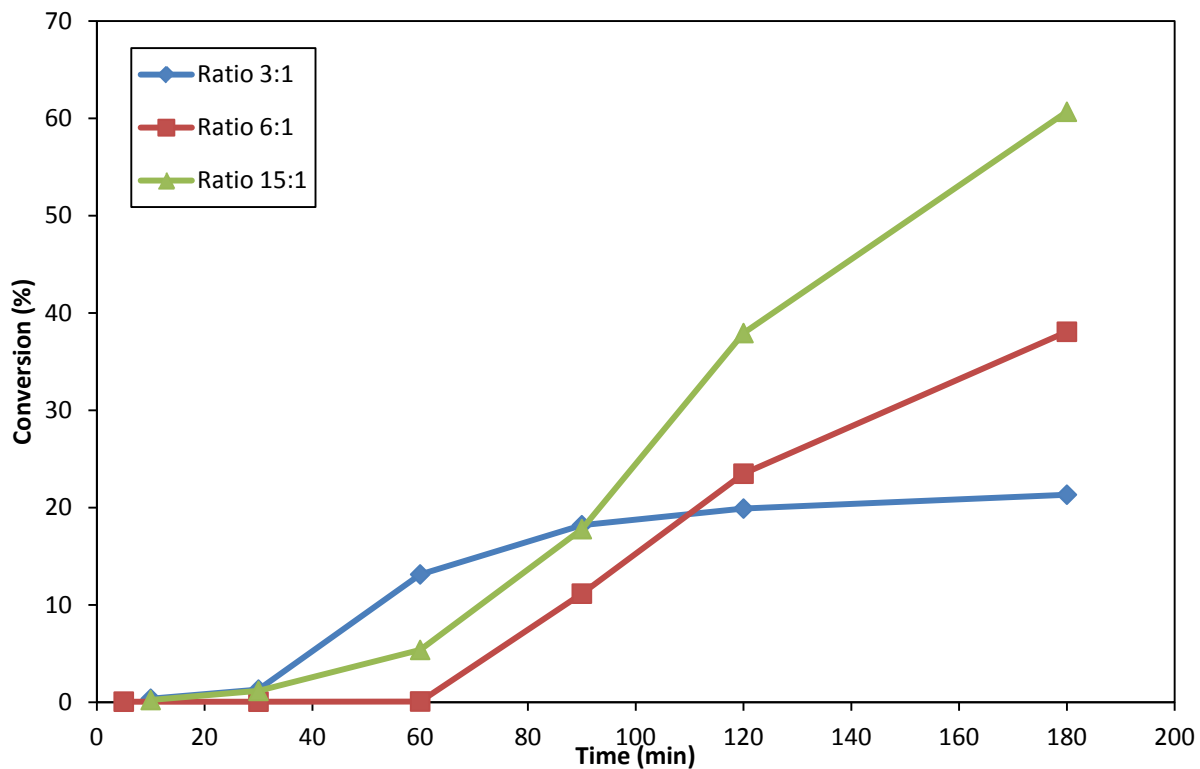


Figure 33 - Transesterification of recycled Jatropha oil with butanol at 115°C using Y-type zeolite (1%wt.) as solid acid catalyst for three butanol-to-oil molar ratios (3:1, 6:1 & 15:1)

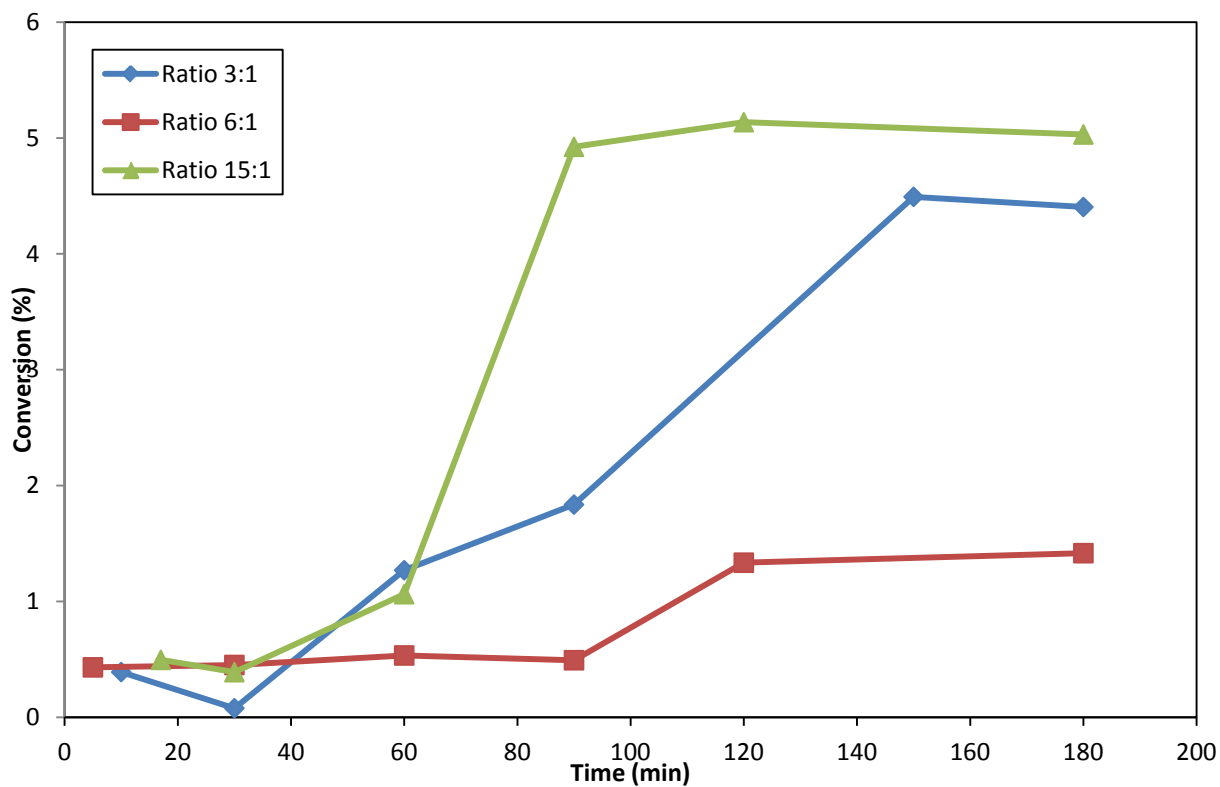


Figure 34 - Transesterification of recycled Jatropha oil with butanol at 115°C using 13-X-type zeolite (1%wt.) as solid acid catalyst for three butanol-to-oil molar ratios (3:1, 6:1 & 15:1)

Regarding the pore size, the particle size and the type of channels, Y-type and 13-X-type zeolites were equivalent. The major difference between both structures was the Si/Al ratio. The Y-type framework exhibited a higher Si/Al ratio (Si/Al=2.43) than the 13-X-type zeolite (Si/Al=1.23). Thus, the 13-X-type zeolite was less hydrophobic than the Y-type zeolite and more sensitive to the presence of water in the medium. However, the gap between the yields obtained with both zeolites (more than 12 times greater with the Y-type zeolite in the case of a butanol-to-oil ratio of 15/1) cannot only be explained thanks to the hydrophobicity difference. The efficiency of the ion-exchange and calcination processes implemented on the 13-X-type zeolite can be questioned. The poor quality of the ion-exchanged catalyst could also be the explanation why the reaction implemented with a 6:1 butanol-to-oil ratio unexpectedly exhibited a lower yield than the reaction done with a 3:1 ratio.

VI.3.3.b – Acidity of the catalyst

Acidity of the catalyst is also influenced by the Si/Al ratio. This ratio was particularly high in the case of the zeolite Beta (Si/Al=75) and had a strong influence on the conversion reached. **Figure 35** and **Figure 36** show the outcome of the reactions catalyzed with zeolite Beta and non-catalyzed.

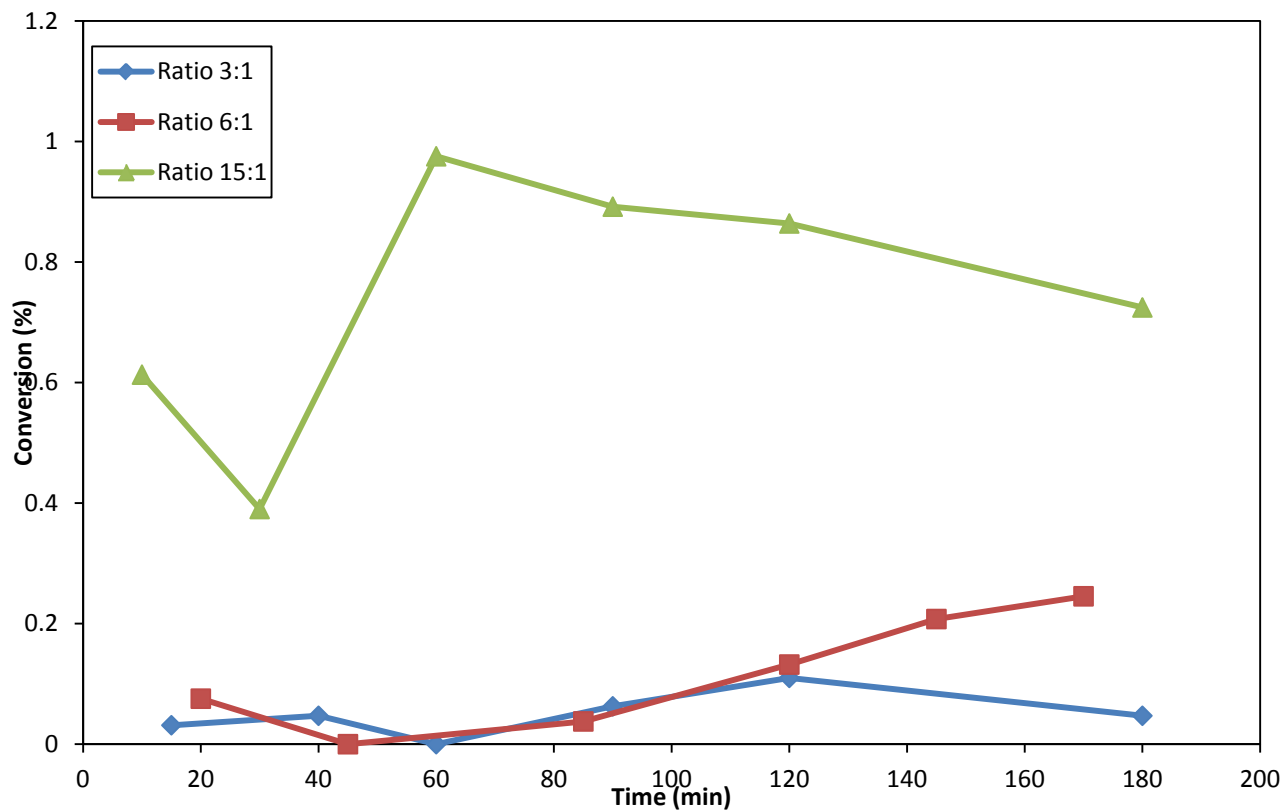


Figure 35 - Transesterification of recreated Jatropha oil with butanol at 115°C using Beta zeolite (1%wt.) as solid acid catalyst for three butanol-to-oil molar ratios (3:1, 6:1 & 15:1)

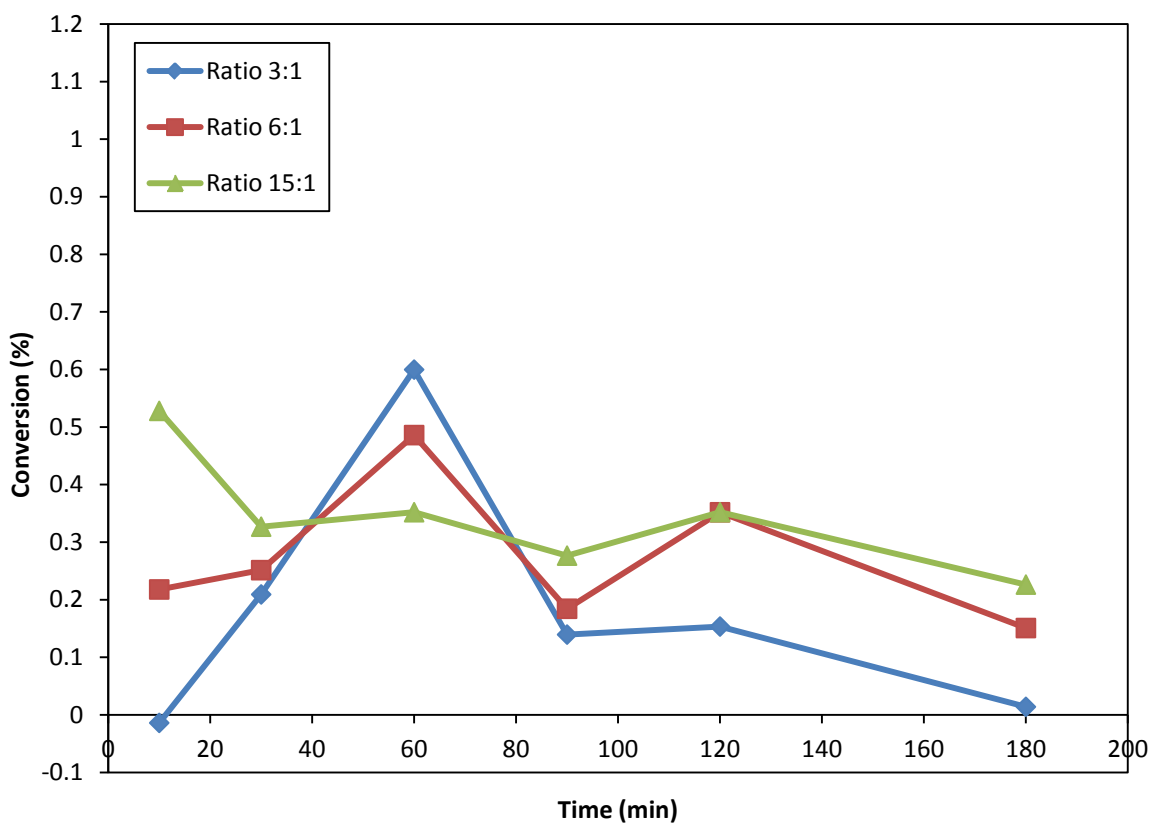


Figure 36 - Non-catalyzed transesterification of recreated Jatropha oil with butanol at 115°C for three butanol-to-oil molar ratios (3:1, 6:1 & 15:1)

The difference between the non-catalyzed reaction and the reaction in which zeolite Beta was used as solid acid catalyst is not significant. The influence of Beta zeolite on the reaction is very limited (almost non-existent). The high silicon-to-aluminum ratio of Beta zeolite implies a very low density of acid catalytic site in the structure of the zeolite and does not enable to catalyze efficiently the transesterification reaction.

This acknowledgement was also confirmed by the outcome of the reactions implemented with Mordenite and presented in **Figure 37**.

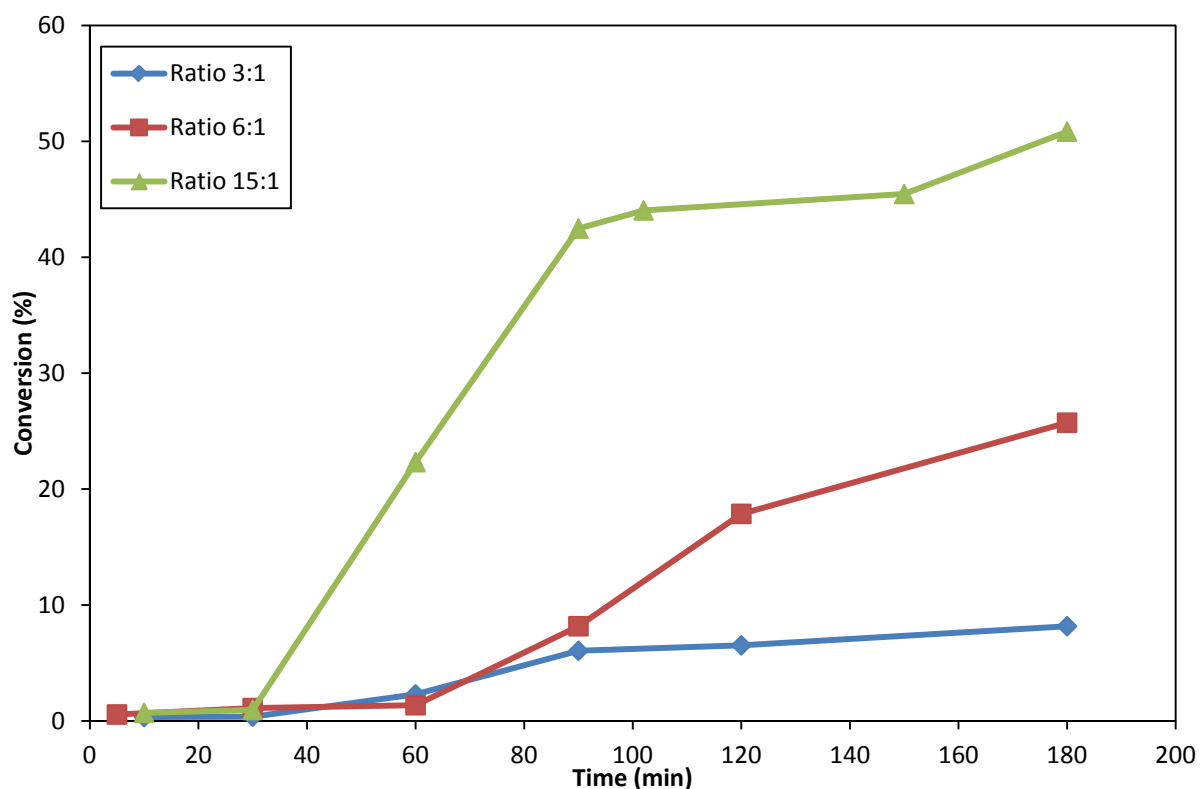


Figure 37 - Transesterification of recreated *Jatropha* oil with butanol at 115°C using Mordenite (1%wt.) as solid acid catalyst for three butanol-to-oil molar ratios (3:1, 6:1 & 15:1)

The yields reached are slightly lower in the case of the use of Mordenite as catalyst than when Y-type zeolite is used. This difference was explained by Si/Al ratio, higher in the case of Mordenite (Si/Al=5) than with the Y-type zeolite (Si/Al=2.43).

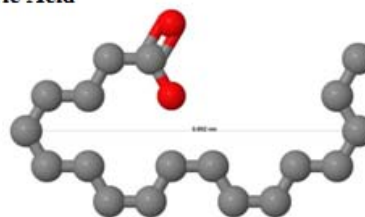
VI.3.3.c – Influence of the pore size

When we tried to correlate the pore sizes of the different zeolites with the outcomes of the transesterification reactions implemented with all the different zeolites, no trend seemed to appear. It does not seem that the pore size has an important influence in the catalytic efficiency of the zeolite. The main explanation comes from the size of the molecules reacting. Modeling the reactants with Jmol (**Figure 38**) gave us estimations of the dimensions of the molecules.

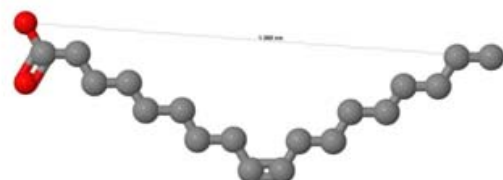
a - Palmitic Acid



b - Stearic Acid



c - Oleic Acid



d - Linoleic Acid

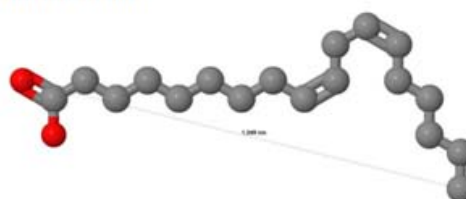


Figure 38 - Models of the four main Fatty Acids and determination of the chain length taking into account the spatial set up of the molecules ($d_{\text{Palmitic acid}} = 1.387 \text{ nm}$, $d_{\text{Stearic acid}} = 0.802 \text{ nm}$, $d_{\text{Oleic acid}} = 1.368 \text{ nm}$, $d_{\text{Linoleic acid}} = 1.249 \text{ nm}$)

The numbers provided by those models show that the molecules involved in the transesterification reaction are much larger than the pore sizes of any zeolite used. The diffusion of the molecules inside the pores of the zeolites is extremely limited. As a consequence, the acidic sites inside the pores cannot be reached by the reactants.

This tends to prove that the transesterification reaction between the tri-, di- and mono-glycerides and butanol as well as the esterification reaction of the FFA by butanol takes place almost exclusively on the surface of the zeolites leaving the inside acidic sites unused.

VI.3.3.d – Influence of particle size

In the case of a reaction involving molecules whose dimensions are larger than the pore size, the size of the particles is essential because it determines the active surface area available to catalyze the reaction. This acknowledgement was proven by the low conversions obtained using ZSM-5 as a catalyst and presented in **Figure 39**.

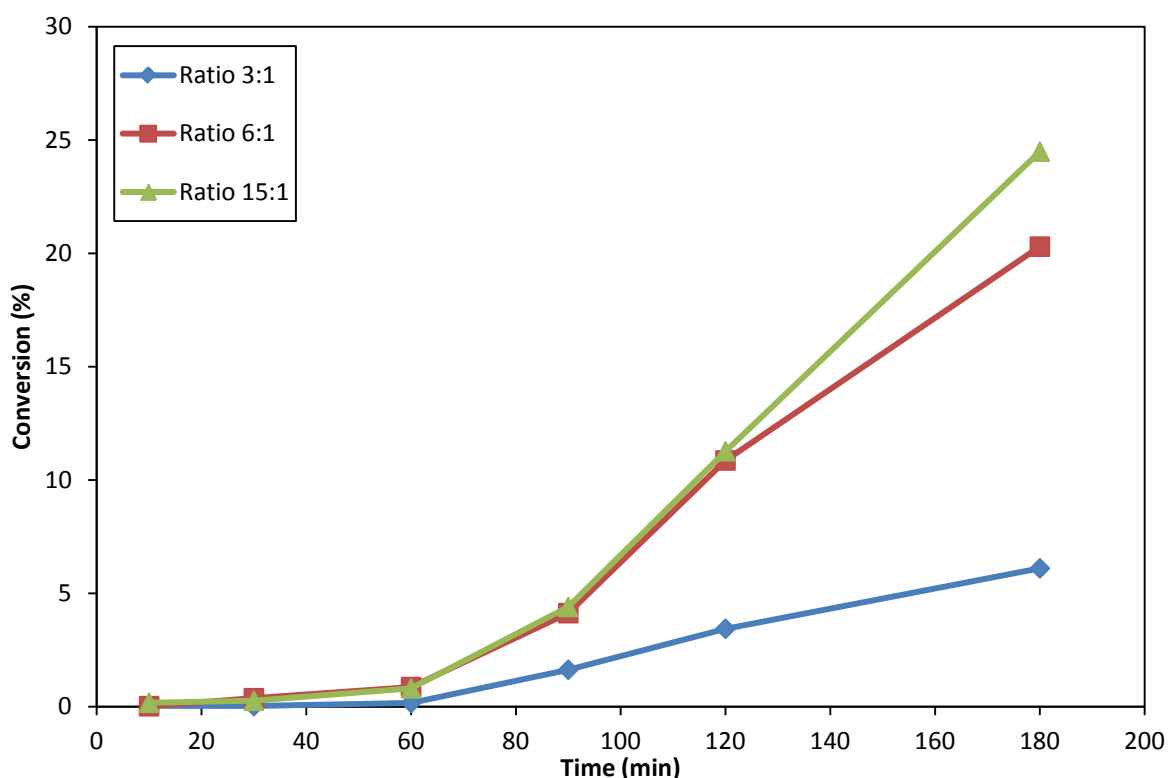


Figure 39 - Transesterification of recycled Jatropha oil with butanol at 115°C using ZSM-5 (1%wt.) as solid acid catalyst for three butanol-to-oil molar ratios (3:1, 6:1 & 15:1)

The fact that the average diameter of the particle of catalyst was 200 times greater than all the other zeolites' particle diameter makes a significant difference in the limiting diffusion process. In the case of the use of 0.4mm ZSM-5 grains, the surface area available for the reaction was 40,000 times smaller than with a powder with an average particle size of 2µm, if particles are assumed to be spherical. The Y-type zeolite and ZSM-5 had similar silicon-to-aluminum ratios (i.e. acidity and hydrophobicity) however, the active surface of the first one was greater than the active surface of the latter causing a significant difference regarding their catalytic power. Nonetheless, comparing the activity of ZSM-5 and the Y-type zeolite, we could note that even with a ratio between the surfaces area of 40,000, the conversions were only 3.5 times, 1.8 times and 2.5 times lower with ZSM-5. This came from the fact that a catalytic site is used multiple times during the transesterification reaction.

VI.3.4 – Global results of the transesterification reactions

Figure 40 gathers the results of all the transesterification reactions implemented with the different catalysts for the three butanol-to-oil ratios.

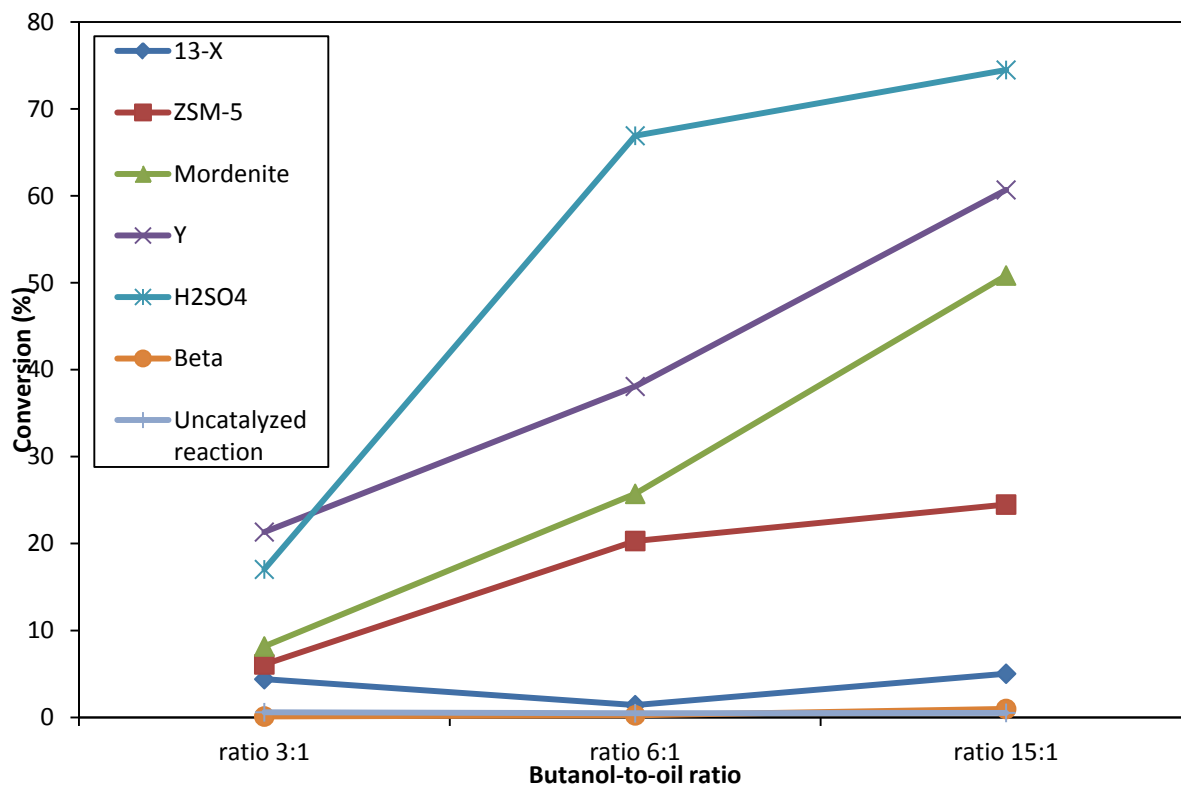


Figure 40 - Maximum conversions reached for each catalyst and each of the three butanol-to-oil molar ratio (3:1, 6:1 & 15:1) in the transesterification reaction of recreated *Jatropha* oil with butanol at 115°C

Yields reached with zeolites were usually much lower than those obtained using the liquid acid catalyst. This is consistent with the results found in the literature. Kiss et al. tested three different types of zeolites (H-ZSM-5, Y and Beta) and only observed a few percents of increase in conversion in comparison to the non-catalyzed reaction. These observations were justified by the limiting diffusion process of the bulky reactants inside the pores of the zeolites.

VI.4 – Conclusions

In our study, we saw that among the three butanol-to-oil ratio tested, the greatest one gave the best conversions with every type of catalyst. However, it is important to keep in mind that beyond the yield aspect of the reaction, the feasibility and cost of separation of the different products and remaining reactants is essential. On the one hand, contrary to homogeneous reactions, the use of zeolites allowed a simple filtration step to remove the catalyst. But on the other hand, using butanol in excess increases the miscibility of the reactants and the products making the separation of the different compounds hard and energy-consuming. On top of that, increasing the solubility and the quantity of the glycerol in the liquid phase containing the products of the transesterification reaction inevitably shifts the reaction equilibrium towards the formation of the reactants and consequently decreases the yield.

The efficiency of each zeolite is closely related to the properties of the catalyst used. At a microscopic scale, the silicon-to-aluminum ratio governs the hydrophobicity and density of acidic sites in the structure which evolve in opposite direction with respect to the Si/Al ratio. The nature of the positive counter-ion also influences the acidity of the zeolite.

The size of the pores determines if the reaction takes place within the pores or if the reactants react only on the surface of the catalyst.

At a macroscopic scale, the size of the zeolite particles have a strong impact on the efficiency of the catalysis, especially when the reaction takes place exclusively on the surface of the zeolite.

VII. *Conclusions*

This project enabled us to achieve several objectives:

- o Determine several properties of the oil used as a starting point for the production of biofuel production (Sesame oil) such as its Acid Value (AV) by titration and the exact composition of its triglycerides by CG-MS analysis. This analysis enabled us to recreate artificial Jatropha oil whose composition was accurate and very close to raw jatropha oil;

- o Implement a four-step ion-exchange process in order to obtain the X-type zeolite initially in the NH_4 -form in the desired H-form. The major issue here was the impossibility to determine accurately the amount of ion exchanged thanks to that process;

- o A further study of the ion-exchanged structure by EDX analysis allowed us to verify the efficiency of the four-step ion-exchange process previously implemented. The EDX analysis on the ZSM-5 zeolite also permitted us to know the nature of the positive counter-ion balancing the negative charge of the structure and consequently revealed to us that the zeolite did not need any other treatment than a simple calcination;

- o Testing different zeolites as solid acid catalysts in the transesterification reaction of Jatropha-type oil with butanol enabled to correlate the results of the follow up of the conversion over time with the nature and properties of the zeolites. The yields of the reaction could be explained regarding, amongst others, the Silicon-to-Aluminum ratios (i.e the acidity and hydrophobicity of the zeolite), the impact of the particle size on the efficiency of the catalysis. The pore size did not have any influence on the yields of reaction because none of the FA (and consequently, none of the mono-, di- and triglycerides) fitted into the zeolites pores. From the comparison of the different catalysts, it appeared that despite its

drawbacks regarding separations steps, homogeneous catalysis with H_2SO_4 enabled to reach better conversions than any of the acid catalysts. Among the zeolites tested, the Y-type zeolite was the more efficient solid acid catalyst and the final conversion reached after 3 hours with a butanol-to-oil molar ratio of 15:1 was around 61%.

o The study of three different butanol-to-oil molar ratios (3:1, 6:1 and 15:1) was a good way to determine the trend observed when the alcohol proportion increased with respect to the oil. In every case, the butanol-to-oil molar ratio which enabled to reach the best yields was 15:1. The comparison of the yields reached with the three tested ratios showed a clear trend: the higher butanol-to-oil molar ratio, the better yield.

VIII. *Recommendations*

This study and more particularly the implementation of the transesterification reactions in batch reactor allowed us to test different parameters of reaction as well as several zeolites as solid acid catalysts. However, it also made us aware of the almost infinite possibilities offered by this simple reaction. Complementary studies could be done in order to understand accurately the mechanism of the reaction as well as the influences of all the parameters in stake in the reaction.

Regarding the follow up of the conversion over time, our method simply enabled us to have access to the conversion of the transesterification reaction only by determination of the glycerol production. It would be worthwhile following the consumption of butanol in parallel of the production of glycerol. Indeed, due to the high FFA content of the oil, a significant proportion of the biodiesel produced comes from esterification of the FFA with butanol. Following the alcohol consumption would enable us to follow the conversions of the transesterification and the esterification at the same time and would give access to the exact quantity of biodiesel produced in the medium.

Concerning the nature of the catalyst itself, we have seen that the size of the reactants involved in that particular reaction makes the pore size almost insignificant when microporous materials are used as catalysts. Dissolving part of the framework of the catalyst could have a strong influence on the pore size and would enable to enlarge those pores increasing the active surface area and thus making the catalyst much more active. Another option would be to choose a solid acid catalyst of another nature and that possesses a much greater surface area. It would be the case with metal and mixed metal oxides such as

Zirconium, Tin, Tungsten or even Titanium oxides. Their acidic properties can be enhanced by functionalizing them by acid treatment with sulfuric or phosphoric acids for instance.

Finally, the use of heterogeneous catalysis makes the separation step much easier than with homogeneous catalysts. On top of saving time and energy thanks to the separation step itself, the interest is also to be able to recover the solid catalyst and to reuse it for the same purpose. Studying the efficiency of the recovered catalyst after several batches as well as a possible deactivation (in batch reactor) and/or leaching effect (In continuous process) would enable to determine if the catalyst can be reused without significantly losing its activity. This would fall within the objectives of finding a process able to meet the sustainable development's requirements.

References

- [1] S. Shafiee and E. Topal, "When will fossil fuel reserves be diminished?," *Energy Policy*, vol. 37, pp. 181-189, 2009.
- [2] R. J. Andres, J. S. Gregg, L. Losey, G. Marland, and T. A. Boden, "Monthly, global emissions of carbon dioxide from fossil fuel consumption," *Tellus B*, vol. 63, pp. 309-327, 2011.
- [3] B. Metz, O. Davidson, H. De Coninck, M. Loos, and L. Meyer, "IPCC special report on carbon dioxide capture and storage," Intergovernmental Panel on Climate Change, Geneva (Switzerland). Working Group III2005.
- [4] J. Chow, R. J. Kopp, and P. R. Portney, "Energy resources and global development," *Science*, vol. 302, pp. 1528-1531, 2003.
- [5] J. Janick and R. E. Paull, *The encyclopedia of fruit and nuts: Cabi*, 2008.
- [6] D. Vyas and R. Singh, "Feasibility study of Jatropha seed husk as an open core gasifier feedstock," *Renewable energy*, vol. 32, pp. 512-517, 2007.
- [7] P. PLANTS, "Jatropha curcas L," *Management*, vol. 10, p. 2.
- [8] R. Singh, D. Vyas, N. Srivastava, and M. Narra, "SPRERI experience on holistic approach to utilize all parts of Jatropha curcas fruit for energy," *Renewable Energy*, vol. 33, pp. 1868-1873, 2008.
- [9] W. Achten, L. Verchot, Y. J. Franken, E. Mathijs, V. P. Singh, R. Aerts, et al., "Jatropha bio-diesel production and use," *Biomass and Bioenergy*, vol. 32, pp. 1063-1084, 2008.
- [10] G. F. R. Staubman, N Foidl, G. M. Gübitz, R. M. Lafferty, V. M. Valencia Arbizu, "Production of biogas from J. curcas seeds press cake," *Biofuels and industrial products from Jatropha curcas roceedings from the symposium "Jatropha 97"*, vol. 31, p. 123, February 23-27 1997.
- [11] P. Radhakrishna, "Contribution of de-oiled cakes in carbon sequestration and as a source of energy," *Proceedings of the fourth international biofuels conference*, , pp. 65-70, February 1-2 2007 2007.
- [12] J. Swana, Y. Yang, M. Behnam, and R. Thompson, "An analysis of net energy production and feedstock availability for biobutanol and bioethanol," *Bioresource technology*, vol. 102, pp. 2112-2117, 2011.
- [13] D. Ramey and S.-T. Yang, "Production of butyric acid and butanol from biomass," *final report to the US Department of Energy*, Contract No.: DE-F-G02-00ER86106, 2004.
- [14] S.-T. Yang, "Extractive fermentation using convoluted fibrous bed bioreactor " USA Patent, 1993.
- [15] D. E. Ramey, "Continuous two stage, dual path anaerobic fermentation of butanol and other organic solvents using two different strains of bacteria," USA Patent, 1996.
- [16] M. Galbe and G. Zacchi, "Pretreatment of lignocellulosic materials for efficient bioethanol production," *Adv Biochem Eng Biotechnol*, vol. 108, pp. 41-65, 2007.
- [17] A. Demirbaş, "Gaseous products from biomass by pyrolysis and gasification: effects of catalyst on hydrogen yield," *Energy Conversion and Management*, vol. 43, pp. 897-909, 2002.
- [18] J. A. Sotolongo, P. Beatón Soler, A. Díaz, S. Montes de Oca, Y. del Valle, S. García Pavón, et al., "Jatropha curcas L. as a source for the production of biodiesel: a cuban experience," in *15th European Biomass Conference and Exhibition*, 2007, 7-10 May, Berlin, Germany, 2007, pp. 2631-2633.
- [19] D. Mohan, C. U. Pittman Jr, and P. H. Steele, "Pyrolysis of wood/biomass for bio-oil: a critical review," *Energy & Fuels*, vol. 20, pp. 848-889, 2006.
- [20] C. Prasad, M. Krishna, C. Reddy, and K. Mohan, "Performance evaluation of non-edible vegetable oils as substitute fuels in low heat rejection diesel engines," *Proceedings of the Institution of Mechanical Engineers, Part D: Journal of Automobile Engineering*, vol. 214, pp. 181-187, 2000.

- [21] T. T. Kywe and M. M. Oo, "Production of biodiesel from *Jatropha* oil (*Jatropha curcas*) in pilot plant," *Proceeding of World Academy of Science and Technology*, vol. 38, pp. 481-487, 2009.
- [22] K. Pramanik, "Properties and use of *Jatropha curcas* oil and diesel fuel blends in compression ignition engine," *Renewable energy*, vol. 28, pp. 239-248, 2003.
- [23] Z. Helwani, M. Othman, N. Aziz, J. Kim, and W. Fernando, "Solid heterogeneous catalysts for transesterification of triglycerides with methanol: A review," *Applied Catalysis A: General*, vol. 363, pp. 1-10, 2009.
- [24] t. N. P. S. Biomass, "*Jatropha* Assessment Agronomy, socio-economic issues, and ecology," Copernicus Institute, Utrecht University Technical University, Eindhoven Plant Research International, Wageningen UR November 2010.
- [25] C. Pohl, "*Jatropha*: money doesn't grow on trees. Ten reasons why *jatropha* is neither a profitable nor sustainable investment," *Friends of the Earth International*, Amsterdam, 2010.
- [26] J. v. Reppert-Bismarck, "Biofuel *jatropha* falls from wonder-crop pedestal," in *Reuters*, ed. Brussels, 2011.
- [27] S. Kumar, A. Chaube, and S. K. Jain, "Sustainability issues for promotion of *Jatropha* biodiesel in Indian scenario: A review," *Renewable and Sustainable Energy Reviews*, vol. 16, pp. 1089-1098, 2012.
- [28] D. Darnoko and M. Cheryan, "Kinetics of palm oil transesterification in a batch reactor," *Journal of the American Oil Chemists' Society*, vol. 77, pp. 1263-1267, 2000.
- [29] B. D. I. F. d. P. Gérard Hillion, "IMPROVED METHOD FOR MAKING ETHYL ESTERS FROM NATURAL FATS," FRANCE Patent, 2006.
- [30] A. T. M. GHAZI, M. G. RESUL, R. Yunus, and T. S. YAW, "Preliminary design of oscillatory flow biodiesel reactor for continuous biodiesel production from *jatropha* triglycerides," *Journal of Engineering Science and Technology*, vol. 3, pp. 138-145, 2008.
- [31] H. Nouredini and D. Zhu, "Kinetics of transesterification of soybean oil," *Journal of the American Oil Chemists' Society*, vol. 74, pp. 1457-1463, 1997.
- [32] G. Kildiran, S. Ö. Yücel, and S. Türkay, "In-situ alcoholysis of soybean oil," *Journal of the American Oil Chemists' Society*, vol. 73, pp. 225-228, 1996.
- [33] M. A. Dasari, M. J. Goff, and G. J. Suppes, "Noncatalytic alcoholysis kinetics of soybean oil," *Journal of the American oil chemists' society*, vol. 80, pp. 189-192, 2003.
- [34] B. Freedman, E. Pryde, and T. Mounts, "Variables affecting the yields of fatty esters from transesterified vegetable oils," *Journal of the American Oil Chemists' Society*, vol. 61, pp. 1638-1643, 1984.
- [35] B. Freedman, R. O. Butterfield, and E. H. Pryde, "Transesterification kinetics of soybean oil 1," *Journal of the American Oil Chemists' Society*, vol. 63, pp. 1375-1380, 1986.
- [36] J. M. Marchetti, V. U. Miguel, and A. F. Errazu, "Possible methods for biodiesel production," *Renewable and Sustainable Energy Reviews*, vol. 11, pp. 1300-1311, 2007.
- [37] A. K. Endalew, Y. Kiros, and R. Zanzi, "Inorganic heterogeneous catalysts for biodiesel production from vegetable oils," *Biomass and Bioenergy*, vol. 35, pp. 3787-3809, 2011.
- [38] S. Zheng, M. Kates, M. A. Dubé, and D. D. McLean, "Acid-catalyzed production of biodiesel from waste frying oil," *Biomass and Bioenergy*, vol. 30, pp. 267-272, 2006.
- [39] H. Fukuda, A. Kondo, and H. Noda, "Biodiesel fuel production by transesterification of oils," *Journal of bioscience and bioengineering*, vol. 92, pp. 405-416, 01/01 2001.
- [40] D. Nimcevic, R. Puntigam, M. Wörgetter, and J. R. Gapes, "Preparation of rapeseed oil esters of lower aliphatic alcohols," *Journal of the American Oil Chemists' Society*, vol. 77, pp. 275-280, 2000.
- [41] A. Srivastava and R. Prasad, "Triglycerides-based diesel fuels," *Renewable and sustainable energy reviews*, vol. 4, pp. 111-133, 2000.
- [42] F. Chai, F. Cao, F. Zhai, Y. Chen, X. Wang, and Z. Su, "Transesterification of Vegetable Oil to Biodiesel using a Heteropolyacid Solid Catalyst," *Advanced Synthesis & Catalysis*, vol. 349, pp. 1057-1065, 2007.

- [43] J. R. Kastner, J. Miller, D. P. Geller, J. Locklin, L. H. Keith, and T. Johnson, "Catalytic esterification of fatty acids using solid acid catalysts generated from biochar and activated carbon," *Catalysis Today*, 2012.
- [44] L. Wang and J. Yang, "Transesterification of soybean oil with nano-MgO or not in supercritical and subcritical methanol," *Fuel*, vol. 86, pp. 328-333, 2007.
- [45] X. Liu, H. He, Y. Wang, and S. Zhu, "Transesterification of soybean oil to biodiesel using SrO as a solid base catalyst," *Catalysis Communications*, vol. 8, pp. 1107-1111, 2007.
- [46] W. Xie and Z. Yang, "Ba-ZnO catalysts for soybean oil transesterification," *Catalysis Letters*, vol. 117, pp. 159-165, 2007.
- [47] W. Xie, H. Peng, and L. Chen, "Calcined Mg-Al hydrotalcites as solid base catalysts for methanolysis of soybean oil," *Journal of Molecular Catalysis A: Chemical*, vol. 246, pp. 24-32, 2006.
- [48] X. Liu, X. Piao, Y. Wang, S. Zhu, and H. He, "Calcium methoxide as a solid base catalyst for the transesterification of soybean oil to biodiesel with methanol," *Fuel*, vol. 87, pp. 1076-1082, 2008.
- [49] J. Jitputti, B. Kitiyanan, P. Rangsunvigit, K. Bunyakiat, L. Attanatho, and P. Jenvanitpanjakul, "Transesterification of crude palm kernel oil and crude coconut oil by different solid catalysts," *Chemical Engineering Journal*, vol. 116, pp. 61-66, 2006.
- [50] S. Furuta, H. Matsushashi, and K. Arata, "Biodiesel fuel production with solid amorphous-zirconia catalysis in fixed bed reactor," *Biomass and Bioenergy*, vol. 30, pp. 870-873, 2006.
- [51] M. Sasidharan and R. Kumar, "Transesterification over various zeolites under liquid-phase conditions," *Journal of Molecular Catalysis A: Chemical*, vol. 210, pp. 93-98, 2004.
- [52] A. Brito, M. Borges, and N. Otero, "Zeolite Y as a heterogeneous catalyst in biodiesel fuel production from used vegetable oil," *Energy & Fuels*, vol. 21, pp. 3280-3283, 2007.
- [53] S. Shah and M. N. Gupta, "Lipase catalyzed preparation of biodiesel from *Jatropha* oil in a solvent free system," *Process Biochemistry*, vol. 42, pp. 409-414, 2007.
- [54] N. U. Soriano, R. Venditti, and D. S. Argyropoulos, "Biodiesel synthesis via homogeneous Lewis acid-catalyzed transesterification," *Fuel*, vol. 88, pp. 560-565, 2009.
- [55] D. Kusdiana and S. Saka, "Effects of water on biodiesel fuel production by supercritical methanol treatment," *Bioresource technology*, vol. 91, pp. 289-295, 2004.
- [56] N. Boz and M. Kara, "Solid base catalyzed transesterification of canola oil," *Chemical Engineering Communications*, vol. 196, pp. 80-92, 2008.
- [57] P. D. Patil, V. G. Gude, and S. Deng, "Biodiesel production from *jatropha curcas*, waste cooking, and *camelina sativa* oils," *Industrial & Engineering Chemistry Research*, vol. 48, pp. 10850-10856, 2009.
- [58] M. L. Granados, M. Poves, D. M. Alonso, R. Mariscal, F. C. Galisteo, R. Moreno-Tost, et al., "Biodiesel from sunflower oil by using activated calcium oxide," *Applied Catalysis B: Environmental*, vol. 73, pp. 317-326, 2007.
- [59] X. Liu, H. He, Y. Wang, S. Zhu, and X. Piao, "Transesterification of soybean oil to biodiesel using CaO as a solid base catalyst," *Fuel*, vol. 87, pp. 216-221, 2008.
- [60] M. C. Albuquerque, I. Jiménez-Urbistondo, J. Santamaría-González, J. M. Mérida-Robles, R. Moreno-Tost, E. Rodríguez-Castellón, et al., "CaO supported on mesoporous silicas as basic catalysts for transesterification reactions," *Applied Catalysis A: General*, vol. 334, pp. 35-43, 2008.
- [61] W. Xie, H. Peng, and L. Chen, "Transesterification of soybean oil catalyzed by potassium loaded on alumina as a solid-base catalyst," *Applied Catalysis A: General*, vol. 300, pp. 67-74, 2006.
- [62] H.-J. Kim, B.-S. Kang, M.-J. Kim, Y. M. Park, D.-K. Kim, J.-S. Lee, et al., "Transesterification of vegetable oil to biodiesel using heterogeneous base catalyst," *Catalysis Today*, vol. 93, pp. 315-320, 2004.
- [63] Z. Yang and W. Xie, "Soybean oil transesterification over zinc oxide modified with alkali earth metals," *Fuel processing technology*, vol. 88, pp. 631-638, 2007.

- [64] W. Xie and X. Huang, "Synthesis of biodiesel from soybean oil using heterogeneous KF/ZnO catalyst," *Catalysis Letters*, vol. 107, pp. 53-59, 2006.
- [65] W. Xie, Z. Yang, and H. Chun, "Catalytic properties of lithium-doped ZnO catalysts used for biodiesel preparations," *Industrial & Engineering Chemistry Research*, vol. 46, pp. 7942-7949, 2007.
- [66] S. Benjapornkulaphong, C. Ngamcharussrivichai, and K. Bunyakiat, " Al_2O_3 -supported alkali and alkali earth metal oxides for transesterification of palm kernel oil and coconut oil," *Chemical Engineering Journal*, vol. 145, pp. 468-474, 2009.
- [67] H.-y. Zeng, Z. Feng, X. Deng, and Y.-q. Li, "Activation of Mg-Al hydrotalcite catalysts for transesterification of rape oil," *Fuel*, vol. 87, pp. 3071-3076, 2008.
- [68] M. Di Serio, M. Cozzolino, R. Tesser, P. Patrono, F. Pinzari, B. Bonelli, et al., "Vanadyl phosphate catalysts in biodiesel production," *Applied Catalysis A: General*, vol. 320, pp. 1-7, 2007.
- [69] S. Ramu, N. Lingaiah, B. Prabhavathi Devi, R. Prasad, I. Suryanarayana, and P. Sai Prasad, "Esterification of palmitic acid with methanol over tungsten oxide supported on zirconia solid acid catalysts: effect of method of preparation of the catalyst on its structural stability and reactivity," *Applied Catalysis A: General*, vol. 276, pp. 163-168, 2004.
- [70] J. Kaita, T. Mimura, N. Fukuoka, and Y. Hattori, "Catalyst for transesterification," ed: Google Patents, 2002.
- [71] B. Delfort, G. Hillion, D. Le Pennec, and C. Lendresse, "Process for transesterification of vegetable oils or animal oils by means of heterogeneous catalysts based on zinc or bismuth, titanium and aluminium," ed: Google Patents, 2006.
- [72] H. Chen, B. Peng, D. Wang, and J. Wang, "Biodiesel production by the transesterification of cottonseed oil by solid acid catalysts," *Frontiers of Chemical Engineering in China*, vol. 1, pp. 11-15, 2007.
- [73] A. Zieba, L. Matachowski, J. Gurgul, E. Bielańska, and A. Drelinkiewicz, "Transesterification reaction of triglycerides in the presence of Ag-doped $\text{H}_3\text{PW}_{12}\text{O}_{40}$," *Journal of Molecular Catalysis A: Chemical*, vol. 316, pp. 30-44, 2010.
- [74] N. Katada, T. Hatanaka, M. Ota, K. Yamada, K. Okumura, and M. Niwa, "Biodiesel production using heteropoly acid-derived solid acid catalyst $\text{H}_4\text{PNbW}_{11}\text{O}_{40}/\text{WO}_3\text{Nb}_2\text{O}_5$," *Applied Catalysis A: General*, vol. 363, pp. 164-168, 2009.
- [75] S. Shamshuddin and N. Nagaraju, "Liquid phase transesterification of methyl salicylate and phenol over solid acids: Kinetic studies," *Journal of Molecular Catalysis A: Chemical*, vol. 273, pp. 55-63, 2007.
- [76] Q. Shu, B. Yang, H. Yuan, S. Qing, and G. Zhu, "Synthesis of biodiesel from soybean oil and methanol catalyzed by zeolite beta modified with La^{3+} ," *Catalysis Communications*, vol. 8, pp. 2159-2165, 2007.
- [77] A. A. Kiss, F. Omota, A. C. Dimian, and G. Rothenberg, "The heterogeneous advantage: biodiesel by catalytic reactive distillation," *Topics in Catalysis*, vol. 40, pp. 141-150, 2006.
- [78] H. Li and W. Xie, "Transesterification of soybean oil to biodiesel with Zn/I_2 catalyst," *Catalysis Letters*, vol. 107, pp. 25-30, 2006.
- [79] P. Sreeprasanth, R. Srivastava, D. Srinivas, and P. Ratnasamy, "Hydrophobic, solid acid catalysts for production of biofuels and lubricants," *Applied Catalysis A: General*, vol. 314, pp. 148-159, 2006.
- [80] O. L. Bernardes, J. V. Bevilaqua, M. C. Leal, D. M. Freire, and M. A. Langone, "Biodiesel fuel production by the transesterification reaction of soybean oil using immobilized lipase," *Applied Biochemistry and Biotechnology*, pp. 105-114, 2007.
- [81] H. He, T. Wang, and S. Zhu, "Continuous production of biodiesel fuel from vegetable oil using supercritical methanol process," *Fuel*, vol. 86, pp. 442-447, 2007.
- [82] W. M. Meier, "Molecular sieves," *Society of Chemical Industry, London*, p. 10, 1968.
- [83] D. W. Breck, *Zeolite molecular sieves: structure, chemistry, and use* vol. 4: Wiley New York, 1973.

- [84] K. Kusakabe, T. Kuroda, A. Murata, and S. Morooka, "Formation of a Y-type zeolite membrane on a porous α -alumina tube for gas separation," *Industrial & engineering chemistry research*, vol. 36, pp. 649-655, 1997.
- [85] K.-i. Okamoto, H. Kita, K. Horii, and K. T. Kondo, "Zeolite NaA membrane: preparation, single-gas permeation, and pervaporation and vapor permeation of water/organic liquid mixtures," *Industrial & engineering chemistry research*, vol. 40, pp. 163-175, 2001.
- [86] V. Van Hoof, C. Dotremont, and A. Buekenhoudt, "Performance of Mitsui NaA type zeolite membranes for the dehydration of organic solvents in comparison with commercial polymeric pervaporation membranes," *Separation and purification technology*, vol. 48, pp. 304-309, 2006.
- [87] J. Purdy, "Chernobyl: Portrait of a Catastrophe," *University of Georgia Research magazine*, 1992.
- [88] T. Okuhara, "Water-tolerant solid acid catalysts," *Chemical Reviews*, vol. 102, pp. 3641-3665, 2002.
- [89] W. Farneth and R. Gorte, "Methods for characterizing zeolite acidity," *Chemical reviews*, vol. 95, pp. 615-635, 1995.
- [90] C. B. L. B. McCusker. Database of Zeolite Structures: <http://www.iza-structure.org/databases/>.
- [91] M. J. Ramos, C. M. Fernández, A. Casas, L. Rodríguez, and Á. Pérez, "Influence of fatty acid composition of raw materials on biodiesel properties," *Bioresource Technology*, vol. 100, pp. 261-268, 2009.
- [92] *Determination of Fatty acid composition of Oils and Fats by Gas Liquid Chromatography vol. Laboratory Manual 2. Manual of Methods of Analysis of Foods oils and Fats*, 2005.
- [93] *Determination of the acid value and the acidity using standard method*, Vysoká škola chemicko-technologická v Praze (Institute of Chemical Technology, Prague (ICT)).
- [94] J.-L. Burgot, "Neutralization or Acid-Base Indicators," in *Ionic Equilibria in Analytical Chemistry*, ed: Springer, 2012, pp. 127-134.
- [95] J. R. Kanicky and D. O. Shah, "Effect of Degree, Type, and Position of Unsaturation on the pKa of Long-Chain Fatty Acids," *Journal of colloid and interface science*, vol. 256, pp. 201-207, 2002.
- [96] L. S. Hwang, "Sesame Oil," ed: Wiley-Interscience [Imprint], 2005.
- [97] L. Peter, F. Schuth, T. S. Zhao, H. Frei, and M. Crocker, *Thermochemical conversion of biomass to liquid fuels and chemicals vol. 1: Royal Society of Chemistry*, 2010.
- [98] R. O'Connor and S. F. Herb, "Specifications of fatty acid composition for identification of fats and oils by gas liquid chromatography," *Journal of the American Oil Chemists Society*, vol. 47, pp. 186A-195A, 1970/05/01 1970.
- [99] C. Alimentarius, "Codex standard for named vegetable oils," *Codex Stan*, vol. 210, p. 1999, 1999.
- [100] A. Kamal-Eldin and L. Å. Appelqvist, "Variation in fatty acid composition of the different acyl lipids in seed oils from four *Sesamum* species," *Journal of the American oil chemists' society*, vol. 71, pp. 135-139, 1994.
- [101] V. Ruiz-Gutiérrez and L. J. Barron, "Methods for the analysis of triacylglycerols," *Journal of chromatography. B, Biomedical applications*, vol. 671, pp. 133-68, 09/15 1995.
- [102] A. S. Braithwaite, F.J.; Stock, R.(Ralph) "Chromatographic methods (4th edition)," pp. 294 - 321, 1985.
- [103] E. Akbar, Z. Yaakob, S. K. Kamarudin, M. Ismail, and J. Salimon, "Characteristic and composition of *Jatropha curcas* oil seed from Malaysia and its potential as biodiesel feedstock," *European Journal of Scientific Research*, vol. 29, pp. 396-403, 2009.
- [104] S. Hachicha, S. Barrek, T. Skanji, Z. Ghrabi, and H. Zarrouk, "Composition chimique de l'huile des graines d'*Onopordon nervosum* subsp. *platylepis* Murb (asteracees)," *JOURNAL-SOCIETE CHIMIQUE DE TUNISIE*, vol. 9, p. 23, 2007.

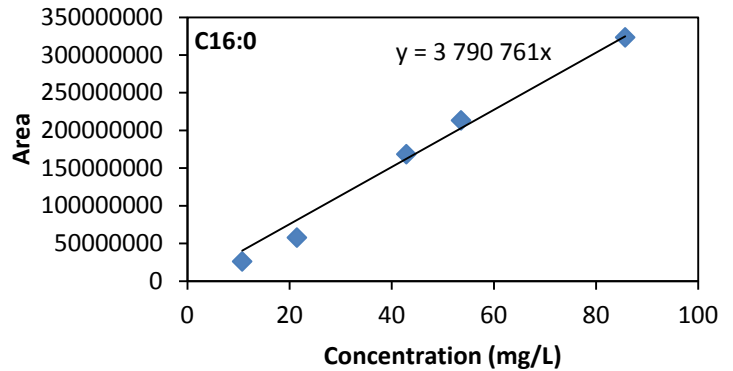
- [105] J. V. Gerpen, "Biodiesel processing and production," *Fuel processing technology*, vol. 86, pp. 1097-1107, 06 2005.
- [106] R. Richard, "Transestérification éthanolique d'huile végétale dans des microréacteurs : transposition du batch au continu," *Doctorat (PhD), Sciences des Agroressources, Institut National Polytechnique de Toulouse (INP Toulouse), Université de Toulouse*, 2011.
- [107] S. H. Khan, "Acid value of vegetable oils and poultry feed as affected by storage period and antioxidants," *Pakistan veterinary journal*, vol. 21, 2001.
- [108] S. Pinzi, L. M. Gandia, G. Arzamendi, J. J. Ruiz, and M. P. Dorado, "Influence of vegetable oils fatty acid composition on reaction temperature and glycerides conversion to biodiesel during transesterification," *Bioresour Technol*, vol. 102, pp. 1044-50, Jan 2011.
- [109] S. Pinzi, J. M. Mata-Granados, F. J. Lopez-Gimenez, M. D. Luque de Castro, and M. P. Dorado, "Influence of vegetable oils fatty-acid composition on biodiesel optimization," *Bioresour Technol*, vol. 102, pp. 1059-65, Jan 2011.
- [110] H. S. Sherry, "The design of ion-exchange processes," *Zeolites*, vol. 13, pp. 377-383, 1993.
- [111] S. M. A. Howard S. Sherry, Kathleen A. Carrado, Prabir K. Dutta, "Ion Exchange," in *Handbook of Zeolite Science and Technology*, I. Marcel Dekker, Ed., ed: Marcel Dekker Inc., 2003.
- [112] T. C. Jorgensen, "Ammonia removal from wastewater by ion exchange in the presence of organic contaminants," *Water research (Oxford)*, vol. 37, pp. 1723-1728, 04 2003.
- [113] C. H. B. Richard D. Bezman, J.B. Butt, *Chemical stability of hydrothermally dealuminated Y-type zeolite: a catalyst manufacturer and user's perspective* In. *Catalyst deactivation. Chevron research and technology company (USA): Elsevier Science publishers*, 1991.
- [114] J. Rabo, "Stability of Zeolites in Acid Media. In: *Zeolite Chemistry and Catalysis*," *American Chemical Society*, pp. 294-298, 1976.
- [115] E. Ivanova, M. Karsheva, and B. Koumanova, "Adsorption of ammonium ions onto natural zeolite," *Journal of the University of Chemical Technology and Metallurgy*, vol. 45, pp. 295-302, 2010.
- [116] H. Zheng, Y. Zheng, L. Han, and H. Ma, "Adsorption characteristics of ammonium ion by zeolite 13X," *Journal of hazardous materials*, vol. 158, pp. 577-584, 01/01 2008.
- [117] U. M. Georg Heinrich Grosch, Andreas Walch, Norbert Rieber, Wolfgang Harder, "United States Patent: 6491861," *Germany Patent*, 2002.
- [118] C. Cuvelier, J.-F. Cabaraux, I. Dufrasne, J.-L. Hornick, and L. Istasse, "Acides gras: nomenclature et sources alimentaires," *Ann. Med. Vet*, vol. 148, pp. 133-140, 2004.
- [119] B. Freedman and M. O. Bagby, "Predicting cetane numbers of n-alcohols and methyl esters from their physical properties," *Journal of the American Oil Chemists' Society*, vol. 67, pp. 565-571, 1990.
- [120] M. Lanza, W. B. Neto, E. Batista, R. J. Poppi, and A. J. Meirelles, "Liquid-liquid equilibrium data for reactional systems of ethanolysis at 298.3 K," *Journal of Chemical & Engineering Data*, vol. 53, pp. 5-15, 2007.
- [121] R. M. Barrer, *Hydrothermal chemistry of zeolites* vol. 15: Academic Press London, 1982.
- [122] S. Pinzi, L. Gandía, G. Arzamendi, J. Ruiz, and M. Dorado, "Influence of vegetable oils fatty acid composition on reaction temperature and glycerides conversion to biodiesel during transesterification," *Bioresource technology*, vol. 102, pp. 1044-1050, 2011.
- [123] H. Wright, J. Segur, H. Clark, S. Coburn, E. Langdon, and R. DuPuis, "A report on ester interchange," *Journal of the American Oil Chemists' Society*, vol. 21, pp. 145-148, 1944.

IX. Appendices

Appendix A: Standard curves obtained for the calibration of the gas chromatograph

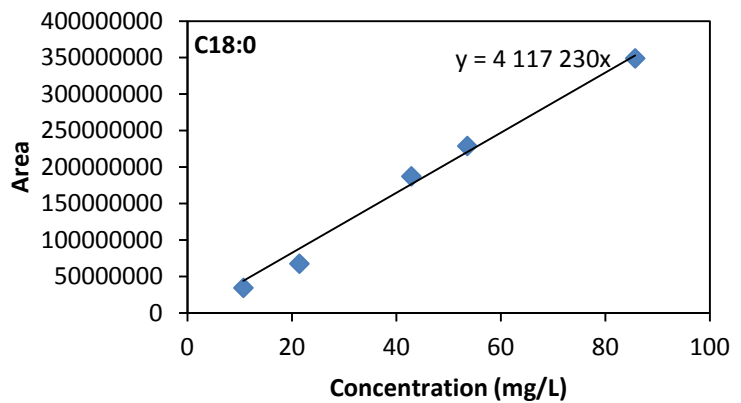
• Palmitic acid (C16:0)

| Concentration (mg/L) | Area 1 | Area 2 | Average Area |
|----------------------|-----------|-----------|--------------|
| 10,71 | 18460738 | 33701595 | 26081167 |
| 21,43 | 57949846 | 57509115 | 57729481 |
| 42,86 | 175942163 | 160765586 | 168353875 |
| 53,57 | 207678116 | 218711866 | 213194991 |
| 85,71 | 292296095 | 354361128 | 323328612 |



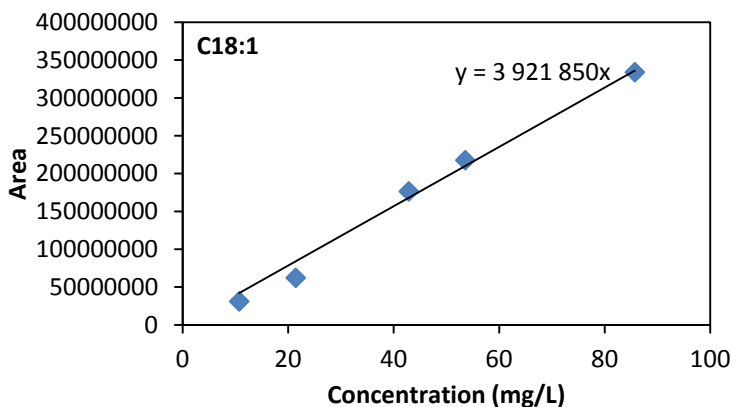
• Stearic acid (C18:0)

| Concentration (mg/L) | Area 1 | Area 2 | Average Area |
|----------------------|-----------|-----------|--------------|
| 10,71 | 29619138 | 39059948 | 34339543 |
| 21,43 | 65964524 | 68917591 | 67441058 |
| 42,86 | 192412754 | 181875514 | 187144134 |
| 53,57 | 223814977 | 233687313 | 228751145 |
| 85,71 | 321211184 | 376479379 | 348845282 |



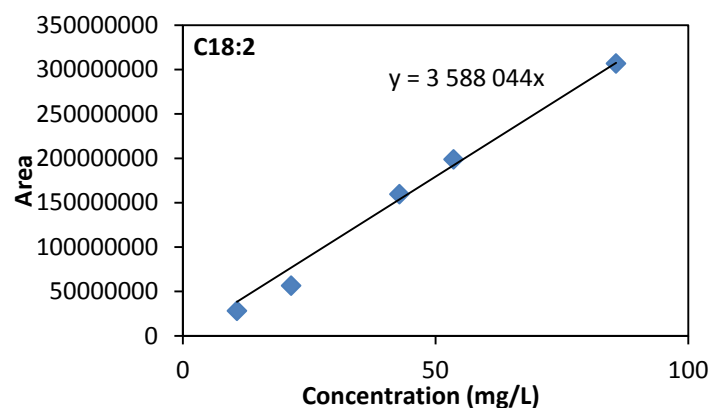
• Oleic acid (C18:1)

| Concentration (mg/L) | Area 1 | Area 2 | Average Area |
|----------------------|-----------|-----------|--------------|
| 10,71 | 25998501 | 36094614 | 31046558 |
| 21,43 | 61244079 | 63212556 | 62228318 |
| 42,86 | 182724237 | 170251804 | 176488021 |
| 53,57 | 212254024 | 223103247 | 217678636 |
| 85,71 | 305969728 | 362081682 | 334025705 |



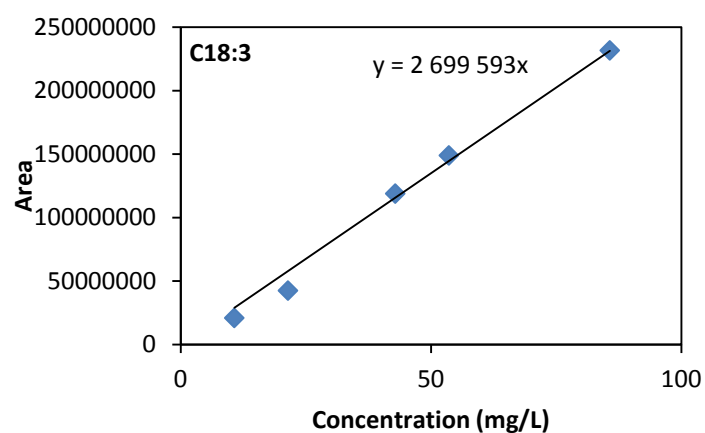
• Linoleic acid (C18:2)

| Concentration (mg/L) | Area 1 | Area 2 | Average Area |
|----------------------|-----------|-----------|--------------|
| 10,71 | 23380765 | 33026347 | 28203556 |
| 21,43 | 55645815 | 57479312 | 56562564 |
| 42,86 | 165292868 | 153954759 | 159623814 |
| 53,57 | 193023693 | 204624675 | 198824184 |
| 85,71 | 281321744 | 332354873 | 306838309 |



• Linolenic acid (C18:3)

| Concentration (mg/L) | Area 1 | Area 2 | Average Area |
|----------------------|-----------|-----------|--------------|
| 10,71 | 17463609 | 24523904 | 20993757 |
| 21,43 | 42035607 | 43057674 | 42546641 |
| 42,86 | 123392966 | 114542144 | 118967555 |
| 53,57 | 144263456 | 153811415 | 149037436 |
| 85,71 | 212694089 | 250914103 | 231804096 |



Appendix B: Determination by calculation of the quantity of FA needed to recreate Jatropha oil from Sesame oil

In the chromatogram obtain thanks to the GC-MS analysis of the transesterified sesame oil, clear peaks corresponding to each FAME present in the solution of FAMES in hexane can be observed.

The area of each peak is related to the concentration of the corresponding FAME in the sample.

However, a calibration of the device had to be done with a standard solution containing the expected FAMES with a perfectly known concentration. The purpose of this calibration is to know correlate the output of the GC-MS analysis with the actual concentration of the compounds in the sample. **Table 21** indicates the area of each peak (arbitrary unit) detected while analyzing the calibration sample (left column) and the studied sample (right column). The sample analyzed for the calibration was a solution of hexane containing the five following FAMES: Palmitic Acid (C 16:0), Stearic Acid (C 18:0), Oleic Acid (C 18:1 cis 9), Linoleic Acid (C 18:2 cis 9, cis 12) and α -Linolenic Acid (C 18:3 cis 9, cis 12, cis 15). It is of paramount importance that the calibration is done with a solution containing the compounds that are going to be detected later with a perfectly well know concentration for each compound and in the same conditions of chromatography. In the calibration sample, the concentration of each FAME was known and equaled to $1\text{mg}\cdot\text{L}^{-1}$.

| | Calibration sample – Peak Area | Studied sample – Peak Areas | Relative peak area |
|--------------------|--------------------------------|-----------------------------|--------------------|
| Palmitic (C16:0) | 3790761 | 10064930 | 265.5122 |
| Stearic (C18:0) | 4117230 | 15494233 | 376.3267 |
| Oleic (C18:1) | 3121850 | 49799556 | 1269.7976 |
| Linoleic (C18:2) | 3588044 | 63611289 | 1772.8681 |
| Linolenic (C18 :3) | 2699593 | ND ¹ | - |
| Total | 17317478 | 138970008 | 3684.5043 |

Table 21 - Peaks' areas for the calibration sample, the studied sample and Relative peak area (Arbitrary unit)
ND¹: Non Detected

On the calibration curve, in spite of the differences observed in the areas of the peaks, all of them correspond to the same concentration ($1\text{mg}\cdot\text{L}^{-1}$) of a different FAME. That is why the area under the peak obtained while analyzing our sample has to be balanced out regarding the area found for the same compound on the standard curve. For each FA, a relative peak area is found following the method detailed below:

$$\text{Relative peak area} = 100 \cdot \frac{\text{Area of the peak in the studied sample}}{\text{Area of the peak in the calibration sample}}$$

The numerical values for each FA detected in the studied sample can be found on the right column of **Table 21**. The relative peak areas allowed us to obtain the molar fraction of each FAME in the studied sample. Also, we assumed that the molar fraction of each FA in the FFA phase was equal to the molar fraction of the corresponding FAME derived from the oil by transesterification. Assuming this and knowing the measured acid value (AV) of the crude sesame oil ($\text{AV}_{\text{sesame oil}} = 1.374 \text{ mg}_{\text{KOH}}/\text{g}_{\text{oi}}$ which corresponds to $2.5 \times 10^{-5} \text{ mol}_{\text{FA}}/\text{g}_{\text{oil}}$) enabled us to know the quantity of matter of each FA present in the FFA part of the crude oil (**Table 22**).

| | Sesame oil | | Jatropha oil [103] | |
|-------------------------|----------------|---|--------------------|---|
| | Molar Fraction | Quantity of matter ($\times 10^{-5}$) [mol] | Molar fraction | Quantity of matter ($\times 10^{-4}$) [mol] |
| Palmitic (C16:0) | 0.0721 | 0.1802 | 0.143 | 0.715 |
| Stearic (C18:0) | 0.1021 | 0.2553 | 0.071 | 0.355 |
| Oleic (C18:1) | 0.3446 | 0.8616 | 0.453 | 2.265 |
| Linoleic (C18:2) | 0.4812 | 1.2029 | 0.333 | 1.665 |
| Total | 1 | 2.5 | 1 | 5 |

Table 22 - Amount of each FA in the FFA fraction of both oils

For each Fatty Acid FA_i , the amount N_{FA_i} of FA_i that needed to be added to the sesame oil was computed according to the formulas below:

$$\text{For the Palmitic acid: } x_{\text{Palm},J} = \frac{N_{\text{Palm}} + N_{\text{Palm},S}}{\sum_{\text{FA}} N_{\text{FA},S} + N_{\text{Palm}} + N_{\text{Stea}} + N_{\text{Olei}} + N_{\text{Lino}}}$$

$$\text{For the Stearic acid: } x_{\text{Stea},J} = \frac{N_{\text{Stea}} + N_{\text{Stea},S}}{\sum_{\text{FA}} N_{\text{FA},S} + N_{\text{Palm}} + N_{\text{Stea}} + N_{\text{Olei}} + N_{\text{Lino}}}$$

For the Oleic acid:
$$x_{Olei,J} = \frac{N_{Olei} + N_{Olei,S}}{\sum_{FA} N_{FA,S} + N_{Palm} + N_{Stea} + N_{Olei} + N_{Lino}}$$

For the Linoleic acid:
$$x_{Lino,J} = \frac{N_{Lino} + N_{Lino,S}}{\sum_{FA} N_{FA,S} + N_{Palm} + N_{Stea} + N_{Olei} + N_{Lino}}$$

With $x_{FAi,J}$ the molar fraction of the particular FAi in the Jatropha oil, Note that $\sum_i x_{FAi,J} = 1$
 N_{FAi} the quantity of matter [mol] of the particular FAi that has to be added to 1g of oil,
 $N_{FAi,S}$ the quantity of matter [mol] of the particular FAi in 1g of the Sesame oil.

We have 4 equations (one for each FA) with the 4 values of N_{FAi} as unknowns. However, those 4 equations are not independent and another one has to be found in order to replace one of the 4 equations of the system and make the new system independent. The new independent equation which is introduced related both AVs:

$$N_{FA,J} = N_{FA,S} + N_{Palm} + N_{Stea} + N_{Olei} + N_{Lino}$$

With $N_{FA,J}$ the total quantity of matter [mol] of FA in 1g of the Jatropha oil,
 $N_{FA,S}$ the quantity of matter [mol] of the particular FAi that has to be added to 1g of oil.

Eventually the system of 4 independents equations where the 4 unknowns are the N_{FAi} is:

$$\left\{ \begin{array}{l} x_{Palm,J} = \frac{N_{Palm} + N_{Palm,S}}{\sum_{FA} N_{FA,S} + N_{Palm} + N_{Stea} + N_{Olei} + N_{Lino}} \\ x_{Stea,J} = \frac{N_{Stea} + N_{Stea,S}}{\sum_{FA} N_{FA,S} + N_{Palm} + N_{Stea} + N_{Olei} + N_{Lino}} \\ x_{Olei,J} = \frac{N_{Olei} + N_{Olei,S}}{\sum_{FA} N_{FA,S} + N_{Palm} + N_{Stea} + N_{Olei} + N_{Lino}} \\ N_{FA,J} = N_{FA,S} + N_{Palm} + N_{Stea} + N_{Olei} + N_{Lino} \end{array} \right.$$

Solving the system lead to the final results:

$$\left\{ \begin{array}{l} N_{Palm} = 6.97 \cdot 10^{-5} \text{ mol} \\ N_{Stea} = 3.29 \cdot 10^{-5} \text{ mol} \\ N_{Olei} = 21.79 \cdot 10^{-5} \text{ mol} \\ N_{Lino} = 15.45 \cdot 10^{-5} \text{ mol} \end{array} \right.$$

Table 23 gathers the weight of each FA per gram of sesame oil that needs to be added in order to obtain oil which has similar properties as Jatropha oil.

| | Molecular weight [g.mol ⁻¹] | Quantity of matter (x10 ⁻⁵) [mol] | Weight added [mg] |
|-------------------------|---|---|-------------------|
| Palmitic (C16:0) | 256.42 | 6.97 | 17.87 |
| Stearic (C18:0) | 284.44 | 3.29 | 9.36 |
| Oleic (C18:1) | 282.44 | 21.79 | 61.54 |
| Linoleic (C18:2) | 280.44 | 15.45 | 43.33 |
| Total | 1 | 2.5 | 132.1 |

Table 23 - Amount of FAs added per gram of sesame oil

Appendix C: Determination of the butanol-to-oil weight ratios corresponding to the three molar ratios

C.1 – Preliminary calculations

Before computing the actual weights of butanol and oil used, it was necessary to determine an average molecular weight of the oil \overline{M}_{oil} .

The nature and amount of each FA (whether as FFA or inside the triglycerides' structure) in the oil is perfectly known (See section III.3 and III.4). This enabled us to compute the average molecular weight of FAs (\overline{M}_{FA}), triglycerides (\overline{M}_{trig}) and finally the number of moles of triglyceride (N_{trig}) per gram of oil.

$$\begin{aligned}\overline{M}_{FA} &= \sum_i x_{FAi,J} M_{FAi} = x_{Palm,oil} M_{Palm} + x_{Stea,oil} M_{Stea} + x_{Olei,oil} M_{Olei} + x_{Lino,oil} M_{Lino} \\ &= 0.142 \times 256.42 + 0.07 \times 284.44 + 0.447 \times 282.44 + 0.328 \times 280.44 \\ &= 274.56 \text{ g. mol}^{-1}\end{aligned}$$

Since the structure of the triglyceride derives from the structure of the FAs, we obtain:

$$\overline{M}_{trig} = 3(\overline{M}_{FA} - M_H) + M_{glycerol} - 3M_{OH} = 3(274.56 - 1) + 92 - 3 \times 18 = 864.68 \text{ g. mol}^{-1}$$

The AV of the oil allows us to compute the weight of FFA per gram of oil:

$$m_{FFA} = N_{FFA} \overline{M}_{FA} = 5 \times 10^{-4} \times 274.56 = 0.1373 \text{ g}$$

This leads to the number of moles of triglycerides per gram of oil:

$$N_{trig} = \frac{m_{trig}}{\overline{M}_{trig}} = \frac{1 - m_{FFA}}{\overline{M}_{trig}} = \frac{0.8627}{864.68} = 9.98 \times 10^{-4} \text{ mol} \approx 1 \text{ mmol}$$

C.2 – Determination of the butanol-to-oil weight ratio for each experiment

The purpose of the calculation is to find, for each butanol-to-oil ratio, the weights of each liquid that have to be mixed in order to fill the Parr reactor (400mL). The density of the butanol was taken from the supplier (Sigma-Aldrich) and the specific gravity of the modified oil was measured.

We had $d_{butanol} = 810 \text{ g.L}^{-1}$ and $d_{oil} = 918 \text{ g.L}^{-1}$.

We solved a two-equation system with two unknowns: the weight of each liquid: m_{but} and m_{oil} . The first equation is a volumetric equation. The second one expresses the molar ratio:

$$\begin{cases} V_{reactor} = V_{oil} + V_{but} = \frac{m_{oil}}{d_{oil}} + \frac{m_{but}}{d_{but}} \\ N_{but} = N_{trig} \end{cases}$$

Knowing the densities of both liquids and the fact that there was $9.98 \times 10^{-4} \text{ mol}$ of triglycerides per gram of oil, we ended up with the following numerical system:

$$\begin{cases} 0.4 = \frac{m_{oil}}{918} + \frac{m_{but}}{810} \\ m_{but} = 74 \times 9.98 \times 10^{-4} \times Ratio_{But/oil} \times m_{oil} \end{cases}$$

Table 24 gathers the amounts of each liquid involved in each reaction depending on the molar ratio.

| Molar Ratio | Weight of butanol [g] | Weight of oil [g] | Weight Ratio |
|----------------|-----------------------|-------------------|--------------|
| 3 to 1 | 65,023 | 293,51 | 0,22 to 1 |
| 6 to 1 | 108,46 | 244,28 | 0,44 to 1 |
| 9 to 1 | 139,21 | 209,44 | 0,66 to 1 |
| 15 to 1 | 180,35 | 162,8 | 1,11 to 1 |
| 30 to 1 | 231,72 | 104,59 | 2,21 to 1 |

Table 24 – Amounts of each liquid according to the butanol-to-oil molar ratio

Eventually, these amounts were the amount used with each zeolite. The amount of zeolite added in each batch was equal to 1% to the total weight of liquid in the reactor. **Table 25** gives the weight of solid acid catalyst used in each batch. Note that the amount of zeolite (in grams) does not depend on its nature.

| Molar Ratio | Weight of zeolite [g] |
|---------------|-----------------------|
| 3 to 1 | 3.58 |
| 6 to 1 | 3.53 |

| | |
|----------------|------|
| 9 to 1 | 3.48 |
| 15 to 1 | 3.43 |
| 30 to 1 | 3.36 |

Table 25 – Weight of each zeolite with respect to the molar ratio in each batch

Appendix D: EDX Analysis reports

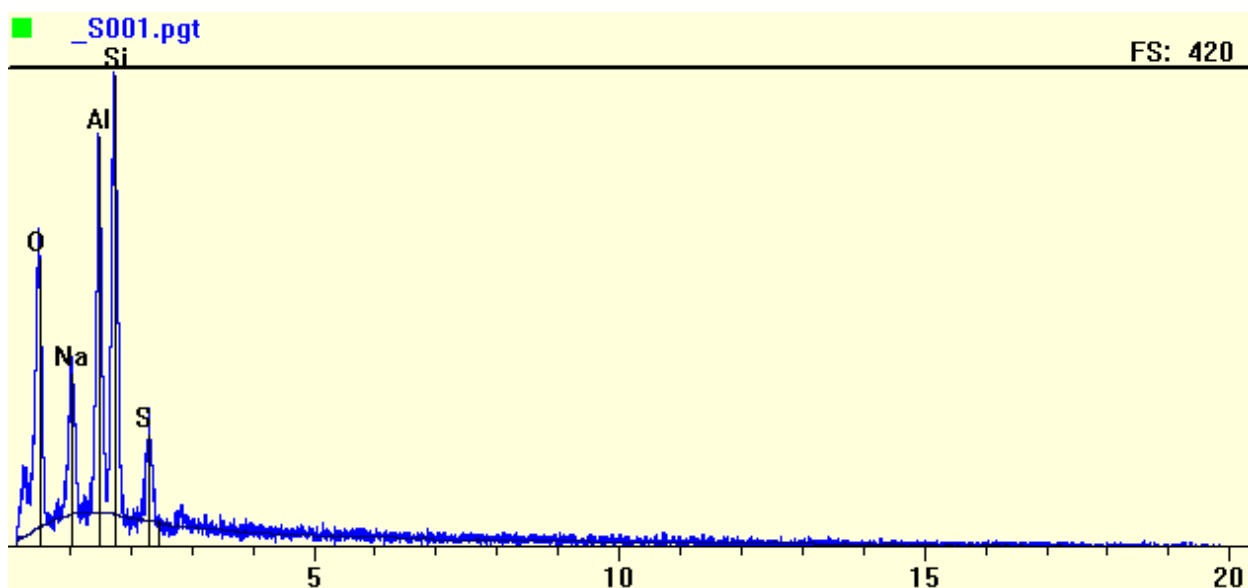
- *First analysis of the powder of 13-X-type zeolite before ion exchange*

Princeton Gamma-Tech, Inc.

Spectrum Report
Monday, December 10, 2012

File: C:\susan\MQP\spray dryer thursday group_S001.pgt
Collected: December 10, 2012 14:17:27

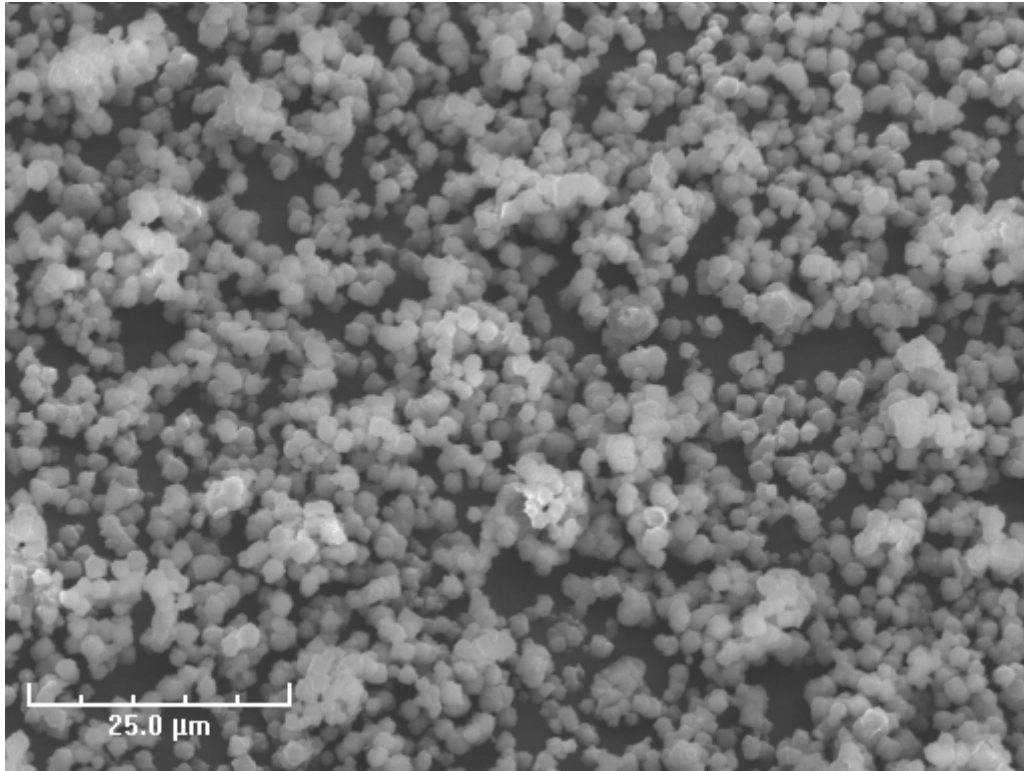
Live Time: 118.95 Count Rate: 471 Dead Time: 14.85 %
Beam Voltage: 15.00 Beam Current: 2.00 Takeoff Angle: 59.51



| Element | Line | keV | KRatio | Wt% | At% | ChiSquared |
|--------------|------|-------|--------|---------------|---------------|-------------|
| Na | KA1 | 1.041 | 0.0747 | 10.48 | 9.90 | 1.66 |
| Al | KA1 | 1.487 | 0.1647 | 20.12 | 16.21 | 2.55 |
| Si | KA1 | 1.740 | 0.2155 | 27.18 | 21.03 | 2.55 |
| O | KA1 | 0.523 | 0.2057 | 35.65 | 48.41 | 21.73 |
| S | KA1 | 2.307 | 0.0523 | 6.56 | 4.45 | 1.59 |
| Total | | | | 100.00 | 100.00 | 5.80 |

| Element | Line | Gross (cps) | BKG (cps) | Overlap (cps) | Net (cps) |
|---------|------|-------------|-----------|---------------|-----------|
| Na | KA1 | 26.1 | 5.5 | 0.0 | 20.6 |
| Al | KA1 | 54.1 | 6.1 | 0.0 | 48.0 |
| Si | KA1 | 67.2 | 6.0 | 0.0 | 61.2 |
| O | KA1 | 39.3 | 3.1 | 0.0 | 36.2 |
| S | KA1 | 18.0 | 4.9 | 0.0 | 13.2 |

| Element | Line | Det Eff | Z Corr | A Corr | F Corr | Tot Corr | Modes |
|---------|------|---------|--------|--------|--------|----------|--------|
| Na | KA1 | 0.783 | 1.034 | 1.367 | 0.993 | 1.403 | Elmnt. |
| Al | KA1 | 0.900 | 1.057 | 1.171 | 0.988 | 1.222 | Elmnt. |
| Si | KA1 | 0.889 | 1.035 | 1.221 | 0.998 | 1.261 | Elmnt. |
| O | KA1 | 0.435 | 0.931 | 1.863 | 0.999 | 1.733 | Elmnt. |
| S | KA1 | 0.898 | 1.057 | 1.187 | 1.000 | 1.254 | Elmnt. |

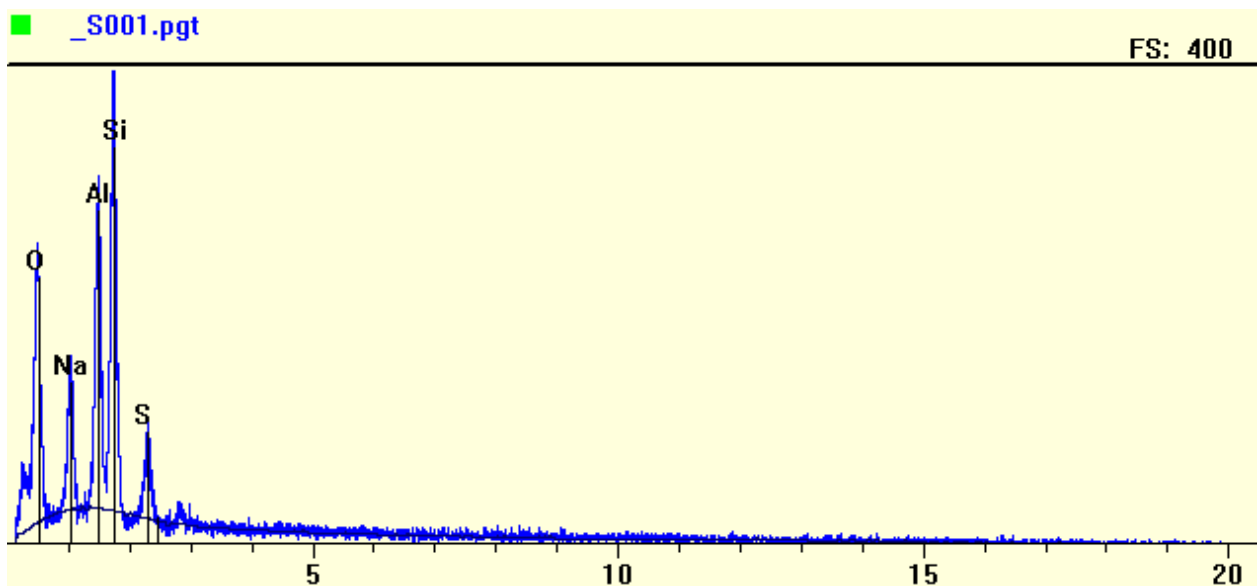


- Second analysis of the powder of 13-X-type zeolite before ion exchange

Princeton Gamma-Tech, Inc.
Spectrum Report
Monday, December 10, 2012

File: C:\susan\MQP\spray dryer thursday group_S001.pgt
Collected: December 10, 2012 14:23:58

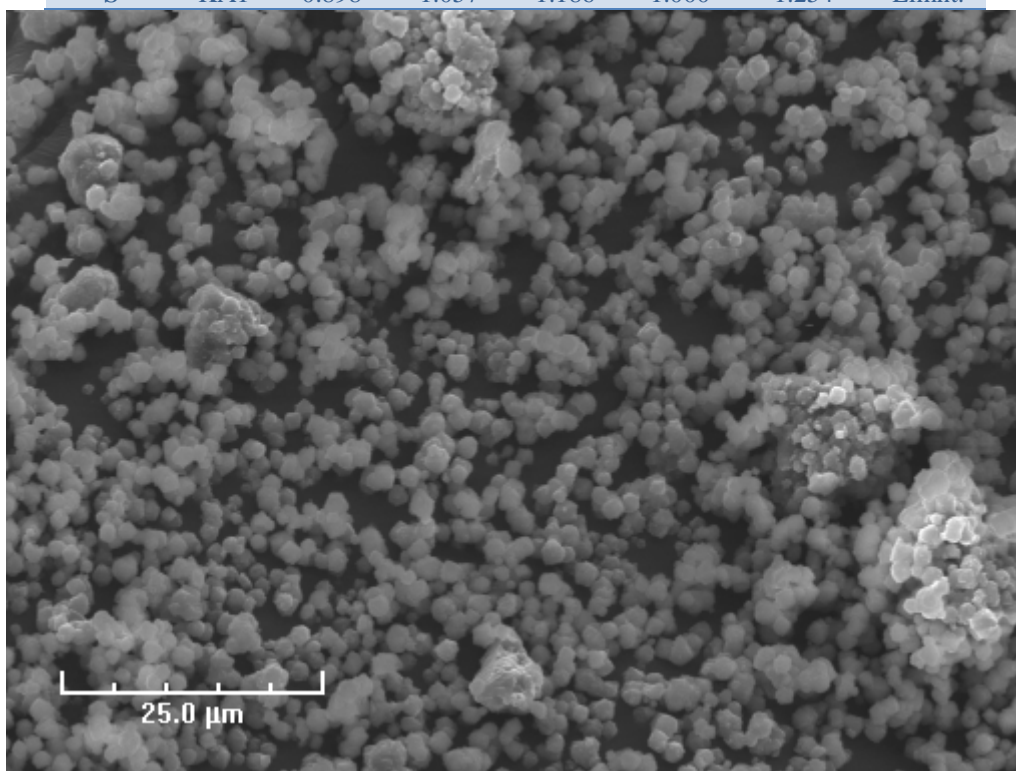
| | | |
|---------------------|--------------------|----------------------|
| Live Time: 106.92 | Count Rate: 474 | Dead Time: 14.78 % |
| Beam Voltage: 15.00 | Beam Current: 2.00 | Takeoff Angle: 59.51 |



| Element | Line | keV | KRatio | Wt% | At% | ChiSquared |
|--------------|------|-------|--------|---------------|---------------|-------------|
| Na | KA1 | 1.041 | 0.0729 | 10.25 | 9.67 | 1.22 |
| Al | KA1 | 1.487 | 0.1637 | 19.99 | 16.09 | 2.50 |
| Si | KA1 | 1.740 | 0.2151 | 27.11 | 20.95 | 2.50 |
| O | KA1 | 0.523 | 0.2069 | 35.90 | 48.71 | 20.76 |
| S | KA1 | 2.307 | 0.0539 | 6.76 | 4.58 | 1.21 |
| Total | | | | 100.00 | 100.00 | 5.48 |

| Element | Line | Gross (cps) | BKG (cps) | Overlap (cps) | Net (cps) |
|---------|------|-------------|-----------|---------------|-----------|
| Na | KA1 | 25.8 | 6.2 | 0.0 | 19.7 |
| Al | KA1 | 53.5 | 6.8 | 0.0 | 46.7 |
| Si | KA1 | 66.3 | 6.5 | 0.0 | 59.7 |
| O | KA1 | 39.3 | 3.6 | 0.0 | 35.7 |
| S | KA1 | 18.3 | 5.0 | 0.0 | 13.3 |

| Element | Line | Det Eff | Z Corr | A Corr | F Corr | Tot Corr | Modes |
|---------|------|---------|--------|--------|--------|----------|--------|
| Na | KA1 | 0.783 | 1.034 | 1.369 | 0.993 | 1.406 | Elmnt. |
| Al | KA1 | 0.900 | 1.057 | 1.170 | 0.988 | 1.221 | Elmnt. |
| Si | KA1 | 0.889 | 1.035 | 1.220 | 0.998 | 1.260 | Elmnt. |
| O | KA1 | 0.435 | 0.932 | 1.864 | 0.999 | 1.735 | Elmnt. |
| S | KA1 | 0.898 | 1.057 | 1.186 | 1.000 | 1.254 | Elmnt. |



- *Third analysis of the powder of 13-X-type zeolite before ion exchange*

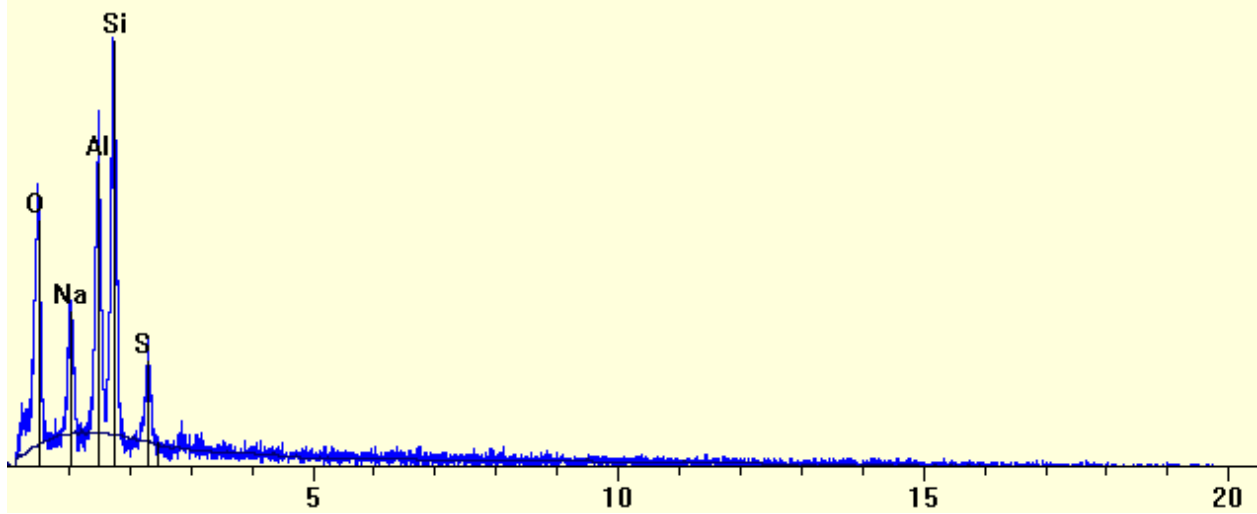
Princeton Gamma-Tech, Inc.

Spectrum Report

Monday, December 10, 2012

File: C:\susan\MQP\spray dryer thursday group_S001.pgt
 Collected: December 10, 2012 14:28:48

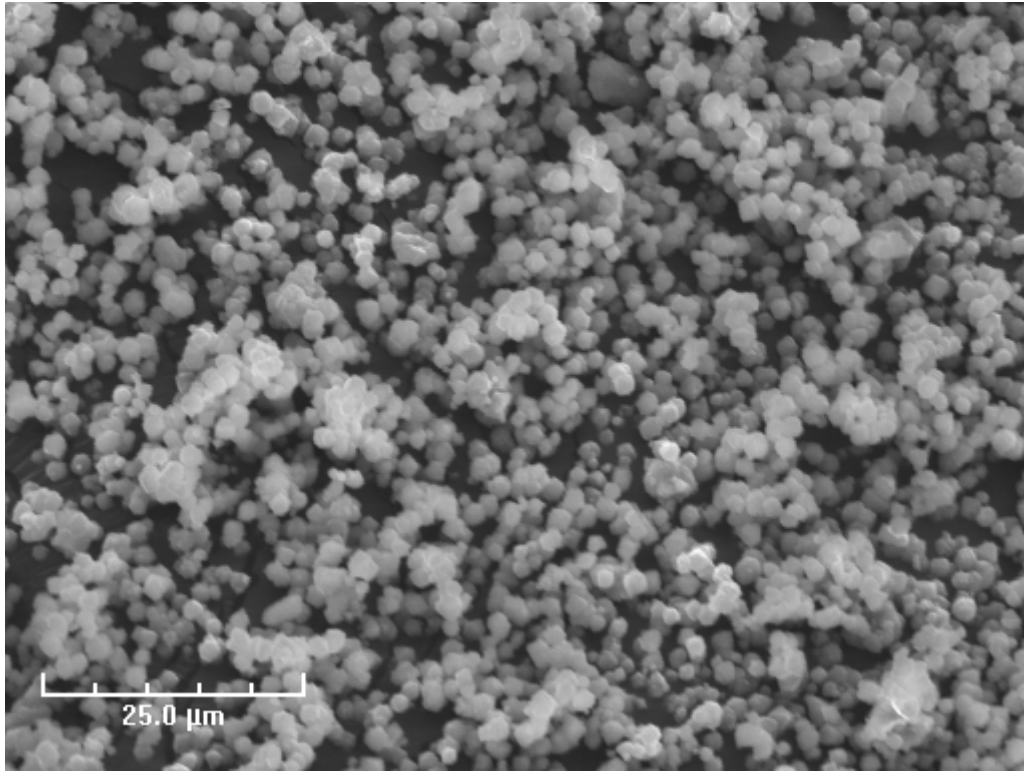
Live Time: 76.50 Count Rate: 474 Dead Time: 14.81 %
 Beam Voltage: 15.00 Beam Current: 2.00 Takeoff Angle: 59.51



| Element | Line | keV | KRatio | Wt% | At% | ChiSquared |
|--------------|------|-------|--------|---------------|---------------|-------------|
| Na | KA1 | 1.041 | 0.0720 | 10.15 | 9.57 | 0.72 |
| Al | KA1 | 1.487 | 0.1597 | 19.51 | 15.69 | 2.35 |
| Si | KA1 | 1.740 | 0.2158 | 27.13 | 20.95 | 2.35 |
| O | KA1 | 0.523 | 0.2083 | 36.17 | 49.03 | 14.57 |
| S | KA1 | 2.307 | 0.0562 | 7.04 | 4.76 | 1.30 |
| Total | | | | 100.00 | 100.00 | 3.85 |

| Element | Line | Gross (cps) | BKG (cps) | Overlap (cps) | Net (cps) |
|---------|------|-------------|-----------|---------------|-----------|
| Na | KA1 | 26.2 | 6.7 | 0.0 | 19.5 |
| Al | KA1 | 52.9 | 7.2 | 0.0 | 45.7 |
| Si | KA1 | 67.3 | 7.2 | 0.0 | 60.2 |
| O | KA1 | 40.2 | 4.2 | 0.0 | 36.0 |
| S | KA1 | 19.4 | 5.5 | 0.0 | 13.9 |

| Element | Line | Det Eff | Z Corr | A Corr | F Corr | Tot Corr | Modes |
|---------|------|---------|--------|--------|--------|----------|--------|
| Na | KA1 | 0.783 | 1.034 | 1.372 | 0.993 | 1.409 | Elmnt. |
| Al | KA1 | 0.900 | 1.057 | 1.170 | 0.988 | 1.222 | Elmnt. |
| Si | KA1 | 0.889 | 1.035 | 1.217 | 0.998 | 1.257 | Elmnt. |
| O | KA1 | 0.435 | 0.932 | 1.865 | 0.999 | 1.737 | Elmnt. |
| S | KA1 | 0.898 | 1.057 | 1.185 | 1.000 | 1.253 | Elmnt. |



- *First analysis of the powder of 13-X-type zeolite after ion exchange*

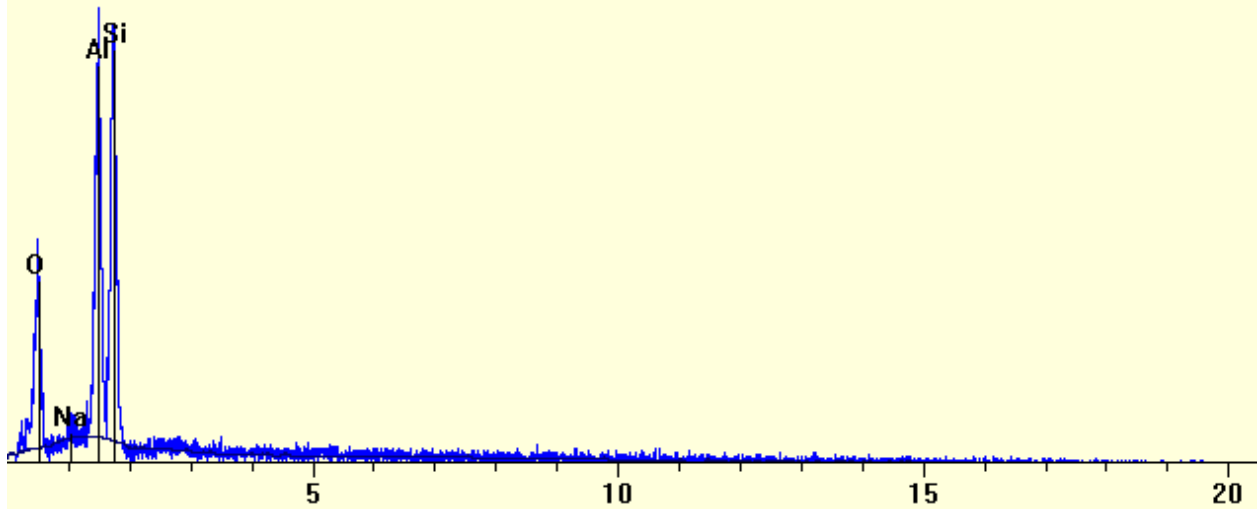
Princeton Gamma-Tech, Inc.

Spectrum Report

Monday, December 10, 2012

File: C:\susan\MQP\spray dryer thursday group_S001.pgt
Collected: December 10, 2012 14:40:33

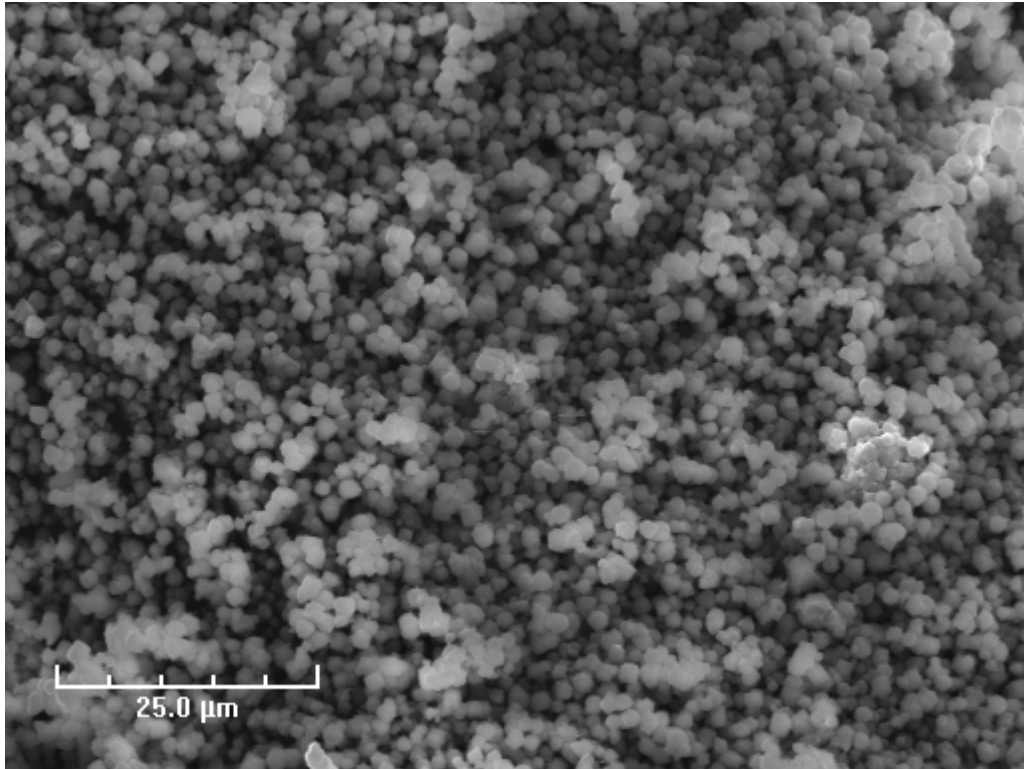
| | | | | | |
|---------------|-------|---------------|------|----------------|---------|
| Live Time: | 40.71 | Count Rate: | 623 | Dead Time: | 17.02 % |
| Beam Voltage: | 15.00 | Beam Current: | 2.00 | Takeoff Angle: | 59.51 |



| Element | Line | keV | KRatio | Wt% | At% | ChiSquared |
|--------------|------|-------|--------|---------------|---------------|-------------|
| Na | KA1 | 1.041 | 0.0064 | 0.87 | 0.85 | 0.90 |
| Al | KA1 | 1.487 | 0.2587 | 29.40 | 24.35 | 2.18 |
| Si | KA1 | 1.740 | 0.2962 | 37.54 | 29.86 | 2.18 |
| O | KA1 | 0.523 | 0.1805 | 32.19 | 44.94 | 9.80 |
| Total | | | | 100.00 | 100.00 | 2.93 |

| Element | Line | Gross (cps) | BKG (cps) | Overlap (cps) | Net (cps) |
|---------|------|-------------|-----------|---------------|-----------|
| Na | KA1 | 10.3 | 8.0 | 0.0 | 2.4 |
| Al | KA1 | 109.4 | 8.6 | 0.0 | 100.8 |
| Si | KA1 | 120.2 | 7.8 | 0.0 | 112.4 |
| O | KA1 | 46.9 | 4.4 | 0.0 | 42.5 |

| Element | Line | Det Eff | Z Corr | A Corr | F Corr | Tot Corr | Modes |
|---------|------|---------|--------|--------|--------|----------|--------|
| Na | KA1 | 0.783 | 1.029 | 1.342 | 0.988 | 1.365 | Elmnt. |
| Al | KA1 | 0.900 | 1.052 | 1.097 | 0.984 | 1.136 | Elmnt. |
| Si | KA1 | 0.889 | 1.030 | 1.230 | 1.000 | 1.267 | Elmnt. |
| O | KA1 | 0.435 | 0.927 | 1.925 | 0.999 | 1.783 | Elmnt. |



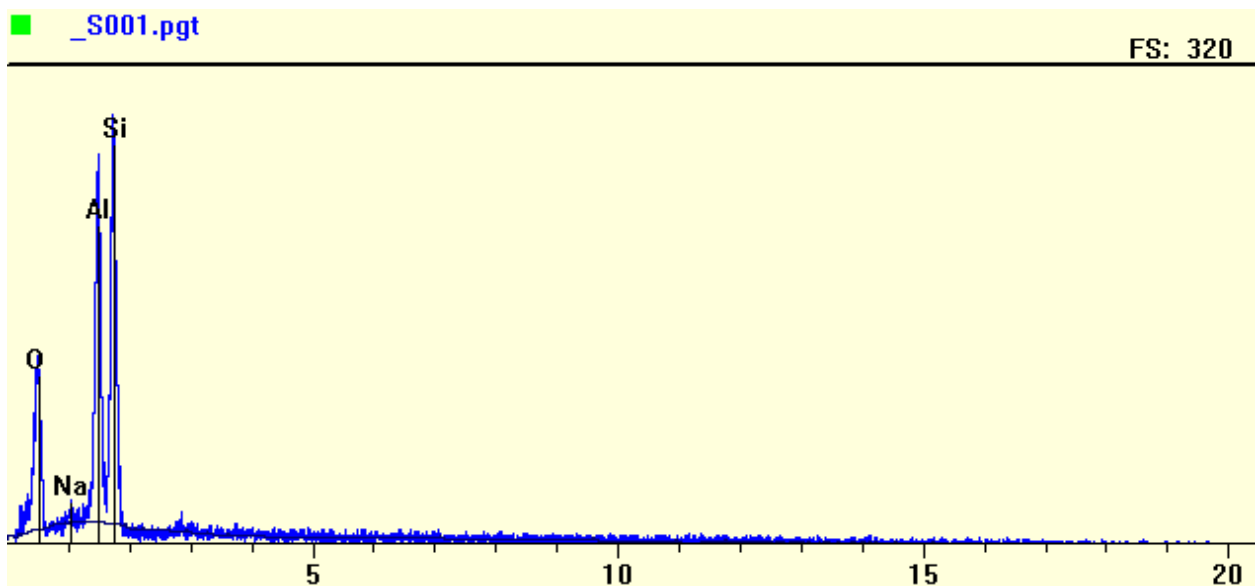
- *Second analysis of the powder of 13-X-type zeolite after ion exchange*

Princeton Gamma-Tech, Inc.

Spectrum Report
Monday, December 10, 2012

File: C:\susan\MQP\spray dryer thursday group_S001.pgt
Collected: December 10, 2012 14:48:13

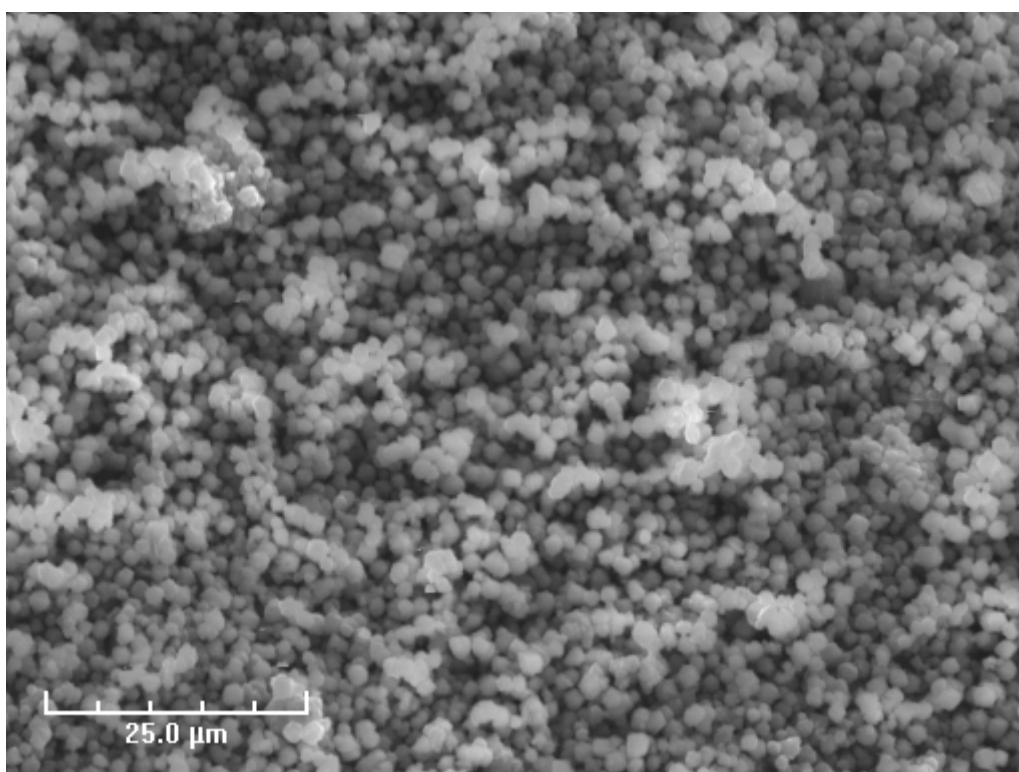
| | | | | | |
|---------------|-------|---------------|------|----------------|---------|
| Live Time: | 37.26 | Count Rate: | 701 | Dead Time: | 18.04 % |
| Beam Voltage: | 15.00 | Beam Current: | 2.00 | Takeoff Angle: | 59.51 |



| Element | Line | keV | KRatio | Wt% | At% | ChiSquared |
|--------------|------|-------|--------|---------------|---------------|-------------|
| Na | KA1 | 1.041 | 0.0065 | 0.90 | 0.87 | 0.96 |
| Al | KA1 | 1.487 | 0.2462 | 28.15 | 23.09 | 2.12 |
| Si | KA1 | 1.740 | 0.2928 | 37.04 | 29.17 | 2.12 |
| O | KA1 | 0.523 | 0.1919 | 33.91 | 46.87 | 11.63 |
| Total | | | | 100.00 | 100.00 | 3.27 |

| Element | Line | Gross (cps) | BKG (cps) | Overlap (cps) | Net (cps) |
|---------|------|-------------|-----------|---------------|-----------|
| Na | KA1 | 11.6 | 8.7 | 0.0 | 2.8 |
| Al | KA1 | 122.7 | 9.4 | 0.0 | 113.3 |
| Si | KA1 | 140.0 | 8.7 | 0.0 | 131.2 |
| O | KA1 | 58.7 | 5.3 | 0.0 | 53.4 |

| Element | Line | Det Eff | Z Corr | A Corr | F Corr | Tot Corr | Modes |
|---------|------|---------|--------|--------|--------|----------|--------|
| Na | KA1 | 0.783 | 1.031 | 1.354 | 0.989 | 1.381 | Elmnt. |
| Al | KA1 | 0.900 | 1.054 | 1.102 | 0.984 | 1.144 | Elmnt. |
| Si | KA1 | 0.889 | 1.032 | 1.225 | 1.000 | 1.265 | Elmnt. |
| O | KA1 | 0.435 | 0.929 | 1.903 | 0.999 | 1.767 | Elmnt. |



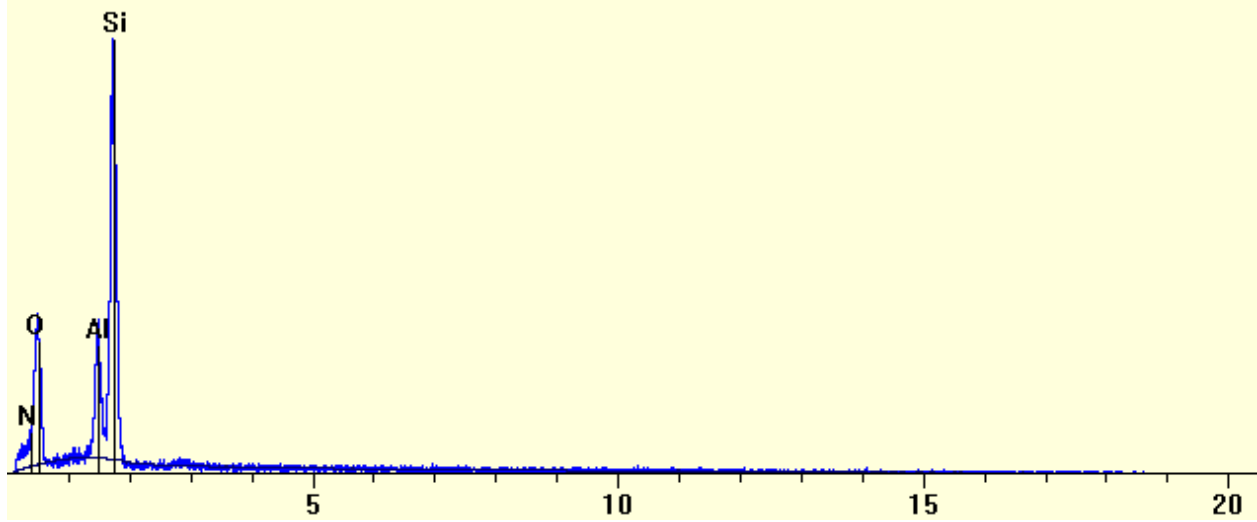
- First analysis of the ZSM-5 particles before calcination

Princeton Gamma-Tech, Inc.

Spectrum Report
Friday, January 18, 2013

File: C:\gaetan lemoine\zsm-5_S001.pgt
Collected: January 18, 2013 15:20:26

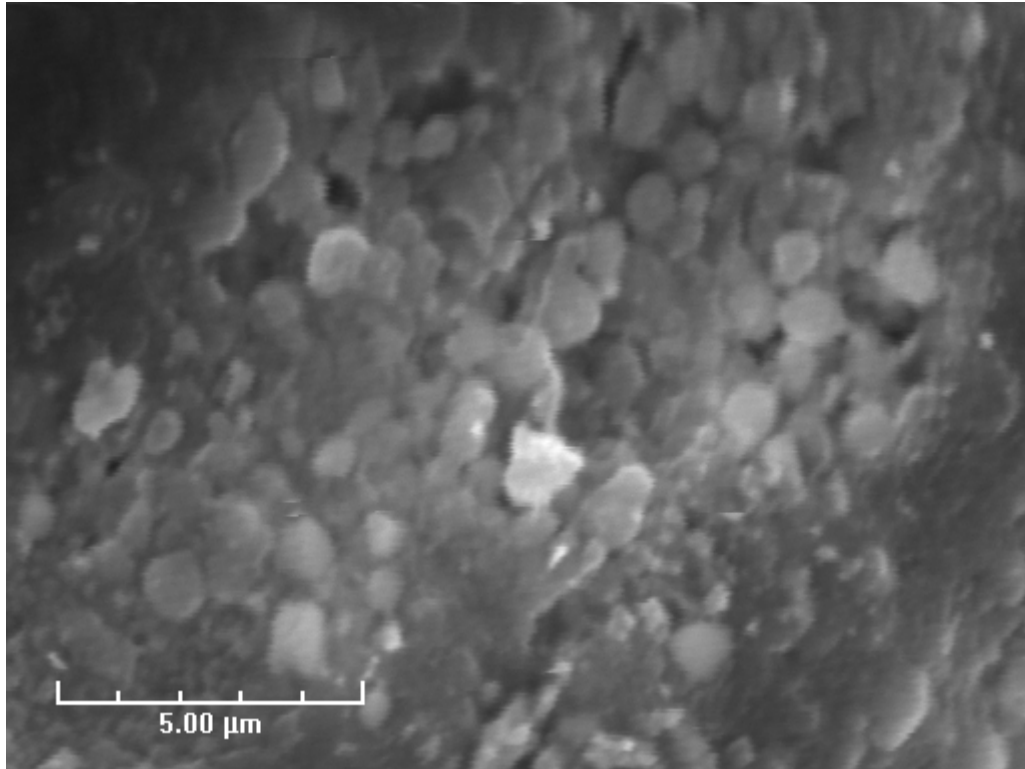
Live Time: 65.65 Count Rate: 737 Dead Time: 18.67 %
Beam Voltage: 15.00 Beam Current: 2.00 Takeoff Angle: 59.51



| Element | Line | keV | KRatio | Wt% | At% | ChiSquared |
|--------------|------|-------|--------|---------------|---------------|-------------|
| Al | KA1 | 1.487 | 0.0626 | 7.82 | 5.08 | 3.12 |
| Si | KA1 | 1.740 | 0.2068 | 25.22 | 15.75 | 3.12 |
| O | KA1 | 0.523 | 0.1027 | 30.13 | 33.04 | 14.14 |
| N | KA1 | 0.392 | 0.1761 | 36.83 | 46.13 | 14.14 |
| Total | | | | 100.00 | 100.00 | 4.57 |

| Element | Line | Gross (cps) | BKG (cps) | Overlap (cps) | Net (cps) |
|---------|------|-------------|-----------|---------------|-----------|
| Al | KA1 | 71.8 | 9.4 | 0.0 | 62.3 |
| Si | KA1 | 209.3 | 8.8 | 0.0 | 200.5 |
| O | KA1 | 67.3 | 4.9 | 0.7 | 61.8 |
| N | KA1 | 23.7 | 3.4 | 1.3 | 19.1 |

| Element | Line | Det Eff | Z Corr | A Corr | F Corr | Tot Corr | Modes |
|---------|------|---------|--------|--------|--------|----------|--------|
| Al | KA1 | 0.900 | 1.106 | 1.145 | 0.986 | 1.249 | Elmnt. |
| Si | KA1 | 0.889 | 1.083 | 1.126 | 1.000 | 1.219 | Elmnt. |
| O | KA1 | 0.435 | 0.976 | 3.009 | 1.000 | 2.935 | Elmnt. |
| N | KA1 | 0.077 | 0.951 | 2.201 | 0.999 | 2.091 | Elmnt. |

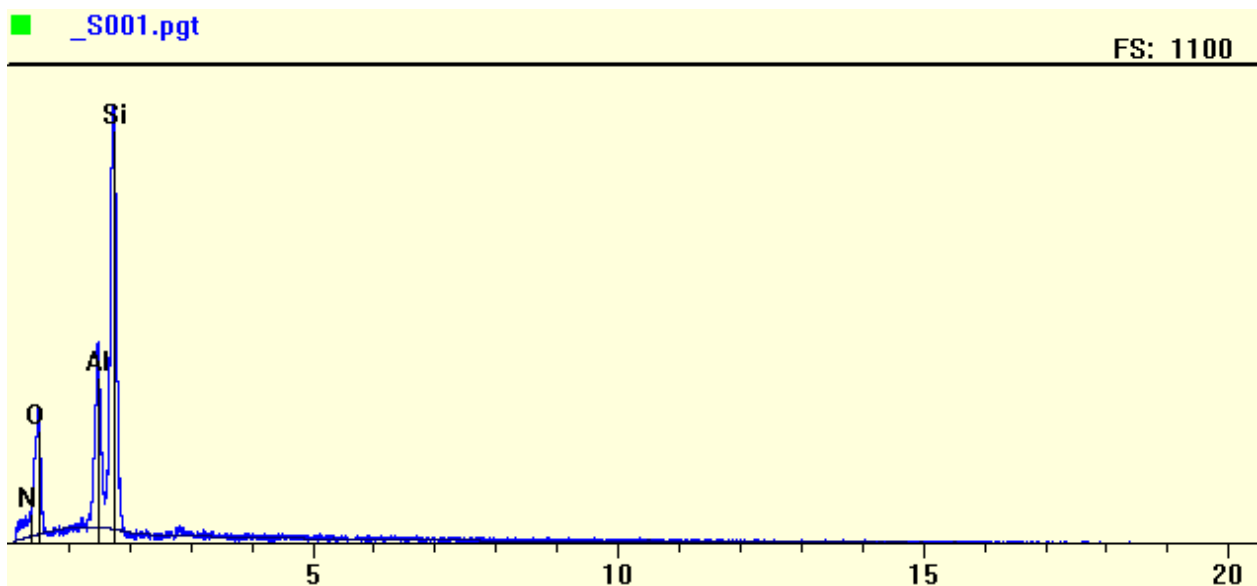


- *Second analysis of the ZSM-5 particles before calcinations*

Princeton Gamma-Tech, Inc.
Spectrum Report
Friday, January 18, 2013

File: C:\susan\MQP\spray dryer thursday group_S001.pgt
Collected: January 18, 2013 15:06:25

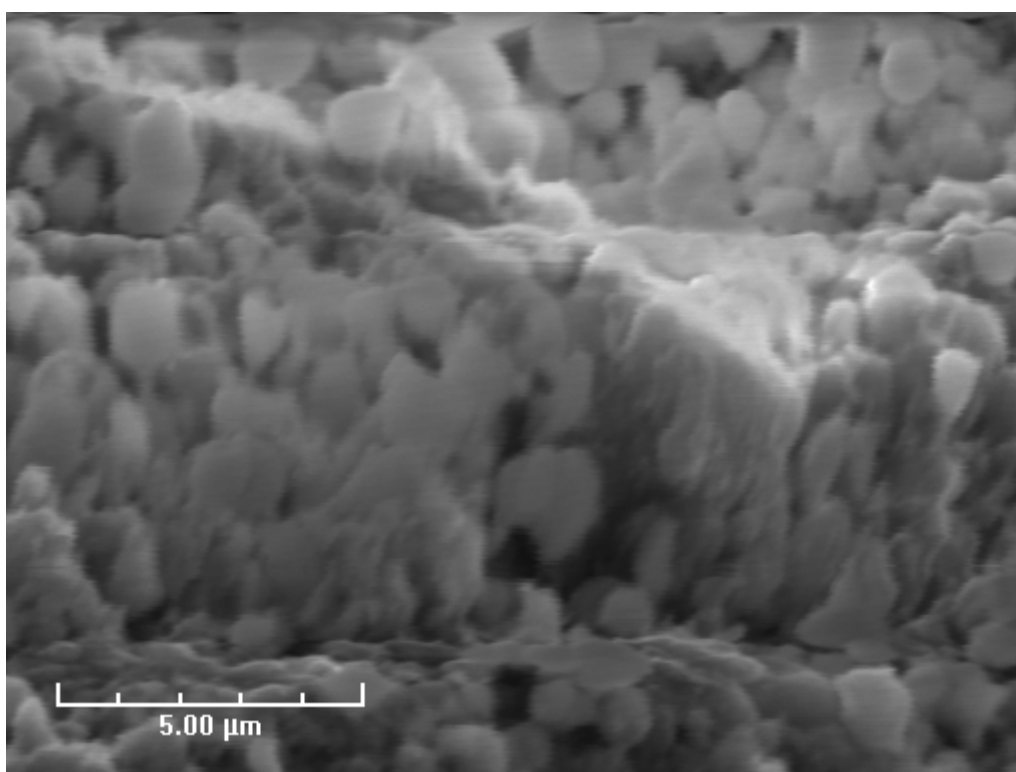
| | | | | | |
|---------------|--------|---------------|------|----------------|---------|
| Live Time: | 102.25 | Count Rate: | 663 | Dead Time: | 17.65 % |
| Beam Voltage: | 15.00 | Beam Current: | 2.00 | Takeoff Angle: | 59.51 |



| Element | Line | keV | KRatio | Wt% | At% | ChiSquared |
|--------------|------|-------|--------|---------------|---------------|-------------|
| Al | KA1 | 1.487 | 0.0916 | 11.18 | 7.55 | 4.54 |
| Si | KA1 | 1.740 | 0.2368 | 28.92 | 18.75 | 4.54 |
| O | KA1 | 0.523 | 0.0892 | 25.82 | 29.38 | 13.87 |
| N | KA1 | 0.392 | 0.1486 | 34.09 | 44.32 | 13.87 |
| Total | | | | 100.00 | 100.00 | 5.05 |

| Element | Line | Gross (cps) | BKG (cps) | Overlap (cps) | Net (cps) |
|---------|------|-------------|-----------|---------------|-----------|
| Al | KA1 | 81.9 | 8.5 | 0.0 | 73.4 |
| Si | KA1 | 192.5 | 7.7 | 0.0 | 184.7 |
| O | KA1 | 48.0 | 4.3 | 0.5 | 43.2 |
| N | KA1 | 16.7 | 2.9 | 0.9 | 12.9 |

| Element | Line | Det Eff | Z Corr | A Corr | F Corr | Tot Corr | Modes |
|---------|------|---------|--------|--------|--------|----------|--------|
| Al | KA1 | 0.900 | 1.097 | 1.130 | 0.984 | 1.220 | Elmnt. |
| Si | KA1 | 0.889 | 1.074 | 1.137 | 1.000 | 1.221 | Elmnt. |
| O | KA1 | 0.435 | 0.967 | 2.993 | 1.000 | 2.895 | Elmnt. |
| N | KA1 | 0.077 | 0.943 | 2.435 | 0.999 | 2.294 | Elmnt. |



- *Third analysis of the ZSM-5 particles before calcination*

Princeton Gamma-Tech, Inc.

Spectrum Report

Friday, January 18, 2013

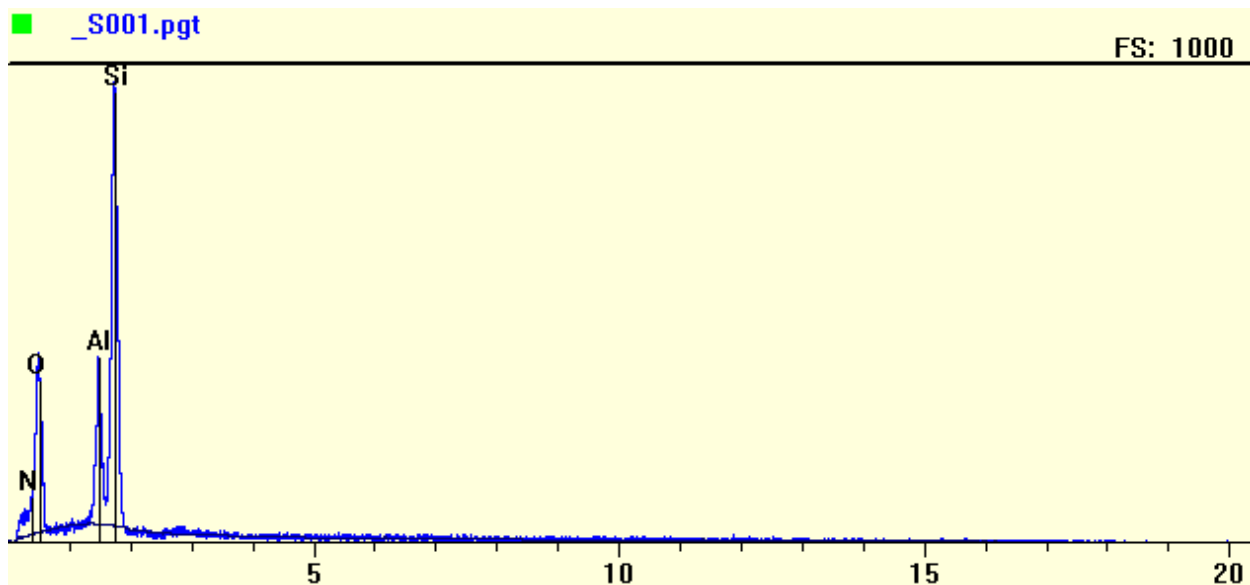
File: C:\gaetan lemoine\zsm-5_S001.pgt

Collected: January 18, 2013 15:15:44

Live Time: 59.19
 Beam Voltage: 15.00

Count Rate: 1144
 Beam Current: 2.00

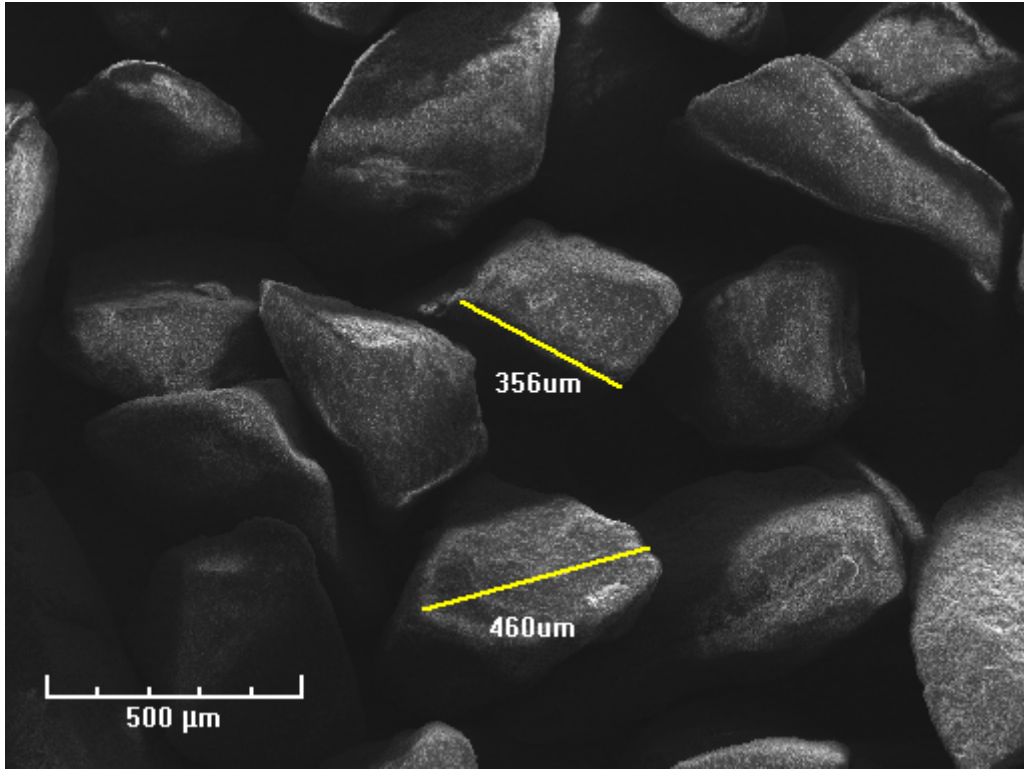
Dead Time: 23.96 %
 Takeoff Angle: 59.51



| Element | Line | keV | KRatio | Wt% | At% | ChiSquared |
|--------------|------|-------|--------|---------------|---------------|-------------|
| Al | KA1 | 1.487 | 0.0629 | 7.89 | 5.10 | 3.52 |
| Si | KA1 | 1.740 | 0.1977 | 24.17 | 15.02 | 3.52 |
| O | KA1 | 0.523 | 0.1037 | 30.56 | 33.32 | 20.52 |
| N | KA1 | 0.392 | 0.1817 | 37.38 | 46.56 | 20.52 |
| Total | | | | 100.00 | 100.00 | 5.95 |

| Element | Line | Gross (cps) | BKG (cps) | Overlap (cps) | Net (cps) |
|---------|------|-------------|-----------|---------------|-----------|
| Al | KA1 | 113.6 | 15.6 | 0.0 | 98.0 |
| Si | KA1 | 314.4 | 14.5 | 0.0 | 299.9 |
| O | KA1 | 106.3 | 7.6 | 1.1 | 97.6 |
| N | KA1 | 38.0 | 5.3 | 2.0 | 30.7 |

| Element | Line | Det Eff | Z Corr | A Corr | F Corr | Tot Corr | Modes |
|---------|------|---------|--------|--------|--------|----------|--------|
| Al | KA1 | 0.900 | 1.108 | 1.147 | 0.987 | 1.254 | Elmnt. |
| Si | KA1 | 0.889 | 1.085 | 1.127 | 1.000 | 1.223 | Elmnt. |
| O | KA1 | 0.435 | 0.977 | 3.016 | 1.000 | 2.946 | Elmnt. |
| N | KA1 | 0.077 | 0.953 | 2.163 | 0.999 | 2.057 | Elmnt. |



Appendix E: EnzyChrom Assay Kit's manual

BioAssay Systems Glycerol

EGLY003.pdf

EnzyChrom™ Glycerol Assay Kit (Cat# EGLY-200) Quantitative Colorimetric/Fluorimetric Glycerol Determination

DESCRIPTION

GLYCEROL [GLYCERIN or GLYCERINE, C₃H₅(OH)₃] is widely used in foods, beverages and pharmaceutical formulations. It is also a main by-product of biodiesel production. Simple, direct and automation-ready procedures for measuring glycerol concentrations find wide applications. BioAssay Systems' glycerol assay uses a single Working Reagent that combines glycerol kinase, glycerol phosphate oxidase and color reactions in one step. The color intensity of the reaction product at 570nm or fluorescence intensity at λ_{em}/ex = 585/530nm is directly proportional to glycerol concentration in the sample.

KEY FEATURES

Sensitive and accurate. Use as little as 10 μL samples. Linear detection range in 96-well plate: 10 to 1000 μM (92 μg/dL to 9.2 mg/dL) glycerol for colorimetric assays and 2 to 50 μM for fluorimetric assays.

Simple and convenient. The procedure involves addition of a single working reagent and incubation for 20 min at room temperature, compatible for HTS assays.

Improved reagent stability. The optimized formulation has greatly enhanced the reagent and signal stability.

APPLICATIONS:

Direct Assays: glycerol in biological samples (e.g. serum and plasma).

Drug Discovery/Pharmacology: effects of drugs on glycerol metabolism.

Food and Beverages: glycerol in food, beverages, pharmaceutical formulations etc.

KIT CONTENTS

Assay Buffer: 24 mL **Enzyme Mix:** 500 μL **ATP:** 250 μL
Dye Reagent: 220 μL **Standard:** 100 μL 100 mM Glycerol

Storage conditions. The kit is shipped on dry ice. Store Assay Buffer at 4°C and other reagents at -20°C. Shelf life of 6 months after receipt.

Precautions: reagents are for research use only. Normal precautions for laboratory reagents should be exercised while using the reagents. Please refer to Material Safety Data Sheet for detailed information.

COLORIMETRIC PROCEDURE

Note: SH-group containing reagents (e.g. mercaptoethanol, DTT) may interfere with this assay and should be avoided in sample preparation.

1. Equilibrate all components to room temperature. Keep thawed Enzyme Mix in a refrigerator or on ice. Dilute standard in distilled water as follows (diluted standards can be used for future assays when stored refrigerated).

| No | STD + H ₂ O | Vol (μL) | Glycerol (mM) |
|----|------------------------|----------|---------------|
| 1 | 10 μL + 990 μL | 1000 | 1.0 |
| 2 | 6 μL + 994 μL | 1000 | 0.6 |
| 3 | 3 μL + 997 μL | 1000 | 0.3 |
| 4 | 0 μL + 1000 μL | 1000 | 0 |

Transfer 10 μL standards and 10 μL samples into separate wells of a clear 96-well plate.

2. For each reaction well, mix 100 μL Assay Buffer, 2 μL Enzyme Mix, 1 μL ATP and 1 μL Dye Reagent in a clean tube. This Working Reagent should be used on the same day of preparation. Transfer 100 μL Working Reagent into each reaction well. Tap plate to mix.
3. Incubate 20 min at room temperature. Read optical density at 570nm (550-585nm).

Note: if the Sample OD is higher than the Standard OD at 1.0 mM, dilute sample in water and repeat the assay. Multiply result by the dilution factor.

CALCULATION

Subtract blank OD (water, #4) from the standard OD values and plot the OD against standard concentrations. Determine the slope using linear regression fitting. The glycerol concentration of Sample is calculated as

$$[\text{Glycerol}] = \frac{\text{OD}_{\text{SAMPLE}} - \text{OD}_{\text{H}_2\text{O}}}{\text{Slope}} \quad (\text{mM})$$

OD_{SAMPLE} and OD_{H₂O} are optical density values of the sample and water. **Conversions:** 1mM glycerol equals 9.2 mg/dL, 92 ppm.

FLUORIMETRIC PROCEDURE

For fluorimetric assays, the linear detection range is 2 to 50 μM glycerol. Mix 10 μL 100 mM Standard with 990 μL H₂O (final 1 mM).

| No | 1 mM STD + H ₂ O | Vol (μL) | Glycerol (mM) |
|----|-----------------------------|----------|---------------|
| 1 | 50 μL + 950 μL | 1000 | 0.050 |
| 2 | 30 μL + 970 μL | 1000 | 0.030 |
| 3 | 15 μL + 985 μL | 1000 | 0.015 |
| 4 | 0 μL + 1000 μL | 1000 | 0 |

Dilute standards as above. Transfer 10 μL standards and 10 μL samples into separate wells of a black 96-well plate.

Add 100 μL Working Reagent (see *Colorimetric Procedure*). Tap plate to mix.

Incubate 20 min at room temperature and read fluorescence at λ_{ex} = 530nm and λ_{em} = 585nm.

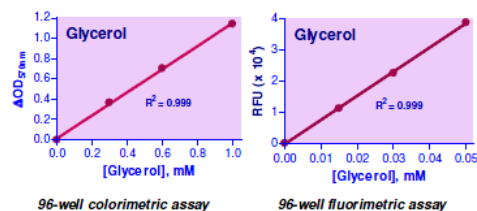
The glycerol concentration of Sample is calculated as

$$[\text{Glycerol}] = \frac{\text{F}_{\text{SAMPLE}} - \text{F}_{\text{H}_2\text{O}}}{\text{Slope}} \quad (\text{mM})$$

MATERIALS REQUIRED, BUT NOT PROVIDED

Pipeting devices, centrifuge tubes, Clear flat-bottom 96-well plates, black 96-well plates (e.g. Corning Costar) and plate reader.

Glycerol Standard Curves



LITERATURE

1. Duncan RE, et al. (2007). Regulation of lipolysis in adipocytes. *Annu Rev Nutr.* 27:79-101.
2. Moller F, Roomi MW. (1974). An enzymatic, spectrophotometric glycerol assay with increased basic sensitivity. *Anal Biochem.* 59(1):248-58.
3. MacRae AR. (1977). A semi-automated enzymatic assay for free glycerol and triglycerides in serum or plasma. *Clin Biochem.* 10(1):16-9.

Appendix F: Determination of the glycerol concentration of a sample

The main purpose of the project is to follow overtime the yield of transesterification reactions implemented with different acid catalysts (5 zeolites and sulfuric acid) and for several butanol-to-oil ratios. In order to follow the degree of conversion of the reaction, a one-step enzymatic method was chosen using the EnzyChrom Glycerol Assay Kit (Cat# EGLY-200) developed by BioAssay Systems. The analysis is based on a colorimetric procedure which allows to have access to the glycerol concentration inside the sample analyzed. The sample's Optical Density (OD) at 570nm is directly related to its concentration in glycerol. Prior to each measurement, a calibration curve based on the OD of standards whose glycerol concentration is perfectly known was done. The measurements of the OD of the calibration samples and the reaction samples were realized thanks to the Spectrometer Spectramax (model 340PC – 384). **Figure 41** shows an example of the pink coloration due to the presence of glycerol in the well.

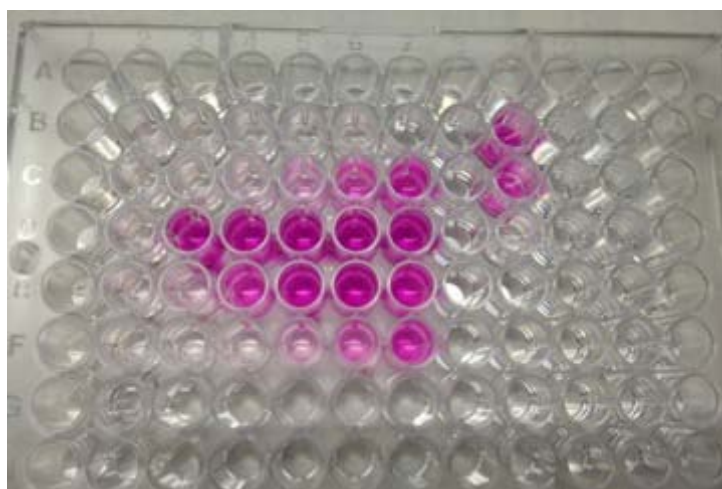


Figure 41 – The OD depends on the glycerol concentration in each well

Using this method, we assumed that glycerol was the only compound having an influence on the OD of the sample. This assumption was justified by the fact that this particular method of analysis combines glycerol kinase (which catalyzes the transfer of a

phosphate from ATP to glycerol thus forming glycerol phosphate), glycerol phosphate oxidase (which catalyzes the reaction leading to glycerone phosphate from glycerol phosphate) and a color reaction in one step. The specificity of the reactions involved in the process makes the assumption reasonable.

We can also note that on top of the precautions taken to keep the buffer and all the reagents in the freezer at -20°C between the experiments, a calibration curve was plotted simultaneously with each analysis for a better accuracy of the measurement.

A detailed method of analysis is provided in Appendix D.

Once the OD of each sample determined, the use of the slope of the calibration curve leads to the value of the concentration of the sample in mmol (1mmol = 0.092g/L of glycerol) thanks to the following formula:

$$C_{glycerol\ sample} = \frac{OD_{sample} - OD_{pure\ water}}{Slope}$$

In our case, the glycerol concentration of the sample is not the actual glycerol concentration in the reactor. Indeed, each sample is the result of a dilution of 0.5mL of reaction medium in 20mL of deionized water. As a consequence a simple dilution calculation has to be implemented to the concentration of the sample $C_{glycerol\ sample}$ in order to obtain the glycerol concentration in the reactor $C_{glycerol\ reactor}$:

$$C_{glycerol\ reactor}(t) = 40 C_{glycerol\ sample}(t)$$

Calculation of conversion

Once the results of the analysis with the EnzyChrom Glycerol Assay Kit found, it was necessary to find the value of the conversion. First of all, as a reference, finding the theoretical concentration of glycerol for each Butanol-to-oil ratio was essential as a reference to compute the yield reached in each sample.

In Appendix B, the number of moles of triglycerides per gram of oil N_{trig} was calculated. We obtained $N_{trig} = 9.98 \times 10^{-4} \text{ mol} \approx 1\text{mmol}$.

Knowing the specific gravity of the oil ($d_{oil} = 918 \text{ g.L}^{-1}$) as well as the molecular weight of the **glycerol** $M_{glycerol} = 92 \text{ g.mol}^{-1}$ and the volume of the reactor $V_{reactor} = 0.4\text{L}$, lead to the expression of the theoretical glycerol concentration $C_{glycerolTOT}$ in the reactor in the case of a total conversion $X_{Tot} = 1$.

$$C_{glycerolTOT} (\text{g.L}^{-1}) = m_{oil} \frac{N_{trig}}{3V_{reactor}} M_{glycerol}$$

Table 24 in Appendix C gives the weight of oil used for each Butanol-to-oil Ratio. As a consequence, $C_{glycerolTOT}$ was calculated for each value of $Ratio_{But/oil}$. The values are gathered in **Table 26**.

| $Ratio_{But/oil}$ | $C_{glycerolTOT} (\text{g.L}^{-1})$ |
|-------------------|-------------------------------------|
| 3 to 1 | 22.457 |
| 6 to 1 | 18.691 |
| 9 to 1 | 16.025 |
| 15 to 1 | 12.456 |
| 30 to 1 | 8.002 |

Table 26– theoretical value of the maximum glycerol concentration reached with respect to the butanol-to-oil ratio

Once those theoretical values obtained, the actual conversion X_t reached at time t (min) for the particular value R_i of butanol-to-oil ratio can be computed thanks to the measurement of the glycerol concentration in the reactor $C_{glycerol reactor}(t)$ and the theoretical maximum glycerol concentration computed for the same ratio R_i :

$$X_t = \frac{C_{glycerol reactor}(t)}{C_{glycerolTOT}}$$

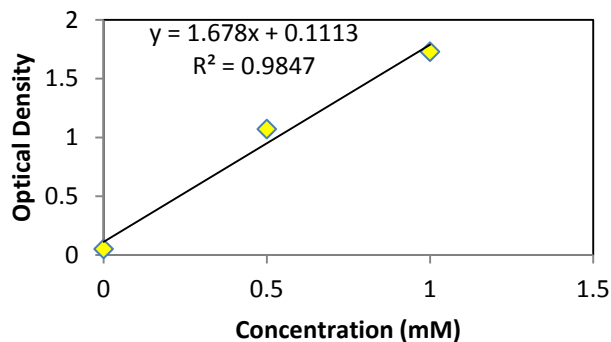
Appendix G: Results of the transesterification reactions with the different catalyts. 5 zeolites (13-X-type, Y-type, ZSM-5, Mordenite & Beta), H₂SO₄ and non-catalyzed reaction. Butanol-to-oil ratios tested: 3:1, 6:1 and 15:1.

- 13-X-type zeolite:

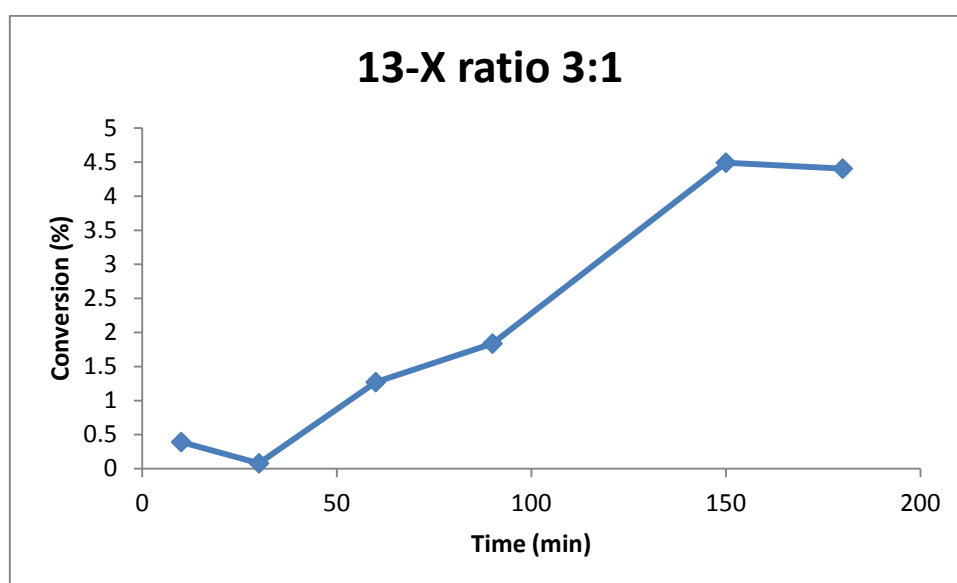
- Butanol-to-oil ratio: 3:1

Calibration data and curve:

| Gly (mM) | OD at t= 20 min |
|----------|-----------------|
| 0 | 0,051 |
| 0,5 | 1,071 |
| 1 | 1,729 |
| | |
| Slope | 1,678 |



| time | OD 20 | concentration Gly (g/L) | Conversion (%) |
|------|-------|-------------------------|----------------|
| 10 | 0,091 | 0,08772348 | 0,39062867 |
| 30 | 0,059 | 0,017544696 | 0,078125734 |
| 60 | 0,181 | 0,285101311 | 1,269543176 |
| 90 | 0,239 | 0,412300358 | 1,835954747 |
| 150 | 0,511 | 1,008820024 | 4,4922297 |
| 180 | 0,502 | 0,989082241 | 4,40433825 |

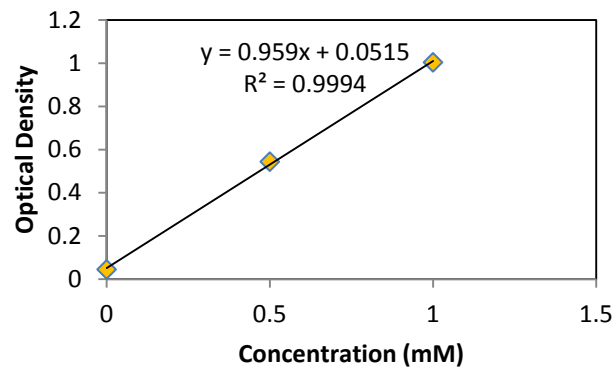


- 13-X-type zeolite:

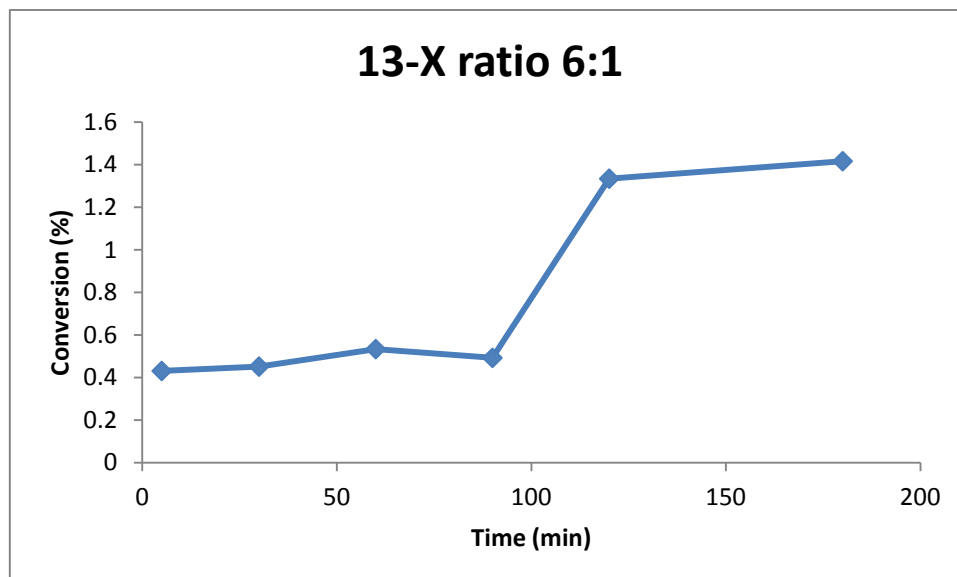
- Butanol-to-oil ratio: 6:1

Calibration data and curve:

| Gly (mM) | OD at t= 20 min |
|----------|-----------------|
| 0 | 0,045 |
| 0,5 | 0,544 |
| 1 | 1,004 |
| Slope | 0,959 |



| time | OD 20 | concentration Gly (g/L) | Conversion (%) |
|------|-------|-------------------------|----------------|
| 5 | 0,066 | 0,080583942 | 0,431137668 |
| 30 | 0,067 | 0,084421272 | 0,451668034 |
| 60 | 0,071 | 0,099770594 | 0,533789494 |
| 90 | 0,069 | 0,092095933 | 0,492728764 |
| 120 | 0,11 | 0,249426486 | 1,334473736 |
| 180 | 0,114 | 0,264775808 | 1,416595196 |

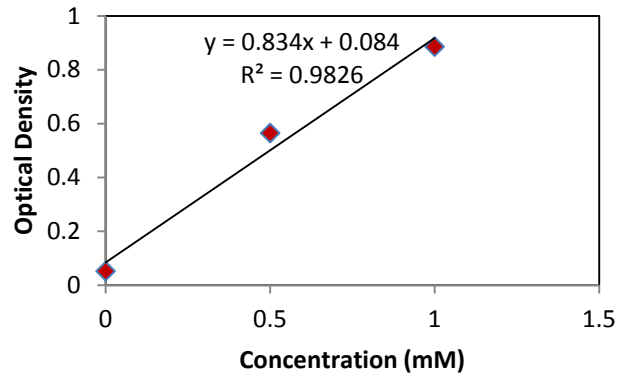


- 13-X-type zeolite:

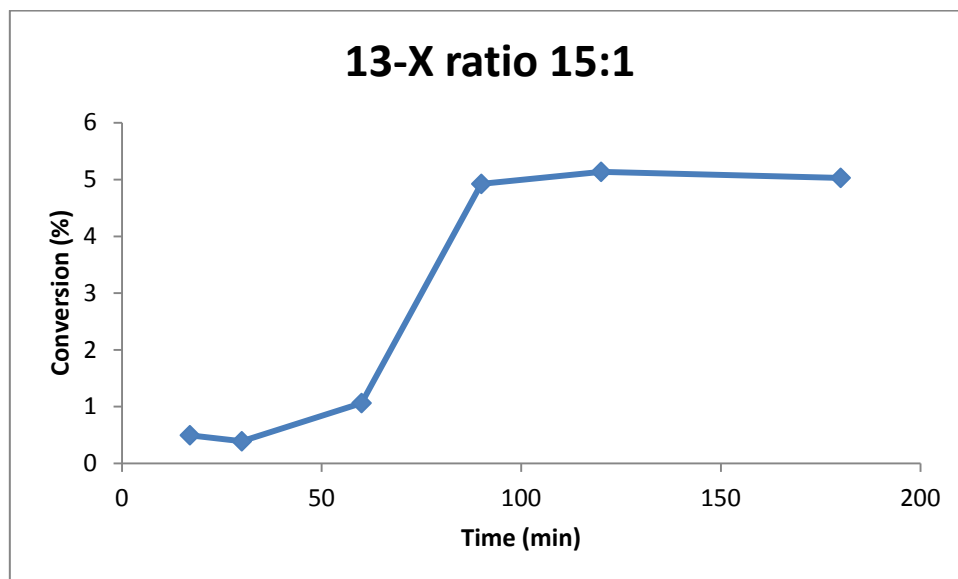
- Butanol-to-oil ratio: 15:1

Calibration data and curve:

| Gly (mM) | OD at t= 20 min |
|----------|-----------------|
| 0 | 0,052 |
| 0,5 | 0,565 |
| 1 | 0,886 |
| | |
| Slope | 0,834 |



| time | OD 20 | concentration Gly (g/L) | Conversion (%) |
|------|-------|-------------------------|----------------|
| 17 | 0,066 | 0,06177458 | 0,49594236 |
| 30 | 0,063 | 0,04853717 | 0,389668997 |
| 60 | 0,082 | 0,132374101 | 1,062733628 |
| 90 | 0,191 | 0,613333333 | 4,923999144 |
| 120 | 0,197 | 0,639808153 | 5,136545869 |
| 180 | 0,194 | 0,626570743 | 5,030272506 |

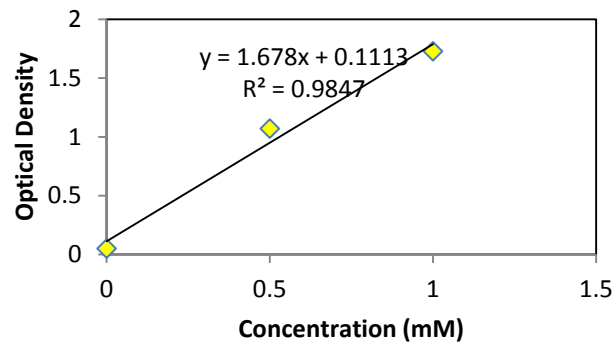


- Y-type zeolite:

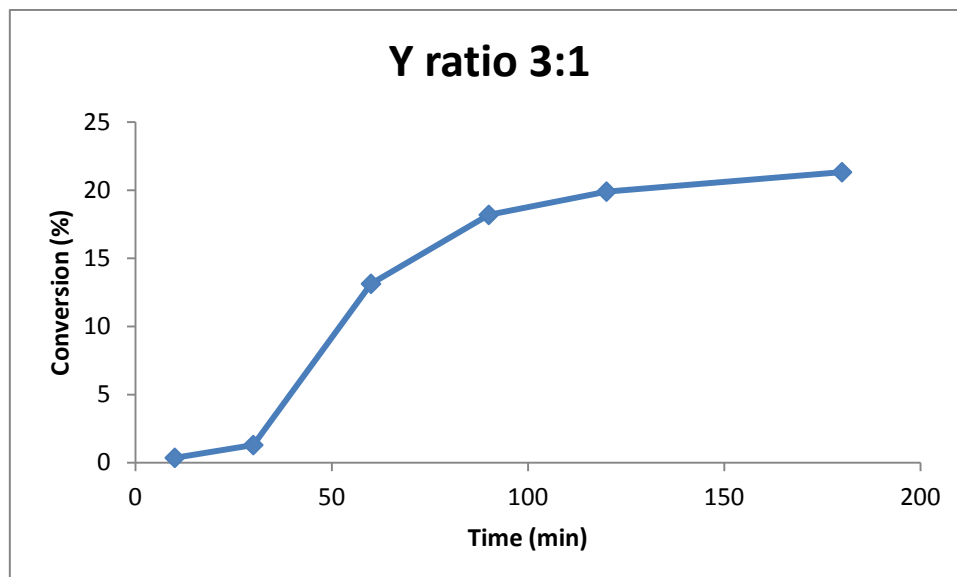
- Butanol-to-oil ratio: 3:1

Calibration data and curve:

| Gly (mM) | OD at t= 20 min |
|----------|-----------------|
| 0 | 0,051 |
| 0,5 | 1,071 |
| 1 | 1,729 |
| | |
| Slope | 1,678 |



| time | OD 20 | concentration Gly (g/L) | Conversion (%) |
|------|-------|-------------------------|----------------|
| 10 | 0,088 | 0,081144219 | 0,361331519 |
| 30 | 0,184 | 0,291680572 | 1,298840326 |
| 60 | 1,396 | 2,949702026 | 13,13488902 |
| 90 | 1,914 | 4,085721097 | 18,19353029 |
| 120 | 2,089 | 4,469511323 | 19,90253072 |
| 180 | 2,235 | 4,789702026 | 21,32832536 |

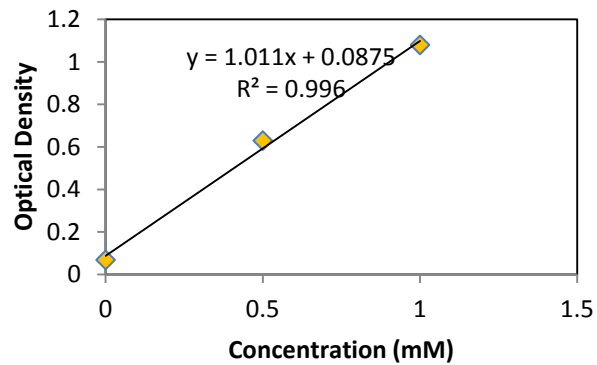


• Y-type zeolite:

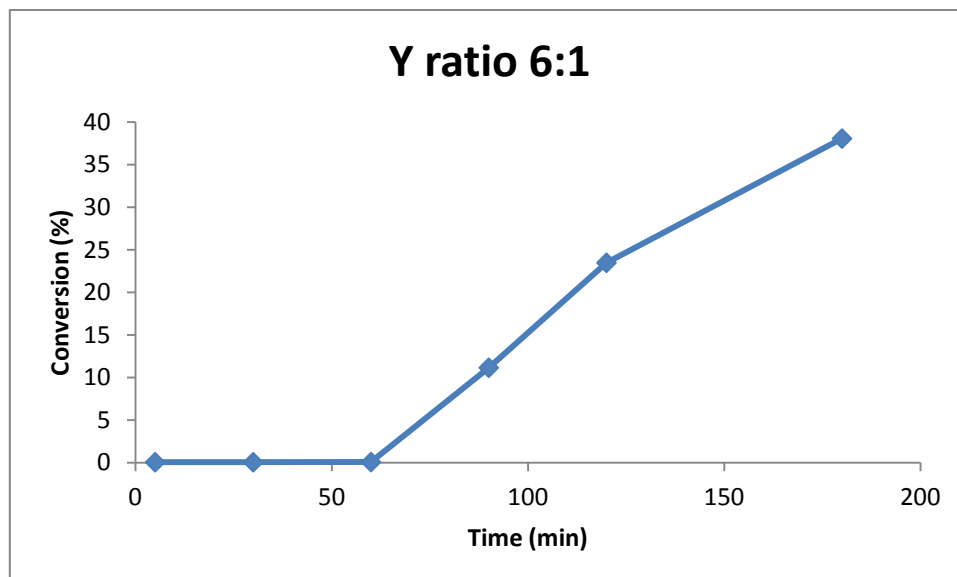
- Butanol-to-oil ratio: 6:1

Calibration data and curve:

| Gly (mM) | OD at t= 20 min |
|----------|-----------------|
| 0 | 0,069 |
| 0,5 | 0,63 |
| 1 | 1,08 |
| | |
| Slope | 1,011 |



| time | OD 20 | concentration Gly (g/L) | Conversion (%) |
|------|-------|-------------------------|----------------|
| 5 | 0,072 | 0,010919881 | 0,058423205 |
| 30 | 0,072 | 0,010919881 | 0,058423205 |
| 60 | 0,073 | 0,014559842 | 0,077897607 |
| 90 | 0,642 | 2,085697329 | 11,15883222 |
| 120 | 1,275 | 4,389792285 | 23,48612854 |
| 180 | 2,024 | 7,116122651 | 38,07245546 |

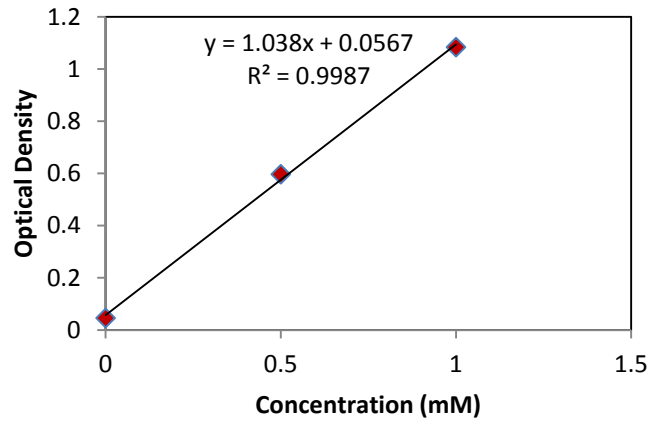


• Y-type zeolite:

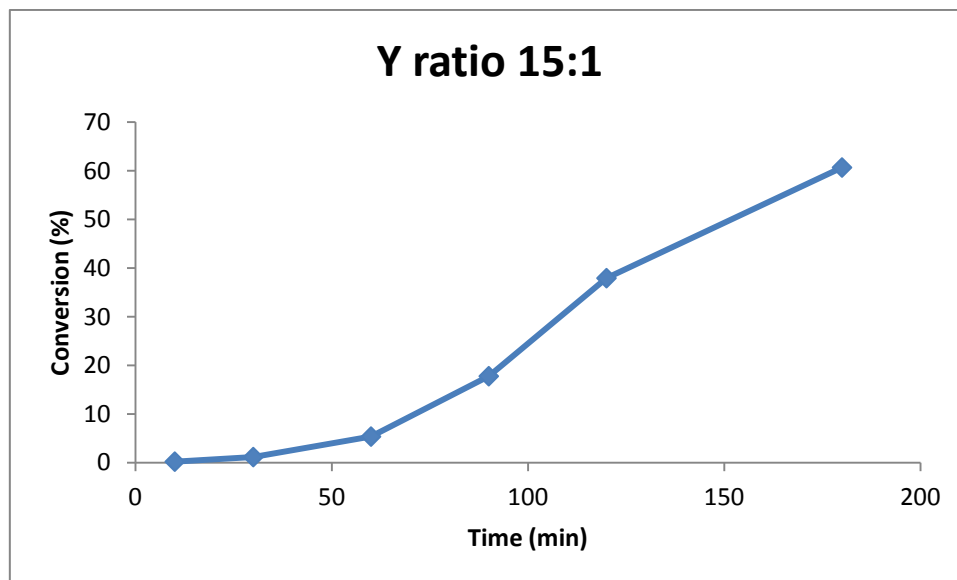
- Butanol-to-oil ratio: 15:1

Calibration data and curve:

| Gly (mM) | OD at t= 20 min |
|----------|-----------------|
| 0 | 0,046 |
| 0,5 | 0,597 |
| 1 | 1,084 |
| Slope | 1,038 |



| time | OD 20 | concentration Gly (g/L) | Conversion (%) |
|------|-------|-------------------------|----------------|
| 10 | 0,054 | 0,028362235 | 0,227699382 |
| 30 | 0,087 | 0,145356455 | 1,166959335 |
| 60 | 0,235 | 0,670057803 | 5,379397908 |
| 90 | 0,671 | 2,215799615 | 17,78901425 |
| 120 | 1,379 | 4,725857418 | 37,94040959 |
| 180 | 2,178 | 7,558535645 | 60,6818854 |

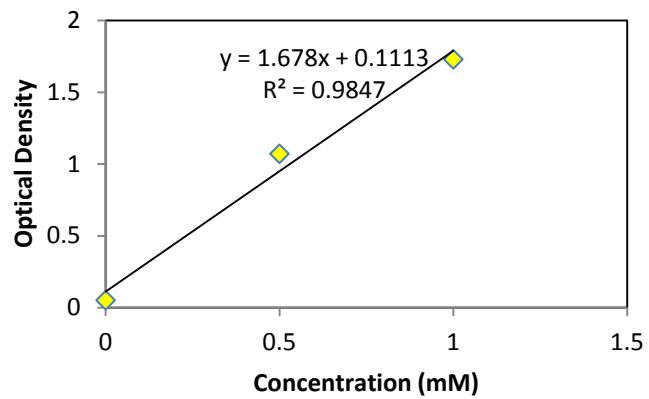


• ZSM-5:

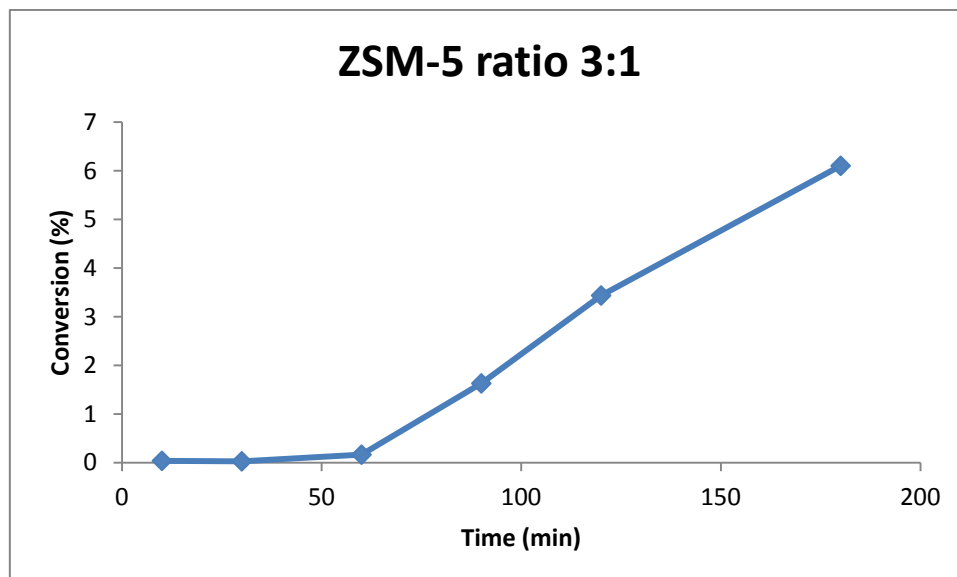
- Butanol-to-oil ratio: 3:1

Calibration data and curve:

| Gly (mM) | t= 20 min |
|----------|-----------|
| 0 | 0,051 |
| 0,5 | 1,071 |
| 1 | 1,729 |
| | |
| Slope | 1,678 |



| time | OD 20 | concentration Gly (g/L) | Conversion (%) |
|------|-------|-------------------------|----------------|
| 10 | 0,055 | 0,008772348 | 0,039062867 |
| 30 | 0,054 | 0,006579261 | 0,02929715 |
| 60 | 0,068 | 0,037282479 | 0,166017185 |
| 90 | 0,218 | 0,36624553 | 1,630874696 |
| 120 | 0,403 | 0,771966627 | 3,437532293 |
| 180 | 0,676 | 1,37067938 | 6,103572963 |

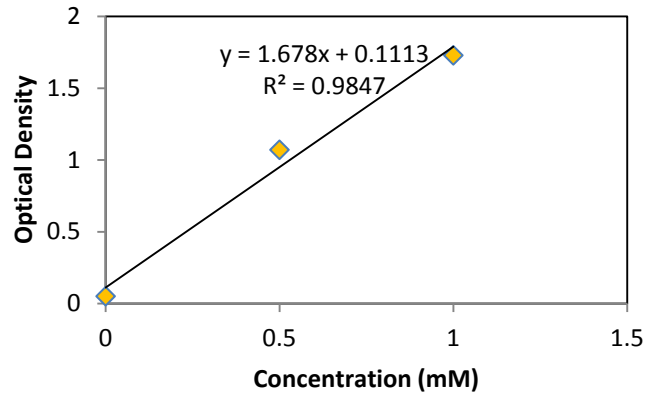


• ZSM-5:

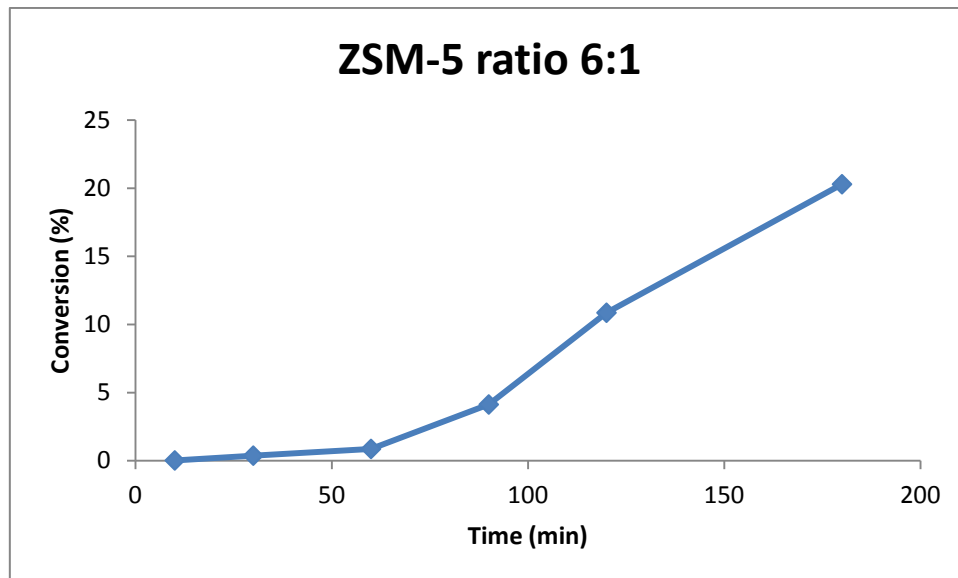
- Butanol-to-oil ratio: 6:1

Calibration data and curve:

| Gly (mM) | t= 20 min |
|----------|-----------|
| 0 | 0,051 |
| 0,5 | 1,071 |
| 1 | 1,729 |
| | |
| Slope | 1,678 |



| time | OD 20 | concentration Gly (g/L) | Conversion (%) |
|------|-------|-------------------------|----------------|
| 10 | 0,053 | 0,004386174 | 0,02346677 |
| 30 | 0,083 | 0,070178784 | 0,375468323 |
| 60 | 0,125 | 0,162288439 | 0,868270497 |
| 90 | 0,403 | 0,771966627 | 4,130151554 |
| 120 | 0,977 | 2,03079857 | 10,8651146 |
| 180 | 1,781 | 3,794040524 | 20,29875622 |

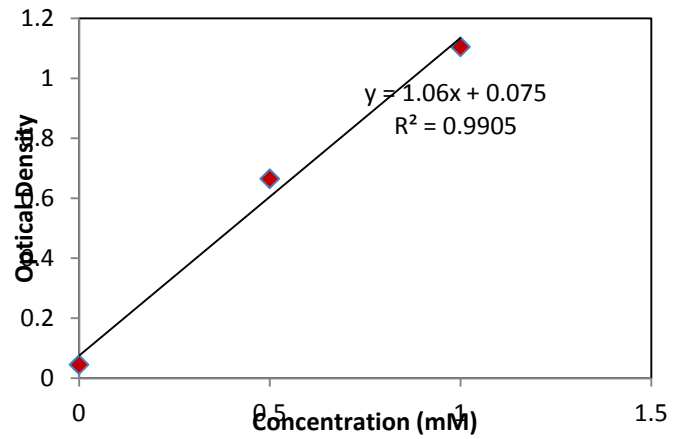


- ZSM-5:

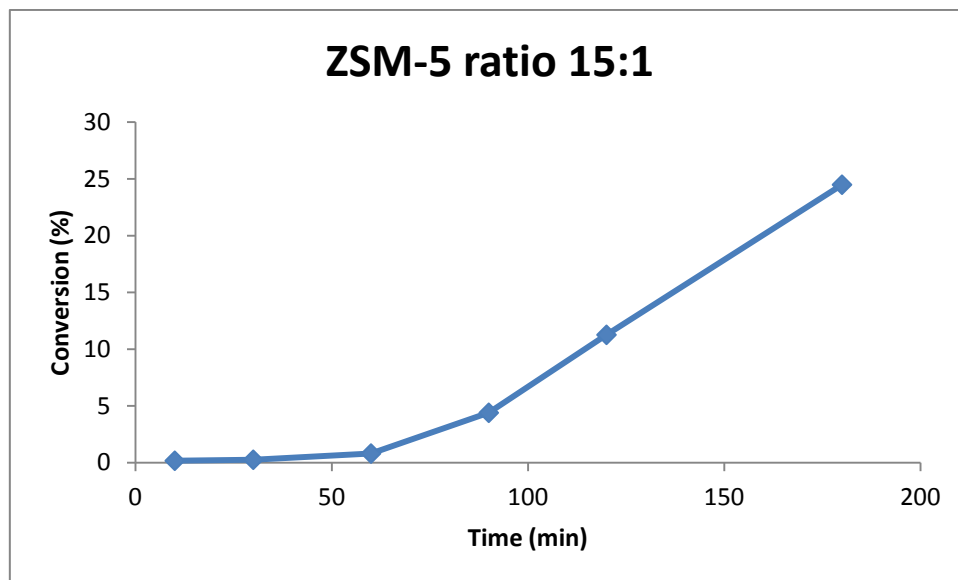
- Butanol-to-oil ratio: 15:1

Calibration data and curve:

| Gly (mM) | t= 20 min |
|----------|-----------|
| 0 | 0,051 |
| 0,5 | 1,071 |
| 1 | 1,729 |
| | |
| Slope | 1,678 |



| time | OD 20 | concentration Gly (g/L) | Conversion (%) |
|------|-------|-------------------------|----------------|
| 10 | 0,061 | 0,02193087 | 0,176066716 |
| 30 | 0,066 | 0,032896305 | 0,264100073 |
| 60 | 0,097 | 0,100882002 | 0,809906891 |
| 90 | 0,301 | 0,548271752 | 4,401667888 |
| 120 | 0,691 | 1,403575685 | 11,26826979 |
| 180 | 1,442 | 3,050584029 | 24,49088013 |

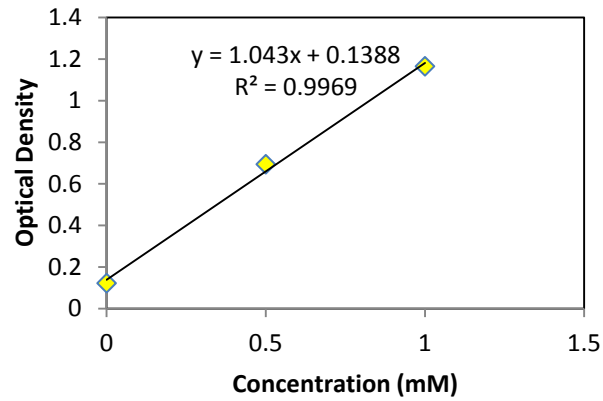


- Mordenite:

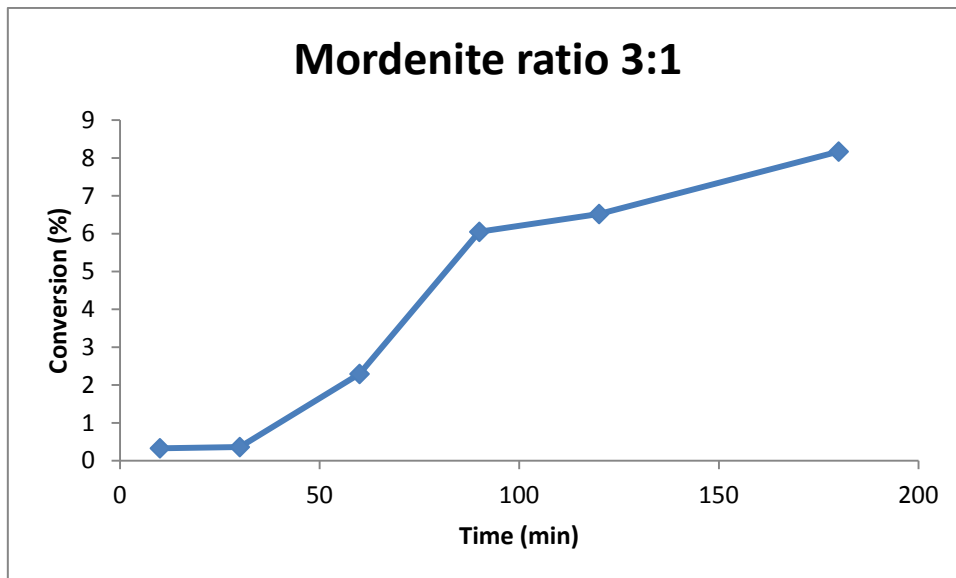
- Butanol-to-oil ratio: 3:1

Calibration data and curve:

| Gly (mM) | OD at t= 20 min |
|----------|-----------------|
| 0 | 0,122 |
| 0,5 | 0,694 |
| 1 | 1,165 |
| | |
| Slope | 1,043 |



| time | OD 20 | concentration Gly (g/L) | Conversion (%) |
|------|-------|-------------------------|----------------|
| 10 | 0,143 | 0,07409396 | 0,329937034 |
| 30 | 0,145 | 0,081150527 | 0,361359609 |
| 60 | 0,268 | 0,515129434 | 2,293847951 |
| 90 | 0,507 | 1,358389262 | 6,048845624 |
| 120 | 0,537 | 1,464237776 | 6,520184244 |
| 180 | 0,642 | 1,834707574 | 8,169869414 |

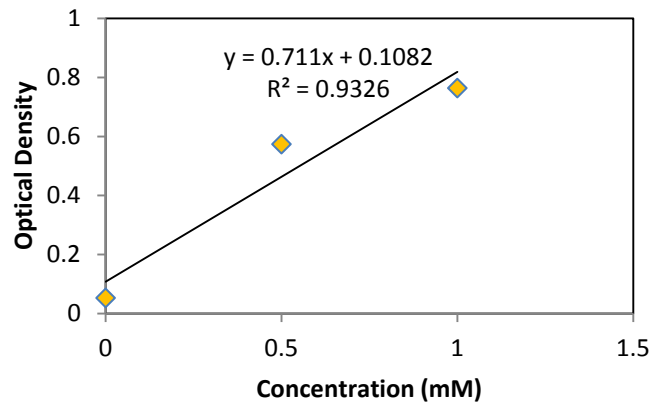


- **Mordenite:**

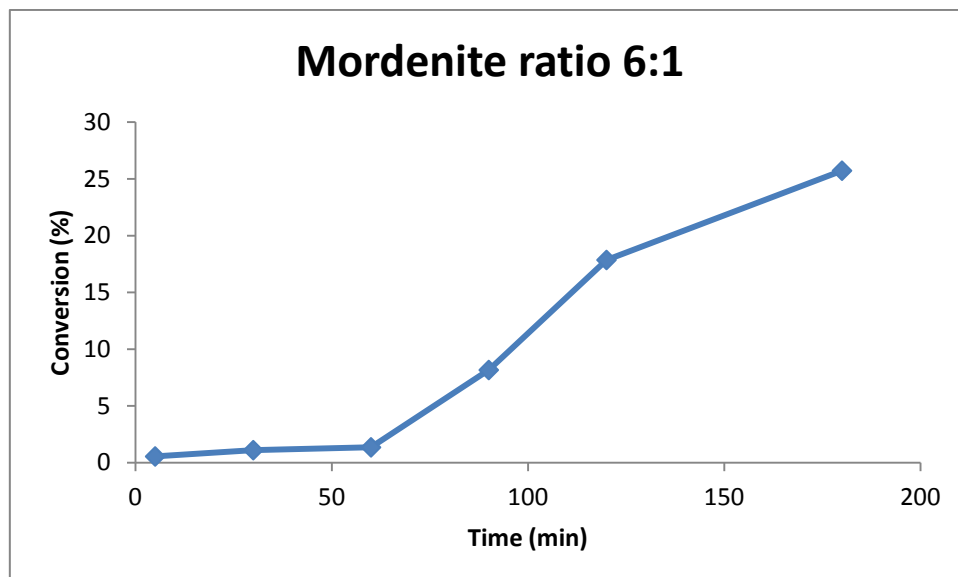
- Butanol-to-oil ratio: 3:1

Calibration data and curve:

| Gly (mM) | OD at t= 20 min |
|----------|-----------------|
| 0 | 0,053 |
| 0,5 | 0,574 |
| 1 | 0,764 |
| Slope | 0,711 |



| time | OD 20 | concentration Gly (g/L) | Conversion (%) |
|------|-------|-------------------------|----------------|
| 5 | 0,073 | 0,103516174 | 0,553828979 |
| 30 | 0,093 | 0,207032349 | 1,107657957 |
| 60 | 0,102 | 0,253614627 | 1,356880998 |
| 90 | 0,348 | 1,526863572 | 8,168977435 |
| 120 | 0,698 | 3,338396624 | 17,86098456 |
| 180 | 0,982 | 4,808326301 | 25,72535606 |

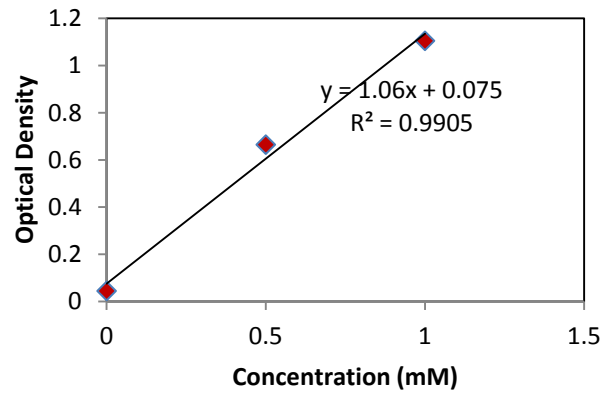


- Mordenite:

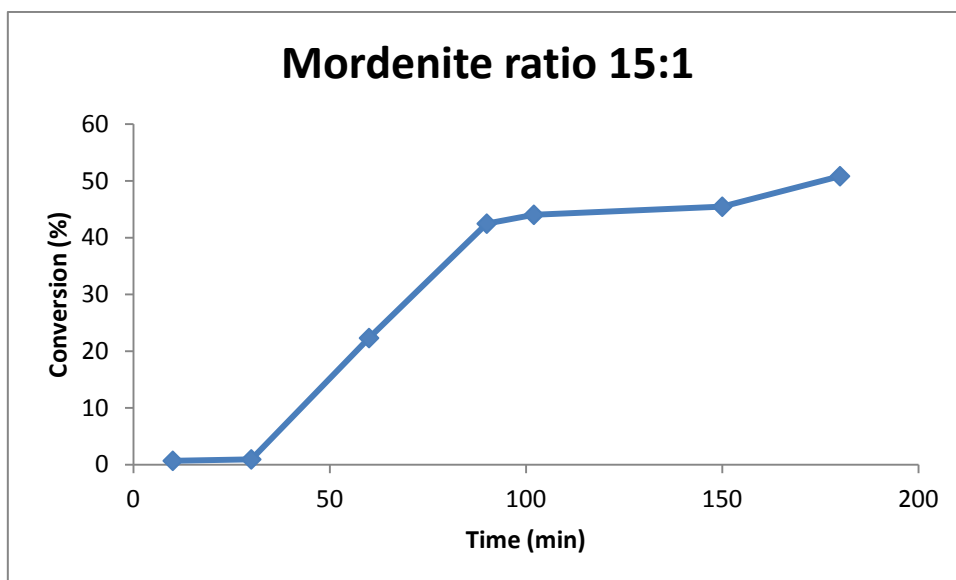
- Butanol-to-oil ratio: 3:1

Calibration data and curve:

| Gly (mM) | OD at t= 20 min |
|----------|-----------------|
| 0 | 0,045 |
| 0,5 | 0,665 |
| 1 | 1,105 |
| | |
| Slope | 1,06 |



| time | OD 20 | concentration Gly (g/L) | Conversion (%) |
|------|-------|-------------------------|----------------|
| 10 | 0,07 | 0,086792453 | 0,696792332 |
| 30 | 0,079 | 0,118037736 | 0,947637571 |
| 60 | 0,846 | 2,780830189 | 22,32522631 |
| 90 | 1,569 | 5,290867925 | 42,47646054 |
| 102 | 1,625 | 5,485283019 | 44,03727536 |
| 150 | 1,676 | 5,662339623 | 45,45873172 |
| 180 | 1,869 | 6,332377358 | 50,83796852 |

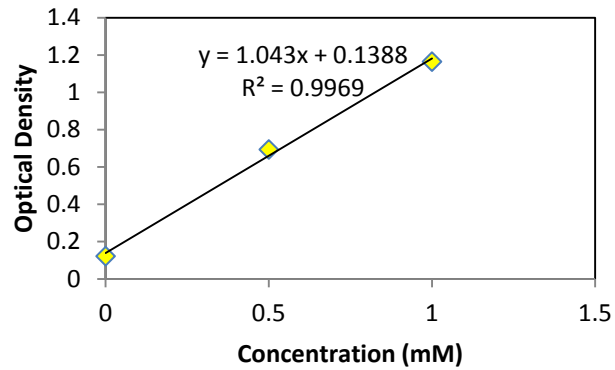


- Beta:

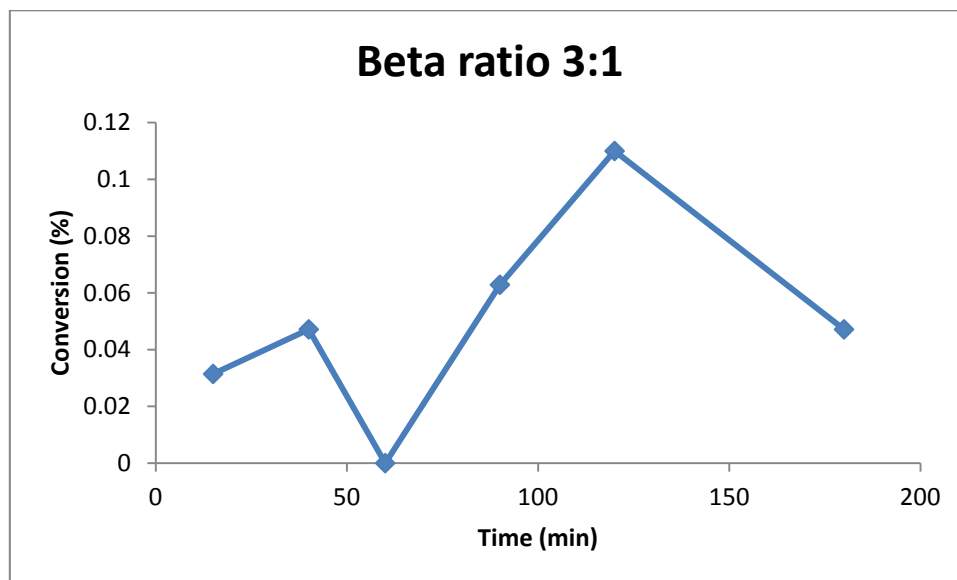
- Butanol-to-oil ratio: 3:1

Calibration data and curve:

| Gly (mM) | OD at t= 20 min |
|----------|-----------------|
| 0 | 0,122 |
| 0,5 | 0,694 |
| 1 | 1,165 |
| | |
| Slope | 1,043 |



| time | OD 20 | concentration Gly (g/L) | Conversion (%) |
|------|-------|-------------------------|----------------|
| 15 | 0,124 | 0,007056568 | 0,031422575 |
| 40 | 0,125 | 0,010584851 | 0,047133862 |
| 60 | 0,122 | 0 | 0 |
| 90 | 0,126 | 0,014113135 | 0,062845149 |
| 120 | 0,129 | 0,024697987 | 0,109979011 |
| 180 | 0,125 | 0,010584851 | 0,047133862 |

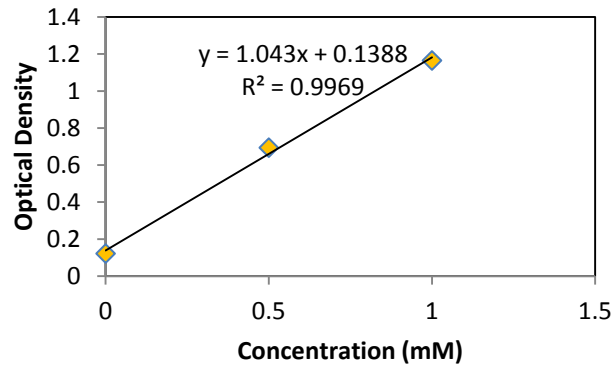


- Beta:

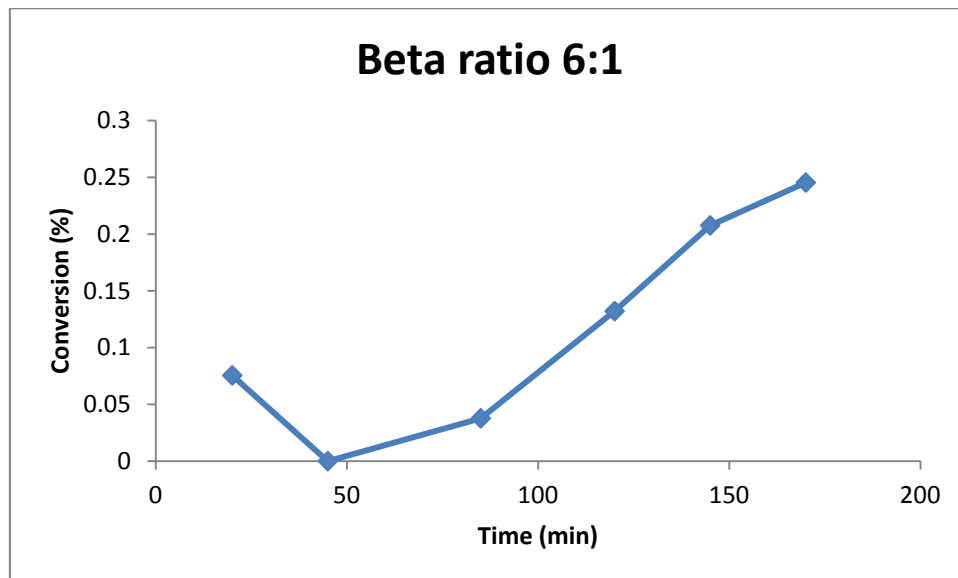
- Butanol-to-oil ratio: 3:1

Calibration data and curve:

| Gly (mM) | OD at t= 20 min |
|----------|-----------------|
| 0 | 0,122 |
| 0,5 | 0,694 |
| 1 | 1,165 |
| | |
| Slope | 1,043 |



| time | OD 20 | concentration Gly (g/L) | Conversion (%) |
|------|-------|-------------------------|----------------|
| 20 | 0,126 | 0,014113135 | 0,075507652 |
| 45 | 0,122 | 0 | 0 |
| 85 | 0,124 | 0,007056568 | 0,037753826 |
| 120 | 0,129 | 0,024697987 | 0,132138391 |
| 145 | 0,133 | 0,038811122 | 0,207646042 |
| 170 | 0,135 | 0,045867689 | 0,245399868 |

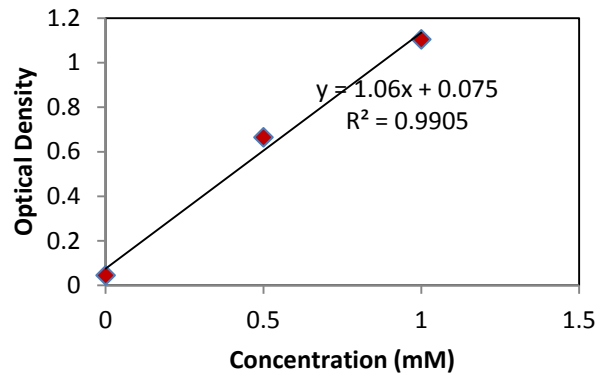


- Beta:

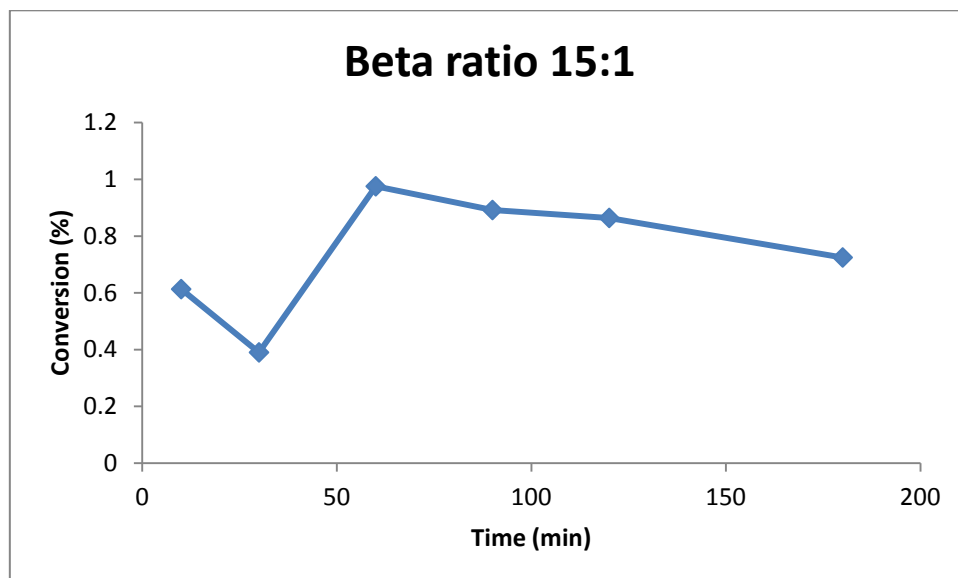
- Butanol-to-oil ratio: 3:1

Calibration data and curve:

| Gly (mM) | OD at t= 20 min |
|----------|-----------------|
| 0 | 0,045 |
| 0,5 | 0,665 |
| 1 | 1,105 |
| | |
| Slope | 1,06 |



| time | OD 20 | concentration Gly (g/L) | Conversion (%) |
|------|-------|-------------------------|----------------|
| 10 | 0,067 | 0,076377358 | 0,613177252 |
| 30 | 0,059 | 0,048603774 | 0,390203706 |
| 60 | 0,08 | 0,121509434 | 0,975509264 |
| 90 | 0,077 | 0,11109434 | 0,891894185 |
| 120 | 0,076 | 0,107622642 | 0,864022491 |
| 180 | 0,071 | 0,090264151 | 0,724664025 |

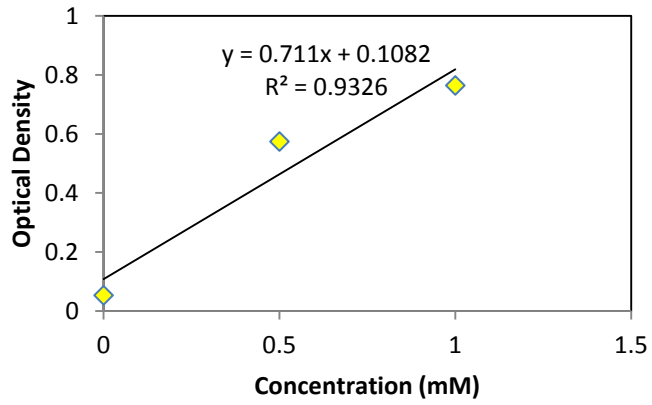


• H₂SO₄:

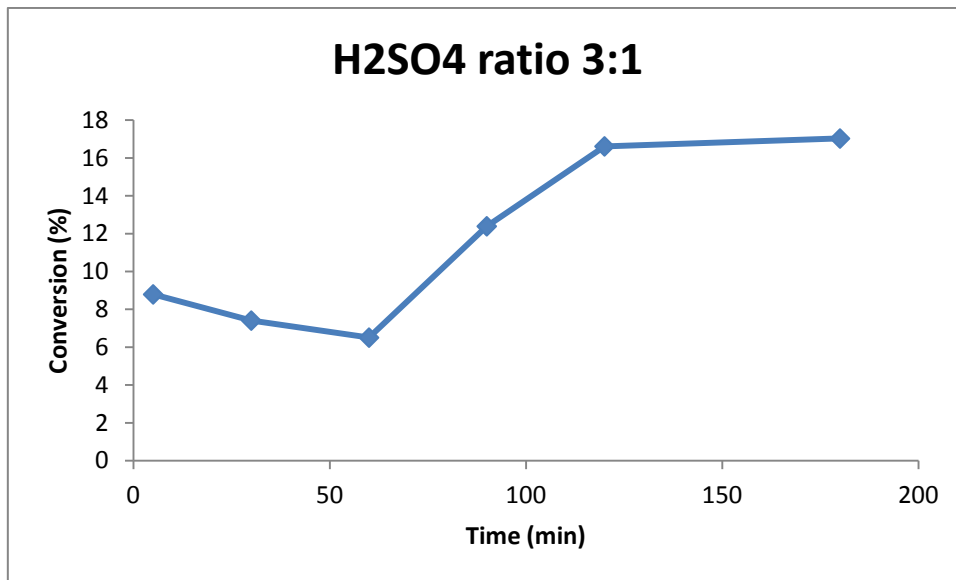
- Butanol-to-oil ratio: 3:1

Calibration data and curve:

| Gly (mM) | OD at t= 20 min |
|----------|-----------------|
| 0 | 0,053 |
| 0,5 | 0,574 |
| 1 | 0,764 |
| | |
| Slope | 0,711 |



| time | OD 20 | concentration Gly (g/L) | Conversion (%) |
|------|-------|-------------------------|----------------|
| 5 | 0,18 | 1,643319269 | 8,792035036 |
| 30 | 0,16 | 1,384528833 | 7,40746259 |
| 60 | 0,147 | 1,216315049 | 6,507490499 |
| 90 | 0,232 | 2,316174402 | 12,3919234 |
| 120 | 0,293 | 3,105485232 | 16,61486936 |
| 180 | 0,299 | 3,183122363 | 17,03024109 |

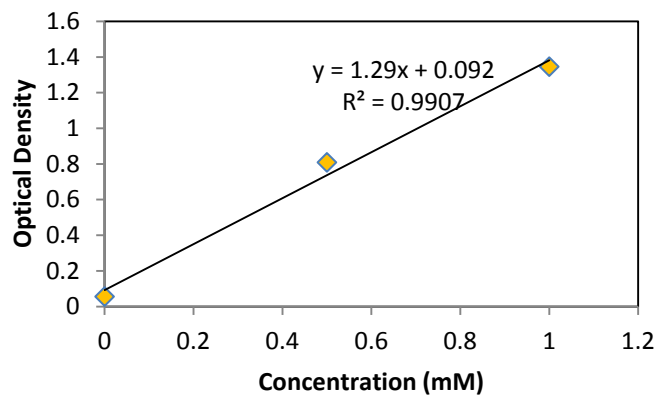


- H₂SO₄:

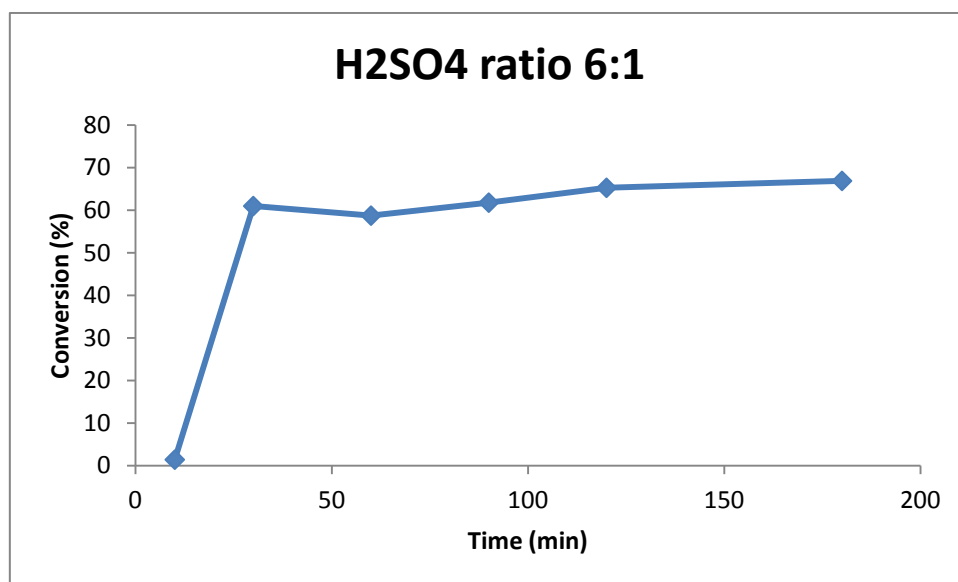
- Butanol-to-oil ratio: 6:1

Calibration data and curve:

| Gly (mM) | OD at t= 20 min |
|----------|-----------------|
| 0 | 0,056 |
| 0,5 | 0,809 |
| 1 | 1,346 |
| | |
| Slope | 1,29 |



| time | OD 20 | concentration Gly (g/L) | Conversion (%) |
|------|-------|-------------------------|----------------|
| 10 | 0,101 | 0,320930233 | 1,429087735 |
| 30 | 1,977 | 13,70015504 | 61,00616751 |
| 60 | 1,906 | 13,19379845 | 58,75138464 |
| 90 | 2,002 | 13,87844961 | 61,80010514 |
| 120 | 2,112 | 14,66294574 | 65,29343072 |
| 180 | 2,163 | 15,02666667 | 66,91306348 |

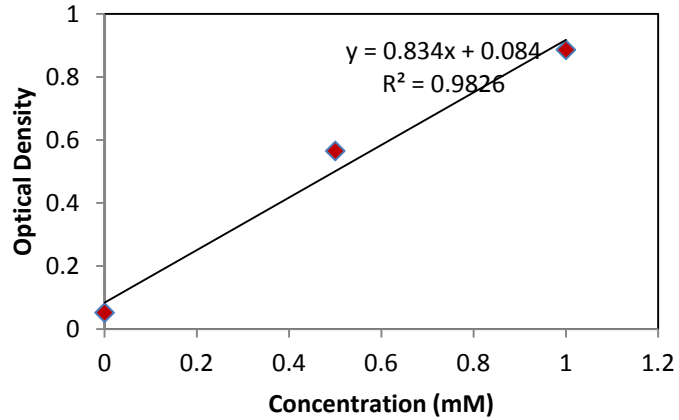


• H₂SO₄:

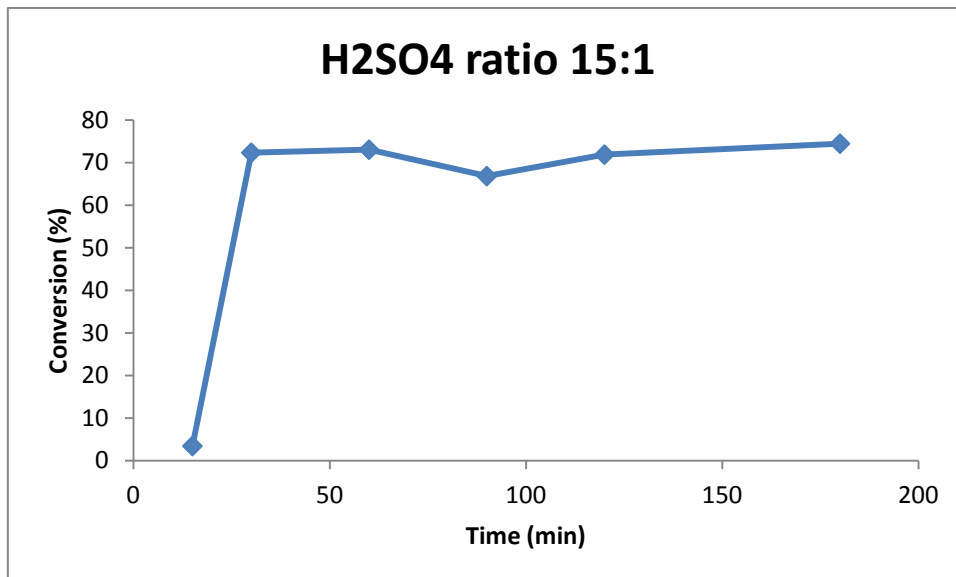
- Butanol-to-oil ratio: 15:1

Calibration data and curve:

| Gly (mM) | OD at t= 20 min |
|----------|-----------------|
| 0 | 0,052 |
| 0,5 | 0,565 |
| 1 | 0,886 |
| | |
| Slope | 0,834 |



| time | OD 20 | concentration Gly (g/L) | Conversion (%) |
|------|-------|-------------------------|----------------|
| 15 | 0,091 | 0,430215827 | 3,453884291 |
| 30 | 0,869 | 9,012470024 | 72,35444785 |
| 60 | 0,877 | 9,100719424 | 73,06293693 |
| 90 | 0,807 | 8,32853717 | 66,86365744 |
| 120 | 0,864 | 8,957314149 | 71,91164217 |
| 180 | 0,893 | 9,277218225 | 74,4799151 |

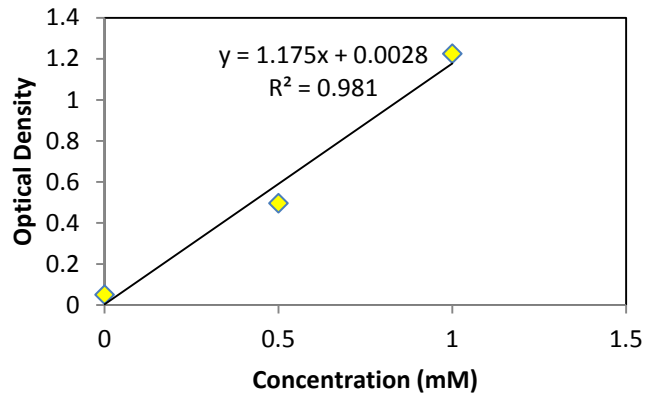


- Non-catalyzed reaction:

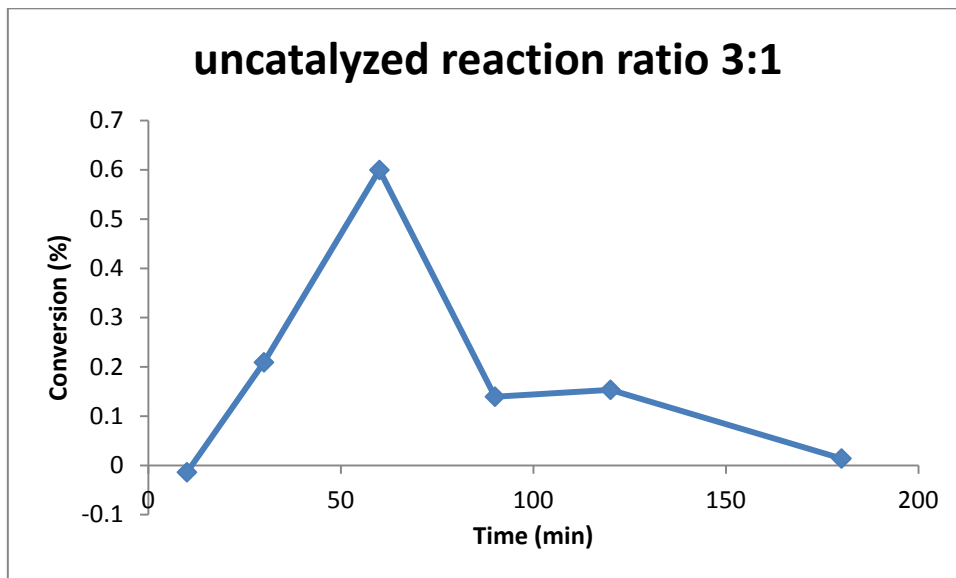
- Butanol-to-oil ratio: 3:1

Calibration data and curve:

| Gly (mM) | t= 20 min |
|----------|-----------|
| 0 | 0,05 |
| 0,5 | 0,496 |
| 1 | 1,225 |
| | |
| Slope | 1,175 |



| time | OD 20 | concentration Gly (g/L) | Conversion (%) |
|------|-------|-------------------------|----------------|
| 10 | 0,049 | -0,00313191 | -0,01394627 |
| 30 | 0,065 | 0,04697872 | 0,20919412 |
| 60 | 0,093 | 0,13467234 | 0,59968981 |
| 90 | 0,06 | 0,03131915 | 0,13946275 |
| 120 | 0,061 | 0,03445106 | 0,15340902 |
| 180 | 0,051 | 0,00313191 | 0,01394627 |

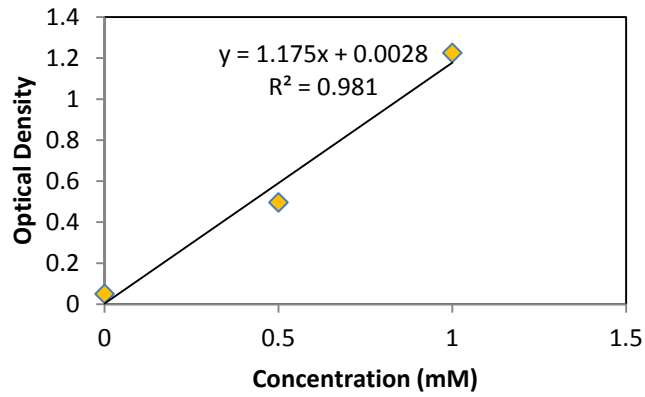


- Non-catalyzed reaction:

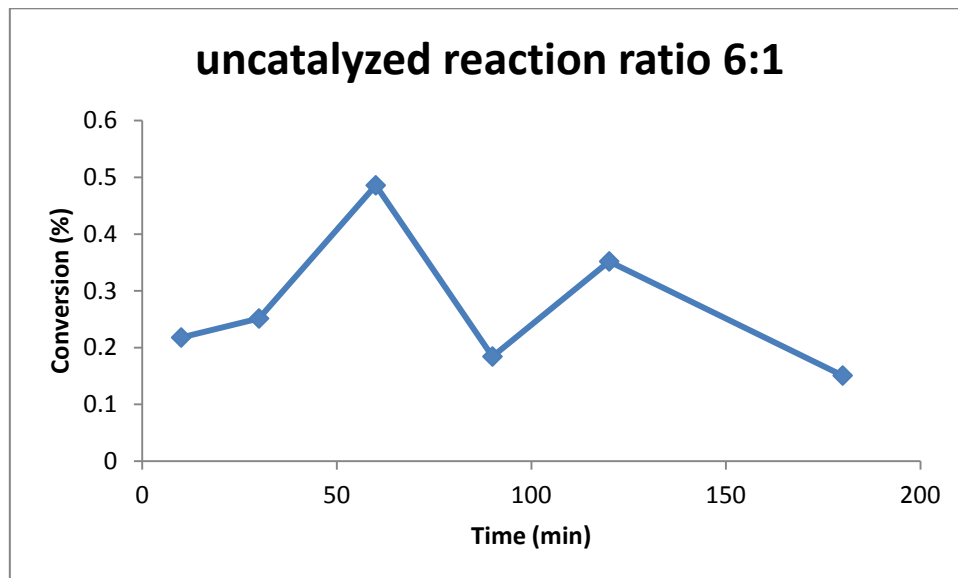
- Butanol-to-oil ratio: 6:1

Calibration data and curve:

| Gly (mM) | t= 20 min |
|----------|-----------|
| 0 | 0,05 |
| 0,5 | 0,496 |
| 1 | 1,225 |
| | |
| Slope | 1,175 |



| time | OD 20 | concentration Gly (g/L) | Conversion (%) |
|------|-------|-------------------------|----------------|
| 10 | 0,063 | 0,04071489 | 0,21783154 |
| 30 | 0,065 | 0,04697872 | 0,25134409 |
| 60 | 0,079 | 0,09082553 | 0,4859319 |
| 90 | 0,061 | 0,03445106 | 0,184319 |
| 120 | 0,071 | 0,06577021 | 0,35188172 |
| 180 | 0,059 | 0,02818723 | 0,15080645 |

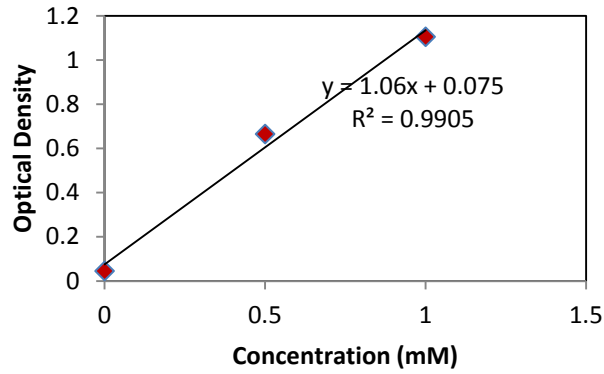


- Non-catalyzed reaction:

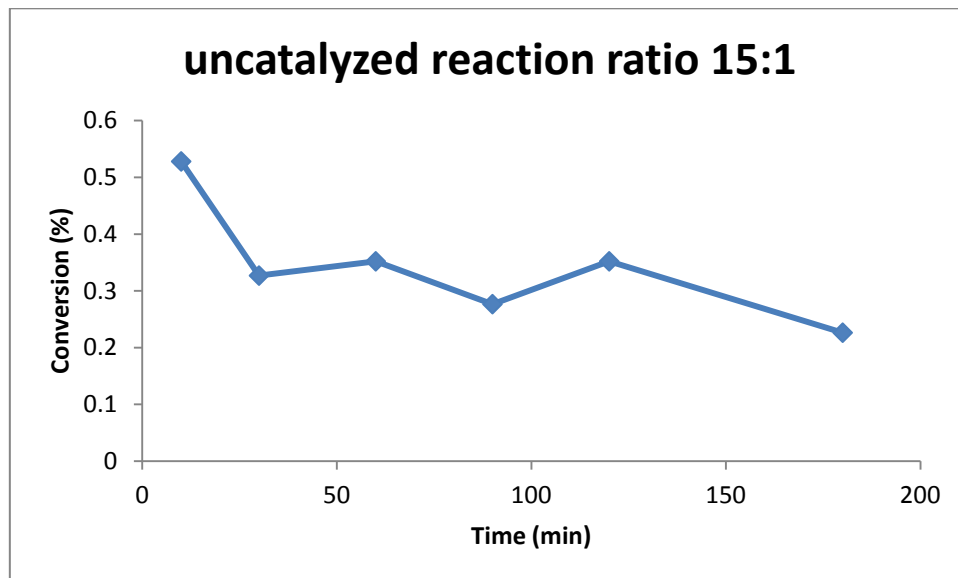
- Butanol-to-oil ratio: 15:1

Calibration data and curve:

| Gly (mM) | t= 20 min |
|----------|-----------|
| 0 | 0,05 |
| 0,5 | 0,496 |
| 1 | 1,225 |
| | |
| Slope | 1,175 |



| time | OD 20 | concentration Gly (g/L) | Conversion (%) |
|------|-------|-------------------------|----------------|
| 10 | 0,071 | 0,06577021 | 0,52802033 |
| 30 | 0,063 | 0,04071489 | 0,32686973 |
| 60 | 0,064 | 0,04384681 | 0,35201356 |
| 90 | 0,061 | 0,03445106 | 0,27658208 |
| 120 | 0,064 | 0,04384681 | 0,35201356 |
| 180 | 0,059 | 0,02818723 | 0,22629443 |



Appendix H: Specifications and characteristics of the Parr reactor



PARR REACTOR SPECIFICATIONS

800-872-7720
309-762-7716

Linda Paradiso
Joe Lambert

A. 450mL PARR Reactor

| Reactor | Model ¹ | Serial Number | Maximum Working Pressure ² |
|----------------|--------------------|---------------|---------------------------------------|
| 450mL: Reactor | 452 HC 2 | 052187 2930 | 2000 psi at 350°C |
| 450mL: Head | 818 HC 2 | 121586 2130 | 2000 psi at 350°C |

1. HC = Hastelloy C, Alloy C-276

2. All materials lose strength at elevated temperature. This number will decrease at higher temperature and increase slightly at lower temperatures. Although lower operating temperatures permit higher pressure ratings, the maximum should only be increased by 20% of the rated amount.

The reactor head is sealed to the body by a split-ring closure and locked together with a drop band. The reactor body is completely removable from the head to aid in charging and cleaning. The reactor's main head is sealed to the body with a flat teflon (PTFE) gasket for temperatures up to 350°C.

The size numbers refer to the free space in the vessel. For safe operation, **the maximum liquid charge held in the vessel used in sealed batch operations should not exceed two-thirds of the available free space.**

The packing gland limits the reactor's pressure to 2000psi, with a magnetic drive, the rating will increase to 3000psig.

The pressure relief valve is installed when any equipment (gauges, sample lines, tubing etc...) is attached to the system and has a lower pressure rating than the system and rupture disk. The benefits are:

- Relief pressure near the operating pressure
- Reseals once excess pressure has been relieved
- Protection of low pressure components

B. System Components:

Hydrogen Tank
Regulator
Nylon Gas Line
Check Valve



Swagelok tube fittings
 Gas inlet valve (SS316 Needle Valve)
 Pressure Safety Valve
 Rupture Disk
 Pressure gauge
 Sampling valve and line
 Thermowell
 Packed Gland Agitator (Magnetic drive)
 Heater
 Temperature Controller
 Vent valve
 Stirrer shaft

| ID | Material | P/N | Temp. Rating | Pressure Rating | Comments |
|----------------------------|--------------------|------------------|--------------|--------------------------|--|
| H ₂ supply line | Nylon | A495HC | Ambient | 2500 psi | Keep away from heated surfaces |
| Pressure relief valve | SS316 | A140VB2PB | Ambient | As set | 150-350 psi adjustable, spring-loaded |
| Pressure relief valve | SS316 | A175VB | Ambient | 750-1500 | Psi, variable |
| Swagelok # | SS-4CPA-X | X=pressure range | | | Refer to specs for flowrate |
| PSV seals | Viton | | -23 to 190°C | | Note: PTFE seals will not be leak free |
| Check valve | SS316 | SS-CHS4-10 | 40°C | Back pressure = 6000psig | Crack at 7-15psi, 40°C |
| Check valve seals | Viton | SS3KCH4-VI | -23 to 204°C | | |
| Check Valve | | 363VBAD | | | PARR |
| Gas inlet valve | | | | | |
| Gas inlet valve seals | | | | | |
| Rupture Disk | Gold faced Inconel | 581HCPF | Ambient | 2000psig | |
| Pressure Gauge | | 593HCPD | | 0-1000psig | 3.5inch gauge |
| Pressure Gauge | | 593HCPF | | 0-2000psig | 3.5inch gauge |



| ID | Material | P/N | Temp. Rating | Pressure Rating | Comments |
|-----------------------|--------------------|---------|--------------|-----------------|----------|
| | | | | | |
| | | | | | |
| | | | | | |
| | | | | | |
| Pressure relief valve | SS316 | A175VB | 240.00 | | |
| Rupture Disk | Gold faced Inconel | 581HCPF | 78.00 | | |
| Pressure Gauge | | 593HCPD | 155.00 | | |
| Pressure Gauge | | 593HCPF | 155.00 | | |

B. 2000mL PARR Reactor

| Reactor | Model | Serial Number | Maximum Working Pressure |
|-----------------|--------------|---------------|--------------------------|
| 2000mL: Reactor | 236 HC 20 | 071790 8030 | 1900 psi at 350°C |
| 2000mL: Head | 1370 HC 2 | 070590 8030 | 1900 psi at 350°C |
| 2000mL: Drive | A1120HC-2235 | | |



Parr Reactors Equipment List
 Tuesday, September 01, 1998
 RJP

Sepracor's Parr Reactor Specifications

| Reactor | Model | New Model Number | Serial Number | Maximum Working Pressure |
|-------------------|--------------|------------------|---------------|--------------------------|
| 450mL: Reactor | 452 HC 2 | 4562 HC | 052187 2930 | 2000 psi at 350°C |
| 450mL: Head | 818 HC 2 | | 121586 2130 | |
| 2000mL: Reactor | 236 HC 20 | 4522 HC | 071790 8030 | 1900 psi at 350°C |
| 2000mL: Head | 1370 HC 2 | | 070590 8030 | |
| 2000mL: Drive | A1120HC-2235 | | | |
| Heater Controller | Parr 4841 | | | |

HC: Hastelloy C

Note: Burst disks are rated at ambient temperature. Their rating goes down as the temperature increases.

Parts List

| Item | Description | Part Number | Comments |
|-----------------------|--|-------------------|-------------------------------|
| 6ft Nylon Hose | Hydrogen tank to reactors | A495HC | Rated to 2500 psi |
| Pressure relief valve | 150-300psig, adjustable. | A140VB2PB | |
| Valve | Hydrogen Inlet | SS-4-JB | Swagelok |
| Teflon Packing | Seal for above valve | <u>T-4JB-K1</u> | \$3.00 |
| 3000psig at 20 °C | Max T=205 °C | 2100psig @ 204 °C | 316SS and Teflon wetted parts |
| Check Valve, SS316 | 10 psi cracking pressure, Viton seal. Swagelok | SS-CHS4-10 | Rated for 6000 psi |
| Safety Rupture Disk | Burst 2000 psig | 581HCPF | Gold faced, Inconel disk |
| Rupture Disk (cont) | ½ diameter rupture disk | | ¼ diameter orifice / |

U:\@MYFILES\FACILITY\EQUIP\Hydrogenator\Parr Equip\Parr Equip List.doc

01/25/01



| Item | Description | Part Number | Comments |
|---------------------------------|-------------------------------|---------------|--|
| | | | NPT connection |
| Spare Parts Kit | 600mL | 4569PB | Replacement gaskets, O-rings, shafts, bearings, rupture disks and a teflon seal for the reactor. |
| Spare Parts Kit | 2000mL | 4509M | Same as above |
| Heater, 450mL | | A2230 HC 2 EB | Standard heater |
| Check valve: | SS316, viton seals (standard) | SS-4CPA2-150 | 150-350psig range |
| Drive Belt | Air motor | 847HC6 | \$4.00 |
| Female Spline Coupling | Mixing shaft coupler | A722HC2 | \$24.00 |
| Check Valve | SS-4C4-10 | 10psig crack | |
| Gaskets | | Kalrez | |
| Relief Valve | SS-4R3-A5 | 750-1500psi | |
| Gaskets | | Kalrez | |
| 9in Type J Thermocouple | | A472E2 | \$54.00 |
| Type J extension wire | For thermocouple | A470E2 | \$ 38.00 |
| Shaft (air stirrer to agitator) | | A860HC | \$19.00 |
| Driven pulley sub-assembly | | A2179HC | \$152.00 |
| | | | |